


12-2013

Caveolins and NJKs Influence Brain Endothelial Permeability after Juvenile TBI

David Olufemi Ajao

Follow this and additional works at: <http://scholarsrepository.llu.edu/etd>

 Part of the [Medical Neurobiology Commons](#), [Medical Physiology Commons](#), [Neurology Commons](#), and the [Physiology Commons](#)

Recommended Citation

Ajao, David Olufemi, "Caveolins and NJKs Influence Brain Endothelial Permeability after Juvenile TBI" (2013). *Loma Linda University Electronic Theses, Dissertations & Projects*. 217.
<http://scholarsrepository.llu.edu/etd/217>

This Dissertation is brought to you for free and open access by TheScholarsRepository@LLU: Digital Archive of Research, Scholarship & Creative Works. It has been accepted for inclusion in Loma Linda University Electronic Theses, Dissertations & Projects by an authorized administrator of TheScholarsRepository@LLU: Digital Archive of Research, Scholarship & Creative Works. For more information, please contact scholarsrepository@llu.edu.

LOMA LINDA UNIVERSITY
School of Medicine
in conjunction with the
Faculty of Graduate Studies

Caveolins and JNKs Influence Brain Endothelial Permeability
after Juvenile TBI

by

David Olufemi Ajao

A Dissertation submitted in partial satisfaction of
the requirements for the degree of
Doctor of Philosophy in Physiology

December 2013

© 2013

David Olufemi Ajao
All Rights Reserved

Each person whose signature appears below certifies that this dissertation in his/her opinion is adequate, in scope and quality, as a dissertation for the degree of Doctor of Philosophy.

_____, Chairperson
William J. Pearce, Professor of Physiology and Basic Sciences

Jérôme Badaut, Assistant Professor of Pediatrics and Physiology

Lorenz Hirt, Associate Professor of Neuroscience, University of Lausanne

Andre Obenaus, Associate Professor of Pediatrics and Basic Sciences

John H. Zhang, Professor of Neurosurgery, Neurology, Anesthesiology, Physiology, Pathology and Human Anatomy

DEDICATION

I dedicate this dissertation to...

My parents, Moses and Deborah Ajao, for inspiring me early on toward higher education,
and for the selflessness they have displayed over the years,

and

My lovely wife, Omolade, for her constant motivation, forbearance, and constructive
criticism.

ACKNOWLEDGEMENTS

I would like to express my sincere gratitude to Dr. Jerome Badaut, my principal investigator (PI), for taking me under his tutelage and mentorship, and generously sponsoring a significant portion of my PhD training through his research funding. For the time, resources, energy, passion, and trust you have invested in me, and for the guidance and numerous counsels provided, I say a big thank you. To current long-standing members and former members of Dr. Badaut's lab, especially Dr. Viorela Pop, Dane Sorensen, and Andrew Fukuda, your expertise (which you generously shared), constructive criticism, friendship, and motivation have been of great assistance in completing this work. The memory of time spent together with you all in the lab will remain cherished.

In the same vein, I would like to thank Dr. John H. Zhang, whose lab provided some pre-doctoral volunteering experience, and Dr. Andre Obenaus, whose lab (the non-invasive imaging lab) provided initial training, especially in juvenile rodent surgery and MRI acquisition and analysis, early on in my PhD studies. Similarly, I appreciate the training provided by Dr. Ubaldo Soto in molecular genetics techniques when I rotated in his lab for one quarter in my first year. I also thank Dr. Richard E. Hartman who, alongside members of his behavioral neuroscience lab, provided training and support in behavioral testing, and made available an equipped lab space for carrying out several of these tests. Moreover, I appreciate the insights of William Rolland (from Dr. John Zhang's lab), Dr. Hartman and Dr. Obenaus which nourished the development of neurological test modalities for this project. I thank various collaborators of Dr. Badaut's lab who have provided insights and practical help in the course of my training.

I would also like to thank all my PhD committee members for their valuable advice and directive. To Dr. John H. Zhang, Dr. William Pearce, and Dr. Andre

Obenaus, I say thank you for your interesting and thought-provoking classes, and for research guidance. To Dr. Lorenz Hirt, a big thank you for the long trips you made, for the time and efforts you have invested, and the valuable insights you provided. And to Dr. Badaut, thank you for patiently reviewing the various preliminary drafts and working documents, and providing valuable feedback.

I would like to thank Loma Linda University (LLU) for offering me admission into the PhD program, for sponsoring the first 2 years of my training, and for the valiant efforts the faculty have put into teaching and mentoring over the years. I would be remiss not to acknowledge several individuals including fellow students, non-teaching staff, and administrators at the university, whose friendship, camaraderie, and patient advice have assisted me tremendously in navigating through this program and making the most of presenting opportunities. In addition, I thank the National Institute of Health (NIH) and the Department of Pediatrics at LLU for funds awarded to my PI which supported this project.

The roles my family members have played in supporting and cheering me on through the duration of this program cannot be overemphasized. To my best partner, friend, and loving wife, Omolade, your unconditional and practical support, forbearance, and motivation have been invaluable in completing this work. I thank you for believing in me. To my parents, siblings, and friends (who are too numerous to mention here), your love and support through this long endeavor is dearly treasured. You have bestowed not only early inspiration, but also the impetus that propels me to the finish line. Highly deserving of mention are two of my former professors at La Sierra University (Prof. Linda Caviness and Prof. Ivan Rouse) whose passion, creative teaching, and motivation spurred me on toward neuroscience research.

Lastly, I thank God for the grace to study a tiny aspect of a small but amazing portion of nature's intricate designs – the brain.

CONTENTS

Approval Page.....	iii
Dedication	iv
Acknowledgements	v
Contents.....	vii
List of Tables.....	xv
List of Figures.....	xvi
List of Abbreviations.....	xix
Abstract.....	xxi
Chapter	
1. Endothelial Tight Junctions, Caveolins, and c-Jun N-terminal Kinases in Context of Juvenile Traumatic Brain Injury.....	1
Traumatic Brain Injury (TBI): Prevalence and Long-Term Outcome	1
Traumatic Brain Injury: Mechanisms of Primary and Secondary Injuries	3
How the Juvenile Brain Differs from Adult Brain with and without TBI	3
Introduction to Blood-Brain Barrier (BBB).....	6
Structural and Molecular Constituents of Brain Endothelial Tight Junction	9
Claudins.....	9
Occludins	10
Junctional Adhesion Molecules (JAMs).....	11
Accessory Proteins – Zona Occludens (ZOs), Cingulin, and Integrins	12
Zona Occludens.....	12
Cingulin.....	13
Integrins.....	13
Changes in Brain Vascular Structure and Functions following Juvenile TBI	15
Changes in Brain Vascular Structure and Functions following Adult TBI.....	18
Search for Therapeutic Avenues for Controlling BBB Disruption and Edema in Juvenile TBI.....	26
Caveolae and Caveolins in Brain Pathologies.....	28

The c-Jun N-Terminal Kinases (JNKs): Expression and Inhibition following Brain Injuries.....	40
Research Aims	45
2A. Traumatic Brain Injury in Young Rats Leads to Progressive Behavioral Deficits Coincident with Altered Tissue Properties in Adulthood	51
Prologue to Chapter 2	51
Abstract	54
Key Words	54
Introduction.....	55
Methods.....	56
Animals	56
Juvenile Traumatic Brain Injury Model.....	57
Magnetic Resonance Imaging and Analysis.....	57
Behavioral Testing	59
Foot-fault.....	59
Beam Balance	59
Rotarod	60
Open Field	60
Zero Maze.....	60
Morris Water Maze (MWM).....	60
Tissue Processing and Immunohistochemistry	61
Electrophysiology.....	64
Statistical Analyses.....	65
Results.....	66
Behavioral Testing	66
MRI-Derived Lesion Volumes and Surface Area of Corpus Callosum.....	70
Immunohistochemical Changes following CCI	72
Corpus Callosum Compound Action Potentials (CAP) following CCI	79
Discussion	79
Conclusion.....	87
2B. Early Brain Injury Alters the Blood-Brain Barrier Phenotype in Parallel with β -Amyloid and Cognitive Changes in Adulthood.....	89
Prologue to Chapter 2	89
Abstract	92
Key Words	92
Introduction.....	93
Materials and Methods	95
Animals	95

Juvenile Traumatic Brain Injury Model.....	95
Water Maze Design and Testing	97
Brain Tissue Processing and Immunohistochemistry	97
Immunoglobulin G Extravasation Staining for Blood-Brain Barrier	97
Immunolabelling of Blood-Brain Barrier Proteins	98
Immunolabelling for A β	99
Quantification of Immunohistochemistry.....	99
Brain Tissue Processing for Western Blotting	101
Statistical Analyses.....	102
Results.....	103
Blood-Brain Barrier Phenotype	103
Widespread A β Accumulation	107
Changes in Strategy during Water Maze.....	112
Discussion	112
Physiopathological Changes in the Blood-Brain Barrier	113
A β Accumulation and Blood-Brain Barrier Changes after Juvenile TBI	117
Parallel Changes in Vascular Phenotype and Behavioral Dysfunction.....	118
Concluding Remarks	119
3. Long-Term Increase of Caveolins in the Endothelium and in Astrocytes after Juvenile Traumatic Brain Injury	122
Prologue to Chapter 3	122
Key Words	124
Abstract	125
Introduction.....	126
Materials and Methods	129
Animals.....	129
Juvenile Traumatic Brain Injury Model.....	129
Tissue Processing and Immunohistochemistry	130
IgG Extravasation Staining for BBB Assessment	130
Double Immunohistochemical Staining.....	130
Western Blotting	132
Statistical Analyses.....	133
Results.....	133
Blood-Brain Barrier Disruption in Early Time Points after jTBI	133
Changes in Vascular Expression of Caveolin-1 and -2 after jTBI.....	134
Caveolin-1 Expression and Distribution after jTBI	134

Acute Change in Vascular Caveolin-2 after jTBI	141
Changes in Astrocytic Caveolin-3 Expression after jTBI	141
Discussion	143
Acute Increase in Endothelial Caveolins-1 and -2 Precedes BBB Recovery.....	143
Long-Term Caveolin-1 Overexpression may be Detrimental.....	146
Caveolin-1 and -3 in Astrocytes: Role in Astrogliosis?	147
Conclusion.....	148
Acknowledgements and Authors' Contributions	148
4. Cavtratin Ameliorates Edema and Reduces Brain Lesion Volume at Acute Time Points after Juvenile Traumatic Brain Injury	150
Prologue to Chapter 4	150
Abstract	154
Introduction.....	155
Materials and Methods	157
Subjects.....	157
Juvenile Traumatic Brain Injury Procedure.....	158
Systemic Administration of Cavtratin	158
Magnetic Resonance Imaging (MRI): Acquisition and Analyses	159
Image Acquisition	159
Lesion Volume Analysis.....	159
T2 Analysis	160
Neurological Tests	160
Foot-fault.....	161
Beam Balance	161
Rotarod	161
Statistical Analyses.....	162
Results.....	162
Cavtratin Reduces Lesion Volume and Ameliorates Some Morphological Alterations	162
Cavtratin Reduces Edema in the Lesion Region Following Brain Injury.....	165
Cavtratin Does Not Improve Sensorimotor Functions at Acute Time Point.....	168
Discussion	168

Reduction of Lesion Volume and Amelioration of Morphological Alterations by Cavtratin.....	170
Reduction of Acute Edema Formation at Lesioned Brain Region by Cavtratin.....	171
Absence of Concrete Improvement in Neurological Function.....	172
A Potential Mechanism of Action for Cavtratin – Blood-Brain Barrier Protection.....	173
Conclusion.....	174
5. Acute Administration of DJNKI-1 following Juvenile TBI in Rats Improves Neuroimaging, Histological and Functional Outcomes.....	175
Prologue to Chapter 5	175
Abstract	179
Introduction.....	180
Materials and Methods	186
Subjects.....	186
Juvenile Traumatic Brain Injury Procedure.....	186
DJNKI-1 Treatment.....	187
Magnetic Resonance Imaging (MRI): Acquisition and Analyses	188
Image Acquisition	188
Lesion Volume Analysis.....	189
T2 Analysis	190
Apparent Diffusion Coefficient (ADC) Analysis.....	190
Area Measurements of Corpus Callosum Thickness.....	190
Neurological and Behavioral Tests.....	191
Foot-fault.....	191
Beam Balance	191
Rotarod	192
Open-field	192
Zero Maze.....	192
Morris Water Maze (MWM).....	192
Tissue Processing and Immunohistochemistry	193
Extravasated Serum Immunoglobulin G (IgG) Staining and Analysis	193
Statistical Analyses.....	194
Results.....	194
DJNKI-1 Reduces Lesion Volume and Ameliorates Morphological Alterations.....	194
DJNKI-1 Reduces Edema and Improves Water Diffusion after Juvenile TBI	203

DJNKI-1 Improves Neurological Functions at Acute Time Points and Cognitive Functions at Chronic Time Points.....	205
DJNKI-1 Protects Blood-Brain Barrier Integrity Acutely after Brain Injury.....	210
Discussion	212
DJNKI-1 and Improvement of Neurological and Cognitive Functions	213
DJNKI-1, Reduction of Lesion Volume and Amelioration of Morphological Alterations	219
DJNKI-1, Blood-Brain Barrier, and Edema Formation	221
Conclusion.....	224
6. General Conclusions and Future Directions.....	226
Model Development for Juvenile TBI.....	226
Histological and Functional Effects of Juvenile TBI in Rodents.....	227
JNK Activation as a Therapeutic Target for Juvenile TBI	229
Caveolins in Brain Homeostasis and in Recovery and Repair after Juvenile TBI.....	232
References	235

TABLES

Tables	Page
Chapter 1	
1. Caveolae-Localized and Caveolin-Interacting Molecules Implicated in Mediating Endothelial Permeability	33
Chapter 2B	
1. Description of MWM swim strategies observed after jTBI	88
Chapter 5	
1. Morphological Observations of Tissue Alterations.....	177

FIGURES

Figures	Page
Chapter 1	
1. Organization and Interactions of Tight Junction and Accessory Proteins in the BBB	13
2. Caveolin Involvement in Endothelial Permeability.....	32
3. JNK Pathway and Proposed Mode of Action of D-JNKI-1 in Juvenile TBI	43
4. Schematic of Proposed Mechanism.....	47
Chapter 2A	
1. Sensorimotor Function Tests.....	62
2. Open Field, Zero Maze and Morris Water Maze Tests.....	64
3. Magnetic Resonance Imaging and Lesion Quantification	66
4. Neuronal Nuclei (NeuN) Immunohistochemistry at 60 Days	68
5. Corpus Callosum Area Measurement and NF200 Immunostaining	70
6. Myelin Basic Protein (MBP) Immunolabeling	72
7. CNPase Immunolabeling along White Matter Tracts at 60 Days	74
8. Electrophysiology in the Corpus Callosum at 60 Days.....	75
Chapter 2B	
1. Changes in Endothelial Tight Junctions 2 Months after jTBI	95
2. Juvenile TBI Changes Proteins Involved in Cellular Trafficking at the BBB	96
3. Immunoreactivity Patterns with a Rodent-A β Antibody	98
4. Anterior to Posterior Patterns of Rodent-A β Distribution.....	100

5. Differences in Water Maze Strategies in Adulthood	102
6. Summary of Parallel Changes in Adulthood after Early Brain Injury	108
Chapter 3	
1. BBB disruption after jTBI	121
2. Caveolin-1 Distribution in Brain Cell Types after jTBI.....	122
3. Increased Caveolin-1 Expression after jTBI	124
4. Caveolin-2 Expression is not Changed after jTBI.....	126
5. Caveolin-3 Expression and Distribution after jTBI.	128
Chapter 4	
A. Proposed Intervention Strategy in Experimental Juvenile TBI.....	137
1. Acute Cavtratin Treatment Reduces Lesion Volume after jTBI	147
2. Acute Cavtratin Treatment Reduces Lesion T2.....	149
3. Neurological Test (Foot-faults, Beam Balance and Rotarod) Outcome following Cavtratin Treatment.....	150
Chapter 5	
1. Proposed Intervention Strategy in Experimental Juvenile TBI.....	159
2. Pathway of JNK Activation in a Generalized Brain Cell and Theorized Mechanism of Action of D-JNKI-1	166
3. Experimental Timeline, and Images and Quantification of Lesion Volume.....	176
4. Changes in Hemispheric Volumes and Brain Morphology	179
5. Corpus Callosum (CC) Area Increases with DJNKI-1 Treatment.....	181
6. Changes in T2 and Apparent Diffusion Coefficient (ADC) with DJNKI Treatment	182
7. DJNKI Treatment Changes Neurological Outcomes	186

8. DJNKI Treatment Effects Behavioral Changes in Open Field and Zero Maze Tests	188
9. DJNKI Treatment Improves Behavioral Outcomes in Morris Water Maze (MWM) Tests	189
10. IgG Extravasation Decreases with DJNKI-1 Treatment.....	191
Chapter 6	
1. Proposed Intervention Strategies in Experimental Juvenile TBI	211

ABBREVIATIONS

TBI	Traumatic Brain Injury
jTBI	Juvenile Traumatic Brain Injury
CCI	Controlled Cortical Impact
CC	Corpus Callosum
E(n)	Embryonic Day (n), where 'n' is a number
P(n)	Post-natal Day (n), where 'n' is a number
dpi	Days Post-Injury
MRI	Magnetic Resonance Imaging
T2WI	T2-Weighted Imaging
DWI	Diffusion-Weighted Imaging
ADC	Apparent Diffusion Coefficient
ROI	Region of Interest
CAP	Compound Action Potentials
NeuN	Neuronal Nuclei
MBP	Myelin Basic Protein
NF200	Neurofilament-200
CNPase	2',3'-Cyclic Nucleotide 3'-Phosphodiesterase
GFAP	Glial Fibrillary Acidic Protein
IBA1	Ionized Calcium Binding Adaptor Molecule 1
CNS	Central Nervous System
Cav-1	Caveolin-1
Cav-2	Caveolin-2
Cav-3	Caveolin-3
IR	Infrared
BBB	Blood-Brain Barrier

TJ	Tight Junction
CBF	Cerebral Blood Flow
ICP	Intracranial Pressure
DCS	Diffuse Cerebral Swelling
DAI	Diffuse Axonal Injury
NO	Nitric Oxide
eNOS	Endothelial Nitric Oxide Synthase
nNOS	Neuronal Nitric Oxide Synthase
CSD	Caveolin Scaffolding Domain
CBM	Caveolin-Binding Motif
IgG	Immunoglobulin G
JNK	c-Jun N-terminal kinase
JIP-1	JNK-interacting peptide-1
MLK	Mixed-Lineage Kinases
MAPKs	Mitogen-Activated Protein Kinases
MKK	Mitogen-Activated Protein Kinase Kinase
MMPs	Matrix Metalloproteinases
GLT1	Glutamate Transporter 1
TGF- α	Transforming Growth Factor-alpha
VEGF	Vascular Endothelial Growth Factor
BMECs	Brain Microvascular Endothelial Cells
MCAO	Middle Cerebral Artery Occlusion
SAH	Subarachnoid Hemorrhage
MS	Multiple Sclerosis
IP/i.p	Intraperitoneal
ROS	Reactive Oxygen Species
MWM	Morris Water Maze

SAL

Saline

ANOVA

Analysis of Variance

rm ANOVA

Repeated Measures ANOVA

ABSTRACT OF THE DISSERTATION

Caveolins and JNKs Influence Brain Endothelial Permeability after Juvenile TBI

By

David Olufemi Ajao

Doctor of Philosophy, Graduate Program in Physiology
Loma Linda University, December 2013
Dr. Jérôme Badaut, Chairperson

Disruption of blood-brain barrier (BBB) is a key secondary event that exacerbates brain damage following traumatic brain injury (TBI). BBB disruption is particularly damaging to the developing brain – which is highly vulnerable to various stress stimuli, resulting in increased brain swelling, disrupted cerebral blood flow (CBF) autoregulation, long-term disabilities and death following TBI in young demographic. Unsurprisingly, BBB disruption and the resultant cerebral edema have emerged as therapeutic targets in juvenile TBI. It is therefore important to understand the molecular players and mechanisms involved in TBI-induced BBB disruption in the juvenile brain. To this end, the endothelial caveolins and c-Jun N-terminal kinases (JNKs) were identified as proteins of interest in the regulation of brain endothelial permeability after injury. These were investigated under a three-fold aim. The first was to characterize the acute and long-term histological and functional changes occurring following injury to the developing brain. Second was the attempt to profile the changes in expression patterns of caveolins after juvenile TBI in conjunction with BBB disruption. And lastly, the effects of molecular agents that target JNK (DJNKI-1) and caveolin (cavtratin) pathways respectively were examined on BBB integrity, and on imaging, histological and functional outcomes.

To achieve these aims, an experimental model of TBI in juvenile rats was developed and characterized. Evidence emerged that long-term white matter dysfunction occurs in this model, in parallel with delayed neurodevelopment and persistence of

behavioral deficits, which mimics data from clinical and longitudinal TBI observations. There was both acute and long-term increase in the expression level of caveolin-1 in the endothelium and reactive astrocytes following juvenile TBI. Furthermore, acute administration of cavtratin, a peptide mimetic of caveolin-1 scaffolding domain, markedly reduced edema formation and lesion volume without improving sensorimotor outcome in the acute time points. However, competitive inhibition of the JNK pathway with acute administration of DJNKI-1 markedly ameliorates BBB permeability, reduced edema formation, and improves neuroimaging and neurological outcomes at both acute and chronic time points. These findings could potentially be exploited for future therapeutic applications in juvenile brain trauma.

CHAPTER ONE

INTRODUCTION:

ENDOTHELIAL TIGHT JUNCTIONS, CAVEOLINS, AND C-JUN N- TERMINAL KINASES IN CONTEXT OF JUVENILE TRAUMATIC BRAIN INJURY

Traumatic Brain Injury (TBI): Prevalence and Long-Term Outcome

Traumatic brain injury (TBI) is 'caused by a bump, blow or jolt to the head or a penetrating head injury that disrupts the normal function of the brain' (Faul, 2010). Increasingly higher incidence rate of TBI and accompanying mortality and disability is seen in the United States (Coronado et al., 2011) and in other countries around the world (Tagliaferri et al., 2006, Kiening and Unterberg, 2007, Moppett, 2007), making it a global menace and potential pandemic. According to Center for Disease Control (CDC) reports, an annual average of 53,014 deaths was associated with TBI in the US alone between 1997 and 2007 (about 18 deaths per 100,000 population) (Coronado et al., 2011). The leading causes of TBI-related deaths during this period are: firearm-related incidents, motor vehicle accidents, and falls (Coronado et al., 2011).

TBI is an increasingly troubling public health concern among childhood/pediatric populations (Schneier et al., 2006, Kochanek et al., 2010), with childhood and pediatric being defined as the developmental period between birth and adolescence (Faul, 2010). In trauma centers in the United States, head injury represents 75 – 97% of all pediatric trauma deaths (Yeates et al., 2002, Schneier et al., 2006). In comparison to other age groups, the pediatric populations have higher proportion of annual TBI-related

emergencies (close to half a million) (Faul, 2010, Dawodu, 2011), and experience longer hospital stays, increased mortality, and protracted neurological and cognitive deficits (Schwartz et al., 2003, Keenan and Bratton, 2006, Coronado et al., 2011), all associated with enormous economic burden (Schneier et al., 2006). These statistics underscore the higher risk of TBI facing the pediatric populations.

Another important point to note is that TBI incidence rate is higher for males than females at every age (Faul, 2010). For example, there is a disproportionate male-to-female TBI incidence ratio of 4:1 in US pediatric populations. Previous investigators have highlighted factors thought to be responsible for this male-to-female disparity, including higher activity levels and increased participation in risky sports by males (Centers for Disease and Prevention, 1997). It has been estimated that nearly 300,000 sports-related TBIs occur in the United States per annum (Sosin et al., 1996, Centers for Disease and Prevention, 1997).

Long-term problems associated with moderate to severe TBI include sensorimotor (postural instability, dyspraxia, pain in the face and extremities, etc.) (Davis and Dean, 2010), neuropsychiatric (e.g. anxiety disorder, depression, etc.) (Brown et al., 1981, Yeates et al., 2002, Schwartz et al., 2003, Nicholl and LaFrance, 2009), and cognitive deficits (e.g. poor attention and executive function deficit; thought and impulse disorder) (Chadwick et al., 1981, Max et al., 2000). These dysfunctions have been shown to last for decades post-TBI (Thomsen, 1984, 1992, Morton and Wehman, 1995, Sbordone et al., 1995, Hoofien et al., 2001). These TBI-associated long-term problems originate from various pathophysiological processes and mechanisms set in motion post-TBI. This is the focus of next sub-section below.

Traumatic Brain Injury: Mechanisms of Primary and Secondary Injuries

TBI processes are generally classified into either primary or secondary injury mechanism. Primary injury consists of the initial insult(s) to the cranium and brain tissue, and may manifest as either focal (e.g. skull fractures, intracranial hematomas, lacerations, contusions, penetrating wounds) or diffuse injuries (e.g. diffuse axonal injury, acceleration and deceleration injury) (Gennarelli, 1993, Dawodu, 2011). Strict adherence to preventative measures such as wearing of helmet (during cycling, sports events or dangerous industrial work) and using seatbelts or child-restraint (in automobiles) may reduce the damage caused by primary injury (Dawodu, 2011).

Secondary injury, however, consists of a complex array of cellular processes and pathophysiological events which are delayed consequences of the initial insult, and may continue for a long time (Park et al., 2008, Dawodu, 2011). Secondary injuries may include: impaired cerebral blood flow and hemodynamics, ischemia, hypoxia, excitotoxicity, impaired metabolism, increased free radical formation, disruption of blood-brain barrier, and edema. Unlike primary injury, the gradual onsets of the secondary injury mechanisms make them theoretically amenable to treatment (Park et al., 2008). Research efforts are therefore geared towards utilizing this window of opportunity through development of therapies (e.g. pharmacological agents aimed at reducing blood-brain barrier damage and curtailing brain edema) that could potentially minimize secondary injury damage and facilitate functional recovery (Donkin and Vink, 2010, Shlosberg et al., 2010).

How the Juvenile Brain Differs from Adult Brain with and without TBI

For the rest of this dissertation, the term 'juvenile TBI' is used to indicate TBI occurring in the pediatric/childhood period. Mounting evidence is showing that juvenile

brain is uniquely different from adult brain both in terms of natural physical and physiological status and also in terms of response to TBI (Giza and Prins, 2006, Giza et al., 2007, Ibrahim et al., 2012, Maxwell, 2012). First, there are differences in the physical attributes of juvenile heads, skulls, and brains versus those of adults. The pediatric skull is thinner, flexible, and more pliable than adult skull (Giza, 2006). There is, for instance, an open fontanelle in infants which is thought to make them more susceptible to subdural hematoma following TBI (Khilnani, 2004, Giza, 2006). This flexibility affects the forces being transmitted to the brain tissue following trauma and the handling of increased intracranial pressure (ICP) (Giza, 2006). Other pediatric anatomical features such as disproportionately large head-to-body ratio, weaker neck muscles, and large subarachnoid space in which the brain can move more freely compared to adults further predispose the pediatric population to TBI (Zuckerman and Conway, 1997, Giza, 2006), and especially increases the rate of occurrence of diffuse axonal injury (DAI) (Gleckman et al., 1999).

Developmental processes in the pediatric brain are unique and different from those of adult brain (Giza et al., 2007, Maxwell, 2012). Maturation of brain cells and structures, and changes of synaptic density and integrated brain functions all continue well into adulthood (Giza et al., 2007, Groeschel et al., 2010). For instance, myelination of axons in some brain regions continues progressively post-partum and lasts into the third decade of life (Ballesteros et al., 1993, Luna et al., 2004, Blakemore and Choudhury, 2006, Maxwell, 2012). The unmyelinated fibers in immature brains are preferentially vulnerable to structural and functional damage after TBI (Reeves et al., 2012), resulting in cognitive and behavioral alterations (Jonsson et al., 2013). TBI-associated injury to unmyelinated axons is thought to affect emerging skills more vigorously than established skills possibly due to disruption of developing neural networks mediating the skills (Lehnung et al., 2001, Jonsson et al., 2013).

Young age is considered a risk factor for complications resulting from secondary injuries such as disruption of neural and sensory-motor pathways (Kriel et al., 1989, Anderson et al., 2005, Anderson et al., 2012, Crowe et al., 2012). In the developing brain, brain water content is higher than in adult brain (Counsell and Rutherford, 2002), resulting in reduced brain compliance and making the brain more susceptible to diffuse swelling (Aldrich et al., 1992, Giza, 2006, Lenroot and Giedd, 2006). The developing brain is associated with higher cerebral blood flow (CBF) which may be related to lower cerebrovascular resistance, and post-traumatic hyperemia and diffuse cerebral swelling which are more common in children (Suzuki, 1990, Zwienenberg and Muizelaar, 1999, Giza, 2006, Udomphorn et al., 2008).

Approximately 50% of children who suffer severe TBI will develop diffuse cerebral swelling (DCS) which has been defined as “compressed or obliterated mesencephalic cisterns, cerebrospinal fluid (CSF) spaces, and/or small to normal size ventricles in the absence of other intracranial pathology” (Aldrich et al., 1992, Adelson, 2009). Although DCS is noted as the most common cause of brain death in both pediatric and adult TBI (Becker et al., 1977, Marshall et al., 1979), it is however about 3.5 times more common in children than adults (Zimmerman et al., 1978, Aldrich et al., 1992, Adelson, 2009). Moreover, childhood victims of TBI who present with DCS have been estimated to have three-fold higher mortality than those without it (Aldrich et al., 1992, Bauer et al., 1999). About 50% of all children who present DCS following jTBI suffer mortality within 6 days (Aldrich et al., 1992), while those that surviving bear long-lasting neurological deficits (Yeates et al., 2002, Schwartz et al., 2003). Neuropathologic changes associated with DCS include: obliterated CSF spaces, vascular congestion, edema (both cytotoxic and vasogenic), varying degrees of herniation, and cell death (Adelson, 2009). Furthermore, DCS in jTBI has been linked to the endangerment of BBB

by oxidative stress due to diminished antioxidant capacity in the juvenile brain compared to adult brain (Bauer et al., 1999, Fan et al., 2003).

Experimental evidence has been provided in support of age-dependent differences in cerebral and systemic hemodynamic responses following brain injury (Armstead, 1999). Younger age is found to be associated with increased impairment of cerebral autoregulation (triggering hypo- or hyperperfusion) and poorer outcomes following moderate to severe TBI (Vavilala et al., 2004, Freeman et al., 2008). Neonates and infants have a limited range of brain autoregulation compared to adults (Armstead, 2005), which predisposes them to cerebrovascular dysfunction following jTBI.

The unique vulnerabilities of juvenile brains to TBI highlighted above have triggered a rethink among scientists on the extent to which 'brain plasticity' (defined as brain's ability to repair itself) during development could make up for the damage done, and foster structural brain repair and functional recovery following jTBI (Anderson et al., 2005, Anderson et al., 2012). An emerging opinion is that brain plasticity is insufficient to make up for the vulnerabilities of the juvenile brain by canceling out the deleterious structural and functional effects of jTBI (Anderson et al., 2005, Giza, 2006). The damage done to the developing brain by jTBI often results in decades-long or life-long complications and deficits of sensory-motor, cognitive, and neuropsychiatric nature (Max et al., 2000, Hoofien et al., 2001, Yeates et al., 2002, Davis and Dean, 2010), and these highlight the need for further research into how to facilitate better outcomes (Anderson et al., 2005, Giza et al., 2007).

Introduction to Blood-Brain Barrier (BBB)

The BBB is a dynamic interface comprising of various cell types and molecules that work in concert to physically and chemically separate the brain parenchyma from the systemic circulation and its cargo (Hawkins and Davis, 2005). It comprises of a

physical and chemical barrier to diffusion of peripheral blood content into the brain, as well as a transport barrier, and a metabolic barrier (Ballabh et al., 2004, Abbott et al., 2006). Three cellular elements form the foundation of the BBB: the capillary endothelial cells, the astrocytic endfeet, and the pericytes (Ballabh et al., 2004). The tight junctions (TJs) between adjacent capillary endothelial cells form the major 'physical barrier' to paracellular transport (Abbott et al., 2006). The molecular constituents of TJs are discussed elaborately in section 2.2 below. The presence of specific transporters and transport systems on the luminal (e.g. breast cancer resistance protein [BCRP]) and abluminal (e.g. lipoprotein receptor-related protein 1 [LRP1]) surfaces of the capillary endothelium ensures selective transcellular transport of compounds in either direction between peripheral blood and brain (Zlokovic, 2008). The selectiveness of these transport systems gives the brain a much less degree of transcytosis and endocytosis than peripheral endothelium, and forms the basis of the 'transport barrier' function of the BBB (Abbott et al., 2006). The 'metabolic barrier' function of the BBB is spearheaded by intracellular and extracellular enzymes (e.g. peptidases and nucleotidases which can metabolize unwanted peptides and ATP, and cytochrome P450 which can inactivate various neuroactive and toxic compounds) (el-Bacha and Minn, 1999, Abbott et al., 2006) marshaled against unwanted substrates. The perivascular endfeet of astrocytes ensheathes more than 99% of the cerebrovascular surface (Iadecola and Nedergaard, 2007). It provides a communication route between brain endothelium and neurons, thereby facilitating the coupling of vascular and neuronal activities in several of the brain's blood vessels (Iadecola and Nedergaard, 2007, Dunn et al., 2013). Pericytes enclosed within endothelial basal lamina perform maintenance, regulatory and repair roles crucial to the integrity of the BBB (Winkler et al., 2011).

Contrary to the belief in previous decades that the BBB of neonates and infants is structurally and/or functionally immature (Barcroft, 1938, Saunders et al., 1999),

growing evidence suggests that tight junctions of the human BBB is fully formed at birth (Abbott et al., 2010, Saunders et al., 2012), although there is progressively increase in the expression of some efflux transporters (e.g. p-glycoprotein) during development (Ek et al., 2010, Ek et al., 2012, Saunders et al., 2012). By the 14th week of gestation, the key TJ proteins – claudin-5 and occludin – are detectable in the fetal capillary endothelium and show the same distribution pattern as seen in adult brain (Virgintino et al., 2004). Furthermore, pioneering studies in the 1950s showed that there is a post-mortem BBB to trypan blue in stillborn human fetuses by the 12th week of gestation (Grontoft, 1954). Observations in rodents corroborate these findings. In experimental mice, BBB begins to form between E11 and E17 with identifiable TJs and restriction of transendothelial movement of polar solutes (Abbott et al., 2010). The high transendothelial electrical resistance (TEER) characteristic of adult BBB is exhibited by E21 using *in situ* measurements of TEER in cerebral blood vessels of anaesthetized rats (Butt et al., 1990, Butt, 1995). Recent experimental data from stroke even suggests that the neonates' BBB may be less permeable compared to adults following induction of ischemic event (Fernandez-Lopez et al., 2012). In spite of the presence of intact BBB at birth however, the developing cerebral vessels are still believed to be more fragile than adult vessels, which could render the brain more susceptible not only to drugs and toxins, but also to neuropathologic conditions underlying cerebral damage and neurological disorders (Saunders et al., 2012). The after-birth loss of placental efflux transporters (Ek et al., 2010, Ek et al., 2012, Saunders et al., 2012) and the vulnerability of blood vessels in the white matter to systemic inflammatory insults at this critical stage of development (Stolp et al., 2005a, Stolp et al., 2005b, Stolp and Dziegielewska, 2009) are possible contributors to this vulnerability.

TJ proteins are crucial to the BBB and play a significant role in the evolution of secondary brain injuries (Castejon, 2012, Thal et al., 2012). As such, limiting and

reversing TJ damage following TBI have become important therapeutic avenues for halting the progression of some secondary injury mechanisms (Ballabh et al., 2004, Hawkins and Davis, 2005, Shlosberg et al., 2010). A brief review of the structural and molecular constituents of brain endothelial TJs under physiological condition follow.

Structural and Molecular Constituents of Brain Endothelial Tight Junction

Endothelial TJ forms a major physical and structural barrier that impedes the movement of substances from the periphery into brain parenchyma between adjacent endothelial cells – paracellular permeability (Reese and Karnovsky, 1967, Brightman et al., 1970, Ballabh et al., 2004). It consists of three main integral membrane protein families (occludins, claudins and junctional adhesion molecules [JAMs]) and several cytoplasmic accessory proteins (including zonula occludens [ZO-1, ZO-2, and ZO-3], cingulin, etc.) (Vorbodt and Dobrogowska, 2004, Liebner et al., 2011). In addition to tight junctions, adherens junctions – which comprise of cadherin-catenin complexes and their associated proteins – further strengthen the mechanical attachments between adjacent endothelial cells and contribute to the regulation of TJ proteins (Schulze and Firth, 1993, Wolburg and Lippoldt, 2002, Taddei et al., 2008, Komarova and Malik, 2010). The main TJ proteins as well as key accessory proteins are described below.

Claudins

The first proteins in the claudin family (claudins-1 and 2) were reported in 1998 (Furuse et al., 1998a, Furuse et al., 1998b). The list soon grew to include up to 24 more claudin proteins (Morita et al., 1999, Furuse et al., 2002). Particularly abundant in brain endothelial TJs are claudins-5 and -12 (Ohtsuki et al., 2008, Guerra, 2011). Unlike occludins, there is a strong consensus that claudins are the indispensable protein

molecules responsible for establishing the physical and structural barrier properties of TJs (Furuse et al., 1999, Morita et al., 1999, Wolburg and Lippoldt, 2002, Liebner et al., 2011). The ~22 kDa claudin proteins show the same structural pattern – four membrane-spanning regions, two extracellular loops and two cytoplasmic domains, a short N-terminus and a long C-terminal sequence (Heiskala et al., 2001). There is no homology between the claudin and occludin protein families, although they are structurally similar (Liebner et al., 2011). Functional investigations showed that transfection of one or more claudin genes into cells that naturally do not possess TJs leads to the formation of TJ morphology with reduced paracellular flux (Amasheh et al., 2005, Ohtsuki et al., 2007). The TJ phenotype is maintained through homophilic and heterophilic interactions between the extracellular loops of claudins (Morita et al., 2003). Furthermore, the carboxyl terminals of claudins are known to bind with cytoplasmic zona occludens to ensure structural integrity of the TJs (Ballabh et al., 2004). Claudins are hence fundamental to both the formation and maintenance of brain endothelial TJs (See **Fig. 1**).

Occludins

Furuse and colleagues (1993) were the first to describe the 65-kD occludins in 1993 as being localized to the TJs of epithelial and endothelial cells. Occludins are made up of two extracellular loops, four transmembrane domains, and C- and N-terminal cytoplasmic domains (Feldman et al., 2005) (See **Fig. 1**). Experiments have revealed that the morphology and functional capacity of TJs are not compromised in occludin-deficient mice (Saitou et al., 2000), although these mice developed some undesirable conditions including chronic inflammation and hyperplasia of gastric epithelium, and calcifications in the brain parenchyma and blood vessels. (Saitou et al., 2000, Wolburg and Lippoldt, 2002). These observations suggest that occludins are not primarily

required for TJ formation at the onset (Saitou et al., 2000). However, phosphorylation of occludin is known to regulate TJ permeability in both G-protein-dependent and -independent manner in mature endothelial cells, independent of cytoskeletal changes (Hirase et al., 2001). Furthermore, the external loops, as well as the transmembrane and C-terminal cytoplasmic domains of occludin were found to be important in regulating paracellular permeability, while the N-terminus was determined to be essential for neutrophil migration during inflammation (Sakakibara et al., 1997, Lacaz-Vieira et al., 1999, Huber et al., 2000, Hirase et al., 2001). Moreover, occludin was demonstrated to be responsible for sealing of TJs (Lacaz-Vieira et al., 1999). These reports suggest that occludin is needed by mature endothelial cells for regulating rather than establishing their barrier properties (Wolburg and Lippoldt, 2002).

Junctional Adhesion Molecules (JAMs)

JAMs (JAM-A, JAM-B and JAM-C) contribute to the assembly of TJ structures (Bazzoni, 2003). They belong to the immunoglobulin superfamily and possess a single transmembrane domain with two immunoglobulin-like loops in their extracellular portion (Ballabh et al., 2004). JAMs codistribute with and help regulate homophilic and heterophilic interactions among TJ component molecules (Martin-Padura et al., 1998, Wolburg and Lippoldt, 2002). Homophilic interactions among JAMs linking adjacent endothelial cells help stabilize intercellular junctions and organize tight junctional structures (Bazzoni, 2003) (See **Fig. 1**). During pathological conditions however, heterophilic interactions between JAMs and leukocyte integrins help facilitate leukocyte transmigration (Wolburg and Lippoldt, 2002). JAMs contribute to the regulation of paracellular permeability. Knocking down JAM-A results in increased barrier permeability together with concomitant reduction in claudins in intestinal epithelial cell cultures (Severson and Parkos, 2009). In rat cold cortical injury, there was an acute decrease in

JAM-A which was concomitant with BBB breakdown (Yeung et al., 2008). Mechanisms through which JAMs regulate endothelial permeability include: control of endothelial actomyosin contractility, modulation of myosin light chain (MLC) phosphorylation, and interactions with TJ scaffolding proteins ZO-1, cingulin, etc. (Orlova et al., 2006, Stamatovic et al., 2008).

Accessory Proteins – Zona Occludens (ZOs), Cingulin, and Integrins

Zona Occludens (ZOs)

Zona Occludens were so named because early micrographs revealed them as a zone or band between adjacent epithelial cells whose membranes have joined together and formed a virtually impermeable barrier to fluid, and therefore, the ZOs 'occlude' the space between the adjacent plasma membranes (Brightman and Palay, 1963, Farquhar and Palade, 1963). ZO-1 (220 kDa), ZO-2 (160 kDa), and ZO-3 (130kDa) have major sequence similarities and belong to the membrane-associated guanylate kinase-like protein family (MAGUKs) (Wolburg and Lippoldt, 2002). They all have three PDZ domains (PDZ1, PDZ2, and PDZ3), one SH3 domain, and one guanyl kinase-like (GUK) domain (Wolburg and Lippoldt, 2002). These domains function as protein binding molecules to facilitate signal transductions and help anchor tight junction proteins to the cytoskeleton (Wolburg and Lippoldt, 2002, Ballabh et al., 2004) (**Fig. 1**). The PDZ1 domain of ZO-1, ZO-2, and ZO-3 has been reported to bind directly to the C-terminus of claudins (Itoh et al., 1999). Furthermore, occludin interacts with the GUK domain on ZO-1 (Mitic et al., 2000). Importantly, actin, the primary cytoskeleton protein, binds to C-terminal of ZO-1 and ZO-2, and this complex cross-links transmembrane elements and thereby provides structural support to the endothelial cells (Haskins et al., 1998, Ballabh et al., 2004).

Cingulin

Cingulin has been reported to be expressed in endothelial cells of the BBB, and the junction-associated coiled-coil protein (JACOP) in other endothelial and epithelial cells (Wolburg et al., 2009). Its structure and organization is conserved throughout the vertebrates. Cingulin is an important component of BBB in that it interacts with actin and myosin, ZO-1 and several other TJ proteins (Bazzoni et al., 2000). Cingulin binds to these tight junction-associated proteins through conserved domains on the targets and therefore help to stabilize tight junctional structures (Heiskala et al., 2001, Wolburg and Lippoldt, 2002, Hawkins and Davis, 2005).

Integrins

Integrins were first described in 1987 (Hynes, 1987). Functionally, they serve as receptors for cell adhesion to extracellular matrix (ECM) proteins, play crucial roles in cell-to-cell adhesions and cell motility, and maintain transmembrane connections to the cytoskeleton (Bazzoni et al., 2000, Juliano, 2002) (See **Fig. 1**). They are vital in the maintenance of signal transduction within and the structural stability of endothelial tight junction (Juliano, 2002). Integrins exist in various affinity states for their ligands, and these affinity states are regulated by calcium ions and R-Ras and Rap1 small GTPases (Juliano, 2002). Knock-out studies of some integrins isoforms resulted in hemorrhage, lack of platelet aggregation, impaired leukocyte recruitment, impaired inflammatory responses, vessel dilation, and cerebral hemorrhage (Chen and Sheppard, 2007, Wolburg et al., 2009). Endothelial integrins also play crucial roles during development in the establishment of proper connections between endothelial cells and astrocytes (gliovascular unit) under physiologic conditions, and are also crucial for angiogenesis (Wolburg et al., 2009).

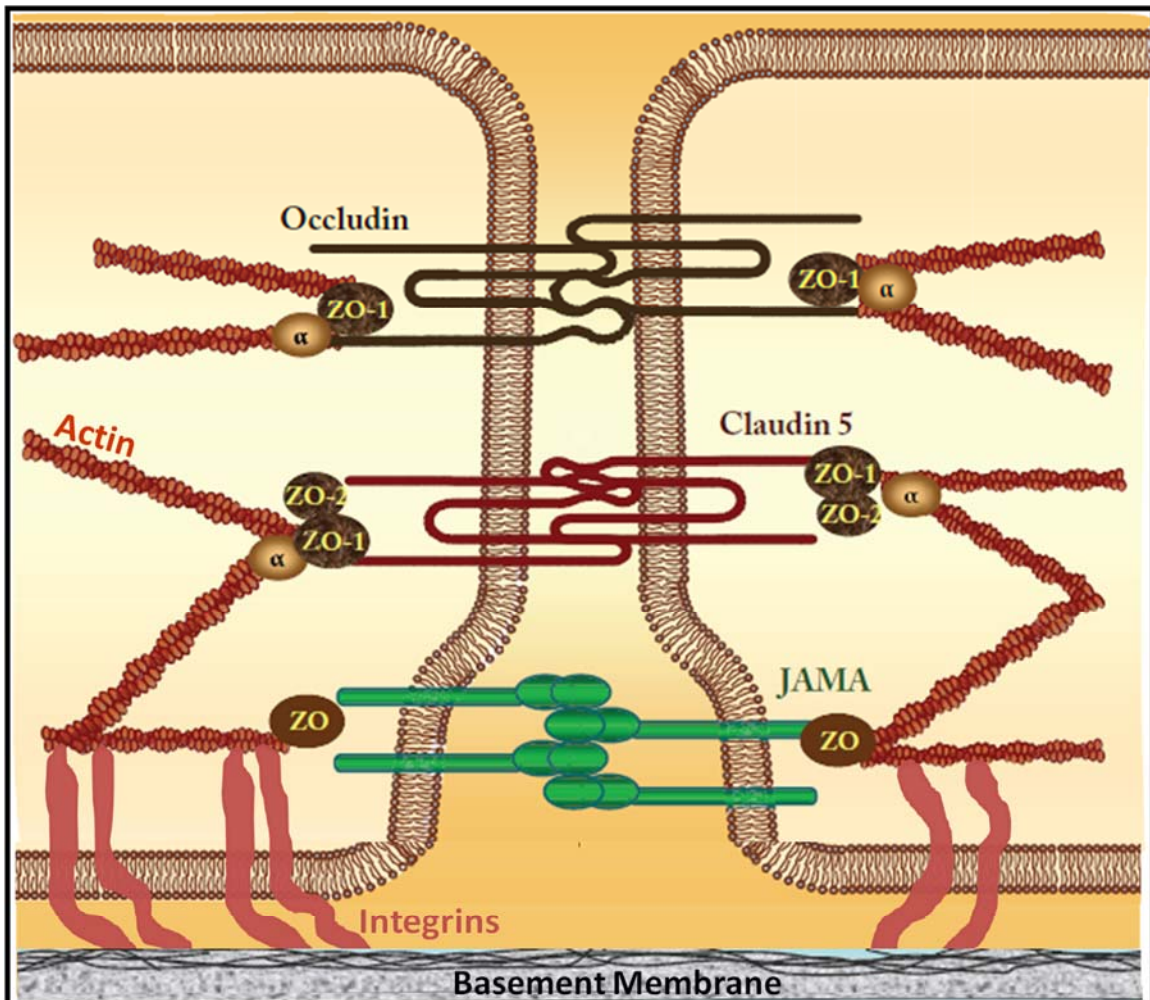


Fig. 1: Organization & Interactions of Tight Junction and Accessory Proteins in the BBB. Adapted from Yuan, S.Y. ; Rigor, R.R. (2010).

The intercellular junction proteins mainly responsible for TJ barrier function are claudin-5 and occludin. JAM-A also contributes to TJ structural stability. The intercellular binding of these TJ proteins is stabilized by connections to the actin cytoskeleton via zona occludens (ZO-1 & ZO-2) and α -catenin. The integrins serve as receptors for cell adhesion to extracellular matrix (ECM) proteins, play crucial roles in cell-to-cell adhesions and cell motility, and maintain transmembrane connections to the cytoskeleton. Additionally, the ZOs, integrins, α -catenin, and other accessory proteins such as cingulin (not shown) all facilitate intracellular and extracellular signal transduction aimed at regulating the tight junction.

Changes in Brain Vascular Structure and Functions following Juvenile TBI

There is paucity of clinical data on changes occurring specifically in the endothelial TJ protein structures and in the BBB in general following TBI in juvenile humans (Graham, 2001). A few postmortem studies have provided some insights into macrostructural changes in jTBI. Intracranial hemorrhages – including subdural (SDH), subarachnoid (SAH), extradural (EDH), and intracerebral (ICH) hemorrhages – are common in postmortem studies of the brains of childhood victims of TBI resulting from falls, with SDH being the most frequently seen (Chadwick et al., 1991, Kim et al., 2000, Agarwal et al., 2005). In addition, Adelson and colleagues reported low cerebral blood flow (CBF) (i.e. hypoperfusion) in the early period after severe TBI in young children which was associated with poor functional outcome measured with Glasgow Outcome Score (GOS) (Adelson et al., 1997, Adelson et al., 2011). Alterations in CBF in the juvenile TBI patients contribute to ischemia and disruption of the BBB (Verive et al., 2012).

Furthermore, as earlier noted in section 1.3 (par. 4), one of the pathologic features of diffuse cerebral swelling (DCS) seen as a clinical presentation of severe jTBI is vascular congestion (Adelson, 2009). Vascular congestion may be indicative of thrombosed cerebral blood vessels (Adams et al., 1982, Adelson et al., 1996) and portends occurrence of further cerebrovascular dysfunctions (Reithmeier et al., 2005). Vascular congestion is preceded and facilitated by cerebral autoregulatory dysfunction and hyperemia (Reithmeier et al., 2005). Clinical and experimental studies both highlight increased intracranial pressure (ICP) as another key consequence of cerebral autoregulatory dysfunction post-jTBI (Barie et al., 1993, Biagas et al., 1996) and cerebral edema (Vink and Van Den Heuvel, 2004).

Experimentally, cerebral autoregulatory dysfunction in the developing brain is linked to excessive activation of N-Methyl D-Aspartate (NMDA) receptor by glutamate (Armstead et al., 2011a), hyperactivation of mitogen activated protein kinase (MAPK) pathways including c-Jun N-terminal Kinase (JNK) (Armstead et al., 2011a), impairment to ATP- and calcium-sensitive potassium (K^+) channels on cerebral vessels (Armstead, 1997, Armstead et al., 2011b), and altered nitric oxide (NO) bioavailability (Verive et al., 2012) and vasodilatory function (Armstead, 2000). Other Endothelium-dependent systems (Verive et al., 2012) such as caveolae and their constituent caveolin proteins in lipid rafts (Prisby et al., 2006) also affect cerebral autoregulation in pediatric head trauma. Interestingly, caveolins, which are known to influence other factors of cerebral autoregulation such as endothelial nitric oxide synthase (eNOS) and nitric oxide (NO) (Bucci et al., 2000, Bernatchez et al., 2005), and possibly JNK (Tourkina et al., 2008), have not been well-researched in juvenile TBI.

Findings from microdialysis show that pro-inflammatory cytokines such as interleukin-1- β (IL-1 β) and tumor necrosis factor- α (TNF- α) are elevated in the CSF of children with moderate to severe TBI (Morganti-Kossmann et al., 1997, Buttram et al., 2007, Cederberg and Siesjo, 2010). These cytokines have been shown experimentally to induce BBB disruption following TBI via upregulation of hypoxia inducible factor- α (HIF-1 α) and vascular endothelial growth factor-A (VEGF-A) (Argaw et al., 2006). In a follow-up study, caveolin-1 and eNOS were shown to mediate the BBB disruption effects of VEGF-A, and the systemic administration of cavtratin – a selective eNOS inhibitor – abrogates this VEGF-A-induced BBB disruption and ameliorates neurologic deficits in a CNS inflammatory model in young adult mice (Argaw et al., 2012). There is also a possibility of developmental differences in cytokines sampled from cerebral microdialysis between juvenile and adult TBI patients (Friess et al., 2012), but more studies need to be designed and carried out to fully compare these two groups.

In experimental juvenile TBI in rodents, genes associated with neuroinflammation, cytokine activities and immune processes were found to be invariably upregulated acutely, while genes associated with development, neurotransmission, neuroplasticity, and, to some extent, metabolism were found to be mostly downregulated (Babikian et al., 2010). These suggest that juvenile brain is assaulted acutely by neuroinflammation following brain injury and it may be more vulnerable to neuroinflammatory insults compared to adult brain (Swaiman et al., 2012). Inflammatory response in the developing brain is more robust than in adult brain and is characterized by greater disruption of the BBB and elaboration of cytokines (Potts et al., 2006). Various studies have determined an increased vulnerability of the juvenile BBB to oxidative stress following jTBI, possibly due to much lower activities of antioxidant enzymes (such as glutathione peroxidase [GPx] and manganese superoxide dismutase [MnSOD]) in the juvenile brain compared to adult brain (Bauer et al., 1999, Bayir et al., 2002, Fan et al., 2003, Babikian et al., 2010).

Activated matrix metalloproteinases (MMPs) are known to cause degradation of vascular basal laminal matrix proteins (e.g. collagen, fibronectin, laminin) and breakdown of tight junction proteins (including claudins and occludins) following injury to adult brain (Morita-Fujimura et al., 2000, Asahi et al., 2001). MMP-2 was found to have increased expression and activity between 12 and 72 hours post-injury in an experimental model of jTBI to P7 rats (Sifringer et al., 2007). In contrast to the prominence of MMP-2 in juvenile TBI, MMP-9 was found to be more prominent in adult rodents with TBI (Wang et al., 2000, Asahi et al., 2001). Baseline activity of MMP-9 was also detectable in infant rodent brains unlike in adult brains (Sifringer et al., 2007). These suggest that the temporal expression and activity profiles for various MMPs may differ dependent on age, and these developmental differences should be considered in therapeutic efforts aimed at MMPs.

From the points reviewed in this section, it is clear that the juvenile brain has a number of vulnerabilities with regards to changes occurring in its cerebral vascular structure and functions following brain trauma. Key molecular targets that could be investigated for pharmacological manipulation aimed at arresting secondary brain damage arising from cerebrovascular dysfunctions also emerged. These include the endothelial caveolins and c-Jun N-terminal kinases.

Changes in Brain Vascular Structure and Functions following Adult TBI

Adult TBI patients (as well as experimental animals) share several similarities as well as differences from juvenile patients in terms of structural and functional changes in the brain vasculature following TBI. A wave of molecular changes that alter both structure and function of brain vasculature is unleashed by the initial TBI impact in the adult brain (Shlosberg et al., 2010, Chodobski et al., 2011). BBB disruption, which is characterized by breakdown of TJ proteins and increased permeability, is typically biphasic in nature according to experimental TBI data in adult rodents (Baldwin et al., 1996, Baskaya et al., 1997). This is also suggested in some clinical data in adult TBI patients (Tomkins et al., 2001, Tomkins et al., 2008). The delayed arm of BBB disruption has been linked with transcriptional changes in the neurovascular unit which precipitates delayed neuronal dysfunction, cell death, and degeneration (Shlosberg et al., 2010). Apoptosis of some endothelial cells following TBI also promotes increased BBB permeability and eventual neuronal loss (Nag et al., 2005). These events have been proposed to influence long-term TBI complications such as cognitive and psychological impairments (Zlokovic, 2008, Shlosberg et al., 2010).

Endothelial structures that form the physical and mechanical barriers to paracellular diffusion or permeability undergo active breakdown in adult TBI (Zhao et al.,

2007, Khan et al., 2009, Chodobski et al., 2011). The levels of expression of claudin-5 and occludin decrease at acute time points following TBI (Zhao et al., 2007). Experimental evidence further suggest that transcellular permeability may also be enhanced following adult brain trauma (Preston et al., 2001), possibly through increased number and activity of caveolae (the caveolins-based, cave-like structures in the endothelial lipid rafts) (Nag et al., 2007, Nag et al., 2009) which facilitate transcytosis – the vesicle-mediated transfer of substances across the cell through binding of ligands to membrane receptors or surface charges, followed by internalization – among other functions (Abbott et al., 2006, Komarova and Malik, 2010). Ultrastructural morphology consistent with increased pinocytotic activity (such as swollen endothelial cells, clearer cytoplasm, increased vacuolization, and increase in number of pinocytotic vesicles) was reported in brain microvessels of adult TBI patients (Vaz et al., 1997). There have been calls (Minshall et al., 2003, Yuan and Rigor, 2010) for more studies to further investigate the role of caveolae and caveolins in the regulation of endothelial barrier permeability in both pediatric and adult TBI.

Compromise of BBB permeability following TBI in the adult brain results in many secondary phenomena which include multi-focal, intraparenchymal hemorrhages in both ipsilateral and contralateral brain regions (Chodobski et al., 2011). There is also a lower regional cerebral blood flow to the pericontusional area (Schroder et al., 1998, von Oettingen et al., 2002). BBB damage following TBI in adult brains results in leakage of blood-borne factors and proteins such as albumin (Shapira et al., 1993), immunoglobulin G [IgG] (Hooper et al., 2005), fibrinogen (Tyagi et al., 2008), thrombin (Xi et al., 2003), extravasation of red blood cells (RBCs) (Chodobski et al., 2011), and aggregation of platelets and leukocytes (Stein et al., 2002, Schwarzmaier et al., 2010).

Each of these leaked or released factors and cells further effect changes in brain vascular structure and function following adult TBI. Extravasated albumin has been

linked with neuroinflammatory processes such as increased calcium concentration and proliferation of microglial cells (Hooper et al., 2005, Chodobski et al., 2011), activation of MAPK pathways and synthesis of proinflammatory cytokines such as IL-1 β in microglia and astrocytes (Ralay Ranaivo and Wainwright, 2010), increase in microglial production of NO which is mediated by MAPK pathway (Hooper et al., 2009), and induction of MMPs (Ralay Ranaivo et al., 2012) which can further degrade the endothelial extracellular matrix. Invading leukocytes can also release degrading MMPs to the traumatized brain parenchyma (Borregaard et al., 2007, Chodobski et al., 2011).

Fibrinogen could induce further endothelial barrier permeability by signaling through the MAPK pathway (Tyagi et al., 2008). Fibrinogen causes rearrangement of microglial cytoskeleton, increases their size and phagocytic activity, thereby influencing post-traumatic neuroinflammation (Adams et al., 2007). Fibrinogen may also inhibit neurite outgrowth and promote post-traumatic astroglial scar formation (Schachtrup et al., 2007, Chodobski et al., 2011).

Although pretreatment with low dose of thrombin is neuroprotective *in vivo* (Chodobski et al., 2011), release of thrombin in high concentration post-TBI exacerbates BBB disruption and edema formation, and causes apoptosis of neurons and astrocytes (Xi et al., 2003). Thrombin stimulates microglial release of pro-inflammatory mediators by signaling through MAPK including c-Jun N-terminal kinases (JNKs) (Waetzig et al., 2005). Thrombin also augments oxidative stress by causing increase in microglial expression of inducible nitric oxide synthase (iNOS) and inducing release of NO (Ryu et al., 2000) which is a potent vasodilator and an inducer of endothelial hyperpermeability (Yuan and Rigor, 2010). It has also been demonstrated *in vitro* that thrombin directly induces contraction of brain endothelial cells which could result in increased paracellular permeability (Nagy et al., 1995).

Release of blood-borne factors and cells into brain parenchyma is a hallmark of what has been traditionally termed 'vasogenic edema' (Donkin and Vink, 2010). Edema in brain pathologies has for several decades been classified as either 'cytotoxic edema' – characterized by swelling of astrocytes and neurons due to failure of sodium-potassium pump and resultant retention of sodium and water while the BBB remains intact – or 'vasogenic edema' – characterized by BBB breakdown and flow of normally excluded intravascular proteins into the parenchyma (Klatzo, 1967, Unterberg et al., 2004, Donkin and Vink, 2010). Recently, however, the complexity of cerebral edema has necessitated the addition of variants of these two traditional categories. These variants include: ionic edema – which occurs when plasma osmolality falls below brain osmolality and results in net movement of water from vasculature into brain interstitial fluid, all in absence of gross BBB breakdown (Simard et al., 2007, Donkin and Vink, 2010); anoxic edema – which occurs within minutes of cessation of CBF to a brain region, depriving it of oxygen and glucose, and characterized by swelling of astrocytes and neurons (Badaut et al., 2011); and hydrostatic edema – which occurs when cerebral perfusion pressure increases to the level where autoregulatory mechanisms fails (Donkin and Vink, 2010). Debates in scientific literature over which classes of edema predominate following TBI has persisted for decades (Donkin and Vink, 2010). The complexity and heterogeneity of TBI which is impossible to replicate in a single experimental model has precluded a consensus regarding the temporal profile of edema following brain injuries. Most researchers, however, agree that post-TBI, edema occurs as a continuum that starts with vasogenic edema (with observable tight junction and BBB breakdown) which occur within hours of TBI, followed by cytotoxic edema which develops over days and may persist for weeks (Barzo et al., 1997, Marmarou, 2003, Donkin and Vink, 2010).

The brain microvessels surrounding major white matter tracts and in the hippocampi are especially vulnerable to damage and leakage following TBI to adult

brains (Dietrich et al., 1994, Chodobski et al., 2011). Hemorrhagic contusions were found at the gray-white matter interphase under somatosensory cortex in lateral fluid-percussion injury model in adult rats (Dietrich et al., 1994). Microvessels coursing the subcortical white matter such as the corpus callosum are also highly susceptible to damage following TBI (Chodobski et al., 2011). Vascular mechanisms is also frequently advanced to explain the selective vulnerability of the hippocampus (especially in the CA1, CA3, and dentate gyrus) to damage following TBI in adult humans and in nonhuman primates (Kotapka et al., 1991) and in rodents (Gao et al., 2011) and other animals (Kirino, 1982). Selective damage to both white matter and hippocampi contribute significantly to sensorimotor and cognitive deficits following adult TBI (Gao et al., 2011, Alwis et al., 2012). Clear-cut vulnerability of the hippocampi and white matter in the juvenile brain compared to those in the adult brain has not been unequivocally demonstrated despite some evidence pointing toward this (Pullela et al., 2006). Vasogenic edema particularly spreads and is more frequently observed in the structured cerebral white matter rather than the less ordered grey matter (Kimelberg, 1995, Vink and Van Den Heuvel, 2004). This is because the movement results from pressure gradients involving the least tissue resistance. The profuse swelling along white matter tracts impacts the structural and functional integrity of the fibers (Feigin et al., 1973, Huh et al., 2008).

Several molecular mediators in the neurovascular unit following TBI to the adult brain demonstrate time-dependent, biphasic effects on the brain, with the acute or chronic phase displaying either beneficial or detrimental impact on the brain's vascular structure and function (Xing et al., 2012). For instance, MMPs degrade neurovascular matrix, damage the BBB, exacerbate edema and hemorrhage, and leads to neuronal death in the acute phase of TBI in patients (Grossetete et al., 2009) and animals (Morita-Fujimura et al., 2000, Wang et al., 2000). MMPs have however been found to promote

neurovascular remodeling in the delayed phases (7 – 14 days) of experimental brain injury in adult rodents (Zhao et al., 2006, Zhang et al., 2010). This biphasic effects are yet to be studied in juvenile rodents. Other mediators displaying these time-dependent effects include trophic factors released by reactive astrocytes (e.g. VEGF, bFGF, PDGF, BDNF, etc.) and NMDA-type glutamate receptors (Xing et al., 2012).

BBB disruption contributes significantly to the development of secondary complications of TBI, one of which is disrupted neurovascular coupling (Golding, 2002, Iadecola and Nedergaard, 2007, Lok et al., 2007). Neurovascular coupling denotes the association of neural activity in a particular brain locale to concomitant changes in cerebral blood flow (CBF) (Pasley and Freeman, 2008). The magnitude and spatial location of blood flow changes are tightly linked to changes in neural activity through a complex sequence of coordinated events involving neurons, glia, and vascular cells (Golding, 2002). In normal brain, local release of metabolic by-products such as carbon dioxide (CO₂), NO, adenosine, lactate, hydrogen ion (H⁺) and potassium ion (K⁺) influence local CBF to match or 'couple' neural activity to blood flow (Lok et al., 2007, Peterson et al., 2011). Following TBI, however, uncoupling often occurs whereby local cerebral glucose utilization increases while local CBF decreases (Golding, 2002, Bor-Seng-Shu et al., 2012). Breakdown in normal activities and interactions between cells making up the neurovascular units (which include endothelium, astrocytes, pericytes, microglia and neurons) results in neurovascular uncoupling (Shlosberg et al., 2010). Influx and release of several vasoactive factors due to BBB disruption (Hawkins and Davis, 2005) and disturbance of cerebral autoregulation (Bor-Seng-Shu et al., 2012) further exacerbate neurovascular uncoupling.

Post-traumatic epilepsy is another well-documented complication of TBI which disruption of BBB contributes to (Tomkins et al., 2001, Tomkins et al., 2008, David et al., 2009). Abnormal brain electrical activities observed on electroencephalogram (EEG)

(which is indicative of abnormal neuronal signaling) were localized to brain regions with clear signs of BBB disruptions in brains of patients suffering from post-traumatic epilepsy (Tomkins et al., 2011). Experimental studies have implicated astrocytic dysfunction together with altered potassium and glutamate homeostasis in this post-traumatic epilepsy (Gupta and Gupta, 2006, David et al., 2009). Hemoglobin/Iron toxicity (Iudice and Murri, 2000) has also been implicated in post-TBI epilepsy. Children who are victims of severe TBI appear to have a lower risk of developing post-traumatic epilepsy compared to their young adult (Pitkanen and McIntosh, 2006) and aged (Herman, 2002) counterparts. In a retrospective population-based study conducted on data from a very large sample of patients (n = 1.6 million people) in Denmark spanning three-and-a-half decades, long-term risk (up to 10 years or longer) of post-traumatic epilepsy was found to be increased with increased injury severity, age, and family history of epilepsy (Christensen et al., 2009). Children are, however, reported to have a slightly higher risk of early (i.e. occurring within 7 days of injury) post-traumatic epilepsy compared to adults following severe TBI (Khan and Banerjee, 2010).

Disruption of BBB has notable negative consequences (besides neurovascular uncoupling) on all major cell types within the brain following adult TBI. Reduced CBF results in the creation of an oxygen- and nutrients-starved zone (Shlosberg et al., 2010), with concomitant neuronal death (Park et al., 2008). Astrocytes (Chodobski et al., 2011) and pericytes (Dore-Duffy et al., 2000) respond to breakdown of BBB following brain trauma (Al Ahmad et al., 2009). Astrocytic foot processes swell due to high intake of potassium ions, and this leads to failure of glutamate transporters and reversal of glutamate uptake (Kimelberg et al., 1995, Park et al., 2008). Reversal of glutamate uptake floods the extracellular space with excessive glutamate, which is a major culprit in neuronal excitotoxicity (van Landeghem et al., 2006, Park et al., 2008). Astrogliosis, marked by abnormal proliferation of the astrocytes, occurs in response to release of

factors (thrombin, albumin, cytokines, etc.) and migration of peripheral cells into the parenchyma following BBB disruption (Chodobski et al., 2011), and neuronal cell death (Myer et al., 2006). Reactive astrogliosis occurs in a graduated fashion depending on injury severity, and is linked with both detrimental and beneficial effects on neurons which may be time-dependent (Myer et al., 2006, Laird et al., 2008, Wu et al., 2010).

NMDA and AMPA receptors on neurons are hyperactivated by the excessive glutamate present in the parenchyma, leading to excessive Ca^{2+} and Zn^{2+} influx – a hallmark of excitotoxicity that eventually kill the cells (Yi and Hazell, 2006, Park et al., 2008, Zhu et al., 2009). Ca^{2+} influx activates several enzymes including proteases such as calpains that damage components of neuronal and axonal cytoskeleton (Saatman et al., 2010). Events such as cellular depolarization, increased oxidative stress, mitochondrial dysfunction and caspase activation are linked to excitotoxicity (Zhao et al., 2003, Park et al., 2008).

Following BBB disruption, intraparenchymal microglial cells become activated and motile, migrating to the injured site within a rapid time frame (Nimmerjahn et al., 2005, Ramlackhansingh et al., 2011). The rapid time frame in which microglia react to BBB disruption suggests involvement of blood-borne and chemoattractive factors (Chodobski et al., 2011). Microglial activation was found to persist in some clinical cases for several years (up to 17 years) after TBI, even at regions distal from the focal impact area (Ramlackhansingh et al., 2011). This highlights chronic inflammatory response that evolves over time and the potential for intervention to be beneficial for long intervals after TBI. It has been linked with both beneficial and deleterious effects.

Blood-derived leukocytes that infiltrate into brain parenchyma following BBB disruption in adult TBI further exacerbate inflammatory response with consequent deleterious effect on BBB integrity, observed as increased permeability and aggravation

of edema (Wedmore and Williams, 1981, Lindbom, 2003, Schmidt et al., 2007, Kenne et al., 2012).

Search for Therapeutic Avenues for Controlling BBB Disruption and Edema in Juvenile TBI

As highlighted in the preceding sections, BBB disruption is central to acute and long-term secondary brain damage following TBI (Shlosberg et al., 2010). The gradual evolution and biphasic nature of BBB breakdown allow a therapeutic window of opportunity to halt the progression of secondary injury on its track (Beauchamp et al., 2008, Park et al., 2008). To this end, the restoration of BBB integrity (Shlosberg et al., 2010) and abrogation of edema formation (Huh and Raghupathi, 2009, Fukuda et al., 2012) are emerging targets for brain protection following juvenile TBI.

Most of past research efforts aimed at investigating interventions for brain trauma have been focused on adult TBI (Adelson et al., 2003), which is reflected in the common use of adult rodents and primates (Prins and Hovda, 2003). Scientific observers have therefore called for more studies focusing on juvenile TBI (Adelson et al., 2003, Taylor, 2004), especially given that majority of TBI cases occur in children and young adults (Langlois et al., 2006, Rutland-Brown et al., 2006, Giza et al., 2007).

Although preclinical studies on drug agents such as corticosteroids, non-steroidal anti-inflammatory drugs (NSAIDs), monoaminergic substances, cyclosporine, and cannabinoids for combating post-TBI secondary damage were highly promising, randomized control trials on these agents have had mostly negative results (Edwards et al., 2005, Beauchamp et al., 2008, CRASH-2, 2011). One of the factors responsible for failure of most of these trials may be the inability of the tested drugs to ameliorate BBB disruption and edema formation on the brain post-TBI (Vink and Van Den Heuvel, 2004). Trials targeting pediatric TBI patients (which are scarce) have also not met with much

success (Natale et al., 2006). A search for safe and potent pharmacological agents that could act at the level of brain vasculature and ameliorate post-traumatic BBB disruption (Shlosberg et al., 2010) is therefore warranted, particularly for the under-researched young demographic. It is not a guarantee that a drug that limits BBB disruption and edema in juvenile TBI will also be effective in adult TBI, due to potential differences in the severity, duration, and mechanisms of BBB disruption and edema following injury to the juvenile brain versus adult brain (Giza et al., 2007, Huh and Raghupathi, 2009).

Another desirable property for any potential pharmacological agent targeting BBB damage and edema in jTBI is the ability to act in more than one cell type and attenuate multiple secondary injury factors (Vink and Van Den Heuvel, 2004). This is important because juvenile TBI, not unlike adult TBI, is a multifactorial and multifaceted pathological phenomenon (Anderson and Yeates, 2010) that affects all major cell types in the brain (Potts et al., 2006, Chodobski et al., 2011). Moreover, BBB is a dynamic interface that is part of the neurovascular unit, and damage to the BBB elicits responses from all cell types that are part of that unit (e.g. endothelial cells, astrocytes, microglia, pericytes, and neurons [see sections 2.3 and 2.4 above]) (Chodobski et al., 2011). Post-traumatic cerebral edema and neuroinflammation also affect all cell types in the neurovascular unit (Chodobski et al., 2011). Therefore, while the search is not for a 'panacea' – an unrealistic universal drug that ameliorates or cures all pathophysiological problems associated TBI in every cell of the developing brain – it is nonetheless desirable that potential drugs have multiple targets and regulate signaling cascades that are not limited to only one cell type in the brain (Vink and Van Den Heuvel, 2004).

Yet another coveted property which a new drug should possess if it to be used in juvenile TBI cases is the ability to reverse the neurological and cognitive deficits that characterize trauma to the developing brain (Adelson et al., 2000, Ajao et al., 2012). The long-lasting nature of some of these deficits highlighted earlier in section 1 often leaves

survivors of moderate to severe TBI saddled with residual and emergent functional problems of sensorimotor, cognitive and psychiatric nature (Max et al., 2000, Yeates et al., 2002, Davis and Dean, 2010). The ability to reverse these deficits and restore normal function long-term will be suitable for a drug to be used in jTBI cases.

Two groups of proteins that are of primary interest to this dissertation with respect to their potential to influence endothelial barrier permeability, edema formation, and a few other pathological processes in the neurovascular unit (such as neuronal apoptosis and disruption in cerebral blood flow autoregulation) are caveolins (cav-1, cav-2 and cav-3) and c-Jun N-terminal kinases (JNK-1, JNK-2, and JNK-3). Varied isoform mix of caveolins and JNKs are present in most of the cell types constituting the neurovascular unit (endothelial, neuronal, astrocytic, etc.) and both affect signaling cascades and processes in these cell types under physiological and pathological conditions. Pharmacological agents that mimic caveolins (see section 4) or inhibit JNKs (see section 5) are available for use in *in vitro* and *in vivo* studies investigating these proteins. These agents have potentials for clinical translation. Ultimately, the main focus of this project is investigating the roles of caveolins and JNKs in regulating BBB disruption and edema formation, and how drugs mimicking or targeting these molecules might correct neurological and cognitive deficits following juvenile TBI both short-term and long-term. The next two sections provide background information and elaborate on the importance of caveolins and JNKs to BBB regulation.

Caveolae and Caveolins in Brain Pathologies

Caveolae were first identified and morphologically described almost simultaneously by Eichi Yamada (who gave the name 'caveolae' which means 'little caves') (Yamada, 1955) and the late Nobel laureate and cell biologist George E. Palade (Palade, 1953) in the early 1950s. Caveolae appear under electron microscope

as vesicular plasma membrane invaginations that are usually 50 – 100 nm in diameter (Palade, 1953). They are early components of what are later called 'lipid rafts' – specialized membrane microdomains that are highly enriched in cholesterol, glycosphingolipids and glycolipoproteins (Simons and van Meer, 1988, Lajoie and Nabi, 2010). George Palade proposed the first functional hypothesis for caveolae – transcytosis (Travis, 1993), but definitive proof of this was delayed by technical restraints for decades until caveolae could be isolated and their structural units examined. Caveolins, the integral membrane structural proteins that form oligomeric assemblies necessary for the characteristic shape and functions of the caveolae in brain lipid rafts (Sargiacomo et al., 1995, Predescu et al., 2007), were discovered in the early 1990s in the lab of Dr. Richard G. Anderson (Rothberg et al., 1992). The lab was able to raise antibodies which label the caveolae membrane proteins. Research into the molecular structure and functions of caveolins blossomed from there onwards.

The caveolin gene is conserved across various species of metazoan (vertebrate and invertebrate animals). It has been studied in some invertebrate (e.g. *Apis mellifera*, honeybee; *C. elegans*, roundworm; *Crassostrea gigas*, pacific oyster; etc.) and non-mammalian (e.g. *Danio rerio*, zebrafish; *Xenopus laevis*, frog; etc.) systems. Amongst mammals, caveolin gene and protein products have been studied notably in mice, rats, pigs, monkeys and humans (Tang et al., 1997, Schlachetzki and Partridge, 2003, Spisni et al., 2005, Kirkham et al., 2008). There are three main isoforms of caveolins – caveolins-1, 2 and 3 – and their presence has been reported in humans and in non-human species (Scherer et al., 1997, Razani et al., 2002a, Shin et al., 2003). The three isoforms enjoy a wide distribution in various tissues and organs of the human body (Virgintino et al., 2002, Das et al., 2007a, Tourkina et al., 2008). Whereas all three caveolin isoforms are present in the brain, their localization differs. Caveolins-1 and 2 usually form hetero-oligomers and predominantly localize to the caveolae (Cohen et al.,

2004, Schwencke et al., 2006) and some cytosolic organelles such as endoplasmic reticulum, mitochondria and Golgi (Li et al., 2001, McCaffrey et al., 2007) in brain endothelial cells (Cameron et al., 1997, Virgintino et al., 2002). However, caveolin-1 has been found in smaller concentrations in some neurons, astrocytes and ependymal cells under both physiological and pathological conditions (Galbiati et al., 1998b, Shin et al., 2005, Head et al., 2008, Head et al., 2010). Caveolin-3 is predominantly found in astrocytes in the brain (Ikezu et al., 1998, Virgintino et al., 2002), and in skeletal, cardiac, and smooth muscles in the periphery (Song et al., 1996).

Early transcription of caveolin gene and expression of its isoforms have been observed in several animal models. Cav-1 immunoreactivity in human fetal tissues has been observed from mid to late gestation (14 to 39 weeks) in patterns similar to that of adult tissues (Barresi et al., 2006). There were, however, some positive staining pattern in the fetal tissues (e.g. in urothelium) not seen in adult tissue, which suggests novel roles for cav-1 during embryogenesis (Barresi et al., 2006). Cav-1 mRNAs have been shown to localize in primitive blood vessels of embryonic mice lungs starting at E10 (Ramirez et al., 2002), suggesting that the caveolins are intact at birth in rodents. The level of cav-1 mRNAs in rodent cortex peaks at P12 – during active brain development (Cameron et al., 1997) – and decreases with age (Head et al., 2010). In chicken, cav-3 immunoreactivity was observed as early as E4, when it is localized to the neural tube and myotome, and seen in glia of chicken brain at E6 (Shin et al., 2003). Cav-3 immunoreactivity changes at various stages of embryogenesis in a non-linear manner, suggesting that the gene and protein play active roles in early development (Shin et al., 2003). Caveolin-1 was shown to be required for proper dorsoventral patterning in zebrafish embryogenesis (Mo et al., 2010). The abnormal phenotypes in zebrafish embryos caused by ablation of Cav-1 – which include weak dorsalization, early tailbud protrusion, curved bodies, deformed notochord and somites, and shortened tails

– were rescued by the expression of human Cav-1, suggesting that cav-1 function is conserved in both species (Mo et al., 2010).

Meanwhile, the caveolins scaffold several signaling molecules through their scaffolding domain (CSD) (Sargiacomo et al., 1995, Cameron et al., 1997, Couet et al., 1997a, Couet et al., 1997c, Garcia-Cardena et al., 1997, Razani et al., 2002b, Lajoie and Nabi, 2010). The CSD binds well-defined caveolin-binding motifs (CBM) present in signaling proteins, such as protein kinases (Galbiati et al., 1998a, Okamoto et al., 1998) and in enzymes such as endothelial nitric oxide synthase (eNOS) (Garcia-Cardena et al., 1996, Couet et al., 1997a, Bucci et al., 2000). For instance, in peripheral endothelial cells, cav-1, via its CSD, functions as a potent endogenous inhibitor of the p42/44-MAPK and JNKs (Wang et al., 2006, Tourkina et al., 2008, Tourkina et al., 2010).

Furthermore, the binding of caveolin to eNOS through CSD-CBM interaction (Garcia-Cardena et al., 1997) is widely implicated in the control of endothelial permeability both in the periphery (Bucci et al., 2000, Siddiqui et al., 2011) and in the brain (Gu et al., 2011). Synthesis of NO by eNOS is negatively regulated by caveolin-1 in both brain and peripheral endothelia (Bucci et al., 2000, Bernatchez et al., 2005). Thus, cav-1 regulates the concentration of NO – the most potent endogenous vasodilator known (Cooke and Dzau, 1997) and a mediator of increased endothelial permeability (Lal et al., 2001, Yuan and Rigor, 2010) (See **Fig. 2**). A synthetic peptide (called Cav-AP, cavtratin, or CSD peptide), made by fusing the CSD of caveolin-1 with a transporter sequence, is being used to investigate mimicry of cav-1 function in experimental studies (Bucci et al., 2000, Argaw et al., 2012).

Caveolin-1 mRNAs, protein levels, and activation states are changed in response to brain injuries such as cold cortical injury (Nag et al., 2007, Nag et al., 2009), brain ischemia (Jasmin et al., 2007), and experimental spinal cord injury (Shin et al., 2005, Shin, 2007). Decrease in cav-1 has been implicated in neurodegenerative disorders

such as Alzheimer's disease (Head et al., 2010). Increase in cav-1 (Nag et al., 2007) and its phosphorylated forms (Nag et al., 2009) was observed up to four days following cold cortical injury model in adult rats, and in the clip compression model of spinal cord injury in rats (Shin, 2007). These reported changes in cav-1 are usually associated with BBB or blood-spinal cord barrier breakdown and vasogenic edema (Shin et al., 2005, Nag et al., 2007, Gu et al., 2011, Li et al., 2012). In both the brain and in peripheral organs, Cav-1 has been recognized as a potent tumor-suppressor in many forms metastatic cancers (Engelman et al., 1998, Gratton et al., 2003, Cohen et al., 2004, Williams and Lisanti, 2005). The Cav-1 gene is localized in a tumor suppressor locus at 7q31.1 (Sloan et al., 2004). There are, however, a few models in which Cav-1 may function as a tumor promoter (Williams et al., 2005, Williams and Lisanti, 2005).

Endothelial caveolins have been associated with various structural components and signaling pathways of the BBB [See (Komarova and Malik, 2010) for a recent review detailing the roles of caveolins in regulating brain endothelial permeability]. It is well-established that caveolins regulate the transcellular route of endothelial permeability via transcytosis (Komarova and Malik, 2010, Yuan and Rigor, 2010). Transcytosis is a process in which solutes can traverse the interior of endothelial cells via receptor-mediated vesicle endocytosis – a form of transcellular transport – originating at caveolae (Predescu and Palade, 1993, Simons and Ikonen, 1997, Predescu et al., 2007) (See **Fig. 2**). However, caveolins also influence the paracellular route of endothelial permeability. For instance, claudins and occludins are found in isolated caveolae, where they interact with caveolins (Nusrat et al., 2000, McCaffrey et al., 2007, Song et al., 2007, Stamatovic et al., 2009, Itallie and Anderson, 2012) (See **Fig. 2**). The level of oligomeric claudin-5 and occludin seen in normal brain endothelial caveolae (McCaffrey et al., 2007) is reduced during pathological conditions such as hypoxia-reoxygenation (McCaffrey et al., 2009). Such reduction engenders tight junction and BBB disruption

(McCaffrey et al., 2008). Several receptors and signaling molecules that are known to mediate endothelial permeability possess caveolin binding motifs (CBMs) and are morphologically and/or biochemically linked with caveolins within the caveolae (See **Table 1**) (Couet et al., 1997a, Couet et al., 1997b, Okamoto et al., 1998, Razani et al., 2002b, Komarova and Malik, 2010).

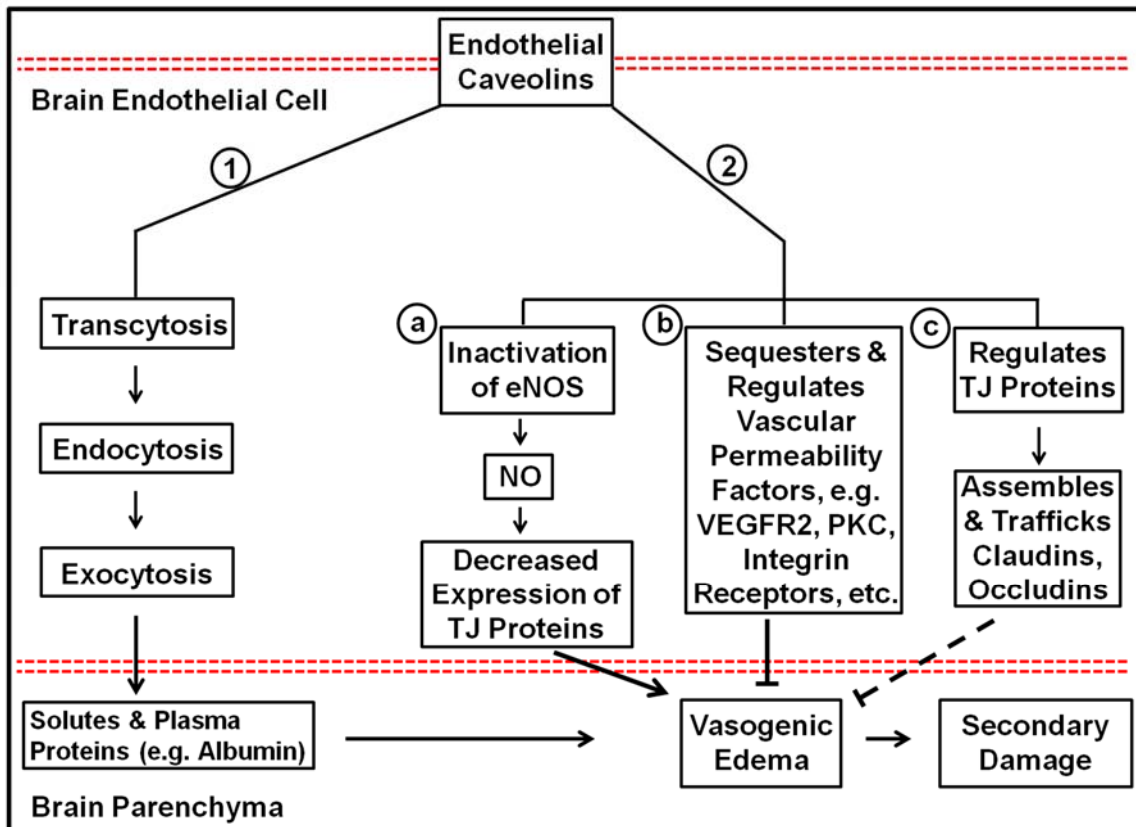


Fig. 2: Caveolin Involvement in Endothelial Permeability.

Caveolins influence endothelial permeability through both transcellular (1) and paracellular (2) routes.

1. The transcellular route of endothelial permeability involves transcytosis, which occurs through receptor-mediated, clathrin-independent vesicular endocytosis, and could also involve exocytosis. These processes are mediated by caveolae, lipid raft microdomains that form “cave-like” invaginations in the plasma membrane for transport of solutes and plasma proteins, such as albumin, into and out of the cell.
2. The paracellular route of endothelial permeability, however, involves regulation of interendothelial junctional proteins (claudins, occludins, zona occludens, etc.). (a) Caveolins inactivates endothelial nitric oxide synthase (eNOS), and thereby reduces nitric oxide (NO) production which has been linked with reduced expression of tight junction (TJ) proteins. (b) Caveolins also sequesters and regulates the signaling of factors such as VEGF receptor-2 (VEGFR2), protein kinase C (PKC), and integrin receptors, which are known to influence TJ permeability. (c) The caveolae assembles and traffics TJ proteins. Hyperpermeability causes vasogenic edema and secondary brain damage.

Table 1: Caveolae-Localized and Caveolin-Interacting Molecules Implicated in Mediating Endothelial Permeability. Adapted from (Razani et al., 2002b).

Molecule with Caveolar Localization	Class	M	B	Interact with Caveolins	References
Receptor Tyrosine Kinase (RTK), e.g. VEGFR-2	Endothelial Receptor	+	+	+	(Feng et al., 1999a, Feng et al., 1999b, Labrecque et al., 2003)
G-Protein Coupled Receptors (GPCR), e.g. Bradykinin B2 receptor	Endothelial Receptor	+	+		(Haasemann et al., 1998, Ju et al., 2000, Chini and Parenti, 2004)
Integrin Receptor	Endothelial Receptor	+	+	+	(Echarri and Del Pozo, 2006, Ning et al., 2007, Shi and Sottile, 2008)
Calcium	Intracellular Second Messenger		+	+	(El-Yazbi et al., 2008, Pani and Singh, 2009)
Cyclic AMP (cAMP)	Intracellular Second Messenger		+	+	(Schwencke et al., 1999, Razani and Lisanti, 2001)
NO-Cyclic GMP (NO-cGMP)	Intracellular Second Messenger		+	+	(Garcia-Cardena et al., 1996, Linder et al., 2005)
Myosin Light-Chain Kinase/Phosphotase (MLCK/MLCP)	Protein Kinase / Phosphotase		+	+	(Somara et al., 2011, Cunningham and Turner, 2012, Rigor et al., 2012)
Protein Kinase C (PKC)	Protein Kinase	+	+	+	(Lisanti et al., 1994, Oka et al., 1997, Rybin et al., 1999)
Focal Adhesion Kinase (FAK)	Protein Kinase		+	+	(Lee et al., 2002, Pelkmans et al., 2005)
Rho Family GTPases	Protein Kinase		+	+	(Somara et al., 2011)
Matrix Metalloproteinases (MMPs), e.g. MMP-2 and MMP-9	Protease		+	+	(Puyraimond et al., 2001, Phillips and Birnby, 2004)

A Disintegrin and Metalloproteases (ADAMs)	Protease		+	+	(Wilke and Bubeck Wardenburg, 2010)
Fibrinogen	Extracellular Matrix Protein	+	+		(Kurozumi et al., 1983)
Bradykinin	Endogenous Vasoactive substance		+	+	(Liu et al., 2010)
Vascular Endothelial Growth Factor (VEGF)	Endogenous Vasoactive substance		+	+	(Feng et al., 1999a, Feng et al., 1999b, Bauer et al., 2005)
Nitric Oxide (NO)	Endogenous Vasoactive substance		+	+	(Garcia-Cardena et al., 1996, Bernatchez et al., 2005, Linder et al., 2005)
Endothelial Nitric Oxide Synthase (eNOS)	Endogenous Vasoactive substance		+	+	(Garcia-Cardena et al., 1997, Bucci et al., 2000)
Sphingosine-1-Phosphate (S1P)	Endogenous Vasoactive substance		+	+	(Rosen and Goetzl, 2005, Singleton et al., 2006, Yuan and Rigor, 2010)
Angiopietin-1 (Ang-1) & Tie-2	Endogenous Vasoactive substance	+	+	+	(Yoon et al., 2003)

M = morphological evidence; B = biochemical evidence

Strong evidence has also emerged from several *in vivo* and *in vitro* brain endothelial and brain disease models that support beneficial roles for caveolins in the maintenance of TJ proteins (Jasmin et al., 2007, Song et al., 2007, Gu et al., 2011). In an *in vivo* brain inflammatory model, VEGF-A was found to reduce claudin-5 expression and induce BBB disruption by signaling through VEGF-2 receptor (VEGFR2) and eNOS (Argaw et al., 2012). Both VEGFR2 and eNOS are negatively regulated by caveolin (Garcia-Cardena et al., 1996, Feng et al., 1999a) and by cavtratin (Bucci et al., 2000, Gratton et al., 2003). Cavtratin also reverses VEGF-mediated decrease in claudin-5 expression (Argaw et al., 2012). This observation, however, is by no means universal, as some reports have suggested that caveolin-1 could play a less beneficial role (e.g. redistribution of claudin-5 and occludin, which may lead to transient increase in BBB permeability early on after brain insults) at least transiently in some models such as *in vitro* inflammatory and drug-stimulated models of brain endothelial cells (Stamatovic et al., 2009, Park et al., 2011) and in early ischemic stroke models (Liu et al., 2012). This highlights the need to investigate the physiologic roles of caveolins and their potential roles in human pathology (Minshall et al., 2003, Sellers et al., 2012).

Interestingly, cav-1 knockouts (-/-) mice display unique defects that include impaired angiogenic response (Woodman et al., 2003), aberrations in endothelium-dependent relaxation, contractility and vascular tone (Drab et al., 2001, Razani et al., 2001), and, importantly, microvascular hyperpermeability (Schubert et al., 2002). The increased microvascular permeability was observed in peripheral organs (lung, heart, spleen, kidney, liver, and skeletal muscle) and in the brain (there is a two-fold increase in the level of extravasated radio-iodinated BSA in the brains of cav-1 knockout mice) (Schubert et al., 2002). *In vivo* knockdown of cav-1 expression in mouse lung endothelia with siRNA resulted in dilated interendothelial junction, with concomitant increase in lung vascular permeability to albumin and increased plasma NO concentration (Miyawaki-

Shimizu et al., 2006). In an ischemic stroke study in mice, cav-1 knockouts have worse outcome than the wild-type (WT), with increased cerebral volume of infarction, impaired cerebral angiogenesis, and increased cerebral apoptotic cell death (Jasmin et al., 2007).

Stimulation of brain microvascular endothelial cells (BMECs) with the chemokine CCL2 reduces expression of cav-1, accompanied with decrease in the expression of occludin (Song and Pachter, 2004, Song et al., 2007). Although, a sharp increase in cav-1 level has been reported to precede the decrease in expression of claudin-5 and occludin in cold cortical injury models in adult rats (Nag et al., 2007), there are no definitive proofs that increase in cav-1 in this model is altogether detrimental. Furthermore, in a cerebral ischemic-reperfusion injury model, Gu and colleagues demonstrated extensively that Cav-1 plays a critical role in protecting BBB integrity through inhibition of MMPs activity in brain microvessels and other brain tissues (Gu et al., 2011, Gottschall and Barone, 2012). This is through cav-1's inhibition of eNOS activity and resultant reduction of NO production – overproduction of NO has been shown to increase MMP-9 activity (Gursoy-Ozdemir et al., 2000, Guroy-Ozdemir et al., 2004). Exposure of human brain endothelial cells (HBMEC) to high concentration of unconjugated bilirubin (a model to mimic hyperbilirubinemia) acutely increases the expression of endothelial caveolin-1 with intact tight junction integrity, whereas prolonged exposure results in reduction in caveolin-1 expression and tight junction compromise (Palmela et al., 2012). The putative beneficial role of cav-1 in these models is possibly related to its regulation of the phosphorylation states, distribution, and oligomerization of TJ proteins, all of which are essential in maintaining functional inter-endothelial TJs (Kachar and Reese, 1982, McCaffrey et al., 2007, Stamatovic et al., 2009, Wolburg et al., 2009).

Regulation of brain endothelial permeability is undoubtedly a complex process with intricately interwoven molecular players and mechanisms (Abbott et al., 2006,

Shlosberg et al., 2010, Yuan and Rigor, 2010). In addition to factors that have been mentioned previously, JNK activation appears to contribute tremendously to TJ and BBB disruption in some brain disease models (Tai et al., 2010, Tu et al., 2011). The 3 JNK isoforms are known to have well-conserved caveolin-binding motif (CBM) (Okamoto et al., 1998). Cav-1 inhibits JNK activation endogenously in the periphery, such as in models of fibrotic lung disease (Tourkina et al., 2008) and in cardiac ischemic-reperfusion (IR) injury (Das et al., 2007b). Such JNK inhibition has been shown to result in increased expression and strengthening of tight junction proteins in the periphery (Kojima et al., 2010, Samak et al., 2010). Furthermore, cav-1 inhibits the expression of proinflammatory cytokines in macrophages and endothelial cells in part by regulating JNK activation (Wang et al., 2006). A drug that restored caveolin-1 expression in a mouse model of pulmonary inflammation and fibrosis was also found to simultaneously inhibit MAPK activation, including JNK activation (Meng et al., 2012). This evidence opens up the possibility that endogenous interaction between cav-1 and JNK within brain endothelial cells may influence BBB permeability. The role of caveolin-1 in mediating JNK inhibition is yet to be researched in brain trauma models.

The roles of caveolin in regulating both transcellular and paracellular routes of endothelial permeability continues to be under investigation in some models (Minshall et al., 2003, Komarova and Malik, 2010). However, to date, there are no reported studies that characterize the expression of brain endothelial caveolins in a juvenile model of TBI in association with BBB dysfunctions. There have also been no reports on how drugs that target or mimic the caveolins (e.g. cavtratin) impact histological, neurological and cognitive outcomes following juvenile TBI.

The c-Jun N-terminal Kinases (JNKs): Expression and Inhibition following Brain Injuries

The c-Jun N-terminal kinases (JNKs) were first described in the early 1990s as consisting of serine/threonine protein kinases which phosphorylate the N-terminal transactivation domain of the c-Jun transcription factor upon activation by stress stimuli (Pulverer et al., 1991, Derijard et al., 1994). JNKs are members of a mitogen activated protein kinase (MAPK) subfamily. The other two MAPK subfamilies are p38 and ERK (Widmann et al., 1999, Plotnikov et al., 2011). There are three JNK genes – JNK1, JNK2 and JNK3 (Pulverer et al., 1991, Derijard et al., 1994, Kallunki et al., 1994, Gupta et al., 1996). Alternative splicing of these genes yield 10 identified JNK isoforms (Waetzig and Herdegen, 2005). All 3 JNK genes are highly conserved across various species ranging from yeast to mammals (Goberdhan and Wilson, 1998, Kirkham et al., 2008).

In mammals, JNK1 and JNK2 are ubiquitously expressed, while JNK3 is primarily expressed in the heart, brain, endocrine pancreas and testis (Waetzig et al., 2006). JNKs are found in various cell types in the brain, including neurons (Lannuzel et al., 1997, Herdegen et al., 1998), endothelial cells (Etienne et al., 1998, Waetzig et al., 2006), and astrocytes (Migheli et al., 1997, Xie et al., 2004). Basal JNK activity level in the brain is 15 to 30-fold higher than in other tissues under physiological conditions (Xu et al., 1997, Coffey et al., 2000). JNKs in the brain are activated even further following external stimuli and pathological events (Borsello and Bonny, 2004).

JNKs are activated by dual phosphorylation of threonine (Thr) and tyrosine (Tyr) residues within a unique Thr-Pro-Tyr motif located in subdomain VIII of the kinases (Ip and Davis, 1998). This phosphorylation is catalyzed by upstream kinases – MKK 4 and 7 (Widmann et al., 1999, Kyriakis and Avruch, 2001, Waetzig et al., 2006). A wide range of environmental and biological stressors are capable of activating JNKs, and these include UV light, inflammatory cytokines, reactive oxygen species (ROS), growth factors, protein

synthesis inhibitors, as well as physical and biomechanical perturbations (Davis, 1999, Borsello and Bonny, 2004). JNKs can also be deactivated by some specific phosphatases (Palacios et al., 2001, Masuda et al., 2010).

In terms of function, JNKs are essential for normal brain development and organogenesis in general during embryonic development (Haeusgen et al., 2009). Postnatally, JNKs play various roles ranging from regulation of cell survival and apoptosis to proliferation (Nishina et al., 2004, Waetzig and Herdegen, 2005, Waetzig et al., 2006, Haeusgen et al., 2009). They are also activated under pathological conditions both in the brain (Brecht et al., 2005, Bogoyevitch, 2006) and in the periphery (Cui et al., 2007, Chaudhury et al., 2010).

Most of the studies on JNK pathway in rodent brains have focused predominantly on neuronal activation triggered by excitotoxic events (Lennmyr et al., 2002, Borsello et al., 2003, Cui et al., 2007, Haeusgen et al., 2009). There is however increasing evidence that JNK is also activated in glial cells (Xie et al., 2004) and brain endothelial cells (Lo et al., 2005, Kacimi et al., 2011), and that such activation in non-neuronal cells negatively impacts neuronal cell death and function (Xie et al., 2004). Zhu and colleagues (2003) reported the hyperactivation of JNK in murine cerebral microvascular endothelial (bEND.3) cells *in vitro*. Such overt JNK hyperactivation in brain endothelial cells has been implicated in clinical pathologies including Alzheimer's disease, strokes and multiple sclerosis (Vukic et al., 2009, Grammas, 2011). Kusaka et al (2004) reported an acute hyperactivation of JNK following subarachnoid hemorrhage (SAH) in rat brain endothelium. Benakis et al (2010) reported the modulation of non-neuronal inflammatory processes in the brain by DJNKI-1, a competitive JNK inhibitor that was injected peripherally. Studies have indicated that DJNKI-1 crossed the BBB and penetrated the cerebral cortex within 1.5 hours after intraperitoneal (i.p.) injection in rodents, and could

remain stable in brain parenchyma for at least 3 weeks (Repici et al., 2007, Ploia et al., 2011, Scip et al., 2011).

Experimental and clinical observations show that JNK phosphorylation initially drops, but begins to rise at 1.5 hours and peaks at 9 hours after stroke (Gao et al., 2005). Phosphorylation of c-Jun, a JNK substrate, follows a similar pattern, peaking at 8 hours post-stroke (Borsello et al., 2003, Gao et al., 2005). Activation of JNK in ischemic strokes has been linked with mitochondrial apoptotic pathway and nuclear translocation of MADD (MAP kinase-activated death domain-containing protein) in neurons (Putcha et al., 2003, Centeno et al., 2007). Increase of Phospho-JNK was also reported in the brain tissues from 6 TBI patients, and experimental reports have confirmed this increase from 1 to 48 hours post-injury in a CCI model in adult mice (Ortolano et al., 2009).

Hyperactivation of JNK in CNS pathologies has been linked with BBB disruption (Tu et al., 2011).

The inhibition of JNK pathway has been shown to be beneficial in some models of adult and juvenile brain damage. Borsello et al (2003) reported that the competitive JNK-inhibitor, DJNKI-1, protects against NMDA-induced neurotoxicity in hippocampal neurons cultured from 2-day old rat pups. Using the drug (DJNKI) after TBI in newborn piglets, Armstead et al (2011a) showed that inhibiting the JNK pathway mitigates cerebral hemodynamic dysfunctions observed in jTBI. Moreover, deletion of JNK3 gene protects neonatal mice against cerebral hypoxic-ischemic (HI) injury (Kuan et al., 2003, Pirianov et al., 2007). Tu et al (2011) also showed that in overweight rat pups (P7 and P21), experimental HI brain injury results in BBB breakage strongly mediated by JNK overactivation.

Experimental evidence suggests that JNK hyperactivation will likely increase endothelial hyperpermeability both in the periphery (Chen et al., 2006, Hu et al., 2013) and in the brain (Yatsushige et al., 2007, Tu et al., 2011) (See **Fig. 3**). Activated JNK

and its substrates (e.g. phosphorylated c-Jun) are strong regulators of TJ proteins in the periphery (Betanzos et al., 2004, Carrozzino et al., 2009, Kojima et al., 2010, Samak et al., 2010). For example, inhibition of JNK pathway in mammary epithelial cells enhances TJ barrier function through modulation of claudin-5 expression (Carrozzino et al., 2009). Furthermore, the protein c-Jun, a substrate phosphorylated by JNK, exerts regulatory control on TJ proteins in epithelial cells (Betanzos et al., 2004). In human pancreatic cells, JNK strongly regulates TJ proteins at the tricellular contacts (Kojima et al., 2010). With regard to brain endothelial cells, activation of JNK and c-Jun has been shown *in vitro* to increase cerebral endothelial cell permeability through disruption of interendothelial TJ complexes (Etienne et al., 1998, Adamson et al., 1999, Wolburg and Lippoldt, 2002).

Meanwhile, certain molecular mediators of endothelial hyperpermeability known to interact with caveolins are also linked with increased JNK activation under pathological conditions such as inflammation. These include VEGF and VEGFR2 (Upon ligand binding, VEGFR2 activates multiple protein kinase-dependent signaling including JNK pathway to induce hyperpermeability) (Kumar et al., 2009), protein kinase C (PKC) (Yuan and Rigor, 2010), and src-kinase (Yoshizumi et al., 2000) (See the preceding section above for literature evidence of links between JNKs and caveolae/caveolins). Inhibitors of JNK pathway have been shown to reduce and reverse TJ disruption in injured brain-derived endothelial cells through decreased inducible nitric oxide synthase (iNOS) activation and NO production (Kacimi et al., 2011). Furthermore, under inflammatory condition in human lung microvascular endothelial cells, bradykinin potentiates eNOS-derived NO generation in part through JNK signaling (Lowry et al., 2013). Hence, mounting evidence suggests that caveolins and JNKs both play key roles in mediating the eNOS-NO pathway in the endothelium (Minshall et al., 2003, Balligand et al., 2009). JNK is also highly activated in laminar shear stress experiments performed

on endothelial cells (Yoshizumi et al., 2003) with concomitant increase in caveolins and caveolae number (Frank and Lisanti, 2006).

Recovery of neurological and cognitive function in both the short- and long-term is a desirable property for any pharmacological agent to be used for juvenile TBI. To this end, it is important to note that DJNKI-1, a competitive JNK inhibitor (see below), has been shown to ameliorate behavioral deficits in experimental models of stroke (Esneault et al., 2008), neuroinflammation (Palin et al., 2008), and spinal cord injury (Repici et al., 2012) in adult rodents, even when injected peripherally. D-JNKI-1 was also successfully used to arrest the progression of hearing loss in a model of cochlear implantation trauma (Eshraghi et al., 2006). The action of DJNKI-1 in various forms of CNS injuries possibly extend beyond brain endothelial cells (where it could reduce BBB disruption) (Tu et al., 2011, Repici et al., 2012) to neurons (where it reduces excitotoxicity and neuronal cell death) (Borsello et al., 2003), astrocytes (Huang et al., 2009, Kang et al., 2011), and microglia (Repici et al., 2012). Hence, DJNKI-1 could potentially mitigate several aspects of secondary brain damage in various cells simultaneously to maximize recovery. Meanwhile, the possibility of systemic mode of action for DJNKI-1, which is beneficial to recovery, has been raised in some *in vivo* experimental studies (Lehnert et al., 2008, Touchard et al., 2010, Benakis et al., 2012).

The drug, DJNKI-1, is a synthetic, protease-resistant and cell-penetrating peptide made by linking HIV-TAT transporter peptide sequence to the 20-amino acid JNK-binding motif of JIP-1 (Borsello et al., 2003). The D-retro-inverso synthesis (i.e. made with D-amino acids) of DJNKI-1 gives it strong resistance against proteolytic degradation and increases its stability in the body (Borsello et al., 2003, Borsello and Bonny, 2004). The peptide functions through competitive inhibition of all JNK isoforms (see **Fig. 3**). DJNKI-1 selectively blocks access of JNK to c-jun and other downstream substrates such as JunB, JunD, and c-myc by competing for the JNK-binding site of JIP-1 (Borsello et al.,

2003, Borsello and Forloni, 2007) (see **Fig. 3**). The potential for therapeutic effectiveness of DJNKI-1 in jTBI is pegged on its ability to modulate upstream and downstream arms of the secondary injury cascade, including excitotoxicity, hypoxia-ischemia, BBB disruption, edema, neuroinflammation and apoptosis (Yang et al., 1997, Kuan et al., 2003, Tu et al., 2011).

Research Aims

Juvenile TBI is a field that has not been well-researched, and in which no pharmacological agent has been successfully translated for clinical use. A reliable and reproducible animal model of jTBI is needed as a starting point to test various hypotheses. A controlled cortical impact (CCI) model of TBI [modeled after one described by Brody et al. (2007)] in juvenile (P17) rats has been developed for this purpose (Ajao et al., 2012). This model could be used to probe the effects of juvenile TBI on neurobehavioral function, brain morphology and molecular structures. Effects of jTBI on brain structures and functions at both acute and latter time point(s) need to be thoroughly studied to enhance the clinical relevance of the model. For instance, effect of TBI on the morphology and function of the developing white matter is not well studied. Neurological and cognitive tests could also be carried out longitudinally to establish functional deficits resulting from brain injury in this model.

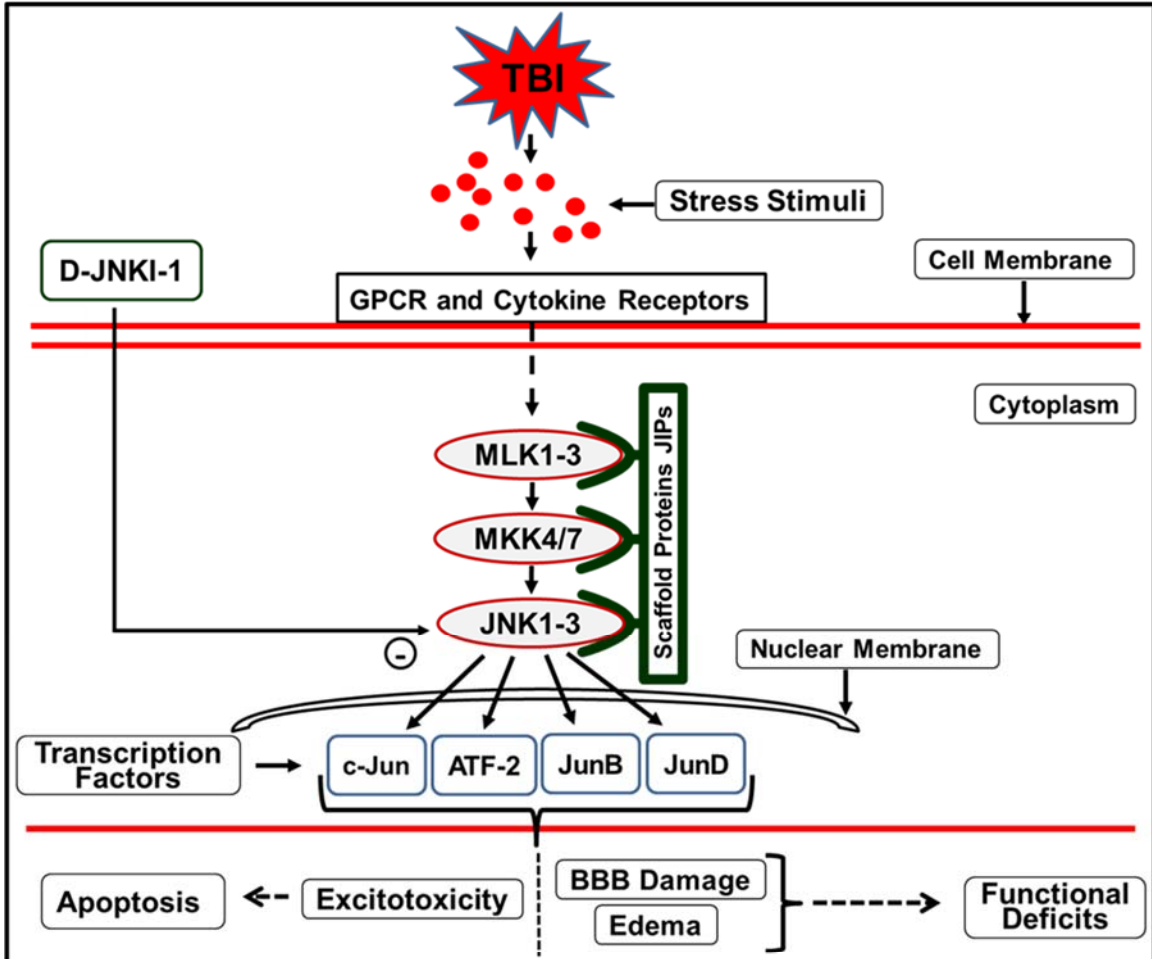


Fig. 3: JNK Pathway and Proposed Mode of Action of D-JNKI-1 in Juvenile TBI.

TBI in the juvenile brain unleashes several stress factors including mechanical forces, blood flow turbulence, cytokines and other ligands, which can stimulate the activation of G protein-coupled receptor (GPCR), cytokine receptors and growth factor receptors. These receptors transduce the extracellular stimuli into intracellular signals through JNK pathway among others. Sequential activation (via phosphorylation) of the mitogen-activated protein kinases (MAPKs) transmits the signal from the mixed-lineage kinases (MLK1-3) to the mitogen-activated protein kinase kinases (MKK4 or 7), which in turn activates JNKs. The JNK-interacting proteins (JIPs) act as a scaffold that structurally aggregates the upstream elements of the MAPK signalling module. Activated JNKs can phosphorylate various substrates, including transcription factors that regulate gene expression. Depending on the cell type, consequences of JNK hyperactivation may include excitotoxicity (e.g. in neurons), apoptosis (neurons and endothelial cells), and production of vascular permeability factors (e.g. NO) that cause BBB damage and edema, followed by functional deficits. DJNKI-1 competitively blocks the interaction between JNK and its various substrates, thereby abrogating their downstream effects.

Having established the relevance of caveolin-1 and JNK activation to secondary events that occur in juvenile brain injury in the preceding sections, the CCI model could be used to study changes in protein expression of caveolin-1 and activation of JNK following jTBI. Moreover, the potential therapeutic effects (functional and/or histological) of pharmacological mimicry of caveolin function and inhibition of JNK could be examined with the use of cavtratin and DJNKI-1 respectively on jTBI animals. The role caveolin-1 and JNK activation are playing in aggravating or reversing BBB disruption could be studied with the use of cavtratin and DJNKI-1 respectively.

Literature evidence reviewed so far suggest parallel molecular pathways that link endothelial caveolins and JNKs to the control of paracellular and transcellular permeability pathways, which may have important consequences on BBB integrity and TBI outcome. This theory has never been examined in the context of jTBI. We therefore hypothesize that:

Following juvenile TBI, upregulation and activation of caveolins-1 in brain endothelial cells endogenously attenuate BBB disruption and edema, while JNK hyperactivation exacerbates BBB disruption, with concomitant morphological damage and functional deficits in the short- and long-term.

This hypothesis will be tested in controlled cortical impact (CCI) model of TBI in juvenile (P17) rats. The questions raised above will be explored under the following three aims.

Aim 1: Characterize the acute and long-term neurological, electrophysiological and histological changes following juvenile TBI.

Hypothesis: *Induction of controlled cortical impact injury in P17 rat pups will engender observable adverse outcomes on neurological function and on brain tissue properties that will last for weeks after the initial insult.*

A battery of neurological and cognitive tests will be carried out longitudinally on rats subjected to CCI and on their sham counterparts. Electrophysiological profiles of these rats as well as their histology will be observed from juvenile period into early adulthood. Lesion volume and T2 changes will also be measured.

Aim 2: Characterize changes in the expression pattern and immunoreactivity of caveolins-1, 2, and 3 after juvenile TBI in conjunction with BBB disruption and edema formation.

Hypothesis: *Decrease in the tight junction protein levels and resultant opening of the BBB will be associated with increase in the expression of caveolins-1, 2 and 3 in brain endothelial cells following juvenile TBI.*

The expression level of caveolins will be determined via immunohistochemistry and immunoblotting at 1, 3, 7 and 60 days post-jTBI. BBB disruption will be confirmed via IgG staining and edema formation will be assessed with MRI.

Aim 3: Examine the effect of DJNKI-1 treatment (JNK Inhibition) and cavtratin treatment (pharmacological mimicry of caveolin scaffolding domain) on BBB integrity and caveolin-1 expression following juvenile TBI.

Hypothesis: *Inhibition of JNK pathway and treatment with cavtratin will reduce and reverse damage to tight junction proteins and prevent BBB disruption.*

A cohort of rats will receive i.p. injection of DJNKI-1 after jTBI. A separate cohort of rats will be treated with cavtratin following jTBI. Changes in the expression of the TJ proteins, caveolin-1 and BBB properties will be assessed at 1, 3, 7, 60 days after injury.

MRI will be used to assess brain water diffusion and edema formation.

The diagrammatic representation below (**Fig. 4**) highlights the key players examined in this project, and illustrates the hypothesized mechanism and effects of the two pharmacological agents used – DJNKI-1 and cavtratin (CSD peptide).

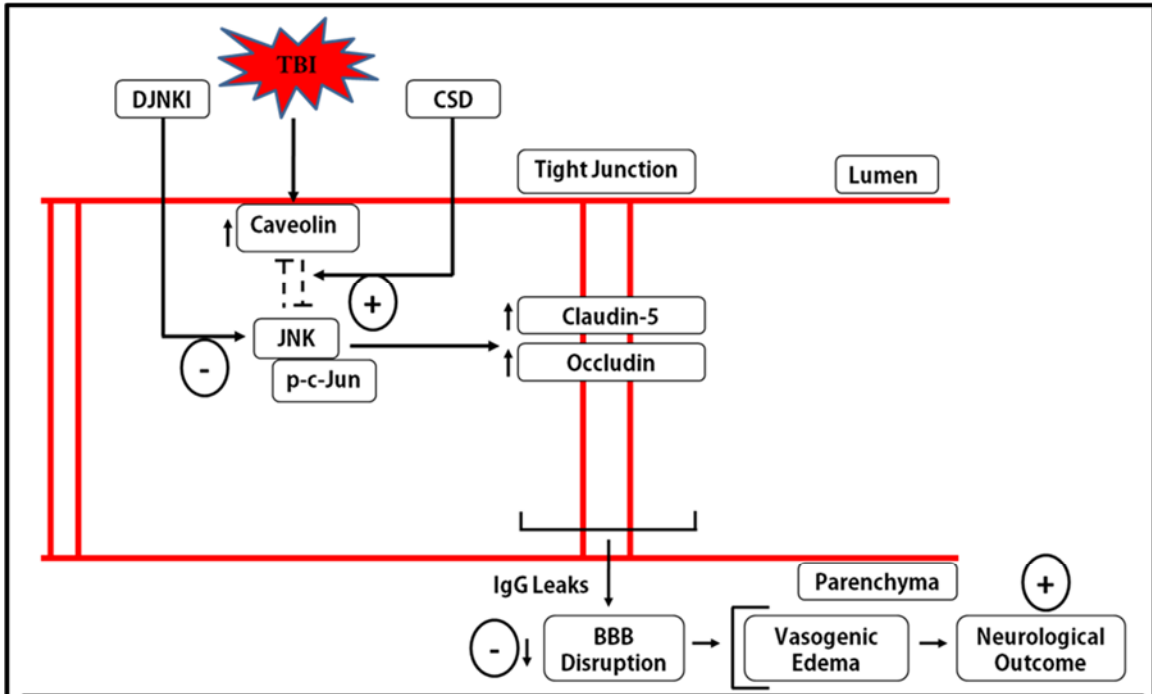


Fig. 4: Schematic of Proposed Mechanism.

TBI induces an increase in caveolin-1 protein level in brain endothelia cells, which endogenously inhibits JNK pathway and counteracts the reduction of tight junction (TJ) proteins levels. DJNKI-1, a competitive JNK inhibitor, was used to investigate the role of JNK hyperactivation in BBB disruption *in vivo*. CSD peptide (cavtratin), which mimics the function of caveolin scaffolding domain, was used to study the interaction between endothelial caveolin-1, BBB permeability and edema formation *in vivo*. We hypothesized that systemic administration of DJNKI-1 and cavtratin (separately) post-TBI will reverse the decrease in TJ proteins, lessen IgG leakage and edema formation, and ultimately result in improved functional recovery.

PROLOGUE TO CHAPTER 2A
TRAUMATIC BRAIN INJURY IN YOUNG RATS LEADS TO
PROGRESSIVE BEHAVIORAL DEFICITS COINCIDENT WITH
ALTERED TISSUE PROPERTIES IN ADULTHOOD

Chapter 2 describes the progressive behavioral deficits resulting from juvenile brain trauma, and their associated morphological and molecular changes, in a rodent model. The clinical relevance of emergent motor and behavioral impairments that persists for months in rodents that were subjected to focal brain injury is emphasized. The chapter highlights the vulnerability of the developing brain to TBI.

The aim of this chapter is to characterize the acute and long-term histological and neurological changes that occur in juvenile TBI using a customized controlled (CCI) model in P17 rats. Morphological and molecular changes in both gray (e.g. at the lesion and perilesion cortex) and white matter (especially the corpus callosum) structures were examined over a 60-day (d) post-injury period. Changes in injury volume across 60 post-injury days, as well as electrophysiological changes were also investigated. A battery of tests was employed to examine neurological and behavioral outcomes following juvenile TBI over the 60d period. The hypothesis for this chapter is that induction of CCI in P17 rat pups will engender observable and testable adverse outcomes on neurological and behavioral functions, and on brain tissue properties, which will last for weeks following the initial insult. The chapter justifies the suitability of the CCI model for carrying out testing of drugs aimed at limiting secondary injury processes, and improving histological and functional outcomes.

This chapter has been published as a scientific article in the July 20, 2012 edition of the *Journal of Neurotrauma* (volume 29, pages 2060 - 2074) under the same title as above. It is complete with abstract, introduction, methods, results and discussion sections. There are 8 figures with detailed figure legends in the manuscript. The authors of the manuscript and their professional affiliations are listed on the first page.

CHAPTER 2A

TRAUMATIC BRAIN INJURY IN YOUNG RATS LEADS TO
PROGRESSIVE BEHAVIORAL DEFICITS COINCIDENT WITH
ALTERED TISSUE PROPERTIES IN ADULTHOOD

**David O. Ajao¹, Viorela Pop², Joel E. Kamper³, Arash Adami⁷,
Emil Rudobeck⁸, Lei Huang⁴, Roman Vikolinsky⁴, Richard E.
Hartman³, Stephen Ashwal², Andre Obenaus^{2, 4-6}, and Jerome
Badaut^{1, 2}**

Departments of ¹Physiology, ²Pediatrics, ³Psychology, ⁴Radiation Medicine, ⁵Biophysics
and Bioengineering, and ⁶Radiology, Loma Linda University, Loma Linda, California.
Departments of ⁷Neuroscience and ⁸Physics, University of California–Riverside,
Riverside, California.

**Running Title: BEHAVIORAL AND WHITE MATTER CHANGES
AFTER JTBI**

Address correspondence to:
Jerome Badaut, Ph.D.
Departments of Pediatrics, Pharmacology, and Physiology
Loma Linda University School of Medicine
Coleman Pavilion, Room A1120
11175 Campus Street
Loma Linda, CA 92354
E-mail: jbadaut@llu.edu

JOURNAL OF NEUROTRAUMA 29:2060–2074 (July 20, 2012)
© Mary Ann Liebert, Inc.
DOI: 10.1089/neu.2011.1883

Abstract

Traumatic brain injury (TBI) affects many infants and children, and results in enduring motor and cognitive impairments with accompanying changes in white matter tracts, yet few experimental studies in rodent juvenile models of TBI (jTBI) have examined the timeline and nature of these deficits, histologically and functionally. We used a single controlled cortical impact (CCI) injury to the parietal cortex of rats at post-natal day (P) 17 to evaluate behavioral alterations, injury volume, and morphological and molecular changes in gray and white matter, with accompanying measures of electrophysiological function. At 60 days post-injury (dpi), we found that jTBI animals displayed behavioral deficits in foot-fault and rotarod tests, along with a left turn bias throughout their early developmental stages and into adulthood. In addition, anxiety-like behaviors on the zero maze emerged in jTBI animals at 60 dpi. The final lesion constituted only ~3% of brain volume, and morphological tissue changes were evaluated using MRI, as well as immunohistochemistry for neuronal nuclei (NeuN), myelin basic protein (MBP), neurofilament-200 (NF200), and oligodendrocytes (CNPase). White matter morphological changes were associated with a global increase in MBP immunostaining and reduced compound action potential amplitudes at 60 dpi. These results suggest that brain injury early in life can induce long-term white matter dysfunction, occurring in parallel with the delayed development and persistence of behavioral deficits, thus modeling clinical and longitudinal TBI observations.

Key words

Behavior; CNPase; juvenile traumatic brain injury; magnetic resonance imaging; myelin; neurofilament-200

Introduction

Traumatic brain injury (TBI) in children is a major cause of death and disability (Schneier et al., 2006, Kuppermann et al., 2009), and it has been suggested that developmental neuroplasticity assists in the recovery of younger individuals (Jane and Francel, 1996, Giza and Prins, 2006). However, clinical and experimental reports indicate that TBI results in lasting structural and functional damage. Clinically, TBI to the frontal cortex has been associated with disruptions in motor function, problem solving, spontaneity, memory, judgment, impulse control, and social behavior (Levin et al., 1987). Although the underlying cellular and molecular pathophysiology is not fully understood, post-TBI behavioral deficits such as aggressive behavior, anxiety, and depression, as well as an increased risk for epilepsy may last for months to years (Fujii and Ahmed, 2002, Giza and Prins, 2006, Lippert-Gruner et al., 2006). Only a small number of experimental TBI studies have evaluated and shown extended behavioral deficits (Prins and Hovda, 1998, Adelson, 2000, Huh and Raghupathi, 2007). Little is known about changes in the tissue properties in association with behavioral modifications.

Several clinical and experimental observations have shown that white matter tracts are highly vulnerable to TBI-induced secondary injury, and that their damage may contribute to cognitive deficits after TBI (Huh and Raghupathi, 2007, Levin et al., 2007, Wagner et al., 2007). Post-natal day (P) 17 in rats, which corresponds to the juvenile population, is a critical myelination period, as it marks the peak of myelin basic protein (MBP) synthesis in the developing rat brain (Bjelke and Seiger, 1989, Akiyama et al., 2002). Previous studies have shown changes in myelination after environmental stress in rats at P17, including changes in MBP (Kodama et al., 2008). Early life stress, such as premature weaning at P17, has been associated with increased anxiety and increased MBP in adulthood (Kodama et al., 2008). To date, experimental juvenile TBI studies have not focused on the timeline of the behavioral deficits seen in association with

alterations in white and gray matter tissue properties using a combinatorial approach of magnetic resonance imaging (MRI), immunohistochemistry, and electrophysiology.

The clinical literature led us to hypothesize that an early-life injury such as TBI would elicit enduring behavioral deficits associated with functional and morphological changes in the brain tissue that persist into adulthood. We used a single controlled cortical impact (CCI) injury to the parietal cortex of P17 rats, at an age of active myelin sheath formation, and evaluated the animals over a period of 60 days post-injury (dpi). We carried out a large battery of behavioral tests to assess a wide spectrum of motor and cognitive functions, and each of the tests that we employed measured a unique aspect of the spectrum of deficits reported after juvenile TBI (jTBI) in humans. We used MRI to evaluate anatomical changes (areas of lesion and corpus callosum [CC]). Tissue was collected to assess morphological and molecular changes in gray and white matter, as well as for *in vitro* axonal conductivity. We present findings of extended behavioral deficits coincident with significant changes in white matter tract properties observed in adulthood, and characterized using MRI, immunohistochemistry, and electrophysiology.

Methods

Animals

All protocols and procedures were approved by the Institutional Animal Care and Use Committee of Loma Linda University, and are in compliance with the U.S. Department of Health and Human Services Guide. Juvenile male Sprague-Dawley rats (P17; Harlan, Indianapolis, IN) were housed with their dams on a 12-h light-dark cycle at constant temperature and humidity. Pups were weaned at P24, housed two rats per cage, and fed with standard lab chow and water ad libitum. All groups of animals used in the study had identical sham or CCI surgical parameters. One group of animals (n = 8 sham, n = 7 CCI) was studied longitudinally for MRI (3, 30, and 60 dpi), and all

behavioral tests (3, 7, 30, and 60 dpi). At 60 dpi, a final immunohistochemistry study was carried out on sham (n = 5) and CCI (n = 6) animals. Additional groups of animals were evaluated at each time point for immunohistochemistry at 3 dpi (n = 3 sham, n = 4 CCI), 7 dpi (n = 5 sham, n = 5 CCI), and 30 dpi (n = 5 sham, n = 5 CCI), and for electrophysiology at 60 dpi (n = 4 sham, n = 4 CCI).

Juvenile Traumatic Brain Injury Model

CCI was induced in juvenile rats as previously described in our adult experiment (Obenaus et al., 2007). Briefly, P17 juvenile rats were anesthetized with isoflurane (Webster Veterinary Supply, Inc., Sterling, MA) and placed in a mouse stereotaxic frame (David Kopf Instruments, Tujunga, CA). Following a midline skin incision over the skull, a 5-mm craniotomy was performed over the right fronto-parietal cortex (bregma: 1mm anterior-posterior and 2mm medial-lateral). CCI was accomplished using a 3-mm rounded-tip metal impactor fixed to an electromechanical actuator and centered over the exposed dura at a 20° angle to be parallel to the cortical surface (Leica Microsystems Company, Richmond, IL). The CCI was delivered at a 1.5-mm depth from the cortical surface with impact duration of 200 msec at a velocity of 6 m/sec. The surgical site was sutured after recording any bleeding or herniation of cortical tissues. Body temperature was maintained at 37°C during surgery. Buprenorphine (0.01 mg/kg; dilution: 0.01 mg/mL) was injected subcutaneously for pain relief before the animals were returned to their dams. The sham animals underwent identical procedures except for the cortical impact.

Magnetic Resonance Imaging and Analysis

MRI was performed *in vivo* at 3 and 30 dpi followed by high resolution *ex vivo* imaging at 60 dpi as previously described (Badaut et al., 2007). For *in vivo* MRI, rats

were anesthetized using isoflurane (1-2%), placed in a temperature controlled cradle containing a volume radiofrequency (RF) coil and imaged on a 11.7T MRI (8.9 cm bore,) or on a larger bore (40 cm) 4.7T MRI (Bruker Biospin, Billerica, MA) based on the size of the animals. T2 weighted imaging (T2WI) to determine TBI volume was acquired using: a repetition time/echo time (TR/TE) = 3278.3/20 ms; 256 X 256 matrix; 1 mm slice thickness; 1 mm interleaved; average of 2 acquisitions; number of slices = 20; and a field of view (FOV) = 2.2 cm for a total imaging time of 28 min on 11.7T MRI; and a repetition time/echo time (TR/TE) = 3563.4/20 ms; 256 X 256 matrix; 1 mm slice thickness; 1 mm interleaved; average of 2 acquisitions; number of slices = 25; and a field of view (FOV) = 2.8 cm for a total imaging time of 30 min on 4.7T MRI. The utilization of two different field strengths did not alter the measurements performed in our experiments (Obenaus et al., 2011).

For *ex vivo* MRI, animals were transcardially perfused with 4% paraformaldehyde (PFA) prepared in phosphate buffered saline (PBS), the brains were immersed in same solution overnight, and then transferred to PBS with sodium azide (0.1%) before *ex vivo* scanning using the 11.7T magnet. T2WI was acquired using: a repetition time/echo time (TR/TE) = 3278.3/20 ms; 256 X 256 matrix; 1 mm slice thickness; 1 mm interleaved; average of 2 acquisitions; number of slices = 20; and a field of view (FOV) = 2.2cm for a total imaging time of 28 min on 11.7T MRI. We previously reported no volumetric differences between *in vivo* and *ex vivo* MRI (Obenaus et al., 2011). Volumetric analyses of the total brain volume and percent lesion/brain volume were performed on T2WI using Cheshire image processing software (Hayden Image Processing Group, Waltham, MA) and Amira (Mercury Computer Systems, Visage Imaging, Inc., San Diego, CA, USA). Lesion volume was defined as those regions containing abnormal hypo- and/or hyper-intense signals. All tissue below the skull level was included, but in the rare instances when tissue herniated and extended above the level of the skull, it was excluded. Injury

volume was adjusted using total brain volume to correct for individual differences and age-related brain growth. Area measurements of the CC at 60 dpi were selected from the MR images at bregma level +1 mm, anterior to the lesion, and included all visible portions of the CC. The coronal section with the same visible anatomical landmarks was chosen for analysis for all animals by a blinded experimenter.

Behavioral Testing

All behavioral tests at each time-point were carried out on sham and CCI animals within a 3-hour morning time-block (8 – 11 am). Sham and CCI animals were interleaved in testing sequence.

Foot-fault

Foot-fault testing was carried out on an elevated wire mesh (2.5 cm X 30 cm rectangular holes/grid spacing) raised 76 cm above the floor at 1, 3, 7, and 60 dpi. Rats were placed in the middle of the wire mesh and movements were video-recorded for a period of 60 sec in two separate trials, 30 min apart (Schmanke et al., 1996). When a rodent's paw slipped completely through the wire mesh, it was considered as an individual fault. The average foot-fault score was calculated from the total number of faults from two 60 sec trials, and a percentage was calculated from sham levels.

Beam Balance

A square Plexiglas beam balance (61 cm long) labeled in 2.5 cm increments was employed in these experiments. Juvenile animals were tested on a 0.65 cm wide beam at 1, 3, and 7 dpi, and adult animals were tested on a 2.5 cm wide beam at 30 and 60 dpi according to size requirements. Animals were placed at the midpoint of the beam, perpendicular to the longitudinal axis, and allowed to walk unrestricted in either direction

for 60 sec, with two trials 20 min apart. The number of falls, total time spent on the beam, and the distance covered by each animal was recorded.

Rotarod

Rotarod evaluation was performed on all the animals at 30 and 60 dpi (Rotamex-5, Columbus Instruments, Columbus, OH). A rotating 7 cm-wide spindle, accelerating at a rate of 2 RPM every 5 sec until the animals fell off, was used to evaluate performance during two trials (15 min apart). Latency to fall was recorded as a measure of motor coordination and balance (Recker et al., 2009), and the two fall latencies were averaged.

Open Field

Open field testing assessed general exploratory behavior and activity levels at 30 and 60 dpi. Each animal was placed in an empty plastic bin (50 cm long, 36 cm wide, 45 cm high), and activity was video-recorded for 30 min (Noldus Ethovision, Noldus Information Technology, Inc., Leesburg, VA). Total distance traveled was assessed as a measure of overall activity levels.

Zero Maze

An elevated zero maze apparatus was used to evaluate anxiety levels at 30 and 60 dpi. The circular apparatus was composed of a 10 cm wide track (100 cm outer-diameter) with walls (30 cm high) enclosing half of the track with the other half remaining open and brightly lit. Animals were given 1 trial of 5 min duration and the percentage of time spent in the enclosed half was recorded. Generally, spending more time in the dark quadrants of the track is associated with increased anxiety-like behaviors.

Morris Water Maze (MWM)

Cued and spatial water maze performance was assessed over 3 days as a measure of learning and spatial memory functions at 30 and 60 dpi. A computerized

tracking device (Noldus Information Technology, Inc., Leesburg, VA) recorded the rodent's swim path (Hartman et al., 2005). The water maze consisted of a 110 cm diameter metal tank filled with opaque water. An escape platform (11 cm diameter) was adjusted so that the platform's surface was 2 cm above the water surface for cued testing, and submerged 1 cm below the water surface for the spatial learning and memory tasks. In the cued task, the platform was placed in one of four quadrants, and the location of the platform changed for each block of trials. Animals were given 10 trials (60 sec maximum) in 5 blocks of 2 consecutive trials with a 5 sec inter-trial interval. For each trial, the rat was released into the tank opposite the platform location and allowed to search for the platform. If the rat had not located the platform within 60 sec, it was guided to it. Animals were allowed to remain on the platform for 15 sec after each trial.

For the spatial testing, the platform remained in the same location for all 10 trials and the rat was released into the tank at one of four release points and allowed to find the platform. A probe trial was administered 1.5 hrs later, in which the platform was removed from the tank, and the rats were allowed to swim for 60 sec. The percentage of time spent in the quadrant where the platform was previously located was calculated. Left/right turn bias and swim speed was also calculated during the probe trial with the percentage of left and right turns measured for each rat.

Tissue Processing and Immunohistochemistry

Rats were transcardially perfused with 4% PFA prepared in PBS at 3, 7, 30 and 60 dpi, the brains were immersed in same solution overnight, and then transferred to PBS with sodium azide (0.1%). Brains were immersed in 30% sucrose at 4°C for 48 hours and then frozen on dry ice and stored at -20°C. Sham and CCI brains were cut as coronal cryostat sections (50µm) throughout the entire length of the brain (Leica CM1850, Leica Microsystems GmbH, Wetzlar, Germany). All antibody incubations were

carried out in PBS (Fisher Scientific, Pittsburg, PA) containing 0.25% Triton X-100 and 0.25% bovine serum albumin (BSA) (both from Sigma-Aldrich Co., St. Louis, MO). After washes in PBS, sections were blocked for 1.5 hours in PBS with 1% BSA, and then incubated overnight at 4°C with mouse anti-neuronal nuclei (mouse anti-NeuN – 1:500, Chemicon International, Temecula, CA), anti-myelin basic protein (mouse anti-MBP – 1:1000 for classical or 1:200 for infra-red analysis, Chemicon International, Temecula, CA; rabbit anti-MBP – 1:1000 for classical or 1:200 for infra-red analysis, Abcam Inc., Cambridge, MA), oligodendrocyte marker anti-CNPase (1:1000 for classical or 1:400 for infra-red analysis, Abcam Inc., Cambridge, MA) or anti-neurofilament-200 (NF200 – 1:1000 for classical or 1:250 for infra-red analysis; Sigma-Aldrich Co., St. Louis, MO) antibodies. After rinsing in PBS, sections were incubated for 2 hours at room temperature with goat anti-mouse secondary antibody coupled with Alexa-Fluor-488 (1:500 or 1:1000; Molecular Probes, Invitrogen) or with goat anti-mouse secondary antibody coupled with Alexa-Fluor-800 and goat anti-rabbit secondary antibody coupled with Alexa-Fluor-680 for infra-red analysis (1:1000; Molecular Probes, Invitrogen) and subsequently washed in PBS 3x10 min. Sections for classical immunofluorescence were mounted on glass slides and coverslipped with anti-fading medium vectashield containing DAPI (Vector, Vector Laboratories, Burlingame, CA). Sections for infra-red analysis were mounted on glass slides and dried. Negative control staining where the primary antibody was omitted showed no detectable labeling. Immunostaining was carried out the same day with the same antibody mix for both sham and CCI animals for each time point.

Automated counting of NeuN positive nuclei was performed as previously described (Badaut et al.) in the dorsal parietal cortex (close to injury) and in the piriform cortex (distant from the injury) in coronal sections that exhibited a visible TBI lesion cavity. NeuN is a specific marker of neuronal nuclei only, allowing the opportunity to

count the number of positive neurons stained with NeuN, but not other cell types such as astrocytes, oligodendrocytes, or microglia (Mullen et al., 1992). The region of interest (ROI) for the ipsilateral parietal cortex (ipsi-parietal cortex) was drawn close to the lesion cavity (Figure 5) and contralateral parietal cortex (contra-parietal cortex) was a mirror image of the ipsi-parietal cortex outline in the contralateral hemisphere. Similar regions were drawn in sham animals at the same anatomical regions. All values were collected using an epifluorescent microscope (Olympus, BX41, Center Valley, PA USA) and each ROI contained 80-95 different fields (422 μm x 338 μm) quantified using Mercator software (Explora-Nova, La Rochelle, France). The threshold and morphological user-defined parameters were selected to maximize visualization of NeuN-positive staining in the regions of interest, and parameters were kept consistent for all animals. The Mercator program automatically counted only NeuN positive nuclei (Figure 4A). Accuracy of counting was previously tested on slices from control rats stained with NeuN, and no significant differences were observed between the two hemispheres (data not shown).

NF200, MBP, and CNPase coronal sections that were immunostained with infra-red secondary antibodies were scanned using the same parameters for sham and CCI with a Licor-Odyssey scanner at 21 μm /pixel resolution (Licor Bio-science, Lincoln, NE, USA). The infra-red method proposed to quantify the immunohistochemistry has been recently described by different authors (Wong, 2004; Brunet et al., 2011) and by our group (Badaut et al., 2007; Badaut et al., 2011). For surface area measurements of the CC with NF200 (Figure 5C) and MBP (Figure 6E), an average area was obtained from fields-of-interest drawn with the Licor-Odyssey analysis software around the entire CC on at least 3 coronal sections located anterior to the injury site at a distance from the disrupted CC directly below the injured area. Tissue processing after MRI and prior to immunohistochemistry (sucrose fixation, freezing, cryosectioning) may result in a

different degree of decrease in CC area from immunohistochemistry compared to MRI. Alternatively, slice thickness on MRI (1mm) compared to immunohistochemistry (50 μm) could also account for these differences. For infra-red analysis on specific regions, integrated intensity (I.I.) values were obtained from 4 – 8 coronal sections spaced at least 1.2 mm apart throughout the longitudinal brain axis (as available per brain region). For NF200 and CNPase, identical fields-of-interest were drawn using Licor-Odyssey software on both ipsilateral and contralateral hemispheres only for an analysis on the medial CC (near longitudinal fissure, adjacent to injury) and lateral CC (dorsal to rhinal fissure, ventral to injury) and a global I.I. average value was calculated for the CC only. For MBP, identical fields-of-interest were drawn using Licor-Odyssey software on both ipsilateral and contralateral hemispheres for the following brain regions: anterior commissure, medial CC (near longitudinal fissure, adjacent to injury), lateral CC (dorsal to rhinal fissure, ventral to injury), cingulate cortex, medial parietal cortex, lateral parietal cortex (dorsal to rhinal fissure, ventral to injury), and temporal/entorhinal cortex (ventral to rhinal fissure, ventral to injury). For MBP, statistical comparisons revealed no within group differences across bregma levels or ipsilateral versus contralateral hemispheres, meaning there was similar immunoreactivity for all white matter structures, and similar immunoreactivity for all gray matter structures within individual sham and CCI groups. Therefore, a global I.I. average value was calculated for the white matter tracts (anterior commissure, medial and lateral CC) and the cortical gray matter (cingulate, medial and lateral parietal, temporal/entorhinal cortices).

Electrophysiology

At 60 dpi, a separate cohort of rats was anesthetized with 3.5% isoflurane, decapitated and their brains dissected to prepare coronal slices of the CC. Slices (400 μm thick) were cut using a vibratome (Electron Microscopy Sciences, Hatfield, PA, USA)

in ice-cold artificial cerebrospinal fluid (ACSF) composed of (in mM): 130 NaCl, 3.5 KCl, 1.25 NaH₂PO₄·xH₂O, 10 MgSO₄·7H₂O, 0.50 CaCl₂, 24 NaHCO₃, 10 glucose and saturated with carbogen (95% O₂ + 5% CO₂) at a pH of 7.4. Slices were prepared from a brain region anterior to the injury site (bregma +0.5mm), transferred to a recording chamber, and superfused for at least 80 minutes with carbogen-saturated ACSF with Mg²⁺ concentration reduced to 1.5 mM and Ca²⁺ concentration elevated to 2.0 mM. During all electrophysiological recordings, slices were continuously perfused at a rate of 2-3 ml/min and maintained at 25°C. A stimulation electrode was placed in the callosal fiber tract ipsilateral to the lesion ~0.5 mm lateral to the longitudinal fissure to deliver square current pulses 0.05 ms in duration at 0.02 Hz (see inset Figure 8). Compound action potentials (CAP) were recorded with glass electrodes (tip resistance 1–3 MΩ) filled with 3 M NaCl and positioned in the contralateral CC, 1.0 mm from the stimulation electrode, and the depth was adjusted to yield a maximal CAP (~140 μm depth). Responses were amplified (Axoclamp, Axon Instruments, Foster City, CA) and digitized at a sampling rate of 10 kHz, and analyzed using Clampfit (Axon Instruments) and MiniAnalyses (Synaptosoft) software. The CAP is characterized as a biphasic waveform produced by fast-conducting, myelinated axons representing the N1 peak and slower, unmyelinated axons representing the N2 peak. The excitability of the myelinated fibers was assayed by evaluating the amplitude of the N1 peak of the CAP at incrementally increasing stimulation intensities (0.5 mA increments) until the maximal CAP amplitude was reached. Maximal CAP amplitude was used from each animal and averaged.

Statistical Analyses

All data are presented as mean ± SEM, and statistical analyses were done using GraphPad InStat version 3.05 (GraphPad Software, San Diego CA) and Sigmastat/Sigmaplot (SPSS Inc.). For behavioral data, a Kolmogorov and Smirnov test

was first performed to assess the Gaussian distribution, and parametric data were analyzed using unpaired Student t-tests and ANOVA testing followed by Tukey-Kramer for multiple comparisons, while non-parametric data was evaluated with Wilcoxon and Kruskal-Wallis tests to assess group differences. Repeated measures ANOVAs were used in cases where longitudinal data were collected on the same groups. MRI and immunohistochemical findings were assessed by unpaired Student t-tests for normally distributed data, or Mann-Whitney U analysis.

Results

All juvenile TBI (jTBI) rats survived the CCI injury (P17) from 1 day to 2 months post-TBI (adulthood; P77). There were no significant weight differences between the CCI and sham groups during the study.

Behavioral Testing

Because the TBI lesion was located in the parietal cortex, which contains somatosensory processing areas, a series of motor tests were performed to evaluate the functional impact of jTBI two months after the initial injury. We found significant impairments on the foot-fault task, with an increased number of faults at 7 dpi ($p < 0.05$) and 60 dpi ($p < 0.001$) (Figure 1A) compared to shams. In the CCI animals, we observed temporal changes from 1 dpi to 60 dpi (repeated ANOVA, $p < 0.001$) in the number of faults (Figure 1A), supporting the concept of progressive motor impairments over time. The beam balance results show impaired performance in CCI animals, with less distance traveled compared to shams from 1 to 60 dpi (Figure 1B, $*p < 0.05$, $**p < 0.01$) and no changes within each group's performance over time. Sensorimotor coordination was assessed using the rotarod (Figure 1C) and revealed that CCI animals were unable to stay on the rotating cylinder as long as shams at 30 dpi ($p < 0.05$). CCI animals

appeared to recover from this deficit by 60 dpi, indicating impaired coordination that resolved over time (Figure 1C). Analysis of turn bias from MWM tests demonstrated a significant left turn bias in CCI rats at 30 dpi ($p < 0.05$) that was maintained at 60 dpi ($p < 0.05$) (Figure 1D). Taken together, these results reveal impaired sensorimotor skills of CCI animals that persisted until adulthood.

We also administered a comprehensive battery of tests to assess exploratory behavior (open field), anxiety-like behaviors (zero maze), and learning and memory (MWM) abilities at 30 and 60 dpi. In open field testing, the total distance traveled in 30 min by the CCI group was significantly less than in sham animals at 30 dpi ($p < 0.05$) but not at 60 dpi (Figure 2A). These and the above rotarod data (Figure 1C) suggest that certain aspects of motor function recovered after TBI, whereas others did not. Analysis of the first 3 minutes of the open field test, as a marker of exploratory behavior in a novel environment (Figure 2B), showed that CCI animals moved significantly less when initially placed into the novel environment compared to sham groups at 60 dpi ($p < 0.05$), consistent with decreased motor/exploratory behaviors. Both CCI and sham animals explored less during the first 3 minutes at 60 dpi than at 30 dpi ($p < 0.001$), suggesting an effect of general maturation and/or repeated exposure to the open field. Similarly, the zero maze-test revealed no group differences in anxiety-like behaviors (measured as increased time spent in the enclosed half of the track) at 30 dpi, but a significant increase in anxiety-like behaviors in CCI animals at 60 dpi ($p < 0.05$) (Figure 2C). Our open field data suggest reduced motor performance at 30 dpi, whereas reduced exploratory behavior may be related to the emerging anxiety-like behaviors in the elevated zero maze occurring at 60 dpi.

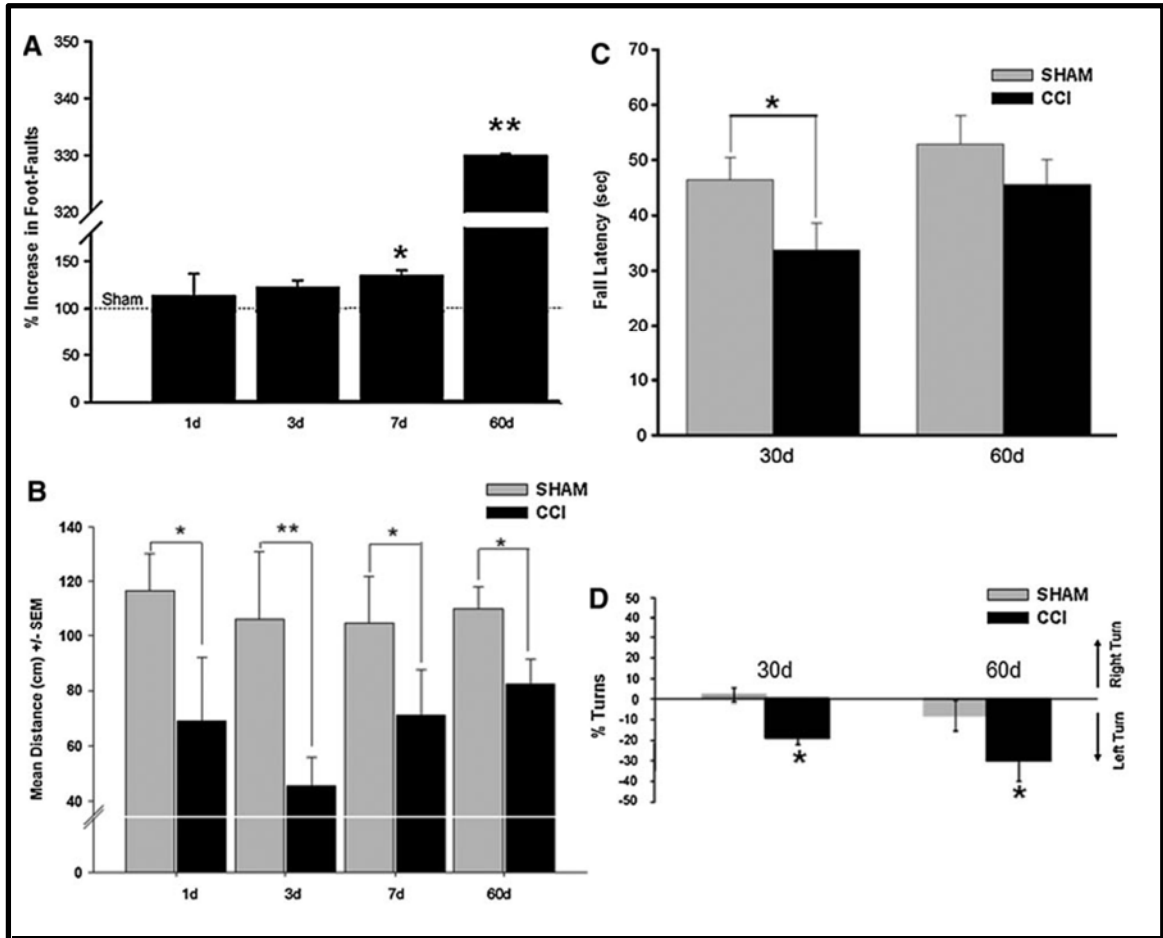


FIG. 1. (A) Sensorimotor functions were tested with the foot-fault test. There was a significant increase in the number of faults in controlled cortical impact (CCI) rats compared to their sham counterparts at 7 and 60 dpi ($*p < 0.05$, $**p < 0.01$). **(B)** Balance and coordination skills were measured with the beam balance test. The distance covered by CCI animals was significantly decreased compared to sham animals at 1, 3, 7, and 60 dpi. **(C)** Balance and coordination skills were tested with the rotarod test. Fall latency was significantly lower in CCI animals at 30 dpi ($*p < 0.05$). **(D)** Turn bias measurements indicated that the percentage of left turns (contralateral to the injury) at 30 and 60 dpi was significantly increased in CCI compared to sham animals ($*p < 0.05$; SEM, standard error of the mean).

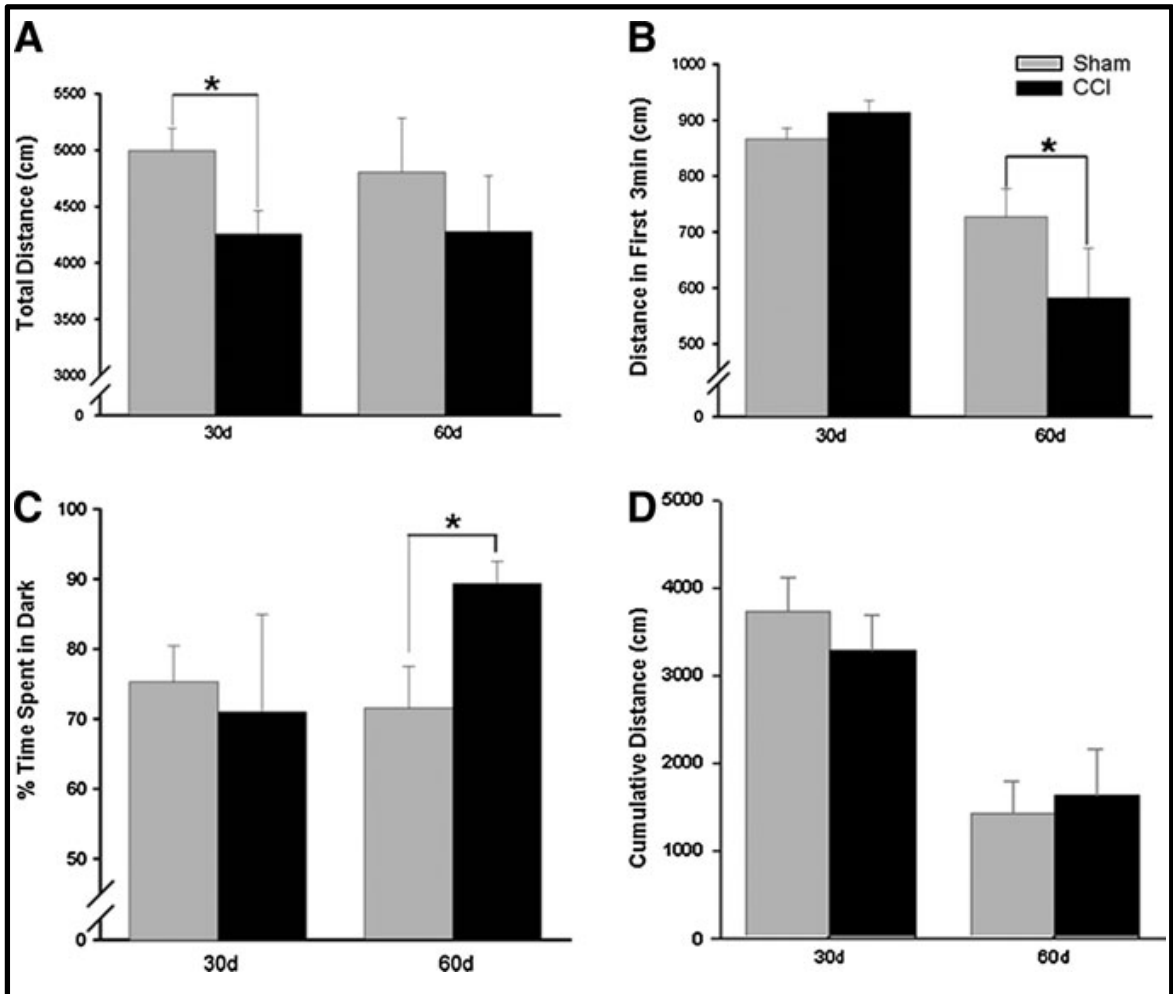


FIG. 2. (A) During open-field testing, the overall distance traveled over 30 min (10 blocks of 3 min each) revealed a significant decrease in activity in the controlled cortical impact (CCI) group compared to sham animals at 30 dpi ($*p < 0.05$). (B) The first 3-min block of activity was evaluated in sham and CCI animals, as this time would normally be used to explore the new environment into which they have been placed. At 60 dpi (but not at 30 dpi) there was a significant difference in the distance traveled in CCI compared to sham animals ($*p < 0.05$), when the CCI animals showed decreased exploratory activity. (C) The zero maze was used to assess anxiety-like behaviors, and in this test more time spent in the dark is thought to correlate with increased anxiety. We observed a significant increase in the time spent in the dark at 60 dpi ($*p < 0.05$). (D) Cumulative distance traveled by the rats to find the platform at 30 and 60 dpi was no different between the CCI and sham groups in the Morris water maze spatial test.

Learning and memory abilities after jTBI were evaluated on the cued and spatial versions of the MWM at 30 and 60 dpi (Figure 2D). Although both groups improved over time, no performance differences in overall swim speed, cued learning or spatial learning / memory were observed between sham and CCI at either time point.

MRI-Derived Lesion Volumes and Surface Area of Corpus Callosum

MRI at 3, 30 and 60 dpi was used to non-invasively measure lesion volumes (Figure 3) and the area of the CC (Figure 5A, B). The relative lesion volume measured from the T2WI might be influenced by edema formation, inflammation and cell death. Sham animals had little or no abnormalities at the site of the craniotomy, whereas CCI animals demonstrated brain injury as evidenced by increased tissue edema (Figure 3A, arrows at 3 and 30 dpi). No prominent midline shift was observed in the MR images in this model and there were only a few CCI animals that exhibited herniation of brain tissue. At 30 and 60 dpi, MRI revealed a cortical cavity that circumscribed the TBI site in fronto-parietal cortex (Figure 3A), and a 3D reconstruction (Figure 3B) revealed the rostro-caudal extent of the lesion cavity in the parietal cortex 60 days after jTBI. Lesion volumes were significantly increased in CCI animals compared to sham controls at 3 dpi (3.5% vs. 0.4% of brain volume; $p < 0.001$), 30 dpi (3.0% vs. 0.3%; $p < 0.001$), and 60 dpi (2.9% vs. 0.1%; $p < 0.001$) (Figure 3C). Lesions volumes, as defined using the parameters of hyper- and hypo-intensity described in the Methods, decreased across the 3 time-points within the CCI and sham groups ($p < 0.05$, Figure 3C). Decreased lesion volume may be a consequence of decreased edema and inflammation over time. MRI at 60 dpi was used to analyze the surface area of the CC, measured at bregma +1mm anterior to the site of the injury in CCI animals and in a comparable coronal section in shams, and showed a global decrease of 21% compared to shams ($p < 0.05$) at 60 dpi (Figure 5A, B).

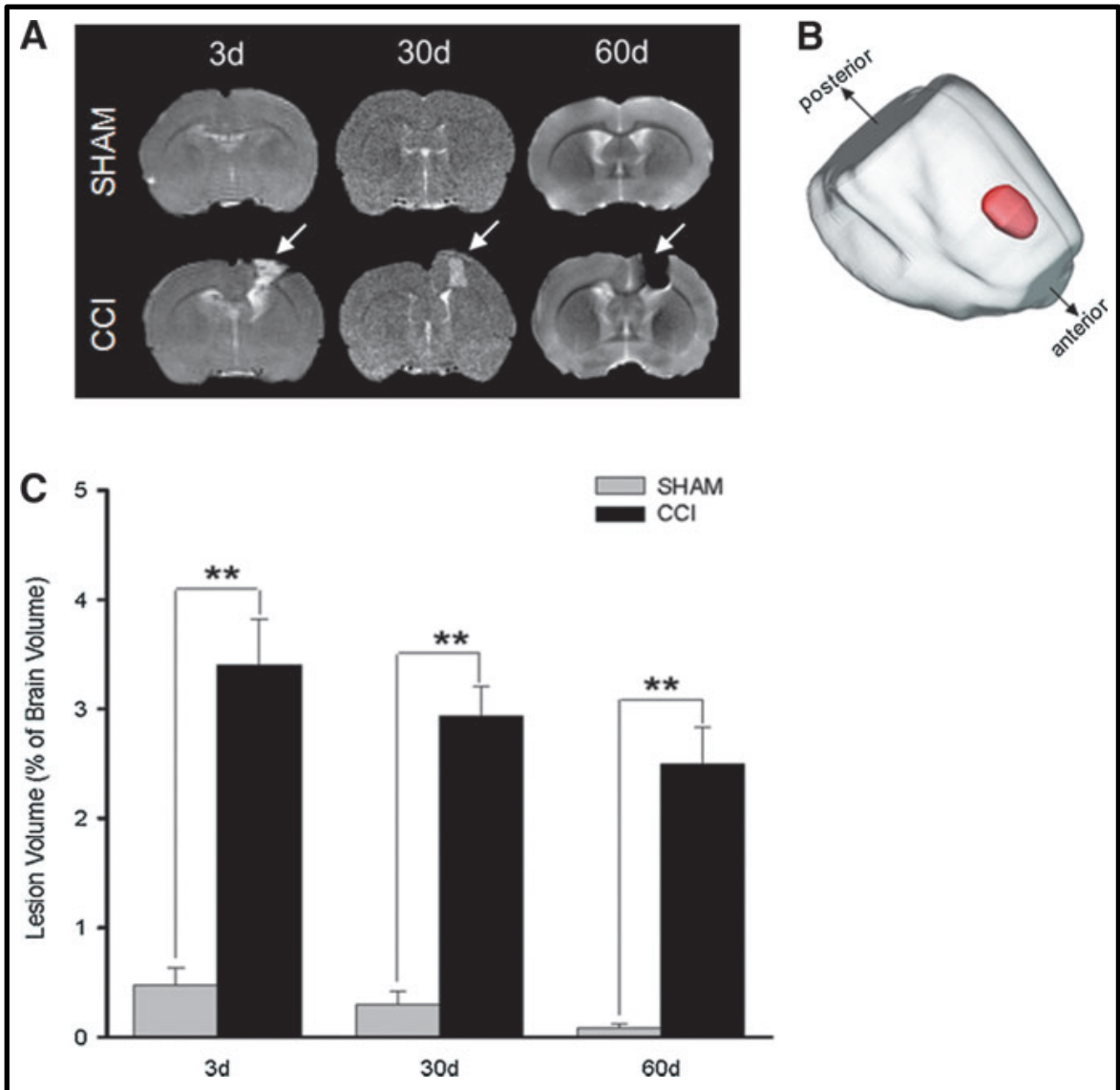


FIG. 3. (A) Magnetic resonance imaging (MRI) at 3, 30, and 60 dpi identifies the lesion (arrows) as an increase in the signal intensity at 3 and 30 dpi, and as a hole at 60dpi, corresponding to the formation of the lesion cavity. (B) A three-dimensional reconstruction of the brain (gray) and lesion (red) at 3 dpi extends to include 3% of the total brain volume. (C) The lesion volumes were significantly larger in controlled cortical impact (CCI) rats compared to their sham counterparts receiving craniotomy only (** $p < 0.001$) at all time points during our 60-day observation period. Color image is available online at www.liebertonline.com/neu

Immunohistochemical Changes following CCI

The consequences of jTBI on gray and white matter were studied at 60 dpi using immunostaining for a neuronal marker (NeuN), neuronal process marker (NF200), oligodendrocyte marker (CNPase) and myelin basic protein (MBP), both at the level of and remote from the site of injury. In sham animals, an intact cortex was observed (Figure 4A, 5A left, 6A left), whereas a cavity at the lesion site extending to the level of the CC was seen in the CCI animals (Figure 4C, arrow). This lesion impacted a relatively small portion of the parietal cortex (in accordance with the results obtained from MRI), and may be directly responsible for some of the observed behavioral deficits.

In Figure 4, NeuN staining reflects the numerical index of NeuN-positive nuclei used to assess neuronal number and DAPI staining shows no difference in cell density in images co-labeled with NeuN. The positive DAPI cells without NeuN are those of non-neuronal cells in the cortex such as astrocytes, microglia, and endothelial cells. Quantitative analyses of NeuN positive cells near the injury, in the ipsilateral and contralateral parietal cortex, revealed a 35% decrease in CCI compared to sham animals ($p < 0.05$) (Figure 4B, D, E). Quantification of NeuN in the piriform cortex, a cortical region distant from the injury site, did not show any changes in the number of neurons between groups (688 ± 117 positive NeuN cells/mm² in sham versus 545 ± 60 positive NeuN cells/mm² in CCI). At 60 dpi, our NeuN staining intensity did not change significantly (Figure 4A, C) in contrast to studies showing increased brain NeuN during the first days after injury (Liu et al., 2009). Therefore, while the intensity level, or actual brightness of NeuN staining is unchanged, the NeuN-positive nuclei reflecting neuronal number is decreased after injury. At 60 days, the observed loss of parietal neurons may be a contributing factor to sensorimotor dysfunction.

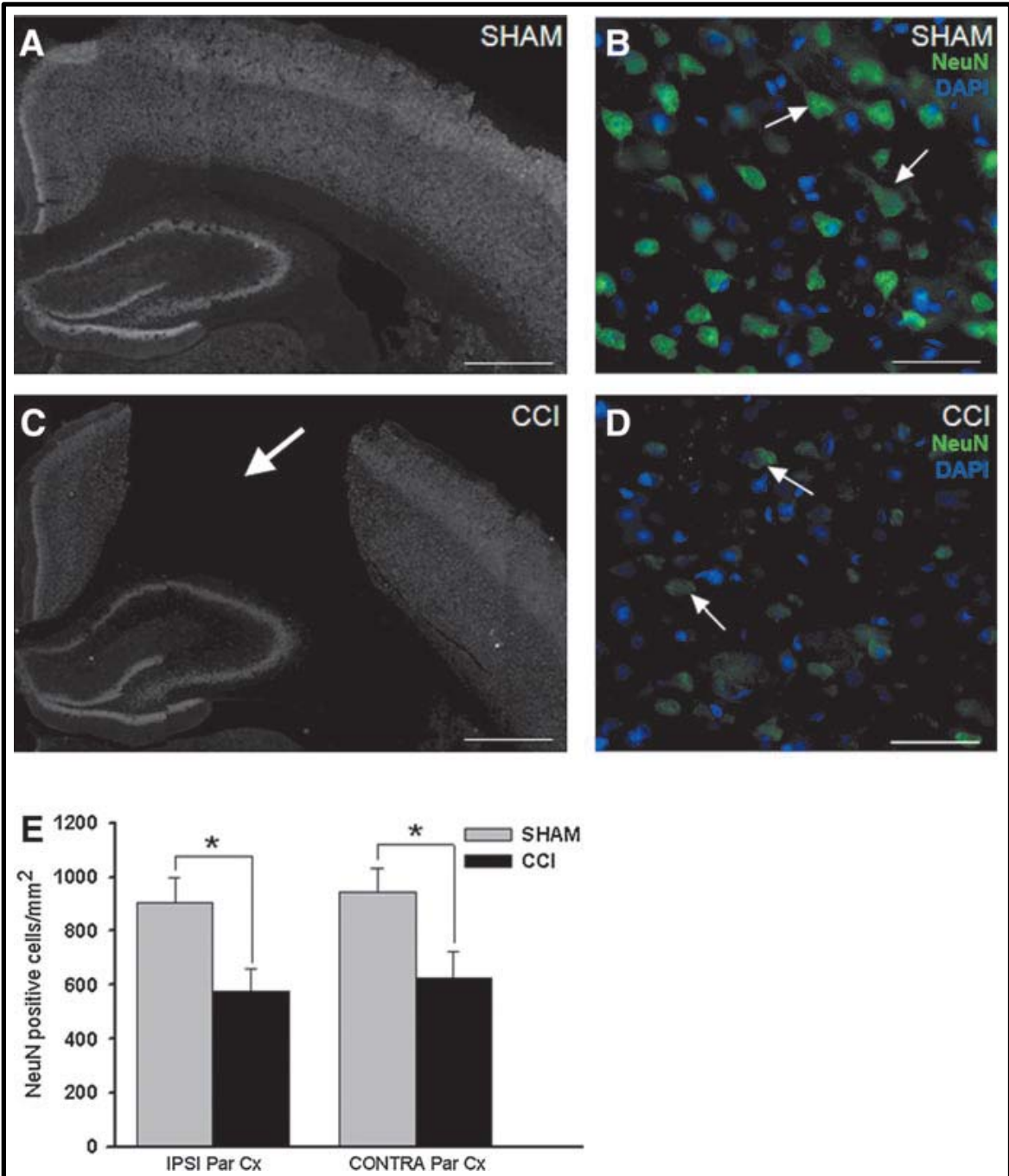


FIG. 4. (A–D) Neuronal nuclei (NeuN) immunohistochemistry at 60 dpi in the sham (A and B) and controlled cortical impact (CCI; C and D) groups showed the lesion cavity in the parietal cortex (arrow in C). The number of NeuN-positive neurons (green) was decreased in CCI (D) compared to sham (B) animals in the parietal cortex (Par Cx) at close proximity to the injury site, in tissue adjacent to the cavity. Nuclei of all cell types were stained with DAPI (blue in B and D), and automated counting of the NeuN-positive cells in the parietal cortex (E) showed a significant reduction in CCI compared to sham animals in the ipsilateral and contralateral hemispheres (* $p < 0.05$; scale bars in A and C= 200 μm ; in B and D= 50 μm ; DAPI, 4,6-diamino-2-phenylindole).

Similar to MRI analysis (Figure 5A, B), area measurements of the CC from infra-red NF200 stained coronal sections (Figure 5A, C) at 60 dpi showed a significant decrease after 7 dpi in the CC ($31\pm 1\%$ of sham, $p<0.01$) that was still present at 60 dpi ($42\pm 4\%$ of sham, $p<0.005$, Figure 5C). CC area measurements from MBP immunostaining also showed a similar decrease in CCI animals compared to shams ($p<0.05$, Figure 6E). CC area changes from MRI were highly correlated with measurements from infra-red NF200 ($r^2= 0.505$, $p<0.05$) or infra-red MBP ($r^2= 0.433$, $p<0.05$). Differences in the size of the decrease in CC area between CCI and shams from MRI and immunostaining are potentially due to tissue processing and analysis (details in Methods). However, it is clear that both quantification methods demonstrate a significant decrease in CC area at 60 dpi following CCI.

In addition to these gross morphological changes to the CC surface area following jTBI, infra-red NF200 (Figure 5), infra-red CNPase (Figure 7) and infra-red MBP (Figure 6) immunoreactivities were quantified to address the question of whether NF200, CNPase and MBP immunoreactivities were altered. Quantification of NF200 infra-red staining intensity in the CC was not significantly changed between sham and CCI at 60 dpi (Figure 5A, H). Classical immunostaining with NF200, including higher magnification images of the CC, showed similar morphological staining patterns between sham and CCI (Figure 5D-G). NF200 appears more punctate in the gray matter cortex in both sham and CCI. In the white matter, there are no obvious distorted fiber tracts, or interrupted fiber tracts that are commonly observed in other white matter injuries and models (e.g. optic nerve injury, Wang et al. 2011; spinal cord injury Cho et al., 2009; Iannotti et al., 2011). In the CC, CNPase staining intensity was not significantly changed (Figure 7A, F), in accordance with our observations at higher magnification showing no gross changes in the pattern of staining between the sham and CCI groups (Figure 7B-E). Classical CNPase immunolabeling identified occasional positive cells in the CC that

were consistent in shape and size with expected oligodendrocyte morphology (Figure 7B-E). Although no changes were detected with these antibodies and quantification methods, it remains possible that other axonal changes are occurring at the ultrastructural or molecular level.

However, in contrast to the NF200 and CNPase staining, the immunostaining and higher magnification images for MBP in Figure 6 reveal stark differences between sham and CCI. As expected during brain development (Bjelke and Seiger, 1989, Akiyama et al., 2002), sham animals demonstrated a significant global increase in MBP immunoreactivity between ages 20 to 60 days in the CC (increased $25\pm 4\%$, $p < 0.005$, data not shown). Quantification of infra-red MBP immunoreactivity in CCI (% of sham) revealed a biphasic change, with an initial increase ($25\pm 5\%$) in CCI compared to sham animals at 3 dpi, normalization at 7 and 30 dpi, and then an increase ($33\pm 9\%$) at 60 dpi in white matter tracts (Figure 6D). MBP immunoreactivity was increased in CCI at 3 dpi and 60 dpi in all anterior-to-posterior white matter tracts (average values of anterior commissure, medial and lateral CC, from bregma +1.7 to -6.0 mm, Figure 6A, D) and was also increased in CCI animals in the CC structure alone (average values of medial and lateral CC only, from bregma +1.7 to -6.0 mm, Figure 6A, $p < 0.05$, graph not shown). MBP staining in the cortex and anterior commissure values alone were higher in CCI compared to sham from bregma +1.7 to -6.0 mm, but did not reach significance (data not shown). MBP staining was consistent across bregma levels within groups, and no differences were detected for comparisons of individual white matter structures within each individual sham or CCI group. Mosaic images and higher magnification of classical immunostaining demonstrate increased MBP after jTBI at 60 dpi (Figure 6B, C). The coronal slices in sham animals show uniform MBP staining throughout individual white matter locations including the CC (Figure 6B). In contrast, CCI animals have a higher staining intensity level in the CC (Figure 6C). Similar results were obtained using a

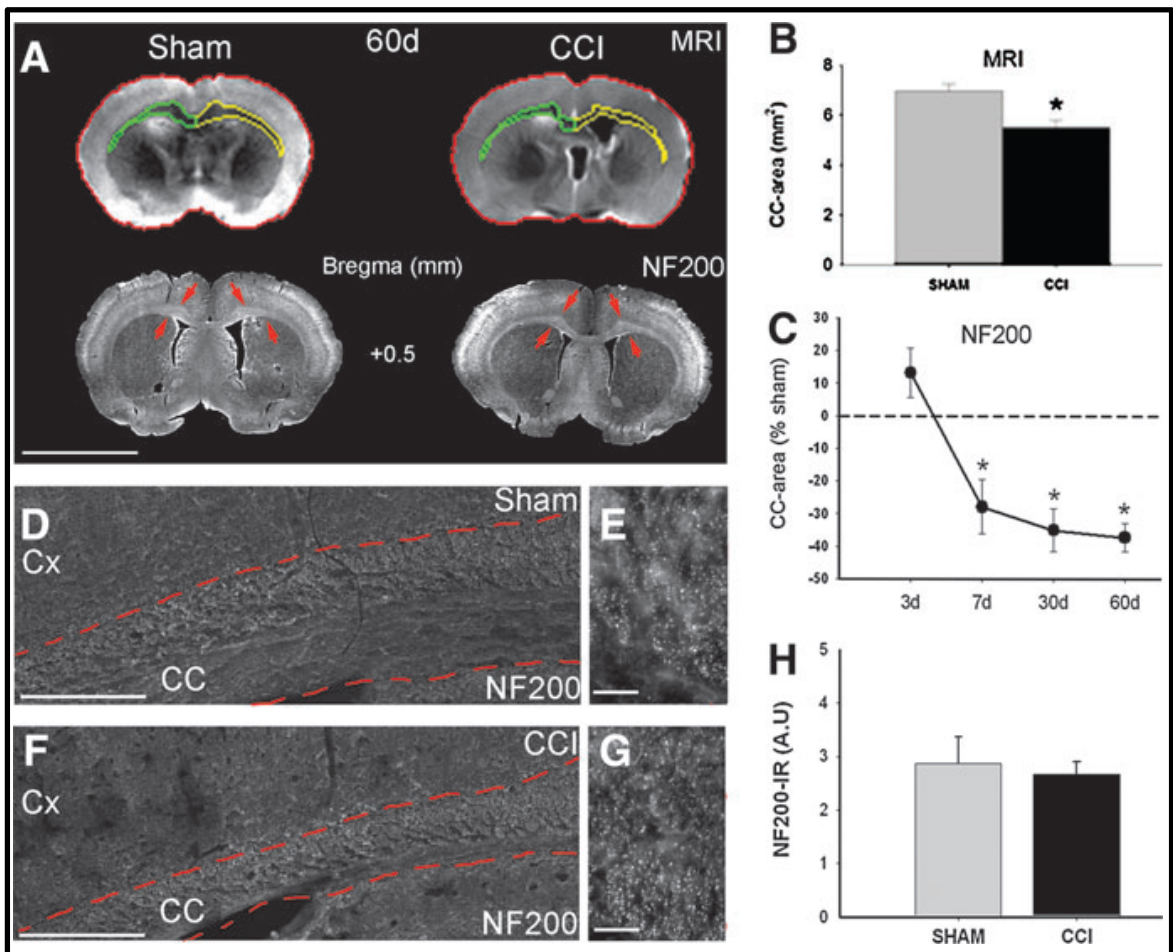


FIG. 5. (A) Slices from magnetic resonance imaging (MRI) and neurofilament-200 (NF200) immunostaining show a decreased corpus callosum (CC) size on MRI (green and yellow outlines), and NF200 immunostaining (arrows). (B) Quantification of the CC area from the MRI at 60 dpi (mm²) showed a significant decrease in CCI animals (**p* < 0.05). (C) Quantification of the CC area from the NF200 infrared immunostaining (% of sham animals) shows a significant decrease in the CCI group at 7, 30, and 60 dpi (**p* < 0.05). (D–G) Classical immunostaining with NF200 images at higher magnification in the corpus callosum (CC, red dashed outlines), and overlying cortex (Cx), showed similar morphological staining patterns, and no changes between the sham (D and E) and CCI (F and G) groups. (H) Infrared (IR) quantification of NF200 staining intensity in the CC was unchanged between groups at 60 dpi (scale bar in A = 1mm; in D and F = 500 μm; in E and G = 50 μm; A.U., arbitrary units).

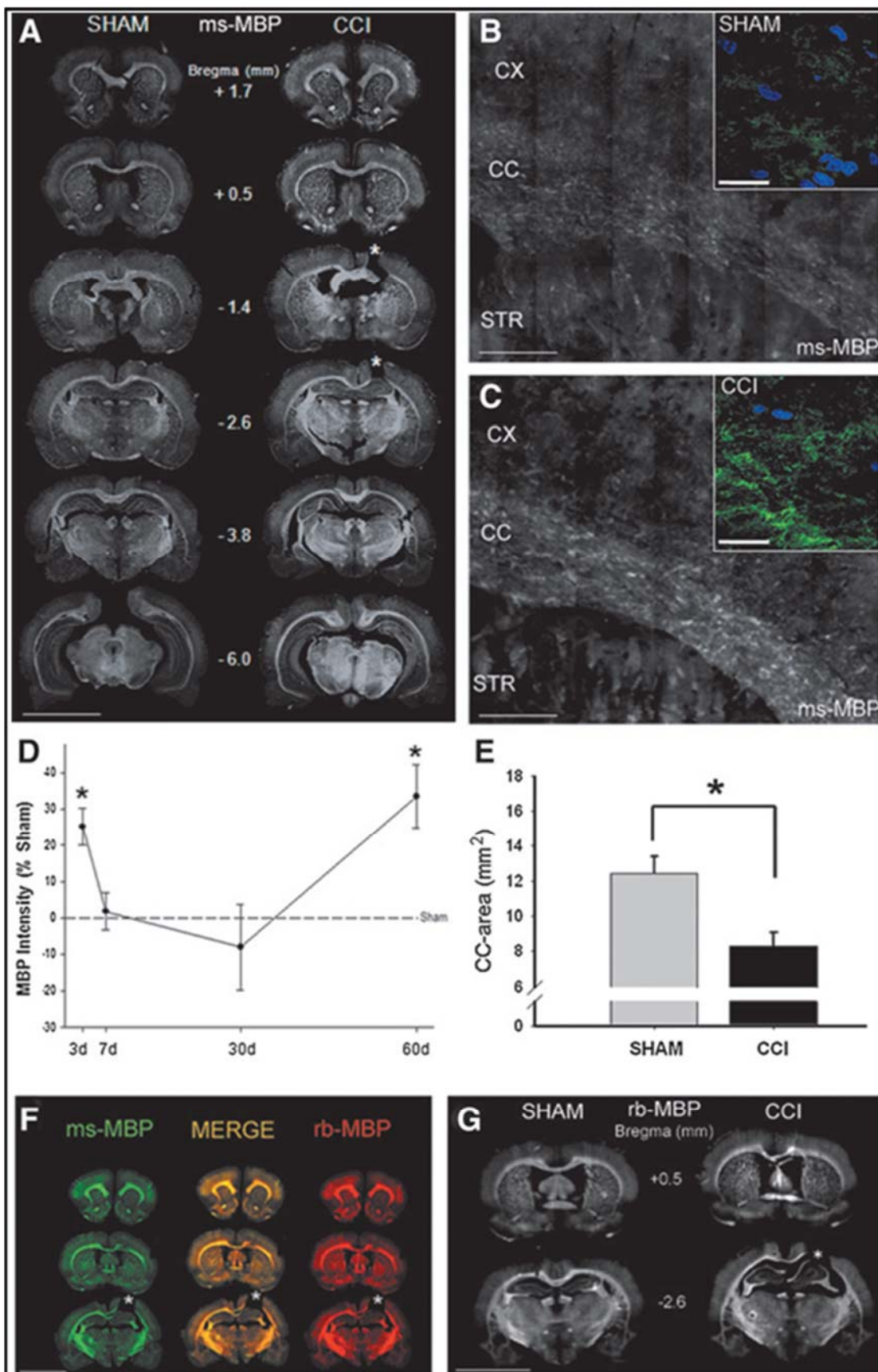


FIG. 6. Myelin basic protein (MBP) immunostaining in the sham (**A**, **B**, and **G**) and controlled cortical impact (CCI; **A**, **C**, **F**, and **G**) animals from bregma + 1.7mm to - 6.0mm. (**A**) MBP immunoreactivity using infrared antibodies with mouse anti-MBP (ms-MBP) was increased in the CCI animals compared to sham animals at the anteroposterior bregma level in white matter tracts. This global increase of MBP was also seen distant from the lesion cavity (asterisk in **A**). (**B** and **C**) Higher magnification images of classical MBP immunostaining show higher intensity in the corpus callosum (CC) compared to the striatum (STR) and cortex (CX), in (**B**) sham and (**C**) CCI animals, and increased MBP staining in the CC white matter of CCI animals (insets in **B** and **C**). (**D**) Quantification of infrared MBP staining showed a significant increase in the white matter tracts (CC and anterior commissure) of CCI animals compared to sham animals at 3 and 60 dpi ($*p < 0.05$). (**E**) CC area measurements of MBP immunostaining showed a decrease in CCI animals compared to sham animals ($p < 0.05$). (**F**) Doubleimmunolabeling with infrared MBP antibodies recognizing two different epitopes, mouse anti-MBP (ms-MBP, green) and rabbit anti-MBP (rb-MBP, red), showed co-localization in the merged images. (**G**) The intensity of the rb-MBP was increased in the CCI compared to the sham group, as indicated by ms-MBP (asterisks in **A**, **F**, and **G** indicate the lesion cavity; scale bars in **A**, **F**, and **G**= 1mm; in **B** and **C**= 200 μ m; in insets in **B** and **C**= 50 μ m).

second antibody raised in rabbit against MBP (Abcam) with a different epitope located from amino acid 150 to the N-terminus, in comparison to the antibody raised in mouse against MBP (Chemicon) that recognizes an epitope from amino acids 116-131. Both antibodies showed similar staining patterns and increases in CCI (Figure 6F-G).

Corpus Callosum Compound Action Potentials (CAP) following CCI

To assess the functional consequences of jTBI on the CC, we evaluated electrical transmission within the CC of CCI and sham animals at 60 dpi. N1 amplitudes of CAP reflect excitability of fast conducting myelinated axons (Figure 8) and represent the sum of all individual action potentials (Bolton and Carter, 1980, Velumian et al.). The average N1 amplitudes in CCI animals were significantly reduced compared to responses recorded from sham operated animals ($p < 0.005$) (Figure 8). This suggests an impairment of axonal conductance in the CC of CCI animals that is possibly associated with a decrease in the thickness of the CC (surface area) and increased MBP (immunoreactivity).

In summary, our data indicates that the CCI is a focal injury at the time of impact with formation of a cavity under the site of the impact, but immunohistochemistry and electrophysiology data suggest that the resulting jTBI continues to pathologically affect the brain in a diffuse pattern, primarily along white matter tracts.

Discussion

Using a CCI model of brain injury in juvenile rats, we have demonstrated for the first time that TBI in the developing brain is associated with acute sensorimotor deficits that persist into adulthood and also showed the delayed appearance at 60 dpi of abnormal anxiety-like behaviors. The morphological changes within the gray matter (the

presence of a cavity and reduced number of neurons) and the white matter tracts (decreased area of the CC from MRI and histology) were associated with increased MBP immunostaining and reduced trans-callosal electrical conductance remote from the lesion site. Our findings on the zero maze are consistent with the accepted notion that anxiety-like behaviors involve several brain regions such as the amygdala, and the parietal and frontal cortical areas. We believe our global analysis of gray and white matter tissue properties also demonstrate that a local impact evolves to a global change that may affect overall brain function. Specifically, our results suggest that TBI in juvenile rats produces long-lasting changes in gray and white matter properties and impairments of electrical signaling in major axonal pathways that may explain the observed sensorimotor deficits and anxiety-like behaviors.

Our observations in this jTBI rodent model corroborate clinical reports that highlight the persistence of neurological, cognitive, behavioral, and psychosocial sequelae after childhood TBI (Lippert-Gruner et al., 2006, Goold and Vane, 2009). In human subjects, these impairments last from a few months to 50 years post-injury and impact activities of daily living (Yeates et al., 2002, Brenner et al., 2007). A wide range of deficits have been clinically described, including slowed information processing, impaired judgment, attention deficit hyperactivity disorder, hampered reasoning and problem-solving skills, mood disorders, anxiety, aggression and anti-social behaviors (Cattelani et al., 1998, Max et al., 2004, Brenner et al., 2007, Prigatano, 2008).

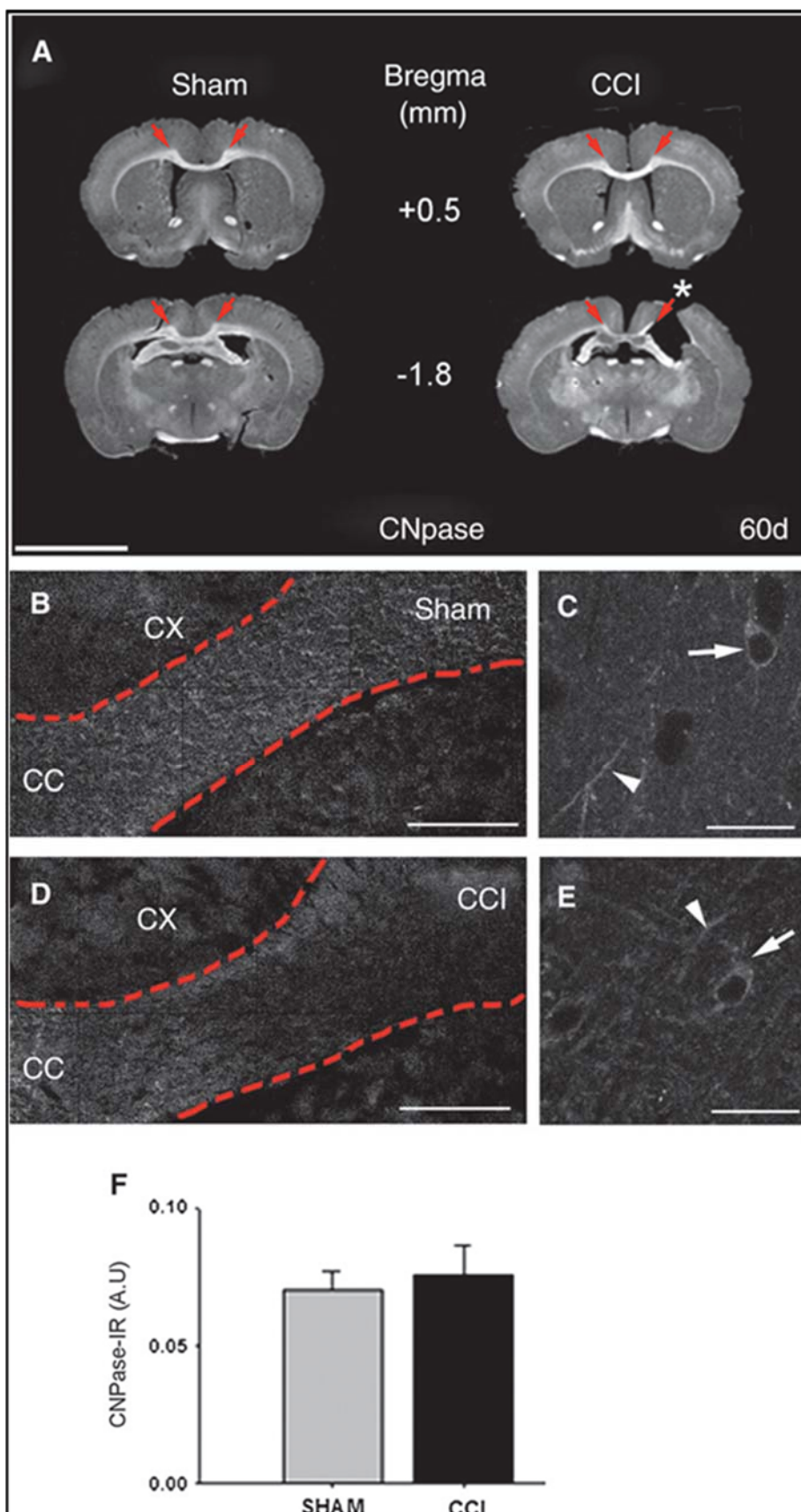


FIG. 7. (A) CNPase immunolabeling along white matter tracts is shown in representative coronal sections near the lesion (bregma - 1.8mm), and anterior to the lesion cavity (bregma + 0.5mm), with bright levels of CNPase staining with infrared (IR) antibodies localized to white matter tracts in the corpus callosum (CC; groups of red arrows). (B–E) Classical CNPase staining at higher magnification shows similar staining patterns in the CC (red dashed outlines), and on individual oligodendrocyte cell bodies (arrows), and processes (arrowheads) of (B and C) sham, and (D and E) controlled cortical impact (CCI) animals. (F) Quantification of infrared staining in the CC across several coronal slices shows no statistically significant differences between the sham and CCI groups for CNPase staining levels (CX, cortex; asterisk in A indicates lesion cavity; scale bar in A=1mm; in B and D= 200 μ m; in insets in C and E = 20 μ m; A.U, arbitrary units).

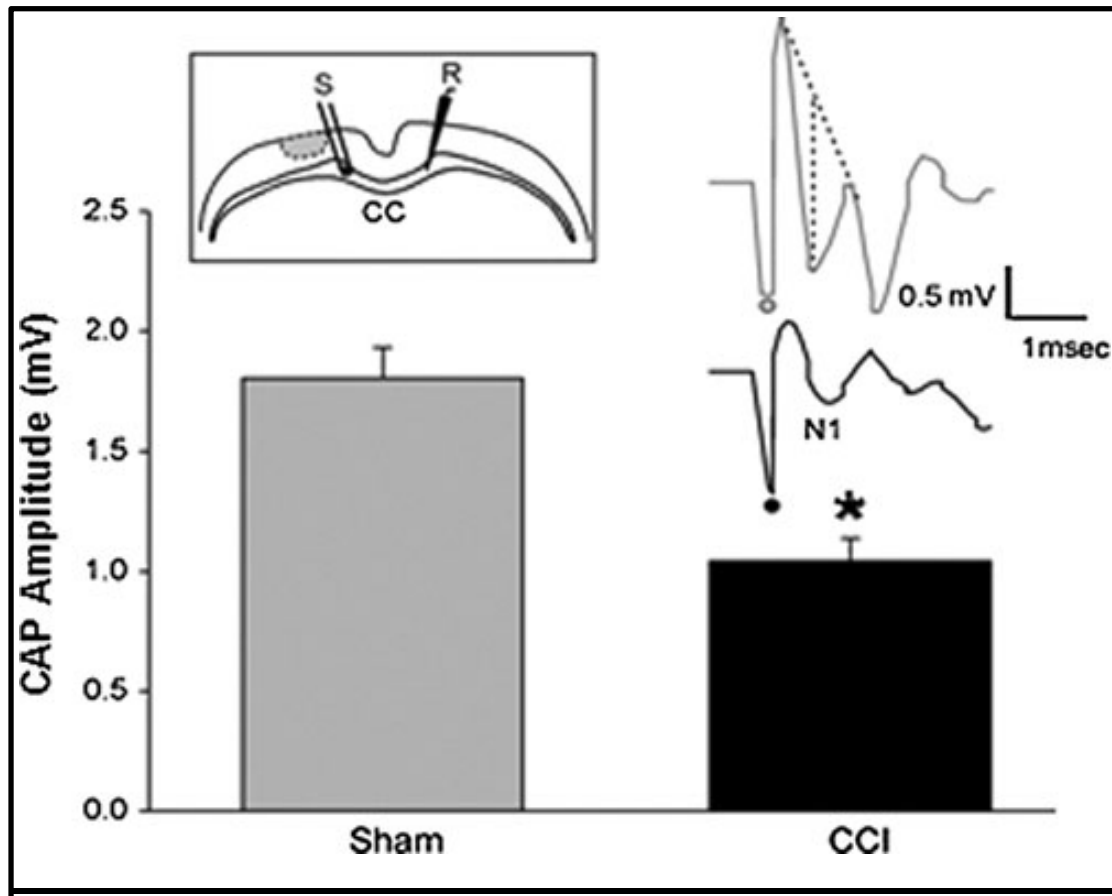


FIG. 8. Electrophysiology in the corpus callosum (CC) at 60 dpi shows N1 amplitudes recorded after compound action potentials (CAP) were evoked. The stimulating electrode (S) was placed on the side of injury (or sham surgery), located approximately 1mm from the recording electrode (R). Quantification shows that N1 amplitudes were significantly decreased in controlled cortical impact animals compared to sham animals (* $p < 0.005$).

A focal injury to the parietal sensorimotor cortex in P17 rats resulted in a 35 mm³ lesion volume (~3% of total brain volume) at 60 dpi (Figure 3B), which is comparable to previously published data (Prins et al., 2005). The lesion volume remained relatively stable over 60 dpi (Figure 3C) despite the emergence of specific motor and behavioral impairments. In fact, motor dysfunction was observed within the first week and persisted until 60 dpi (Figure 1). Early increases in foot faults and decreased distance covered on beam balance tests are similar to results described in a closed head injury model using P17 mice (Adelson et al., 2000). The recovery that we observed in rotarod testing in the CCI group at 60 dpi may be due to a combination of learning effects, age-related brain development, and reduced sensitivity of this particular test to small deficits in motor planning, proprioception and coordination which other tests such as foot fault can detect (Barreto et al., 2010). In accordance with other investigators (Prins and Hovda, 1998), we did not find major deficits in spatial learning and memory using water maze testing at 30 and 60 dpi. However, jTBI induced the development of anxiety-like behaviors that emerged only in adulthood (Figure 2C), which was revealed by the longer time spent in the enclosed part of the zero maze combined with reduction of the exploratory activity in the first 3 minutes of open field testing (Figure 2B). These results are similar to clinical observations of the delayed onset of anxiety in adult patients after TBI (Whelan-Goodinson et al., 2009). The acute decrements in motor function (i.e., increased of incidence of foot faults and asymmetric turning behavior) are likely the result of the initial lesion and local neuronal cell death in the sensorimotor cortex (Nishibe et al., 2010) (Figures 1 - 4). The persistence and progressive worsening of these motor functions could possibly be due to the cavitation of the motor cortex as well as to impaired axonal conductance associated with the global changes in white matter tracts (Figure 1, 4 - 8). As noted above for the rotarod test, the absence of differences between the groups for

open field testing at 60 dpi (Figure 2A) may be due to learning or habituation effects resulting from repeated testing (Russell and Williams, 1973).

Clinical imaging studies have emphasized the vulnerability of white-matter pathways, such as the CC and anterior commissure, after TBI (Holshouser et al., 2005, Wilde et al., 2006, Wu et al., 2010). These structural changes may alter the level of MBP, a primary protein involved in myelin sheath formation. Several reports have studied MBP in human serum and cerebrospinal fluid (CSF) following pediatric and adult TBI, as a potential biomarker of injury severity (Berger et al., 2005, Sandler et al., 2010). For example, serum MBP was increased in children for up to 2 weeks following TBI (Berger et al., 2005). Thus, we sought to explore the relation between white matter tract changes using MRI, histology and electrophysiology and behavioral changes in adulthood after jTBI. Morphological analysis of white matter tracts using MRI and histology revealed decreased callosal thickness starting at 7 dpi that persisted to 60 dpi, findings that are similar to white matter loss observed in humans (Kraus et al., 2007, Wu et al., 2010). Our data show the CC is damaged in this CCI model at the site of the impact, but also at distance from the lesion site, with no recovery over time (Fig 3-8).

The permanently decreased area of the CC over the 60-day observation period (measured with MRI, NF200 and MBP) contrasts with the temporal callosal changes in MBP staining that we measured by infra-red quantitative-immunohistochemistry (Figure 5, 6). We found early increased MBP staining at 3 dpi, which may reflect injury-induced myelin changes. Indeed, increased MBP levels were previously reported in an adult rat TBI model and attributed to MBP fragmentation at 3 dpi (Liu et al., 2006). MBP staining was normalized to sham levels at 7 dpi and 30 dpi, despite the significant decreases in CC thickness (Figure 5, 6). In adult TBI models, early myelin fragmentation is due to increased calpain activity that also normalizes 7 days after TBI (Liu et al., 2006). However, our MBP staining normalization was transient and by 60 dpi we observed a

global increase in MBP staining in white matter tracts throughout the anterior-posterior extent of the brain in CCI compared to sham (bregma +1.7 to -6.0 mm) (Figure 6A). We also showed an absence of CNPase and NF200 staining changes in the CC, in parallel with increased MBP staining at 60 dpi. Thus, increased MBP staining is likely not a result of increased number of oligodendrocytes (CNPase) in the white matter. It remains possible that MBP fragmentation may play a role, or overexpression associated with an attempt of the brain to compensate for myelin loss (Ihara et al., 2010), but the exact mechanism needs further exploration in this CCI model. Previous studies indicate that glucocorticoids may influence MBP, as they are known to enhance the rate of myelin formation (Chan et al., 1998) and are elevated after brain injury as part of the innate immune response (Glezer and Rivest, 2004).

In conjunction with decreased callosal white matter thickness and increased MBP-staining, we found electrophysiological evidence of deficient CC conductivity after jTBI compared to shams (Figure 8), suggesting a possible functional basis for some of the behavioral deficits. The decreased CAP suggests that the increase of MBP observed in CCI animals is non-functional and insufficient to compensate for the loss of axons after CCI. Our findings are similar to a recent report in mice showing that myelin proteolipid protein (PLP1) overexpression was associated with decreased axonal conductance velocity (Tanaka et al., 2009). Interestingly, Kodama et al (2008) used the same mouse anti-MBP antibody (Chemicon) and found increased MBP protein levels in adulthood following early weaning. They ascribed their MBP increase to the 21.5 kDa isoform only, which suggests that increased MBP observed in their study and our jTBI model may not be necessarily localized in the myelin sheath. This hypothesis is supported by our electrophysiological data that showed decreased axonal conductance in spite of increased MBP staining, but additional electron microscopy studies would be needed for confirming precise localization. Further, our data showing decreased CC

thickness post-TBI is consistent with a decrease in the number of fibers that may contribute to a decrement in function.

Morphological and functional changes in white matter tracts after jTBI may explain the persistence of motor dysfunction and the development of anxiety-like behaviors in adulthood. Clinically, non-mechanical stressors early in life are associated with long-term behavioral changes and can also result in altered myelin development and reduced size of white matter tracts. For example, children with post-traumatic stress disorder have a smaller CC volume compared to healthy subjects when they reach adulthood (Bremner et al., 1995). In rodent models, early weaning of rats pups at P17 induces an increase in MBP and development of anxiety-like behaviors (Kodama et al., 2008). Our induction of a cortical mechanical-stress (CCI) at the same developmental age also induced an increase in MBP immunoreactivity and development of anxiety-like behaviors that emerged during adulthood. In the rodent, P14-P21 is a critical maturation period for central axonal myelination (Akiyama et al., 2002), and it is likely that a stressor (early weaning or TBI) during this critical period may induce long-term changes in myelination and behavior. The developmental changes in myelin proteins (MBP, PLP) were associated with a physiological response to stress and emotional states, including anxiety and depression in adulthood (Kodama et al., 2008, Ono et al., 2008, Tanaka et al., 2009). Thus, despite the presumed neuroplasticity of the juvenile brain after jTBI, there is likely insufficient cortical reorganization or compensation to completely reverse injury-induced deficits.

Conclusion

Our findings showed that a focal TBI results in lasting behavioral deficits (decrements in motor function and late emergence of anxiety-like behaviors) similar to those seen in human TBI patients, as well as global alterations in white matter

(decreased thickness of white matter tracts, increased MBP immunoreactivity), leading to long-term changes in neuronal function (decreased neuronal number and axonal conduction). A mechanical stress to the cortex during a sensitive developmental window of myelin formation resulted in long-term changes in the morphology of white matter tracts as seen with changing MBP immunoreactivity that appear concurrently with decreased axonal output and behavioral changes. However, the molecular mechanisms and changes in oligodendrocytes underlying MBP increases in adulthood after TBI have yet to be determined, and would suggest new avenues for development of novel pharmacological therapies.

Acknowledgements

The authors thank Mr. Dane W. Sorensen for his technical help in this work, and Monica Rubalcava at the Advanced Imaging and Microscopy facility at Loma Linda. This work was supported in part by the National Institutes of Health (R01HD061946), the Pediatric Research Fund, the Swiss Science Foundation (FN 31003A-122166 and IZK0Z3-128973), the Department of Pediatrics, and a NASA Cooperative Agreement (NCC9-149) to the Radiobiology Program, Department of Radiation Medicine, at Loma Linda University.

Author Disclosure Statement: No competing financial interests exist.

PROLOGUE TO CHAPTER 2B
EARLY BRAIN INJURY ALTERS THE BLOOD–BRAIN BARRIER
PHENOTYPE IN PARALLEL WITH *B*-AMYLOID AND COGNITIVE
CHANGES IN ADULTHOOD

This second section of chapter 2 describes alterations to blood-brain barrier (BBB) phenotype which are detectable in adult rodents that had been subjected to juvenile traumatic brain injury (jTBI) at a developmental time period (P17). This change in BBB phenotype was studied in conjunction with: (a) accumulation of β -amyloid ($A\beta$), and (b) changes in cognitive function. The section demonstrates that there are both structural and functional changes in the BBB at long-term, brought about by jTBI at a developmental time period. It provides some evidence in support of the theory that TBI at a young age could predispose the brain's blood vessels as well as the BBB to detrimental long-term changes with possible functional deficiencies, such as alteration in clearing of $A\beta$ and lowering of cognitive abilities. BBB alterations may therefore be explored as a therapeutic avenue in jTBI.

The customized controlled cortical impact (CCI) injury model in P17 rats (reported in section 2A) was used as a developmental model of TBI. Morris Water Maze (MWM) test was customized to assess not only spatial learning and spatial memory, but also preferred swim strategies used by the tested rodents at 30 and 60 days post injury (dpi). Immunohistochemical methods were used to test for both BBB marker proteins such as claudin 5 and Immunoglobulin G (IgG). Immunolabeling and western blotting techniques were also employed to assess $A\beta$ accumulation. The hypothesis for this section is that acquisition of TBI in early life may yield detectable long-term changes in

BBB components, such as tight junctions and influx/efflux transporters, in parallel with aberrant A β accumulation and cognitive dysfunction.

This section of chapter 2 has been published as a scientific article in the November 14, 2012 edition of the *Journal of Cerebral Blood Flow & Metabolism* (volume 33, pages 205 - 212) under the same title as above. It is complete with abstract, introduction, methods, results and discussion sections.

CHAPTER 2B

EARLY BRAIN INJURY ALTERS THE BLOOD-BRAIN BARRIER
PHENOTYPE IN PARALLEL WITH *B*-AMYLOID AND COGNITIVE
CHANGES IN ADULTHOOD

**Viorela Pop^{1,5}, Dane W. Sorensen^{1,2,5}, Joel E. Kamper³, David O.
Ajao², M. Paul Murphy⁴, Elizabeth Head⁴, Richard E. Hartman³,
and Jerome Badaut^{1, 2}**

¹Department of Pediatrics, Loma Linda University, Loma Linda, California;

⁷Department of Physiology, Loma Linda University, Loma Linda, California; ⁸Department of Psychology, Loma Linda University, Loma Linda, California; ⁴Sanders-Brown Center on Aging, University of Kentucky, Kentucky, USA.

⁵These authors contributed equally to this work.

Correspondence: Dr. J. Badaut, Department of Pediatrics, Pharmacology and Physiology, Loma Linda University, School of Medicine Coleman Pavilion, Room A1120 11175, Campus Street, Loma Linda, CA 92354, USA. E-mail: jbadaut@llu.edu

This study was supported in part by the NIH R01HD061946 and the Swiss Science Foundation (FN 31003A-122166 and IZK0Z3-128973) (to J. Badaut).

Running title: Blood-Brain Barrier changes after juvenile TBI

Received 12 May 2012; revised 14 September 2012; accepted 25 September 2012

Journal of Cerebral Blood Flow & Metabolism advance online publication, 14 November 2012; doi:10.1038/jcbfm.2012.154

© 2012 ISCBFM All rights reserved 0271-678X/12

Abstract

Clinical studies suggest that traumatic brain injury (TBI) hastens cognitive decline and development of neuropathology resembling brain aging. Blood–brain barrier (BBB) disruption following TBI may contribute to the aging process by deregulating substance exchange between the brain and blood. We evaluated the effect of juvenile TBI (jTBI) on these processes by examining long-term alterations of BBB proteins, β -amyloid ($A\beta$) neuropathology, and cognitive changes. A controlled cortical impact was delivered to the parietal cortex of male rats at postnatal day 17, with behavioral studies and brain tissue evaluation at 60 days post-injury (dpi). Immunoglobulin G extravasation was unchanged, and jTBI animals had higher levels of tight-junction protein claudin 5 versus shams, suggesting the absence of BBB disruption. However, decreased P-glycoprotein (P-gp) on cortical blood vessels indicates modifications of BBB properties. In parallel, we observed higher levels of endogenous rodent $A\beta$ in several brain regions of the jTBI group versus shams. In addition at 60 dpi, jTBI animals displayed systematic search strategies rather than relying on spatial memory during the water maze. Together, these alterations to the BBB phenotype after jTBI may contribute to the accumulation of toxic products, which in turn may induce cognitive differences and ultimately accelerate brain aging.

Keywords

Amyloid; claudin 5; endothelial; juvenile; P-glycoprotein; traumatic brain injury

Introduction

Traumatic brain injury (TBI) is defined as damage resulting from a direct or indirect biomechanical force on the brain, and pathophysiological outcomes emphasize damage to neurons and glia. However, the blood-brain barrier (BBB) and vascular integrity are also compromised following TBI. Primary injury occurs at the moment of TBI impact, with disruption of blood vessels and the BBB, contributing to vasogenic edema formation (Pop and Badaut, 2011). BBB disruption precedes several downstream events contributing to secondary injuries, such as changes in cerebral blood-flow and hypometabolism, brain swelling and increased intracranial pressure, hypoxia/ischemia, and related molecular events such as cell death, inflammation, oxidative stress, and pathology (Pop and Badaut, 2011). BBB disruption normalizes within one week in several injury models, yet recent studies show BBB permeability up to 30 days after ischemic insult (Strbian et al., 2008). Collectively, these observations suggest that BBB integrity represents a complex and dynamic sequelae meriting attention during acute and delayed stages post-TBI.

Vascular dysfunction is a critical element of brain aging and neurodegeneration, especially in Alzheimer disease (AD) (Nicolakakis and Hamel, 2011). Age-related brain $A\beta$ accumulation may depend on progressively impaired clearance mechanisms, as measured by *in vivo* kinetics of $A\beta$ in cerebrospinal fluid of AD and control patients (Mawuenyega et al., 2010). At the endothelial interface, the central molecular participants in the bidirectional flow of substances are the transporters P-glycoprotein (P-gp) and low-density lipoprotein-related receptor protein 1 (LRP1) for brain-to-blood efflux, and the receptor for advanced glycation end products (RAGE) for blood-to-brain influx (Ueno et al., 2010). In fact, decreased P-gp or LRP1 on endothelial cells are linked to increased $A\beta$ and neurodegeneration in human brain aging, AD, and aging rodents (Silverberg et al., 2010). In addition, P-gp knock-out mice administered intra-cerebral $A\beta$

peptides have decreased brain-to-blood clearance and increased brain $A\beta$ (Cirrito et al., 2005), suggesting P-gp as a key player in parenchymal $A\beta$ clearance. After brain trauma, little is known about the pathophysiological timeline of vascular damage and healing, or whether BBB changes affect long-term TBI outcome.

Clinically, several lines of evidence demonstrate long-term pathological and behavioral modifications after TBI. These long-term changes may lead to premature aging and neurodegenerative processes like AD with higher risk for aberrant $A\beta$ protein accumulation (Johnson et al., 2010). In support of this, brain $A\beta$ immunolabeling was detected within hours after clinical TBI (Ikonovic et al., 2004) and in long-term survivors (1 to 47 years) of a single injury (Johnson et al., 2012). As for patient outcome, many TBI survivors endure lifelong consequences, with 3.2 to 5.3 million US residents currently suffering physical and/or mental disability which can result in long-term complications (Zaloshnja et al., 2008). Young children, followed by adolescents and older adults, are at greatest risk for incurring TBI (Faul et al., 2010). Therefore, long-term studies on cellular and molecular changes after TBI are needed in juvenile experimental models, especially regarding collective changes in the BBB phenotype, neuropathology, and behavior.

We hypothesized that an early life juvenile TBI (jTBI) may result in several brain changes. We evaluated BBB components (tight junctions, influx/efflux transporters) in parallel with neuropathology and aberrant protein accumulation ($A\beta$) and cognitive outcomes (learning and memory). A controlled cortical impact (CCI) was delivered to the parietal cortex of juvenile (17 day old) rats and outcomes are described in adults at 60 days post injury (dpi).

Materials and Methods

Animals

All protocols and procedures were approved by the Institutional Animal Care and Use Committee of Loma Linda University. Juvenile (Literature descriptions for “juvenile” include a broad range of post-natal ages (Babikian et al., 2010). Based on previous publications and our recently published data (Ajao et al., 2012) , we used post-natal day 17 as “juvenile” which is identical to methods in the present manuscript.) (17 day old) male Sprague-Dawley rats (Harlan, Indianapolis, IN) were housed with their dams on a 12-hour light-dark cycle at constant temperature and humidity. Only male rats were selected, as prior studies suggest the existence of gender differences following TBI (Wagner et al., 2004). Pups were weaned 7 days after the surgery, housed 2 rats per cage, and fed with standard lab chow and water *ad libitum*. At 60 dpi, animals were euthanized, and brain tissue was collected for immunohistochemical studies (n=8 sham and n=8 jTBI). An additional group of animals (n=10 sham, n=10 jTBI) was studied longitudinally in the water maze (30 and 60 dpi).

Juvenile Traumatic Brain Injury Model

Controlled cortical impact (CCI) was induced in rats as previously described (Ajao et al., 2012). Briefly, rats were anesthetized with isoflurane (Webster Veterinary Supply, Sterling, MA) and given a 5 mm diameter craniotomy over the right fronto-parietal cortex (1 mm posterior, 2 mm lateral from Bregma) and CCI was delivered to jTBI animals using a 3 mm impactor at a 20° angle to cortex, 1.5 mm depth, 200 ms impact duration, 6 m/s velocity. Body temperature was maintained at 37°C during surgery. A subcutaneous buprenorphine injection was administered for pain relief (0.01mg/ml/kg at 1 hr and 24 hrs post-surgery) and animals were returned to their dams. All Sham animals underwent the same procedures as jTBI animals, except for the CCI.

Table 1. Description of MWM swim strategies observed after jTBI		
<i>Learning Strategy</i>	<i>Swim pattern</i>	<i>Description</i>
Spatial	Spatial direct	Animal swims directly to the platform
	Spatial indirect	Animal swims to the platform with slight deviation from a true course
	Focal correct	Animal swims to and searches in proximal quadrant for platform
Systematic	Scanning	Animal searches the interior portion of the tank without spatial bias
	Random	Animal searches entire tank without spatial bias
	Focal incorrect	Animal swims to and searches in an incorrect portion of the tank
	Chaining	Animal swims in repetitive loops in the middle of the tank
Looping	Peripheral looping	Animal swims in repetitive loops around the tank's perimeter

jTBI, juvenile traumatic brain injury; MWM, Morris Water Maze

Water Maze Design and Testing

Water maze (WM) testing has been previously described for this model (Ajao et al., 2012). Briefly, testing occurred at 30 and 60 dpi over a 3-day paradigm, with 5 blocks of 2 trials each (10 total trials) including cued testing (visible platform), spatial learning (hidden platform) and probe trials for spatial memory (no platform). Swim strategy analysis (Brody and Holtzman, 2006) revealed 8 different swim patterns grouped into three general learning strategies (Table 1 and Figure 5A): Spatial strategy (spatial direct, spatial indirect, focal correct), Systematic strategy (scanning, random, focal incorrect), or Looping strategy (chaining, peripheral looping).

Brain Tissue Processing and Immunohistochemistry

At 60 dpi, rats were anesthetized with a combination of Ketamine (Ketaject 100mg/ml, Phoenix, St. Joseph, MO) and Xylazine (AnaSed 100mg/ml, Lloyd Laboratories, Shenandoah, IA) at the appropriate dose/body weight, and then transcardially perfused with 4% paraformaldehyde. Brains were excised and cryoprotected in 30% sucrose solution for 48 hrs, and frozen on dry ice. Coronal cryostat free floating sections (50 μ m) were cut and collected as serial sections spaced 1.2 mm apart, then processed for standard immunohistochemistry experiments as previously described (Ajao et al., 2012).

Immunoglobulin G Extravasation Staining for Blood–Brain Barrier

Sections were rinsed in PBS and blocked for 1 hour in 1% bovine serum albumin (BSA) (Sigma-Aldrich Co., St. Louis, MO) made in PBS, pH=7.4 (Fisher Scientific, Pittsburg, PA) prior to incubation for 2 hrs at room temperature with Alexa-Fluor-800 biotin conjugated affinity purified goat anti-rat IgG (1:500, Rockland Immunochemicals,

Gilbertsville, PA) in PBS containing 0.25% Triton X-100 and 0.25% BSA (Sigma-Aldrich Co., St. Louis, MO) made in PBS, pH=7.4. After washing, sections were scanned on an Odyssey infra-red scanner to quantify fluorescence in the cortex and striatum.

Immunolabeling of Blood–Brain Barrier Proteins

For P-gp staining, sections were pre-treated for antigen retrieval using 33% acetic acid + 66% EtOH solution for 10 min at 20°C (Fisher Scientific, Pittsburg, PA). For claudin 5, glial fibrillary acidic protein (GFAP), P-gp, LRP1, and RAGE, sections were blocked for 1 hour in 1% BSA in PBS prior to overnight primary antibody incubation at 4°C. All antibody incubations were in 0.25% BSA with 0.25% Triton X-100 made in PBS, pH=7.4. For immunolabeling, we used mouse anti-claudin 5 (1:500, Life Technologies: Invitrogen, Grand Island, NY), mouse anti-P-gp (1:100, Abcam Inc., Cambridge, MA and Calbiochem, EMD Chemicals, Merck KGaA, Darmstadt, Germany), mouse anti-LRP1 (1:1000, Calbiochem, EMD Chemicals, Merck KGaA, Darmstadt, Germany), rabbit anti-RAGE (1:500, Abcam Inc., Cambridge, MA) and chicken anti-GFAP (1:1000, Millipore, Temecula, CA). After PBS rinses, we incubated in secondary antibody for 2 hrs at room temperature at 1:1000 as appropriate for each primary antibody: goat anti-mouse secondary antibody coupled with Alexa-Fluor-488 or with Alexa-Fluor-594, goat anti-chicken coupled with Alexa-Fluor-568, and for infra-red analysis either goat anti-mouse secondary antibody coupled with Alexa-Fluor-800 or goat anti-rabbit secondary antibody coupled with Alexa-Fluor-680 (all secondaries from Invitrogen, Grand Island, NY). After washes in PBS, sections for classical immunofluorescence were mounted on glass slides and coverslipped with vectashield anti-fading medium containing DAPI (Vector, Vector Laboratories, Burlingame, CA). Sections for infra-red analysis were mounted on glass slides and air-dried. Control sections for all studies in which primary or secondary antibodies were omitted resulted in negative staining (not shown).

Immunolabeling for A β

Sections for amyloid analysis were pre-treated for 4 min in 88% formic acid at room temperature and all other immunostaining procedures were identical to the procedure described above. We used a monoclonal antibody raised in mouse, against rodent A β at the N-terminal amino acids 1-16 (1:1000, from M. Paul Murphy) and visualized staining with goat anti-mouse secondary antibody Alexa-Fluor-488 (1:1000; Life Technologies: Invitrogen, Grand Island, NY). Adjacent sections were co-incubated with the mouse rodent-A β antibody and either the C-terminal antibody against A β 1-42 (rabbit, 1:1000, Covance, Emeryville, CA), or the microglial marker ionized calcium binding adaptor molecule 1 (IBA1) (rabbit, 1:1000, Wako Chemicals, Richmond, VA). To control for non-specific binding of mouse antibodies on rat tissue (Figure 3F), sections received only the secondary antibody, goat anti-mouse Alexa-Fluor-594 (staining was negative), followed by a full protocol with both the rodent-A β antibody and goat anti-mouse Alexa-Fluor-488. Sections were also stained with the 6E10 anti-human-A β 1-16 antibody (mouse, 1:5000, Covance, Emeryville, CA) or using protocols excluding primary or secondary antibodies, resulting in negative staining (not shown).

To determine any fibrillar beta-pleated sheet structures, sections were double stained with a rodent-A β (see above) followed by Thioflavin S staining. Briefly, tissue was immersed for 5 min in double-distilled (dd) H₂O, followed by a 5 min incubation in 1% Thioflavin S (Sigma-Aldrich Co., St. Louis, MO) made in ddH₂O, and subsequent differentiation using consecutive 5 min washes in 70% EtOH, 95% EtOH, and ddH₂O (Fisher Scientific, Pittsburg, PA). Slides were then coverslipped as described above.

Quantification of Immunohistochemistry

Coronal sections immunostained with infra-red secondary antibodies (IgG and RAGE) were scanned using the same parameters for sham and jTBI at a 21 μ m

resolution (Li-Cor Odyssey Bio-Science, Lincoln, NE) and identical regions-of-interest (ROIs) were drawn using Li-Cor Odyssey software (Ajao et al., 2012). For IgG, average values per animal were obtained from ROIs in the perilesional parietal cortex and striatum in the hemisphere ipsilateral to the lesion, and analogous areas were evaluated in the hemisphere contralateral to the lesion or craniotomy, for a total of 3-5 serial coronal sections as available (n=4 sham, n=4 jTBI). For RAGE, average values per animal were obtained from ROIs in the parietal and temporal cortex in hemispheres both ipsilateral and contralateral to the lesion or craniotomy from 4 coronal sections at bregma levels -1.6 mm, -2.8 mm, -4.0 mm, and -5.2 mm (n=3 sham, n=3 jTBI).

For quantification of classical immunolabeling of claudin 5, P-gp, LRP1, and A β , images were evaluated and collected using an epifluorescent microscope (Olympus, BX41, Center Valley, PA). The threshold and morphological user-defined parameters were selected to maximize visualization of positive staining in the ROIs for each protein staining pattern. These parameters were kept consistent for all animals during image acquisition. For claudin 5, P-gp, and LRP1 a series of images were taken in the parietal and temporal cortex, both above and below the rhinal fissure on each hemisphere ipsilateral and contralateral to the lesion or craniotomy using a 20X objective (422 μ m X 338 μ m). For claudin 5, images of large intra-parenchymal vessels (30-100 μ m diameter) and a separate analysis on microvessels (10-20 μ m diameter) were acquired from two serial coronal sections at bregma level -2.8 mm and -4.0 mm (n=4 sham, n=4 jTBI; 8 images/animal for large vessels and 8 images/animal for small vessels). For P-gp, images were acquired from four serial coronal slices at bregma level -2.8 mm, -4.0 mm, -5.2 mm, and -6.4 mm (n=6 sham, n=6 jTBI; 24 images per animal). For LRP1, images were acquired from two serial coronal slices at bregma level -4.0 mm and -5.2 mm (n=3 sham, n=3 jTBI; 8 images per animal). Individual images were analyzed with MorphoPro software (Explora-Nova, La Rochelle, France), using the following procedure: 1) Top Hat

morphologic filter to outline vascular staining, 2) user-defined thresholding value applied to each image, 3) calculation of area of staining from background for each protein of interest (claudin 5, P-gp, or LRP1). Final values are represented as a percentage of the sham group.

For quantification of rodent-A β immunoreactivity, we used 8 whole serial coronal slices per animal spaced 1.2 mm apart, from bregma levels +3.2 mm to -5.2 mm as shown in Figure 4 (n=8 sham, n=6 jTBI; 112 total individual values). Mercator software (Explora-Nova, La Rochelle, France) was used to automatically calculate the area (μm^2) of positive staining that was normalized to the total area (μm^2) of each respective coronal slice and presented as % of A β load.

Brain Tissue Processing for Western Blotting

A Protein FFPE extraction kit (Qiagen, Hilden, Germany) was used to process perfused brain slices for Western blotting. Parietal and temporal cortical tissue above the rhinal fissure was excised from three coronal sections at bregma levels -1.6 mm, 2.8 mm, and -4.0 mm, that were adjacent to slices of interest used for immunohistochemistry. Briefly, tissue was homogenized and processed according to kit instructions, and then samples were assayed for total protein concentration by bicinchoninic assay (BCA, Pierce Biotechnology Inc., Rockford, IL). The human A β 1-40 and A β 1-42 peptides (Biopeptide Co., San Diego, CA) were prepared using a 1mg sample that was reconstituted to obtain 231 μM A β 1-40 and A β 1-42 peptides in NaOH (Sigma-Aldrich Co., St. Louis, MO). Peptides were then incubated overnight at 37°C and aliquoted for storage at -80°C, then thawed on ice when ready for use. For gel electrophoresis, all samples were prepared with loading sample buffer and reducing agent (Invitrogen, Carlsbad, CA) for a total of 40 μg of rat protein, 4 μg of A β 1-40

peptide, and 0.5 µg of Aβ1-42 peptide, loaded on a 4-12% SDS polyacrylamide gel (Nupage, Invitrogen, Carlsbad, CA). Proteins were transferred to a polyvinylidene fluoride membrane (PVDF, PerkinElmer, Germany), blocked for 1 hr in Odyssey blocking buffer (Li-Cor Bio-Science, Lincoln, NE), and incubated with the same monoclonal antibody against rodent-Aβ used in immunohistochemistry (1:2000; from Dr M. Paul Murphy, University of Kentucky) or a monoclonal antibody anti-human-Aβ 6E10 (1:750; Covance, Emeryville, CA). P-gp and claudin 5 antibodies were used as in the immunostaining, namely mouse anti-P-gp (1:100, EMD Chemicals, Merck KGaA, Darmstadt, Germany) and mouse anti-claudin 5 (1:200, Life Technologies: Invitrogen, Grand Island, NY), and these blots were incubated with Biotin-SP-conjugated goat anti-mouse (1:5000; Jackson ImmunoResearch Laboratories, West Grove, PA) for 1.5 hours at room temperature, followed by PBS washes. The blots were then incubated for 1 hour at room temperature with Streptavidin-conjugated-IRDye 800 (1:10000; Li-Cor Bio-Science, Lincoln, NE), before scanning. Each western blot was co-incubated with a rabbit polyclonal antibody against beta-actin (1:1250; Sigma-Aldrich Co., St. Louis, MO) in Odyssey blocking buffer (Li-Cor Bio-Science, Lincoln, NE) overnight at 4°C. After PBS washes, proteins were visualized using a co-incubation with goat anti-mouse secondary antibody coupled with Alexa-Fluor-800 (1:10,000; Rockland Immunochemicals, Gilbertsville, PA) and goat anti-rabbit secondary antibody coupled with Alexa-Fluor-680 (1:10,000; Life Technologies: Molecular Probes, Grand Island, NY) for 2 hrs at room temperature. After PBS washes, the PVDF membrane was visualized using the Li-Cor infra-red scanner.

Statistical Analyses

All data are presented as mean ± SEM, statistical analyses were done using SPSS, and graphs obtained using SigmaPlot. For the Aβ analyses, we utilized a

repeated measures ANOVA with group (jTBI, sham) x bregma level (8 serial coronal sections) and a conservative Huyhn-Feldt adjustment to the degrees of freedom was used to protect against any violations of the sphericity and compound symmetry assumptions underlying this ANOVA model. For the behavioral strategy analysis, data were analyzed using independent samples t-tests to test between-group differences at each time point, and paired-samples t-test to analyze within-group effects across time points. All other histological data between sham and jTBI animals met statistical assumptions and were analyzed using student *t*-tests.

Results

Blood–Brain Barrier Phenotype

While disruption of the BBB after jTBI lasts only for a short period of about 7 days (Pop and Badaut, 2011), little is known about its recovery and structural properties at a delayed post-jTBI time point. We evaluated several BBB markers at anatomical sites near the lesion, as well as on coronal slices at a distance from the injury site at 60 dpi.

IgG extravasation staining (Figure 1A, B) and quantification (Figure 1C) did not show any difference between sham and jTBI groups in perilesional parietal cortex and striatum, suggesting that the BBB is no longer disrupted. IgG extravasation was observed as expected in regions without a BBB, such as the median eminence (Figure 1A, B). In accordance with this result, claudin 5 immunolabeling was positive and outlined the elongated endothelial membrane structure of large vessels (Figure 1D,E) and microvessels (Supplemental Figure 1A-B) of both sham and jTBI animals. Claudin 5 staining was significantly increased in the large intracortical blood vessels of jTBI animals compared to sham (Figure 1F, $p < 0.045$), but no changes were observed in microvessels (Supplemental Figure 1C). Collectively, these data indicate that although BBB disruption is no longer present at 60 dpi, protein expression within the BBB is

changed long after injury.

To further address phenotypic changes at the BBB, we characterized the distribution of P-gp, LRP1, and RAGE proteins known to be involved in BBB trafficking. P-gp immunostaining was observed primarily on endothelial cells, in both jTBI and sham animals co-labeled with the astrocytic marker, GFAP (Figure 2D-F). Sham animals exhibited more intense and widespread staining patterns on microvessels (Figure 2D), whereas jTBI had more diffuse vascular staining of P-gp (Figure 2E). Quantification of images from the parietal and temporal cortices revealed significantly decreased levels of P-gp immunoreactivity in jTBI cortical vessels compared to sham (Figure 2F, $p < 0.05$). Similarly, western blot analysis revealed significantly lower P-gp protein levels in jTBI compared to sham, as shown in representative cases (Figure 2G) and blot quantification (Figure 2H, $p < 0.05$). LRP1 immunostaining in the parietal and temporal cortices showed a positive signal in both neuronal and vascular compartments (Figure 2A-B), that are consistent with prior reports of LRP1 staining in neurons, endothelial cells, and astrocytes (Silverberg et al., 2010). Quantification of LRP1 immunoreactivity showed a decrease in jTBI animals without reaching significance (Figure 2C, $p < 0.1$). RAGE immunolabeling also revealed a ubiquitous staining pattern encompassing several cell types. No differences were found in RAGE immunoreactivity between sham and jTBI in the parietal and temporal cortex, as measured using infra-red immunolabeling (data not shown). Altogether, our data indicate jTBI alters BBB proteins involved in efflux (P-gp) without significant changes to LRP1 or influx (RAGE) at the endothelial interface between the blood and brain.

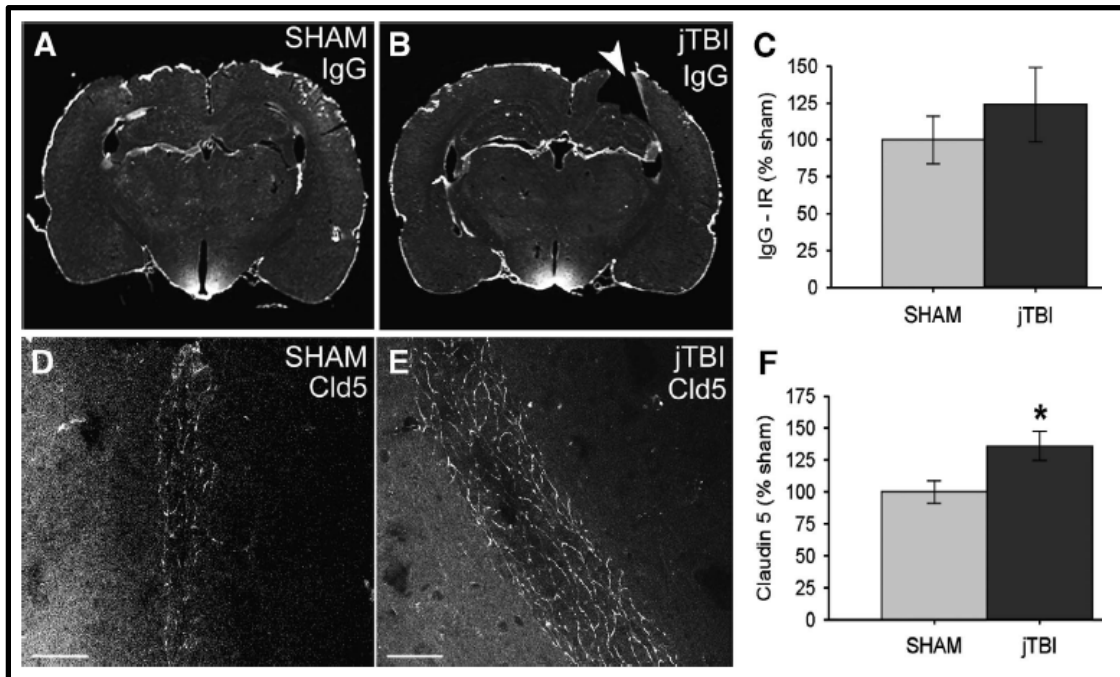


Figure 1. Changes in endothelial tight junctions 2 months after juvenile traumatic brain injury (jTBI). **(A, B)** Immunoglobulin G (IgG) extravasation using infrared immunolabeling showed higher staining intensity at the median eminence and glia limitans of both **(A)** sham and **(B)** jTBI. **(C)** IgG levels were unchanged as quantified in the bilateral parietal cortex and striatum, thus indicating an overall lack of overt blood–brain barrier (BBB) leakage. **(D, E)** Endothelial tight-junction protein claudin 5 (Cld5) was observed on endothelial cells of intraparenchymal vessels in both **(D)** sham and **(E)** jTBI and **(F)** Cld5 quantification in the parietal and temporal cortices shows that jTBI have significantly increased Cld5 staining ($p < 0.05$), perhaps as a restorative mechanism to improve BBB function ($*p < 0.05$; values are represented as mean \pm s.e.m.; IR, infrared; Cld5, claudin 5; white arrowhead in B = lesion cavity; scale bar in **(D, E)** = 50 μ m).

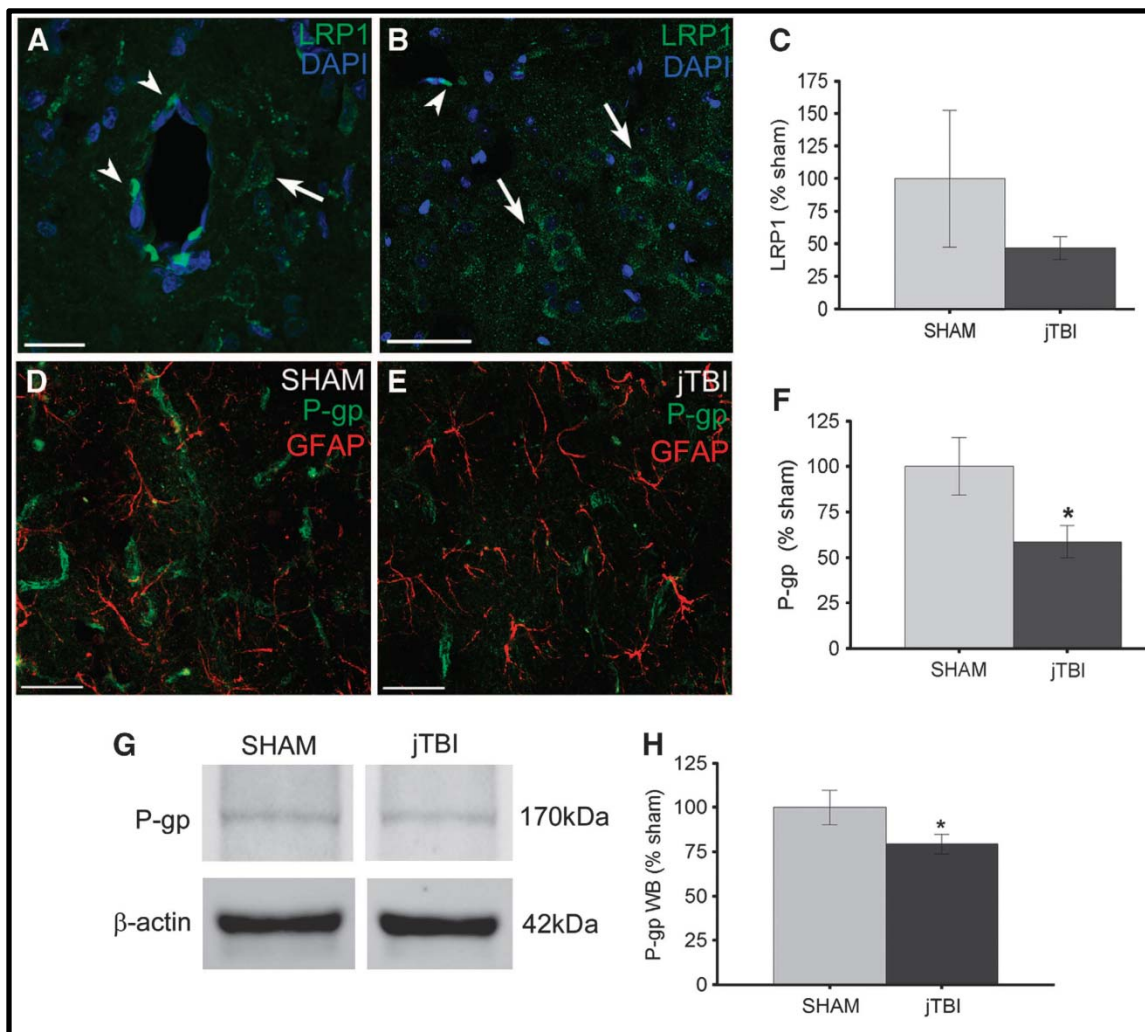


Figure 2. Juvenile traumatic brain injury (jTBI) changes proteins involved in cellular trafficking at the blood-brain barrier. (**A, B**) LRP1 immunostaining is demonstrated in both the vascular walls (white arrowheads in **D, E**) as well as neuronal compartments (white arrows in **A, B**) in the cortex of a representative sham. (**C**) Quantification of LRP1 immunostaining in the parietal and temporal cortex shows that jTBI animals have lower overall staining of LRP1, but no significant differences were found between groups. (**D, E**) P-gp immunostaining is specific for endothelial cells (green), as shown in close proximity to the end-feet of GFAP-positive astrocytes (red) in both (**D**) sham and (**E**) jTBI. (**F**) P-gp quantification in the parietal and temporal cortices shows a significant decrease in vascular P-gp transporter in jTBI compared to sham ($p < 0.05$). (**G, H**) Protein levels of jTBI are also significantly lower than sham, as shown in representative cases and quantification ($p < 0.05$). (* $p < 0.05$; values as mean \pm SEM; BBB, blood-brain barrier; jTBI, juvenile traumatic brain injury; LRP1, lipoprotein receptor-related protein 1; P-gp, p-glycoprotein; GFAP, glial fibrillary acidic protein; scale bar in **A** = 20 μ m; **B, D, E** = 50 μ m)

Widespread A β Accumulation

Using a rodent-A β antibody specific to the N-terminus and a formic acid pre-treatment, we detected a diffuse pattern of immunoreactivity that is both extracellular (Figure 3 A, C-H) and perivascular (arrowheads in Figure 3C, E-H). Examples of positive rodent-A β immunolabeling are shown at a distance from the injury, such as the frontal (Figure 3C, E-H), temporal (Figure 3A), and parietal cortex (Figure 3D). Positive staining was also detected in the entorhinal cortex, striatum, and thalamus (Figure 4A), with no staining using the secondary antibody alone (Figure 3A).

Western blot showed that the rodent-A β antibody was specific for rat tissue but not for human A β 1-40 and A β 1-42 peptides, while the anti-human 6E10 antibody detected bands for human A β peptides, but no signal for rat tissue (Figure 3B). The 6E10 antibody detected monomeric A β species (4kDa) in both human A β 1-40 and A β 1-42 peptide preparations, and several A β aggregates that are more abundant in the A β 1-42 preparation (Figure 3B). In the rat tissue, the rodent-A β antibody reveals a beta-amyloid precursor protein (APP) signal near the expected region ~110kDa and several additional bands, possibly APP fragments or A β aggregates of various sizes (Figure 3B).

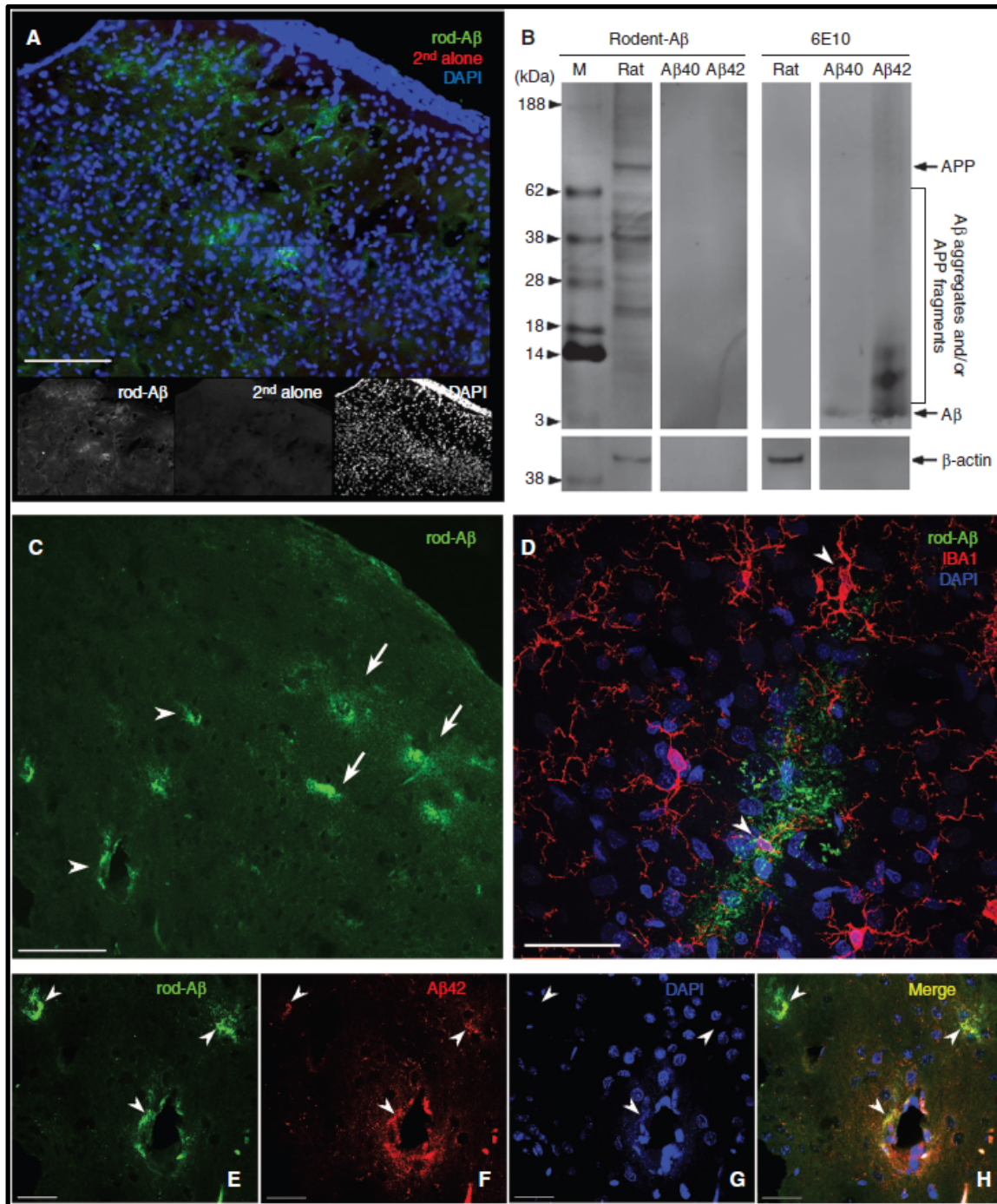


Figure 3. Immunoreactivity patterns with a rodent-A β antibody. **(A-H)** Positive staining is detected in several brain regions following formic acid pre-treatment and classical immunostaining using the specific rodent-A β antibody, as shown in representative sections from jTBI animals. **(A)** Temporal cortex shows specificity of the rod-A β antibody (labeled with goat anti-mouse λ 488 nm), with negative staining using the secondary antibody alone on the same section (2^{nd} alone, pre-incubation protocol with goat anti-mouse λ 594 nm). **(B)** Western blotting from the parietal/temporal cortex shows the rod-A β antibody has high specificity for rat cortex, but not for human A β 1-40 or A β 1-42 peptides, while the 6E10 antibody has high specificity for human A β peptides at 4kDa and larger aggregates, but no signal for rat tissue. In the rat, the rod-A β antibody reveals a prominent APP band and several smaller fragments, indicating positive immunoreactivity for both A β aggregates or APP fragments. **(C)** In an example from the frontal cortex, rod-A β stains a cluster of several extracellular diffuse deposits (white arrows) and vascular labeling (white arrowheads) near the molecular and superficial cortical layers. **(D)** In an example from the parietal cortex, rod-A β staining is often surrounded by IBA1-positive microglial processes with an abnormal morphology (white arrowheads) suggestive of an immune response. **(E, F, G, H)** Co-incubation with both rod-A β antibody (raised in mouse, secondary λ 488 nm) and a C-terminal antibody against A β 42 (raised in rabbit, secondary λ 594 nm) in the frontal cortex, shows several areas of colocalization (white arrowheads) as well as areas without overlap, indicating the presence of several A β species.

(A β , beta-amyloid; rod-A β , rodent beta-amyloid antibody; 2^{nd} alone, secondary antibody alone; APP, beta-amyloid precursor protein; M, marker; kDa, kilodalton; IBA1, ionized calcium binding adaptor molecule 1; scale bars in **A, C** = 100 μ m, **D** = 40 μ m; **E, F, G, H** = 30 μ m)

Rodent-A β immunoreactivity was associated with microglial cells, stained with IBA1. Microglia exhibited an elongated soma, little somatic cytoplasm, and multiple thinner processes, as shown in an example from the jTBI parietal cortex (Figure 3D). No activated microglia were detected at this time point (data not shown). Rodent-A β immunoreactivity colocalized with C-terminal-A β 1-42 staining in several brain regions, such as the frontal cortex (Figure 3E-H). Thioflavin S staining (data not shown) is negative despite positive rodent-A β immunoreactivity, suggesting a lack of fibrillar beta-pleated sheet structures. Overall, these data are consistent with an early A β accumulation pattern having a diffuse morphology and containing A β 1-42 species. Total rodent-A β immunoreactivity was quantified using the Mercator program and expressed as % A β load relative to total coronal brain area at each bregma level (Figure 4A-C). Representative jTBI animals are shown with the lesion location (black arrowheads in Figure 4A) and outlines of positive staining at individual bregma levels (Figure 4A). By 60 dpi, the cortical jTBI lesion cavity is apparent from bregma -1.0 mm up to -4.0 mm (not shown) and higher rodent-A β immunoreactivity was observed in more anterior and posterior levels from the lesion site (Figure 3B). Repeated measures ANOVA showed significant changes across all coronal sections regardless of group (Figure 4B, $p < 0.042$), with moderate changes across bregma levels in jTBI group alone ($p < 0.057$), but no changes observed in sham alone ($p > 0.1$). Similarly, the jTBI group showed a trend for higher staining in total brain compared to sham (Figure 4C, $p < 0.073$). These data suggest that early brain injury may exacerbate a process of endogenous rodent-A β accumulation throughout vulnerable regions over time.

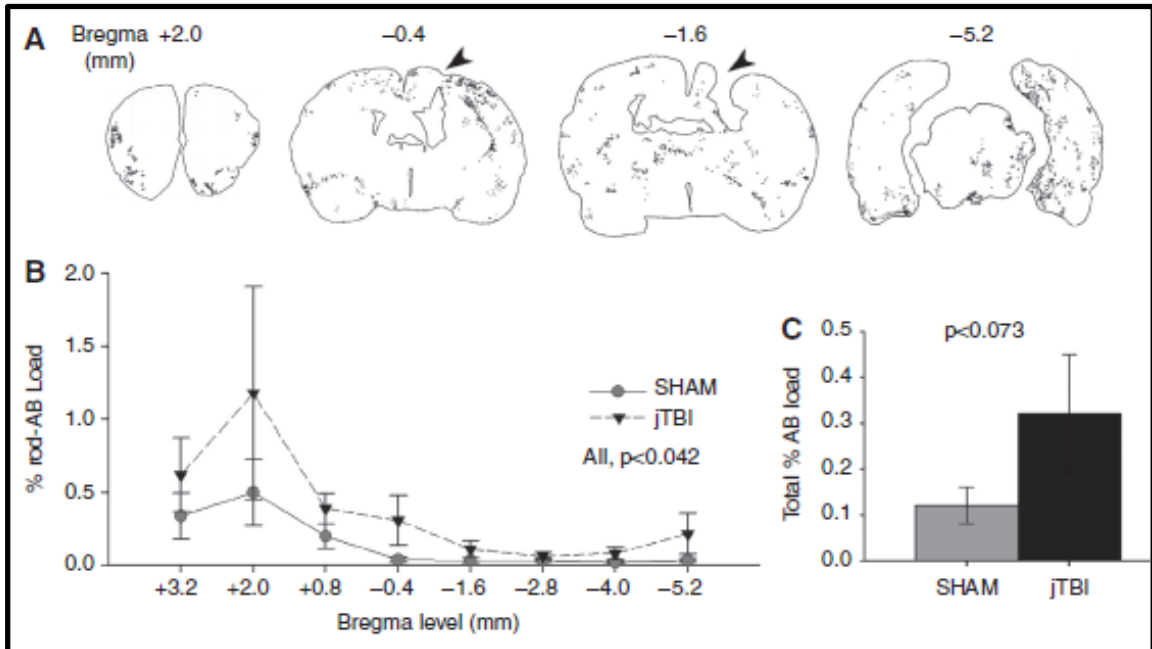


Figure 4. Anterior to posterior patterns of rodent-A β distribution. **(A)** Representative coronal sections with outlines of rodent-A β positive staining in jTBI are shown at bregma +1.7 mm, -0.4 mm, -1.4 mm, and -5.2 mm. The jTBI lesion cavity is apparent in the parietal cortex at -1.4 mm and still visible at bregma -0.4 and -3.8 mm to a lesser extent (black arrowheads). **(B)** All positive rodent-A β immunoreactivity was quantified to obtain %A β load relative to total brain area at 8 bregma levels, with significant changes along the anterior-to-posterior axis ($p < 0.042$), but no significant changes between groups at any single level. **(C)** Summation of total brain A β load was higher in jTBI versus sham ($p < 0.073$), with jTBI animals showing high staining variability common in models of natural A β accumulation. (Values are represented as mean \pm SEM; mm, millimeter; A β , beta-amyloid; jTBI, juvenile traumatic brain injury)

Changes in Strategy during Water Maze

As previously reported, sham and jTBI animals showed no overall performance differences across trials on swim speed, cued learning, or spatial learning/memory at 30 or 60 dpi (Ajao et al., 2012). The cumulative distance travelled for both groups showed no differences in spatial learning at 30 dpi (Figure 5B) and 60 dpi (Figure 5C). As expected due to repeated testing, performance during block 1 of day 60 was better than block 1 of day 30 (Figure 5B versus 5C, $p < 0.05$) for both jTBI and sham animals, and both groups traveled the same average distance for remaining blocks. In addition, we analyzed swim patterns and learning strategies for individual spatial trials (Table 1, Figure 5A). Generally, jTBI animals used fewer spatial strategies, and more systematic and looping strategies, compared to sham animals at 60 dpi (Figure 5E) but not at 30 dpi (Figure 5D). Specifically, the stacked bar graphs (Figure 5D, E) represent a breakdown of the % spatial testing trials classified under spatial, systematic, or looping swim strategies. We observed no significant differences between groups in any strategy categories at 30 dpi. However, we detected significant changes at 60 dpi where shams used more spatial strategies than jTBI animals (88.9% versus 62.5% respectively, $p < 0.05$). In addition, shams exhibit an increased use of spatial strategies from 30 to 60 dpi (37.5% versus 88.9% respectively, $p < 0.05$). In contrast, jTBI animals have nearly identical strategy groupings at both time points, displaying an inability to improve performance over time.

Discussion

We evaluated long-term changes following TBI in a juvenile rat model to address the concordance with clinical observations of delayed behavioral modifications, and emerging data on changing BBB properties during brain aging and neurodegenerative disease. Our results at a delayed two-month time point show parallel changes in

structural BBB phenotypes of claudin 5, altered P-gp expression, rodent-A β immunoreactivity, and altered water maze performance. Together, our data suggest that an early brain injury may commence with vascular damage that promotes long-term phenotypic changes to the BBB that can influence cognition.

Physiopathological Changes in the Blood–Brain Barrier

We explored BBB phenotypes at a delayed time point after juvenile injury as a unique platform for addressing whether jTBI disrupts the neurovascular unit (NVU) and contributes to brain pathophysiology. Within the first days post-injury, we observe high IgG staining (Pop and Badaut, 2011). BBB disruption is repaired by two months in our jTBI model, as evidenced by the absence of IgG extravasation and increases in tight junction protein claudin 5 (Figure 1). Other studies also report that improved BBB integrity coincides with altered expression of tight junction proteins at later time points. Similar to our model, claudin 5 levels are up-regulated after Evans blue and IgG leakage subsides at 1 and 2 weeks after rat cortical injury (Lin et al., 2010). Claudin 5 is also increased, along with resolution of Evans blue staining, after 4 and 8 weeks in mice exposed to an infectious agent targeting the BBB (Liao et al., 2008). Thus, altered levels of claudin 5 long after jTBI suggest delayed modifications in BBB structural properties. Furthermore, our differential observations on large and small vessels (Figure 1, Supplemental Figure 1) indicated a more complex phenotypic response of the endothelium which may be related to location along the vascular tree.

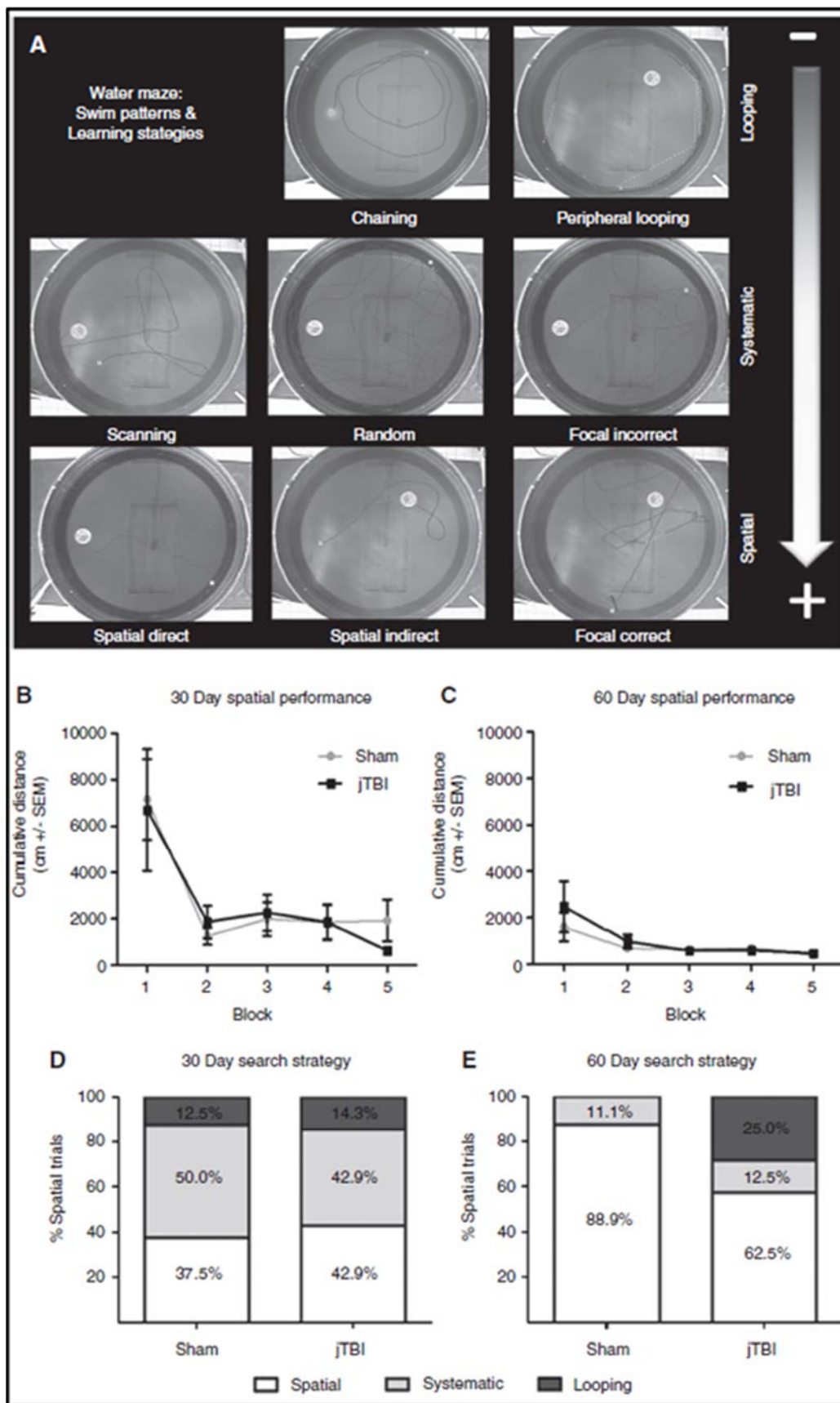


Figure 5. Differences in water maze strategies in adulthood. **(A)** Eight swim patterns/learning strategies (red lines) were identified and divided into 3 categories from the most (+) to the least (-) efficient: spatial, systematic, and looping. **(B-C)** Water maze performance is unchanged between groups at **(B)** 30 days and **(C)** 60 days post-jTBI, however both groups improve and learn the task within each time point (Block 1 to 5) and between testing time points (comparison of Block 1 at 30 versus 60 days). **(D)** Swim strategy use was evenly distributed among sham and jTBI groups at 30 days, but not at 60 days. By 60 days, jTBI animals used strategies similar to those used at 30 days (primarily systematic and looping patterns), but sham controls relied on significantly more spatial memory strategies compared to jTBI and to their prior performance at 30 days ($p < 0.05$). (Values as mean \pm SEM; jTBI, juvenile traumatic brain injury; + and - in **A** = most and least efficient, respectively)

We investigated the triad of endothelial cell proteins (P-gp, LRP1, and RAGE) previously shown as potential mediators of A β trafficking and other proteins across the BBB (Figure 6) (Miller, 2010, Ueno et al., 2010). P-gp is well known as an efficient gatekeeper on the luminal side and often pharmaceutically by-passed to allow efficient drug delivery. Its expression is influenced by several distinct molecular pathways and its putative role in disease and injury is emerging (Kooij et al., 2010, van Assema et al., 2012). We observed a significant decrease in P-gp in cortical vessels following jTBI by immunostaining and protein blot analyses. Similar to our findings, brain P-gp protein level and function decreased after irradiation of normal rats (Bart et al., 2007), in aged 3 year old rats (Silverberg et al., 2010), and in sporadic AD (van Assema et al., 2012). Additionally, P-gp expression and function were impaired during multiple sclerosis pathology and its dysfunction coincides with lymphocyte infiltration and inflammation in experimental allergic encephalomyelitis (Kooij et al., 2010).

Our observed P-gp decreases may be one result of long-lasting neuroinflammation, contributing to an increase in rodent-A β immunoreactivity. Importantly, P-gp knockout mice exhibited decreased LRP1 in brain capillaries without changes in RAGE proteins (Cirrito et al., 2005) and aged 3 year old rats showed decreased vascular levels of P-gp and LRP1 associated with accumulation of A β (Silverberg et al., 2010). We did not detect significant changes in LRP1 between sham and jTBI, but LRP1 was positive in blood vessels and neurons within the temporal cortex of jTBI animals. Our findings are in line with several model systems and age groups, which emphasize the putative role of the BBB in chronic brain pathophysiology after acute injury. Our observed P-gp decrease may have a complex relationship to accumulation of rodent-A β in multiple brain areas. Frontal and temporal lobes are vulnerable to neuropathology after TBI (Johnson et al., 2012). In our model, these same regions exhibited reduced P-gp (Figure 1) and increased rodent-A β immunoreactivity in

the brain parenchyma and vessel walls (Figure 3, 4). Clinically, our findings are similar to low endothelial P-gp that correlated with increased parenchymal A β 1-40 or A β 1-42 plaques in the medial temporal lobe of aged non-demented humans (Vogelgesang et al., 2002). Following peripheral A β 1-42 injections in adult mice, brain endothelial cells show downregulated expression of RAGE, LRP1 and P-gp at the mRNA level, however P-gp immunostaining remained unchanged (Brenn et al., 2011). Collectively, these findings highlight complex interactions between A β species and the BBB transporters that may be influenced by injury type and study time point.

A β Accumulation and Blood–Brain Barrier Changes after Juvenile Traumatic Brain Injury

The important consequences of cerebrovascular dysfunction and the role of the BBB neuropathological protein trafficking are gaining momentum. In normal rodents, classical AD-like pathology with fibrillar amyloidosis is rare. This may be due to A β sequence differences of three amino acids at the N-terminal (Istrate et al., 2012). However, we used an N-terminal specific antibody for rodent A β (McGowan et al., 2005), and endogenous accumulation has been reported long after a brain insult in normal experimental injury models. For example, increased APP and A β immunostaining was observed in thalamic nuclei for up to 9 months after stroke in normal rats (van Groen et al., 2005). In normal adult rats, intranasal nerve growth factor administration resolved increases of A β 1-42 for up to two weeks post-TBI (Tian et al., 2012). In a rodent model of aging, senescence accelerated mice (SAMP8) showed increased BBB disruption at 12 months and exhibited vascular A β compared to their littermate controls (Del Valle et al., 2011). These data indicate the close relationship of BBB disruption and brain pathology in aging and post-injury.

BBB phenotypic changes at 2 months occurred in parallel with higher rodent-A β

immunolabeling in the parenchyma and vasculature of jTBI animals (Figure 3, 4). Notably, we observed diffuse A β deposition in regions remote to the original site of impact, especially in the superficial cortical layers. Additionally, diffuse A β in superficial cortical layers is the primary conformation present in other models of natural A β accumulation, such as aged beagles (Pop et al., 2012). Diffuse A β is also more common in clinical cases with mild cognitive impairment (MCI) (Jicha et al., 2006) and is becoming recognized as an important contributor to disease progression by the National Institute of Aging-Alzheimer's Disease (Montine et al., 2012). A β load, evaluated by immunohistochemical staining similar to our methodology, was the best predictor for dementia in very old individuals (Robinson et al., 2011). Interestingly, we observed sparse rodent-A β immunoreactivity in some shams (n=3 of 8 total) and only modest effects of increased rodent-A β immunolabeling throughout the brain of jTBI animals (n=6 total). In a similar TBI model, sham animals with a craniotomy exhibited brain tissue modifications and deficits in learning and memory post-surgery (Bertolizio et al., 2011). Therefore, we expect that inclusion of additional animals or a more appropriate naïve control group may improve our data variability and improve statistical power.

Parallel Changes in Vascular Phenotype and Behavioral Dysfunction

In our injury model, we observed changes in behavioral outcome by two months post-injury (Ajao et al., 2012), which indicate the brain may be undergoing compensatory mechanisms. Here, we observed strategic water maze impairment without overt memory deficits, which may reflect underlying brain-repair mechanisms occurring post-injury. Interestingly, clinical defects of initial strategy formulation affected performance on a task of complex visuospatial executive function in individuals with amnesic MCI who are more likely to develop AD (Papp et al., 2011). In a CCI study in adult mice, sham and

TBI animals exhibited similar water maze outcomes after two months, but TBI animals exhibited thigmotaxic strategy impairment with increased percent time swimming along maze walls, similar to our looping category (Blais et al., 2011). In comparison with adult models, juvenile rats may be especially vulnerable due to a lack of cognitive reserve. While the neural correlates are unclear, clinically it is thought that having increased cognitive reserve from education and other life experiences may be protective against brain aging and disease (Honer et al., 2012). Thus, brain injury at a developmental stage may influence underlying mechanisms and reduce cognitive reserve. Our observations of delayed impairments in jTBI suggest a parallel with acceleration of brain aging and disease due to trauma.

Concluding Remarks

Juvenile traumatic brain injury may induce initial BBB dysfunction which progresses over time to affect protein trafficking at a time point relevant for cognition. Our data are consistent with clinical and experimental findings in studies of TBI and $A\beta$ in transgenic models, as well as studies on BBB dynamics with aging and non-traumatic brain injuries. However, only the use of further target-specific studies may address whether these changes are interconnected, or whether they are independent parallel events in the same trauma-affected brain. In this study, we described lasting effects of jTBI with phenotypic BBB changes after two months, including a lack of IgG extravasation and compensatory increases in structural tight junction protein claudin 5 (Figure 6) (Andras et al., 2010). However, the reduction in P-gp may be sufficient to impair normal $A\beta$ clearance and promote its accumulation inside the brain. Overall, we show the presence of continued modifications in the BBB phenotype long after injury, and propose the BBB as a meaningful therapeutic target for resolving detrimental post-traumatic dysfunction.

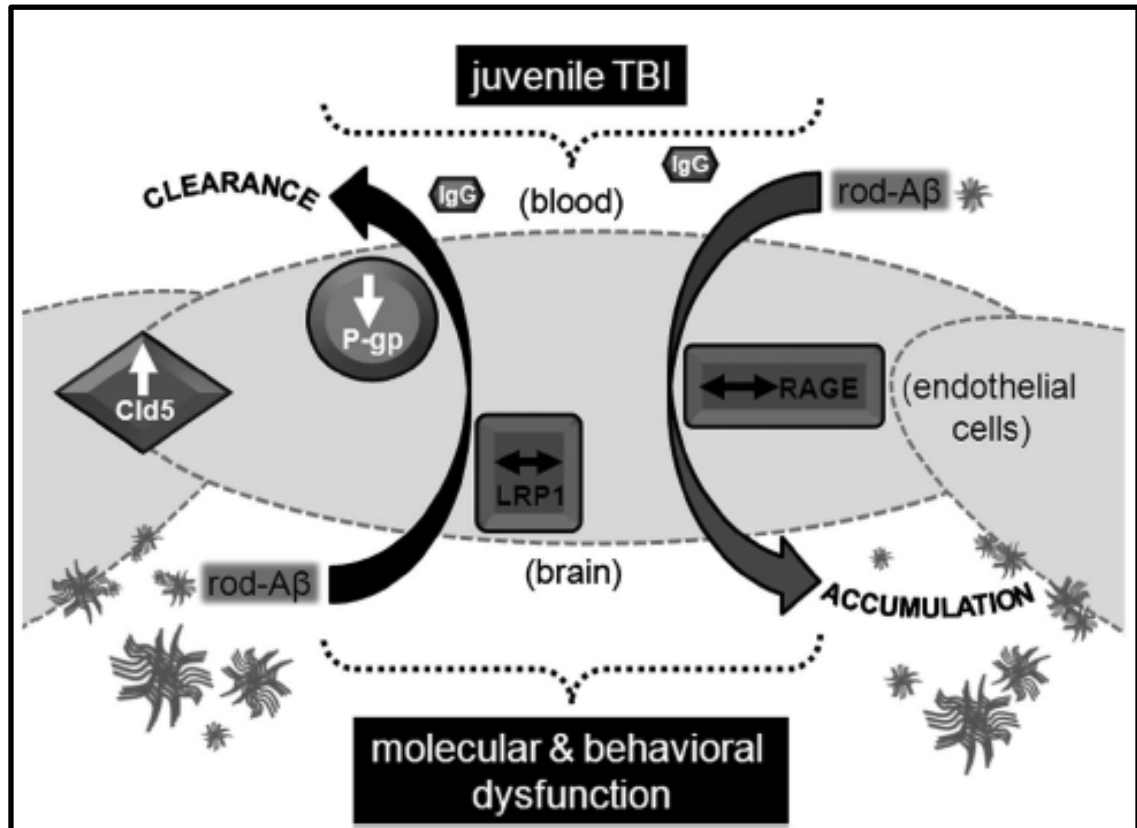


Figure 6. Summary of parallel changes in adulthood after early brain injury. A schematic representation of events two months after jTBI shows phenotypic alterations to the BBB changes occurring in parallel with molecular and behavioral dysfunction. Specifically, lack of IgG extravasation from the blood into the tissue and increased levels of tight-junction marker Cld5 indicate an intact BBB during adulthood. However, in an environment with decreased levels of P-gp, and unchanged levels of LRP1 and RAGE, proper metabolism of toxic proteins such as A β can be hindered. As a result, the BBB phenotype impairs normal clearance of rod-A β and may promote its abnormal accumulation inside the brain in the parenchyma and vascular walls (figure adapted from Andras et al., 2010).

Disclosure/Conflict of Interest

The authors declare no conflict of interest.

Acknowledgements

We thank Dr. André Obenaus (Loma Linda University) for project assistance and Monica Rubalcava for a portion of imaging performed at the Loma Linda University School of Medicine Advanced Imaging and Microscopy Core (LLUSM AIM) supported by NSF Grant, MRI-DBI 0923559 (to S.M. Wilson).

Support

Supported in part by the NIH R01HD061946 and the Swiss Science Foundation (FN 31003A-122166 and IZK0Z3-128973) (to J. Badaut).

PROLOGUE TO CHAPTER 3
LONG-TERM INCREASE OF CAVEOLINS IN THE ENDOTHELIUM
AND IN ASTROCYTES AFTER JUVENILE TRAUMATIC BRAIN
INJURY

A reproducible juvenile TBI (CCI in P17 rat pups) model and the histopathological features and functional deficits resulting from the injury at both acute and chronic time points have been described in chapters 2. In keeping with the experimental aims of this project, chapter 3 focuses on caveolins and their association with BBB disruption, and possibly with other secondary processes following juvenile TBI. Caveolin-1, -2, and -3 are a family of integral membrane proteins that constitute the coat of caveolae – small invaginations of plasma membrane in lipid rafts – and perform various roles ranging from transcytosis and endocytosis to cholesterol metabolism and modulation of numerous intracellular signaling pathways. Regulation of tight junction permeability is suspected to be one of the functions of caveolins in the developing brain following TBI.

The relevance of caveolin expression and activation to the secondary pathophysiology of juvenile TBI has been reviewed in chapter 1 (and is also reviewed in the introductory section of this chapter 3). In chapter 4, the therapeutic potential of cavtratin – an injectable peptide mimetic of the caveolin scaffolding domain is investigated with respect to slowing and/or reversing BBB disruption and cerebral edema, and also in terms of improving functional outcomes.

The aim of this chapter is to characterize changes in the expression pattern and immunoreactivity of caveolin-1, -2 and -3 following juvenile TBI in conjunction with BBB disruption and edema formation. The hypothesis is that decrease in tight junction protein

levels and the resultant opening of BBB will be associated with increased expression of caveolins-1, 2, and 3 in brain endothelial cells and other cells following juvenile TBI.

The chapter follows the blueprint of a scientific manuscript. It contains 5 figures with detailed figure legends. Authors' names and affiliations are on the first page.

CHAPTER 3
LONG-TERM INCREASE OF CAVEOLINS IN THE ENDOTHELIUM
AND IN ASTROCYTES AFTER JUVENILE TRAUMATIC BRAIN
INJURY

**David O. Ajao¹, Andrew M Fukuda¹, Dane Sorensen^{1, 2}, Jérôme
Badaut^{1, 2*}**

Departments of Physiology¹ and Pediatrics², Loma Linda University, Loma Linda, CA.

Running Title: Expression of caveolins after juvenile TBI

Key words

Blood-brain barrier, endothelium, astrocyte, juvenile traumatic brain injury, caveolin

Highlights

- 1) Long-term change in blood-brain barrier after jTBI
- 2) Distribution of the 3 isoforms of caveolin after jTBI
- 3) Time course of protein expression for the 3 caveolin isoforms after jTBI
- 4) Increase of caveolin-1 in cerebral endothelia
- 5) Increase of caveolin-1 and -3 in astrocytes

Abstract

Caveolins are structural proteins involved in caveolae formation as well as in modulating the activities of a wide variety of signaling molecules. Three isoforms of caveolin are known to be present in the mammalian brain and hypothesized to be involved in blood-brain barrier (BBB) dysfunctions after brain injury with vascular phenotypic changes. Traumatic brain injury (TBI) is one of the major causes of death and disability in children and adolescents, and results in a complex cascade of events including the disruption of BBB. Juvenile TBI (jTBI) induces long-term alterations on endothelial phenotypes such as increase of claudin-5 and a decrease in p-glycoprotein. In the present study, we explored the changes of the caveolin expression and distribution after jTBI. Using a controlled cortical impact on post-natal 17 day-old rats as a model of jTBI, BBB was observed to be disrupted from 1 to 3 days after injury and went back to normal at day 7. Caveolin (cav)-1 was increased from day 1 to 60 after injury in the endothelial cells and in the reactive astrocytes. In contrast, cav-2 expression, only present in the endothelium, was not modified over time after injury. Cav-3 was observed in astrocytes and increased in the border of the lesion in the reactive astrocytes at 1 and 3 days after injury. The long-term change observed in cav-1 after jTBI makes this a good molecular candidate for controlling endothelial phenotypic changes after injury. Increase of cav-1 and 3 in the astrocytes also raises an interesting question regarding their roles in the reactive astrocytes after jTBI.

Introduction

Traumatic brain injury (TBI) affects about 1.7 million people annually and accounts for about 30.5% of all injury-related deaths in the United States. Children and adolescents aged between 0 to 14 years represent a vulnerable population with half a million TBI-related emergency department visits annually (Faul et al., 2010). As such, juvenile TBI (jTBI) is a leading cause of death and disability in children and adolescents in the United States (Schneier et al., 2006). TBI is defined as brain damage that results from an external mechanical force (e.g. rapid acceleration or deceleration), blast waves, penetration by a projectile, or direct impact, and it is often accompanied by a post-injury concussion or similar form of altered consciousness (Maas et al., 2008). In connection with the primary injury, TBI is associated with secondary events, which include hemorrhage, disruption of blood-brain barrier (BBB), and vasogenic edema (Pop and Badaut, 2011). TBI in the juvenile population has been associated with greater risks of cerebral hemodynamic dysfunction, hypoxic-ischemic injury, and diffuse cerebral edema compared to adults (Armstead, 1999, Suh et al., 2001, Giza et al., 2007, Freeman et al., 2008). In an experimental model of jTBI, we have previously shown an increase in brain water content during the first week post-injury using T2-weighted MRI (Fukuda et al., 2012). Further post-traumatic secondary events include brain swelling, decrease in cerebral blood flow (CBF), perturbation of ionic homeostasis that induce dysfunction in neuronal firing, excitotoxicity, apoptosis, oxidative stress, and inflammation (Baethmann et al., 1988, Armstead, 1999, Sahuquillo et al., 2001, Gaetz, 2004, Zweckberger et al., 2006). All these events contribute to neurological deterioration, leading to mortality and morbidity after TBI.

TBI-induced vascular changes have been shown to alter endothelial phenotypes both acutely and chronically after injury (Pop and Badaut, 2011, Pop et al., 2012). In addition to early breakdown of BBB and edema formation, we have observed a

compensatory increase in the expression of claudin-5, a protein involved in tight junction formation, and a decrease in p-glycoprotein (P-gp), an ATP-binding protein, at 2 months post-injury (Pop et al., 2012). The molecular mechanisms contributing to these long-term endothelial phenotypic changes are still unknown. However, recent studies showed that the caveolins are involved in molecular signaling and contribute to the changes in claudin-5 and P-gP (McCaffrey et al., 2007, McCaffrey et al., 2012).

Caveolins are structural proteins that form the backbone of the caveolae, which are known to function in endocytosis, transcytosis, and exocytosis in endothelial cells (Predescu and Palade, 1993, Jodoin et al., 2003, Salaun et al., 2005, Choudhury et al., 2006, Predescu et al., 2007). Three isoforms of caveolin are known to be present in the mammalian brain (Cameron et al., 1997, Virgintino et al., 2002). Caveolins-1 (cav-1) and 2 were mostly observed in brain endothelial cells (Lisanti et al., 1994, Virgintino et al., 2002) although cav-1 has also been observed in some neurons and astrocytes (Cameron et al., 1997, Virgintino et al., 2002, Head et al., 2010). Cav-3 has been predominantly described in the astrocytes (Virgintino et al., 2002, Shin et al., 2005). Besides facilitating the caveolae sequestration of several receptors and ligands, the caveolins also serve as active modulators of activities of a wide variety of signaling molecules, including inhibition of endothelial nitric oxide synthase (eNOS) (Bucci et al., 2000, Bauer et al., 2005, Lajoie et al., 2009). This modulation is performed via the caveolin scaffolding domain (CSD), a 19-amino acid sequence (amino acids 82 – 109) that binds proteins via a binding site, caveolin-binding motif (CBM), that are present on proteins such as eNOS (Sargiacomo et al., 1995, Cameron et al., 1997, Lajoie et al., 2009).

Despite abundant literature on the role of cav-1 in modulating eNOS and its physiological consequences in the periphery (Bernatchez et al., 2005), little is known about the potential roles of caveolins after brain injury (Nag et al., 2007). In an adult rat

model of cold cortical injury, the level of expression of cav-1 is increased in the endothelium for several days following injury (Nag et al., 2007, Nag et al., 2009). Similar increases have been reported in models of brain ischemia (Jasmin et al., 2007) and experimental spinal cord injury (Shin et al., 2005, Shin, 2007). Although cav-1 increase in some of these brain injury models was associated with BBB or blood-spinal cord barrier breakdown (Nag et al., 2007, Nag et al., 2009), the exact role of these changes in cav-1 is still unclear. Experiments using cav-1 knockout (cav-1^{-/-}) mice suggest beneficial roles for cav-1 in rodent models of brain disorders (Jasmin et al., 2007, Gu et al., 2011). In fact, cav-1^{-/-} mice presented higher vascular permeability (Schubert et al., 2002, Miyawaki-Shimizu et al., 2006, Siddiqui et al., 2011) and intriguingly have a worse outcome than the wild-type (WT) with increased cerebral volume of infarction after stroke (Jasmin et al., 2007). Interestingly, claudin-5, a protein involved in tight junction (TJ) formation, was shown to bind to cav-1 and be stabilized by it in some cases (McCaffrey et al., 2007, Stamatovic et al., 2009). It is therefore plausible that increase in cav-1 expression may be contributing to the recovery of TJ and BBB functions after injury.

However, cav-2 is also abundant in the endothelial cells, and cav-2^{-/-} mice showed a decreased lesion volume compared to WT (Jasmin et al., 2007). This suggests that cav-2 may have a detrimental role in brain injury, in contrast with cav-1.

Lastly, cav-3 expression was also shown to change in spinal cord astrocytes in a model of experimental autoimmune encephalomyelitis (Shin et al., 2005). The changes in expression of these caveolins are potentially contributing to the neurovascular dysfunctions observed after jTBI (Fukuda et al., 2012, Pop et al., 2012). The expression and distribution profiles of cav-1, 2, and 3 within the neurovascular unit after jTBI in conjunction with BBB disruption have not been investigated. The goal of this present study is, therefore, to report changes in the level of expression of cav-1, 2, and 3 after jTBI, in parallel with the changes in the BBB.

Materials and Methods

Animals

All animal related protocols and procedures in this study were approved by the Institutional Animal Care and Use Committee of Loma Linda University. Male Sprague-Dawley rat pups at postnatal day 10 (P10, Harlan, Indianapolis, IN) were housed on a 12-hour light-dark cycle at constant temperature and humidity for one-week prior to surgery to allow sufficient time for acclimatization. Following induction of experimental brain injury or sham procedure at P17 (30 ± 4 g, $n=36$ rats), the pups were returned to their cages with their dams and subsequently weaned at 7d. They were housed two rats per cage, and fed with standard lab chow and water *ad libitum*. Identical sham or controlled cortical impact (CCI) surgical parameters were used for the experimental brain injury.

Juvenile Traumatic Brain Injury Model

Controlled cortical impact (CCI) was induced in P17 old rat pups as previously described (Ajao et al., 2012, Fukuda et al., 2012). Briefly, rat pups were anesthetized with isoflurane (Webster Veterinary Supply, Inc., Sterling, MA) and placed into a stereotaxic frame (David Kopf Instruments, USA). A 5 mm diameter craniotomy was drilled over the right parietal cortex at 3 mm anterior-posterior and 4 mm medial-lateral to bregma. CCI was induced in the jTBI group using a 2.7mm diameter rounded-tip metal impactor fixed to an electromechanical actuator (Leica Microsystems Company, Richmond, IL) and centered over the exposed dura at a 20° angle to the cortical surface. The impact was delivered at a velocity of 6 m/s, with impact duration of 200 ms, and to a depth of 1.5 mm from the cortical surface. Bleeding and convexity of the injured cortex were recorded and showed no significant difference within the jTBI animals. The surgical site was sutured closed. Appropriate pain management was provided through subcutaneous administration of Buprenorphine (0.01 mg/kg; dilution: 0.01 mg/ml)

immediately following end of suturing. The body temperature was maintained at 37°C throughout the surgical procedure. Sham animals underwent identical procedures with the exception of cortical impact. All rats recovered from anesthesia within 25 minutes post-injury. No seizures resulting from experimental procedure was observed within the 2 to 3-hour observation period immediately following injury when the animals were returned to their cages.

Tissue Processing and Immunohistochemistry

Rats were transcardially perfused with 4% PFA prepared in PBS at 1d, 3d, 7d, and 60d with n=5 rats per group (jTBI and sham) for each time points. The brains were removed and immersed in 30% sucrose at 4°C for 48 hours and then frozen on dry ice and stored at -20°C pending tissue cutting. Coronal cryostat sections (Leica CM1850, Leica Microsystems GmbH, Wetzlar, Germany) were prepared.

IgG Extravasation Staining for BBB Assessment

To evaluate the BBB disruption, IgG extravasation staining was performed as previously described (Badaut et al., 2011). Briefly, the sections were incubated with biotin conjugated affinity purified goat anti-rat IgG coupled with Infrared-Dye-800-nm (1:500 dilution; Rockland, Gilbertsville, PA) in PBS containing 0.1% Triton X-100 and 1% bovine serum albumin (BSA) for 2 hours at room temperature. After washing, sections were dried and scanned on an infra-red scanner (Odyssey-system, LiCor, Germany) to quantify the area of the IgG extravasation for three adjacent slices covering the lesion with the LI-COR Odyssey system.

Double Immunohistochemical Staining:

All antibody incubations were carried out in PBS (Fisher Scientific, Pittsburgh,

PA) containing 0.25% Triton X-100 and 0.25% BSA (both from Sigma-Aldrich Co., St. Louis, MO). After washes in PBS, sections were blocked for 1.5 hours in PBS with 1% BSA, and then incubated overnight at 4°C with one of the following: mouse anti-cav-1 or -2 or -3 (each diluted 1:200; BD Biosciences, San Jose, CA), rabbit anti-cav-1 (1:200; Abcam Inc., Cambridge, MA), mouse anti-claudin-5 (1:100; Invitrogen, Camarillo, CA), mouse monoclonal antibodies for NeuN (1:500; Abcam Inc., Cambridge, MA), rabbit polyclonal antibodies for IBA-1 (1:300; Wako), and chicken anti-gial fibrillary acidic protein (GFAP, 1:1000; Millipore, Billerica, MA). After 3x10min PBS rinses, sections were incubated for 2 hours at room temperature with a mixture of goat anti-mouse secondary antibody coupled with Alexa-Fluor-488 and goat anti-rabbit secondary antibody coupled with Alexa-Fluor-568 (both at 1:1000; Invitrogen, Camarillo, CA) and subsequently rinsed again in PBS for 3x10 minutes. Sections stained with the antibodies mentioned were all mounted on glass slides and coverslipped with anti-fading medium vectashield containing DAPI (Vector, Vector Laboratories, Burlingame, CA).

Negative control staining where the primary antibody was omitted showed no detectable labelling.

The area of cav-1 and cav-2 immunolabeling was quantified at 1, 3, 7, and 60d from a series of images collected at 20X objective (422 μm X 338 μm) in perilesional parietal cortex and ipsilateral temporal cortex using an epifluorescent microscope with the same parameters for all animals (Olympus, BX41, Center Valley, PA). Images were acquired from five serial coronal slices separated by 500 μm (24 images per animal). The area of cav-1 and cav-2 staining was measured for each individual image with MorphoPro software (Explora-Nova, La Rochelle, France) according to the following procedure: 1) Top Hat morphologic filter to outline vascular staining from the background, 2) user-defined thresholding value applied to each image. Final values were represented as a percentage of the sham group.

Cav-3 was mainly observed in astrocytes and scored in the perilesional parietal cortex adjacent to the lesion site on 5 sections separated by 500 μm per animals. Scoring was given a value from 0-4 with (0) no staining seen; (1) faint staining in a few positive cells, (2) bright staining in a small area, or low intensity staining in a larger area (more positive cells), (3) bright staining in a larger area, or (4) very intense staining over a large area.

Western Blotting

A second set of rats was prepared with four animals per group at 1d and brains were freshly dissected and the cortical tissue adjacent to the site of the impact was collected. Tissues were prepared in RIPA buffer with a cocktail of protease inhibitors (Roche, Basel, Switzerland) and sonicated for 30 s (Hirt et al., 2009). After BCA protein assay, 10 μg of protein was then subjected to SDS polyacrylamide gel electrophoresis on a 4-12% gel (Nupage, Invitrogen, Carlsbad, CA). Proteins were then transferred to a polyvinylidene fluoride membrane as indicated by the supplier (PerkinElmer, Germany). The blot was incubated with a rabbit polyclonal against cav-1 (BD Biosciences, 1:2000) and a monoclonal antibody against Tubulin (Sigma, USA, 1:10,000); a monoclonal antibody against cav-2 or cav-3 (BD Biosciences, 1:2000) and a polyclonal antibody against actin (Sigma, USA, 1:25,000) in Odyssey blocking buffer (LI-COR, Bioscience, Germany) overnight at 4°C. After washing, the blot was incubated with two fluorescence-coupled secondary antibodies (1:10,000, anti-rabbit Alexa-Fluor-680nm, Molecular Probes, Oregon and anti-mouse IR-Dye-800-nm, Roche, Germany) for 2 hours at room temperature. After washing, the degree of fluorescence was measured using an infra-red scanner (Odyssey, LI-COR, Germany).

Statistical Analyses

All data are presented as mean \pm SEM, statistical analyses were done using SPSS, and graphs obtained using SigmaPlot. The IgG extravasation, cav-1, cav-2 immunolabeling, and western blot data were analyzed using student t-tests for normally distributed data with comparison between the sham and jTBI groups for each individual time points. Cav-3 data were analyzed using a non-parametric Mann-Whitney test with a comparison between the sham and jTBI.

Results

Blood-Brain Barrier Disruption in Early Time Points after jTBI

IgG extravasation staining was used to evaluate BBB disruption from 1d to 7d (Fig. 1). Increased staining of extravasated IgG was observed in the perilesion and contralateral cortex of jTBI animals (Fig. 1) at 1d and 3d compared to the sham group. The IgG staining decreased back to the normal (i.e. sham) level at 7d (Fig. 1A). Quantification of the surface area of extravasated IgG showed a significant increase in the perilesion cortex of the jTBI rats at 1d and 3d compared to sham (respectively $0.023 \pm 0.033 \text{ mm}^2$ vs. $0.002 \pm 0.001 \text{ mm}^2$ and $0.035 \pm 0.042 \text{ mm}^2$ vs. $0.002 \pm 0.001 \text{ mm}^2$, $p < 0.05$, Fig. 1E). This suggests that BBB disruption is maximum at 1d and 3d post-injury, which is in agreement with our previous observations that showed vasogenic edema formation between 1d and 3d, followed by normalization after 7d (Fukuda et al., 2012).

In parallel with increased IgG extravasation staining, immunostaining for claudin-5 showed a decrease at 1d and 3d in the cortical perilesion in the jTBI group (Fig. 1D) compared to the sham group (Fig. 1C). At 7d, claudin-5 immunoreactivity was comparable to the sham level (Fig. 1D), suggesting a return to normal as observed for the IgG extravasation (Fig. 1A, B).

Changes in Vascular Expression of Caveolin-1 and -2 after jTBI

Caveolin-1 Expression and Distribution after jTBI

Mouse and rabbit cav-1 antibodies were used in double immunostaining to identify the cell distribution of cav-1 after jTBI in the tissue adjacent to the lesion and remotely. As previously described in adult brain (Nag et al., 2007), the rabbit anti-cav-1 antibody was observed in brain endothelium and also in other cell types such as astrocytes and neurons (Fig. 2A, B, C, D). At 1d and 3d, when BBB disruption was maximal (Fig. 1), double immunolabeling of GFAP and cav-1 showed co-localization, suggesting the presence of cav-1 in the reactive astrocytes at the border of the lesion at 1d and 3d in jTBI (Fig. 2A, B, C). Rabbit anti-cav-1 staining also co-localized with mouse anti-NeuN staining (Fig. 2D), suggesting an increased immunoreactivity of cav-1 in neuronal nuclei located around the lesion site at 3d post-injury. However, cav-1 staining did not co-localize with IBA-1 staining, a marker of microglia cells (Fig. 2E). As previously described in literature, mouse anti-cav-1 staining showed that cav-1 is predominantly expressed in brain endothelial cells (Fig. 2E, F) of all cerebral blood vessels, independent of the diameter (from the pial vessels to intracerebral arterioles and capillaries) in normal brain (not shown) and at distance from the site of the injury. The presence of cav-1 in the endothelium was also observed with the rabbit anti-cav-1 (Fig. 2C, D).

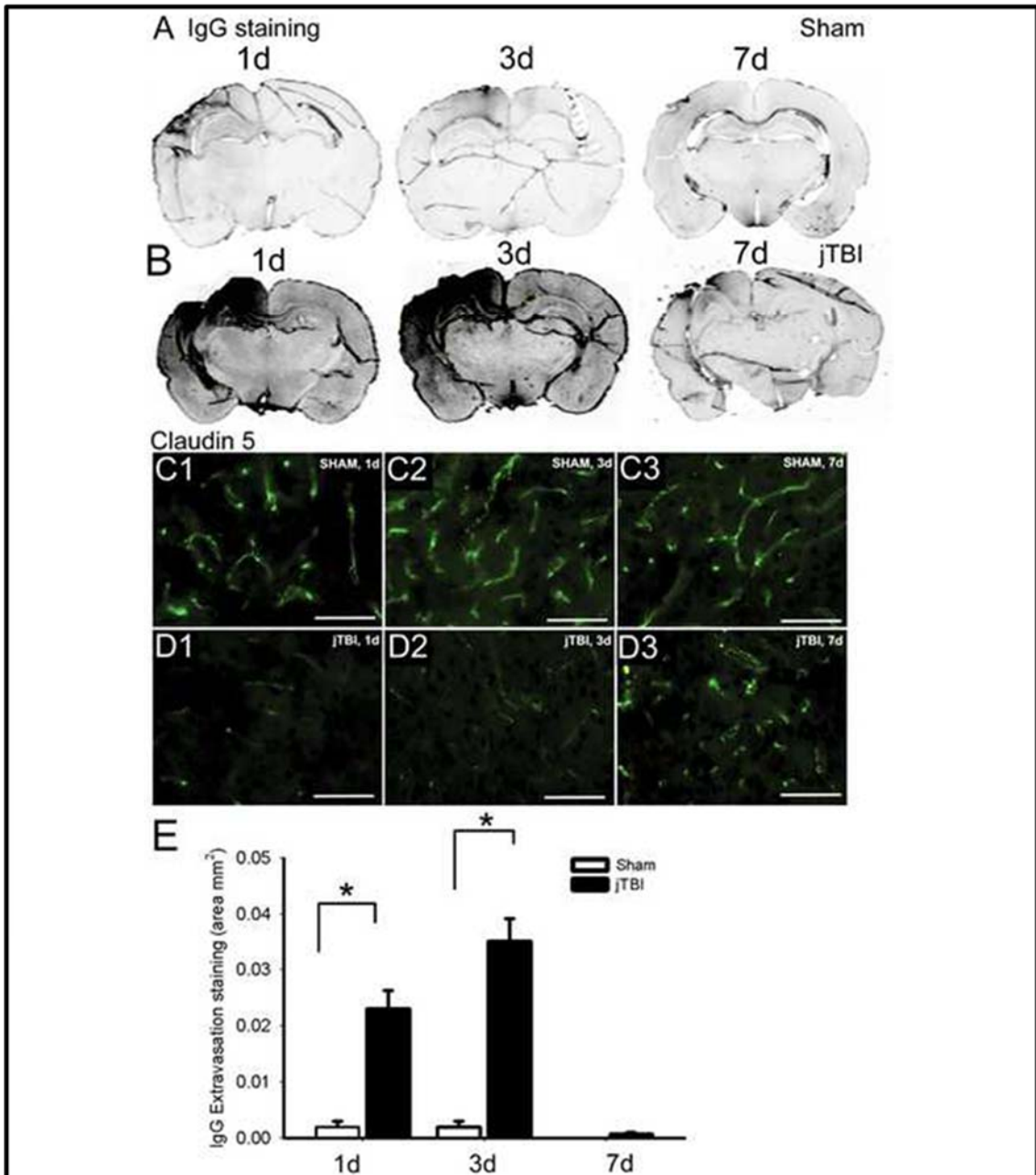


Figure 1. BBB disruption after jTBI: (A, B) IgG extravasation staining in sham (A) and jTBI (B) at 1, 3, and 7d post injury. Area of IgG staining (black) is enlarged at 1 and 3d in jTBI animals (B) compared to sham (A), but normalizes by 7d (A, B). (C, D) A tight junction protein Claudin-5 staining in the sham (C) and jTBI (D) at 1d (C1, D1), 3d (C2, D2) and 7d (C3, D3). In accordance with IgG staining (A, B), the staining of claudin-5 is lower in jTBI (D1, D2) than sham group (C1, C2) at 1d and 3d. Intensity of claudin-5 staining in jTBI group is going back to the sham value at 7d after the injury (C3, D3). (E) Quantification of IgG immunoreactivity shows a significant increase at 1 and 3d, but not at 7d (E; $p < 0.05$). Taken together, increased IgG extravasation signifies a more disrupted BBB and a decreased claudin-5 signifies less intact tight junction proteins. C, D, bar = 100 μ m

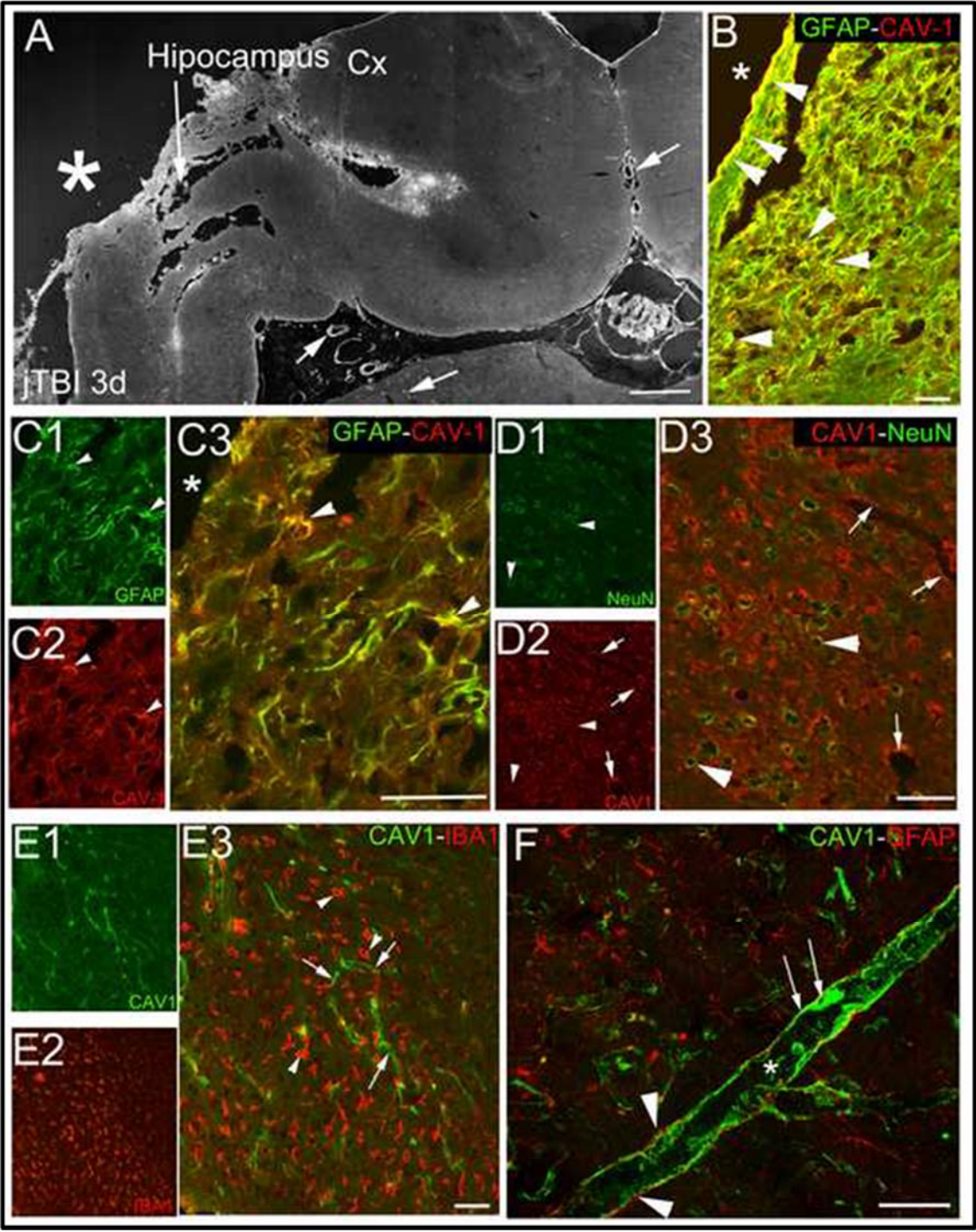


Figure 2. Caveolin-1 Distribution in brain cell types after jTBI. (A) Caveolin-1 (cav-1) staining was studied in regions directly bordering the lesion cavity (*), at the perilesional cortex, and hippocampus under the site of impact. Pial blood vessels of various sizes as well as intraparenchymal blood vessels were stained by Cav-1 (arrows). There was a visual gradient of cav-1 staining that was brightest around the cavity border, and decreasing further from the impact site. (B, C) In the perilesional areas, cav-1 staining (red, B, C2, C3) was co-localized with GFAP labeling (green, B, C1, C3) (arrowheads), which is an astrocytic marker and increased in reactive astrogliosis. (D) NeuN labeling (green, D1, D3) and Cav-1 staining (red, D2, D3) co-localized (yellow, arrowheads), suggesting presence of cav-1 in neurons in periphery of the lesion. Cav-1 staining (red, D2, D3) is also observed in intracortical microvessels (arrows) (E) Cav-1 labeling (green, E1, E3, arrows) and IBA1 staining (red, E2, E3, arrowhead), a marker of microglial cells, did not show co-localization. (F) Cav-1 labeling (green) and GFAP (red) staining did not show co-localization in parietal cortex at distance to the injury site, suggesting that astrocytic cav-1 staining may be contained within reactive astrogliosis around the injury (arrowhead = astrocyte endfeet, arrow = cav-1 in endothelium). A, bar = 500 μ m; B, C, D, E, F, bar = 100 μ m

The regional observation of the cav-1-IR showed an increase in the staining of brain cortical blood vessels from 1d to 60d (Fig. 3B) in the perilesion compared to the sham groups (Fig. 3A). The quantification showed that cav-1-IR at the perilesional cortex is significantly increased by 36% at 1d, 105% at 3d, 92% at 7d and 88% at 60d compared to the sham groups ($p < 0.05$, Fig. 3C). The relative change in cav-1-IR at 1d was confirmed by western blot quantification performed on the perilesional cortical tissue at 1d. Both monomeric (molecular weight at ~ 22 kDa) and oligomeric forms (molecular weight at ~ 66 kDa) of cav-1 were significantly increased in jTBI compared to sham (Fig. 3D, E; $p < 0.05$).

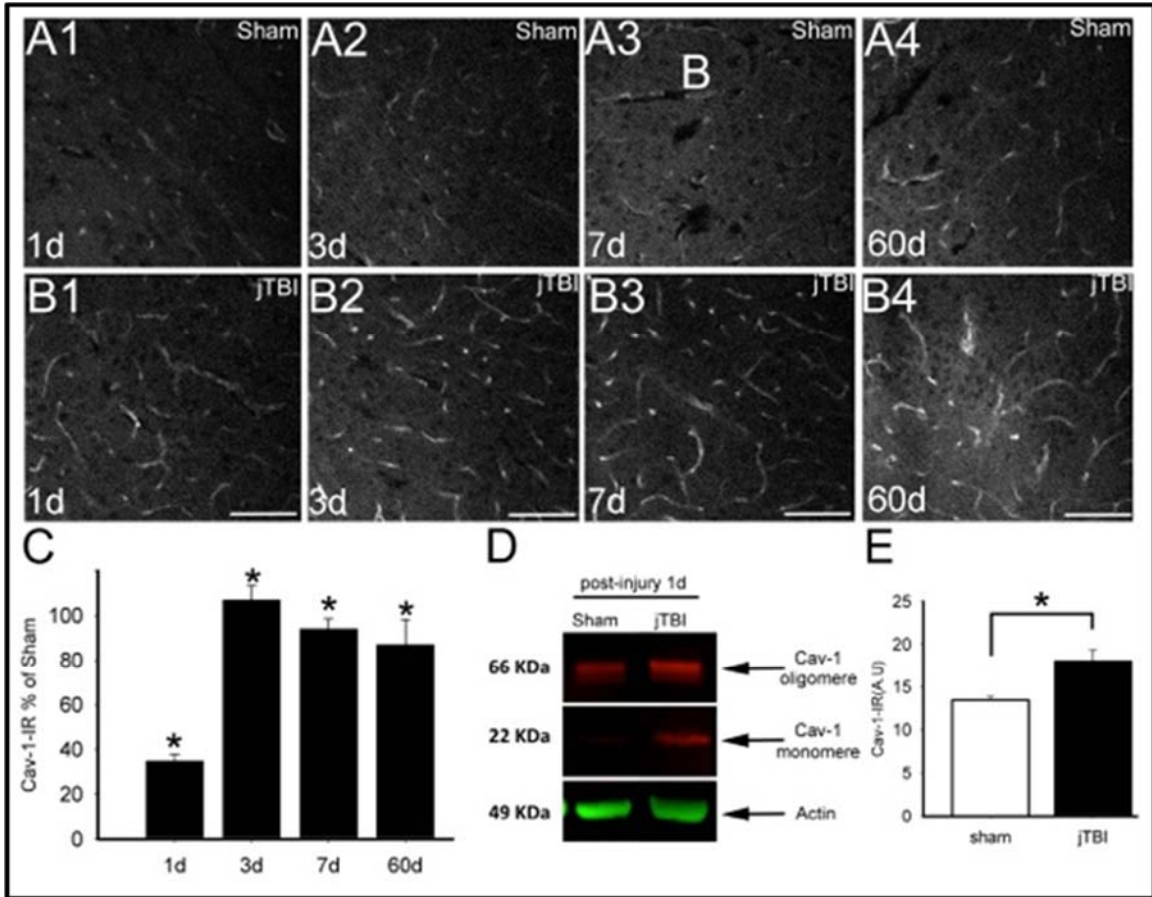


Figure 3. Increased Caveolin 1 Expression after jTBI

(A, B) Caveolin-1 (cav-1) staining in the sham (A) and jTBI (B) at 1d (A1, B1), 3d (A2, B2), 7d (A3, B3) and 60d (A4, B4) after the injury. Less endothelial cav-1 staining was observed throughout the time points studied in sham (A) compared to jTBI (B). (C) Quantification of cav-1 immunoreactivity (IR) showed significant increases in jTBI animals compared to sham at 1, 3, 7, and 60d ($p < 0.05$). (D) Western blot for cav-1 showed monomer at 22 kDa (red), oligomer at 66 kDa and tubulin (green) at 55kDa in sham and jTBI cortex. Both cav-1 monomer and oligomer are increased when tubulin did not show changes. (E) The quantification of the blot showed significant increase in cav-1 staining intensity in jTBI animals after normalization with Tubulin compared to sham group (E, $p < 0.05$). A, B, bar = 100 μ m

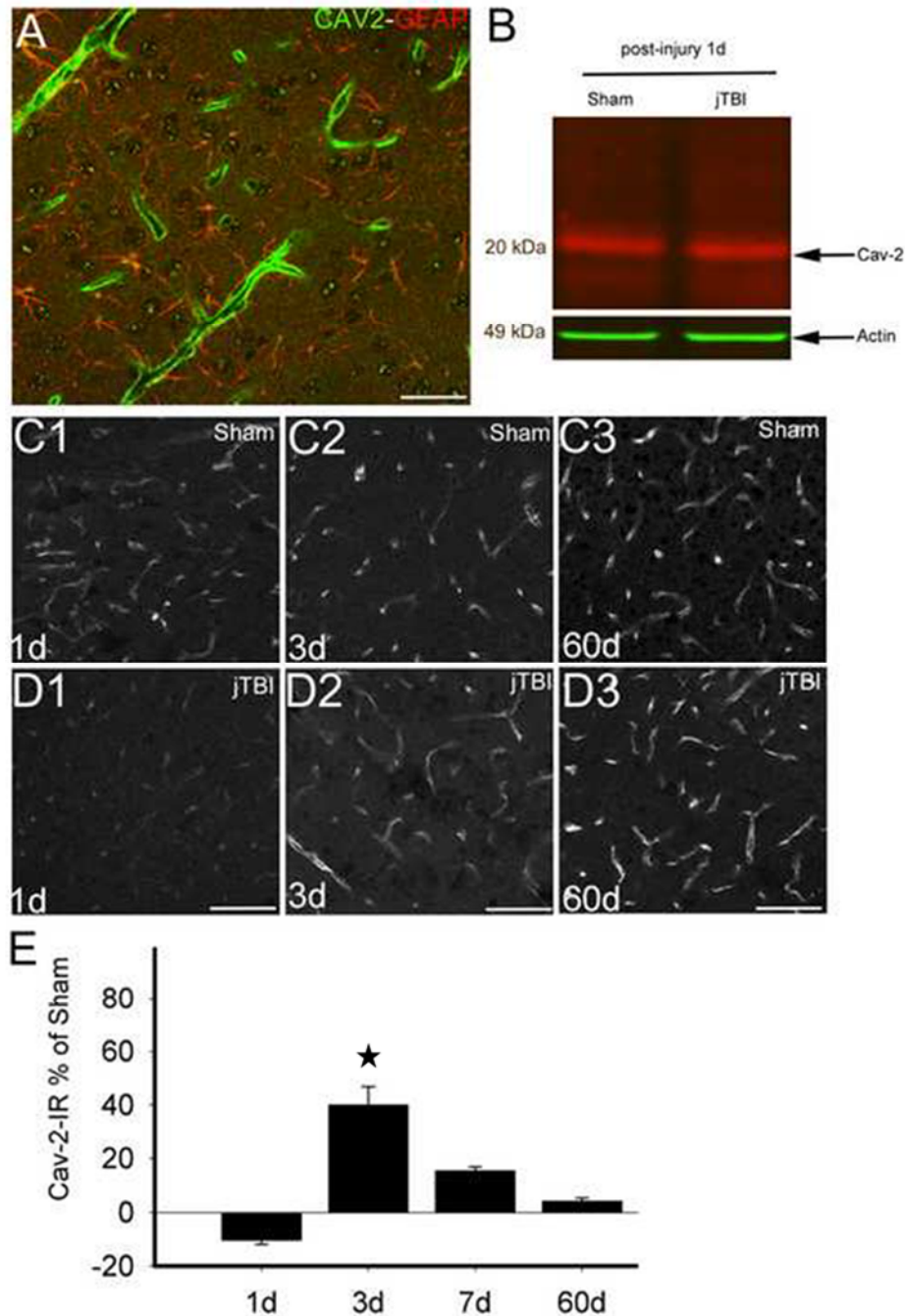


Figure 4. Acute Increase in Caveolin 2 Expression after jTBI. (A) Caveolin-2 (cav-2, green) and GFAP (red) did not exhibit co-localization, unlike cav-1 (Fig. 2), and only endothelial staining was observed. (B) Western blot of cav-2 (red) showed a band around 20kDa with no difference in intensity between sham and jTBI group at 1d post-injury. Actin (green) at 49 kDa was used as protein of reference to assess the loading. (C, D) Cav-2 staining in the sham (C) and jTBI (D) at 1d (C1, D1), 3d (C2, D2) and 60d (C3, D3). Cav-2 was more intensely stained in jTBI (D2) versus sham (C2) only at 3d post-injury. (E) Quantification of immunoreactivity showed significant change in cav-2 only at 3d ($p < 0.05$) compared to sham. C, D, bar=100 μ m

Acute Change in Vascular Caveolin-2 after jTBI

Similar to cav-1-IR, cav-2-IR was observed in brain endothelial cells in brain blood vessels of all sizes (Fig. 4A, C, D) including pial blood vessels in both shams and jTBI group. The western blot showed a band around 20 kDa in both sham and jTBI, without any difference between the groups (Fig. 4B). The analysis of the level of cav-2 IR was performed on the same regions of interest that was used for cav-1. There was a slight decrease of cav-2 IR in jTBI group at 1d post-injury (Fig 4C, D; not significant). This was followed by a significant increase in cav-2 in the jTBI animals on at 3d post-injury ($p < 0.05$; Fig. 4, C2, D2 and E). No significant changes were seen between the sham and jTBI animals at 7d (not shown) and 60d post-injury (Fig. 4C, D, E). This result was confirmed by quantification of Cav-2-IR in the perilesional cortex over the timeline (Fig. 4E) and by the western blot quantification (not shown).

Changes in Astrocytic Caveolin-3 Expression after jTBI

Cav-3 staining was observed in astrocytes located in the glia limitans, cortex, hippocampus, white matter tract (Fig. 5A, B), and hypothalamus (data not shown). Double immunolabeling of GFAP and cav-3 confirmed the presence of cav-3 in astrocytes (Fig. 5B). Interestingly, cav-3-IR is also highly co-localized with eNOS staining in the astrocytes at the border of the lesion cavity (Fig. 5C). Western blot of cav-3 showed a band around 20kDa (Fig 5D) that is significantly higher in the jTBI group compared to sham at 1d (Fig. 5D). Immunohistochemical observation showed increase of cav-3-IR in reactive astrocytes in the vicinity of the lesion in the cortex (Fig 5A, E). In addition, increase of cav-3 staining was also observed in the corpus callosum and in hippocampal structures below the site of the impact, but there was no such increase in the contralateral cortex (data not shown). These observations were confirmed by categorical

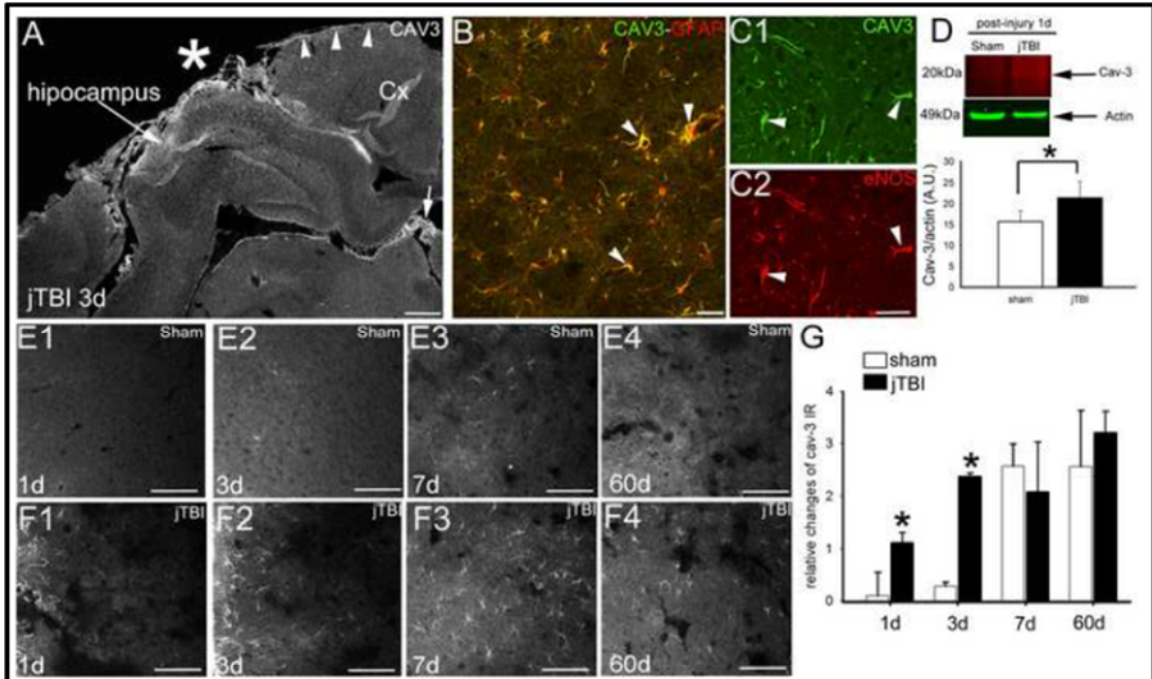


Figure 5. Caveolin-3 Expression and Distribution after jTBI. (A) Caveolin-3 (cav-3) staining was studied in regions directly bordering the lesion cavity (*), at the perilesional cortex, and hippocampus under the site of impact. Cav-3 staining was observed in astrocytes located in the glia limitans (arrowhead), cortex, hippocampus, white matter tract and choroid plexus (arrow). (B) Cav-3 staining (red) and GFAP labeling (green) showed co-localization (yellow, arrowheads), showing the presence of cav-3 in astrocyte process and cell bodies. (C) Cav-3 labeling (red, C1, arrowheads) and eNOS (green, C2, arrowheads) are also co-localized, suggesting association between eNOS and cav-3. (D) Western blot of cav-3 (red) showed a band around 20kDa and is significantly higher in jTBI compared to sham. The quantification of the intensity of the band for cav-3 was normalized to the actin (green, 49kDa). (E, F) Cav-3 staining in the sham (E) and jTBI (F) at 1d (E1, F1), 3d (E2, F2), 7d (E3, F3) and 60d (E4, F4) after the injury. Cav-3 staining is increased in the jTBI animals (F) compared to sham (E), mostly in the acute phase after injury at 1 and 3d (E1, E2, F1, F2). (G) Categorical scoring of cav-3 staining showed that the immunoreactivity (IR) of cav-3 was significantly higher in jTBI compared to sham at 1 and 3d ($p < 0.05$) in the perilesional cortex. A, bar = 500 μ m; B, C, E, F, bar = 100 μ m

scoring of the Cav-3 staining over several sections covering the lesion. It showed that cav-3 staining was increased in jTBI compared to sham groups in the perilesional brain structures at 1d (Fig. 5F1, G) and 3d (Fig. 5F2, 5G) compared to the sham groups (Fig. 5E1, E2, G). After 7d and 60d, there were no longer differences between the groups where the cav-3 staining was observed in the astrocytes in both groups (Fig. 5E3, E4, F3, F4, G).

Discussion

The level of expression of cav-1 is increased in the endothelium and astrocytes, cav-2 increased only in the endothelium, and cav-3 is increased in astrocytes after jTBI during the first week post-injury, which is also known to be a period of active BBB disruption. This increased expression level for cav-1 is still maintained even at 2 months after injury, suggesting phenotypic changes in the endothelium after jTBI, in accordance with our previous studies showing an increased claudin-5 and decreased Pgp (Pop et al., 2012). These observed changes in caveolin expression following jTBI, coupled with the fact that caveolins are central to caveolae formation and function, as well as in the regulation of several endothelial signaling pathways, indicate that cav-1, cav-2, and cav-3 may be good molecular targets to mitigate the neurovascular changes at early and later time points after jTBI. The functional roles of these proteins, however, need to be determined *in vivo* in this pathological model.

Acute Increase in Endothelial Caveolins-1 and -2 Precedes BBB Recovery

As indicated in the introduction, TBI in the juvenile population is known to be associated with greater risks of cerebral hemodynamic dysfunction, BBB disruption, and diffuse cerebral edema, compared to adults (Armstead, 1999, Suh et al., 2001, Campbell

et al., 2007, Giza et al., 2007, Freeman et al., 2008). BBB disruption in clinical patients is known to be a major cause of mortality and long-term neurological deficits in victims with moderate to severe TBI (Shlosberg et al., 2010). There are also more recent evidence indicating that in mild-TBI such as in blast injury, the BBB is impaired early on after the injury (Readnower et al., 2010). Hence, there is a need to study BBB changes in jTBI at early and long-term.

The jTBI model showed a significant increase in IgG extravasation at 1 and 3d, paralleled with the loss of claudin-5 staining in the cortex (Fig. 1), and these indicate a physical BBB disruption during the development of the secondary injuries. It is interesting to note that BBB disruption parallels the peak of edema formation previously observed on the T2-weighted MRI in a similar jTBI model (Fukuda et al., 2012). At 7d, the extravasation of IgG as well as the claudin-5 staining returned to sham levels, suggesting a recovery of the BBB. Similarly, BBB recovery parallels the decrease in vasogenic edema previously observed as a return to the normal T2 values on T2-weighted MRI scans at 7d in a similar injury model (Fukuda et al., 2012). Despite this return to normal T2 values at 7d, long-term phenotypic changes at the endothelium still occur (Pop et al., 2012).

Endothelial cav-1 and 2 could be good molecular candidates to study with regard to changes in BBB properties because of their possible involvement in the regulation of several intracellular signaling processes (Bucci et al., 2000, Razani et al., 2002, Schubert et al., 2002, Minshall et al., 2003, Stamatovic et al., 2009, Gu et al., 2011). Cav-1 was shown to be involved in the regulation of eNOS activity (Garcia-Cardena et al., 1997, Bucci et al., 2000, Bernatchez et al., 2005), c-Jun N-terminal kinase activation (Tourkina et al., 2008, Tourkina et al., 2010), as well as in the stabilization of tight junction proteins such as claudin-5 within the lipid raft domain and P-gp (Jodoin et al., 2003, McCaffrey et al., 2007, McCaffrey et al., 2012).

In the juvenile rodent population, cav-1 and cav-2 distribution were observed in the endothelial layer of brain blood vessels of all sizes (from capillaries to pial arteries, Fig. 2A) in accordance with previous studies carried out in adult mammalian brains (Cameron et al., 1997, Virgintino et al., 2002). In contrast to the distribution of cav-2, cav-1-IR was also observed in some astrocytes and neurons in the jTBI group, which is in accordance with previous studies (Ikezu et al., 1998, Virgintino et al., 2002, Head et al., 2008, Head et al., 2010). The potential role of cav-1 changes in the astrocytes after jTBI is reviewed later in the discussion. Cav-2 expression was changed significantly only at 3d after jTBI, which was the peak of edema formation. In contrast, increased cav-1 in the endothelial cells in the ipsilateral cortex was observed not only throughout the acute injury phase (from 1d to 7d), but also at a later time point (2 months) after the injury. Similar findings were reported from other adult rodent models of CNS insults with an early increase of cav-1 in the endothelial cells preceding the decrease of claudin-5 and occludin (Nag et al., 2007, Nag et al., 2009). From that study, the authors concluded that the increase of cav-1 could potentially contribute to BBB disruption (Nag et al., 2007, Nag et al., 2009).

Intriguingly, tight junction proteins, claudin-5 and occludin, have been shown to bind to and be stabilized by cav-1 within the caveolae (McCaffrey et al., 2007). After hypoxia-reoxygenation, levels of claudin-5 and occludin found within the caveolae were all together reduced (McCaffrey et al., 2007, McCaffrey et al., 2009). Cav-1 was therefore proposed to play key roles in the maintenance of these tight junction protein subunits (McCaffrey et al., 2007, McCaffrey et al., 2009, Stamatovic et al., 2009). Moreover, cav-1^{-/-} mice presented higher endothelial permeability in the systemic vasculature compared to WT (Razani et al., 2001, Schubert et al., 2002). Therefore, a decrease in cav-1 may suggest a disruption in the BBB integrity, whereas an early increase of cav-1, as observed in our model during the first week, may be beneficial

toward the recovery of the BBB integrity after jTBI. In support of this hypothesis, *cav-1^{-/-}* mice showed a larger lesion volume compared to WT in a transient middle cerebral artery occlusion model (Jasmin et al., 2007). That study concluded that the absence of *cav-1* is detrimental due to a decrease in angiogenesis in the *cav-1^{-/-}* mice compared to WT (Jasmin et al., 2007). Cav-1 has a CSD sequence that binds to eNOS and inhibits its activity (Bucci et al., 2000). A decrease of NO formation following increase of Cav-1 in a stroke model was shown to be associated with decreased activation of MMPs (Gu et al., 2011) and consequently protected the BBB. The recent experiments with *cav1^{-/-}* suggest that early increase of *cav-1* in endothelium following jTBI may be an endogenous mechanism aimed at facilitating BBB recovery during the first week. Until now, the exact role of *cav-1* in brain injury and especially in jTBI is still unknown, and detrimental effects of acute *cav-1* increase cannot be ruled out.

Long-Term Caveolin-1 Overexpression may be Detrimental

In our model, the level of *cav-1* expression was also increased in the endothelium (Fig. 3) when claudin-5 is up-regulated at 2 months after injury (Pop et al., 2012). Long-term changes of *cav-1* expression was also reported at 14d after spinal cord injury in adult rodent (Shin et al., 2005), when usually the tight junctions and BBB have already recovered. This higher expression of *cav-1* at 2 months after injury is possibly a part of the endothelium phenotypic changes observed after jTBI (Pop et al., 2012). Cav-1 could be a molecular pathway in the increase of claudin-5 as well as the decrease of p-glycoprotein. In fact, increase of *cav-1* was associated with a decrease of the P-gp activity (McCaffrey et al., 2012). We cannot rule out the possibility that an increase in *cav-1* staining could be associated with an increase in the number of caveolae, which in turn is responsible for increased transcytosis (Jodoin et al., 2003,

Regina et al., 2004) and the entrance of albumin, which may contribute to the dysfunction of the brain tissue homeostasis (Komarova and Malik, 2010).

Caveolin-1 and -3 in Astrocytes: Role in Astrogliosis?

Reactive astrocytes after jTBI showed increase in cav-1 and 3 expressions during the first week. As described previously, the increase of cav-1 staining in the reactive astrocytes was mostly detected with rabbit polyclonal anti-cav-1 (Virgintino et al., 2002, Shin et al., 2005). Cav-1 and 3 are co-localized with GFAP staining, which is consistent with previous studies in adult models (Ikezu et al., 1998, Shin et al., 2005). Although cav-3 has been reported in smooth muscles (Ikezu et al., 1998), we did not observe any staining in intraparenchymal cerebral blood vessels. The expression and localization of cav-3 in the jTBI brains appears to coincide with astrogliosis, which is similar to findings in experimental autoimmune encephalomyelitis (Shin et al., 2005). The exact roles of these proteins in the astrocyte functions *in vivo* are still unknown. Caveolins were associated with eNOS, which was previously shown in the astrocytes in the rat brains (Colasanti et al., 1998, Wiencken and Casagrande, 1999). Excess NO produced after brain injury can overload its inactivating enzyme, superoxide dismutase, resulting in a cascade of events that have several cytotoxic effects on the brain tissue as well as activation of the MMPs (Gu et al., 2011). Activated MMPs cleave key proteins that are important for maintaining the BBB including matrix proteins in the basement membrane and inter-endothelial junctional proteins such as the claudins and occludins (Yang et al., 2007).

After jTBI, both cav-3 and cav-1 are present in the astrocytes and cav-3 was co-localized with eNOS. In the periphery, cav-3 was shown to interact with neuronal NOS (nNOS), and in astrocytic culture, cav-1 was observed to function as an endogenous inhibitor of eNOS (Colasanti et al.). Therefore, increase of Cav-1 and 3 in the astrocyte

may be linked with the regulation of eNOS activity to prevent the release of excess NO. Interestingly, the changes of the level of expression of cav-1 in astrocyte cultures were associated with the glutamate transporter, GLT1 (Zschocke et al., 2005, Gonzalez et al., 2007). The application of transforming growth factor-alpha (TGF- α) induced a decrease of cav-1 and an increase of GLT1 (Zschocke et al., 2005, Gonzalez et al., 2007). Increase of cav-1 in the astrocytes may, therefore, induce a decrease of GLT1 in the astroglia. This decrease will have a consequence on the glutamate uptake and the excitotoxicity after jTBI.

Conclusion

Cav-1 and cav-3 showed immunoreactivity changes in the astrocytes and endothelial cells after jTBI at early time point as well as long-term. These proteins have several physiological roles within the cells and in the neurovascular unit. This study shows for the first time changes in the expression of these molecules in a model of jTBI. Further studies will be needed to characterize the role of each caveolin in each cell type after jTBI.

Acknowledgements

The authors thank Dr. Viorela Pop for her help for part of the histology and tissue analysis.

This work was supported in part by NINDS grant R01HD061946 (JB), Loma Linda University Department of Pediatrics Research Fund, and the Swiss Science Foundation (FN 31003A-122166, JB) at Loma Linda University.

A portion of this work was performed at the Loma Linda University School of Medicine Advanced Imaging and Microscopy Core, which is supported by the National Science Foundation under Major Research Instrumentation, Division of Biological

Infrastructure Grant No. 0923559 (Dr. Sean M Wilson), and by Loma Linda University School of Medicine.

List of Abbreviations

jTBI (juvenile traumatic brain injury), TBI (traumatic brain injury), BBB (blood brain barrier), Cav-1 (caveolin 1), Cav-2 (caveolin 2), Cav-3 (caveolin 3), CSD (caveolin scaffolding domain), d (days post injury), CCI (controlled cortical impact)

Author's contributions

DA, AF, DS, and JB generated the data, and carried out the analyses and writing; JB carried out the experimental design.

PROLOGUE TO CHAPTER 4
CAVTRATIN AMELIORATES EDEMA AND REDUCES BRAIN
LESION VOLUME AT ACUTE TIME POINTS AFTER JUVENILE
TRAUMATIC BRAIN INJURY

In chapter 3, we described acute and long-term changes in the immunoreactivity and protein expression levels of caveolin-1, -2, and -3 in rat brains following juvenile TBI, and highlighted the potential beneficial role of caveolin-scaffolding domain in the recovery of brain endothelial tight junctions and regulation of BBB permeability following injury. Chapter 4 now focuses on the therapeutic potential of cavtratin – an injectable peptide mimetic of the caveolin scaffolding domain – with respect to repair of BBB tight junctions, reduction of cerebral edema, and improvement in functional outcomes during the peak of edema (See Figure A below for a diagrammatic illustration of the proposed intervention strategy with cavtratin). The question of long-term impact of cavtratin treatment on the histopathology and functional outcome of juvenile TBI is not addressed in this project, and will be a subject of future studies.

The aim of this chapter is therefore to examine the effects of cavtratin treatment on tight junction disruption and associated vasogenic edema, and on functional (mainly neurological and sensorimotor) outcomes following juvenile TBI at acute time point. The hypothesis is that acute treatment with cavtratin (dose = 2.5 mg/kg; injected at 3 hours, 1 day, 2 day, and 3 day post-injury time points) following juvenile TBI will reverse the damage to brain endothelial tight junction proteins and restore its function, thereby reducing cerebral edema and consequently leading to improved functional outcomes. The rationale for the technique and drug dosage used is explained in the section.

The chapter follows the blueprint of a scientific manuscript with detailed figures and figure legends. The data contained in this chapter are yet to be submitted for journal publication.

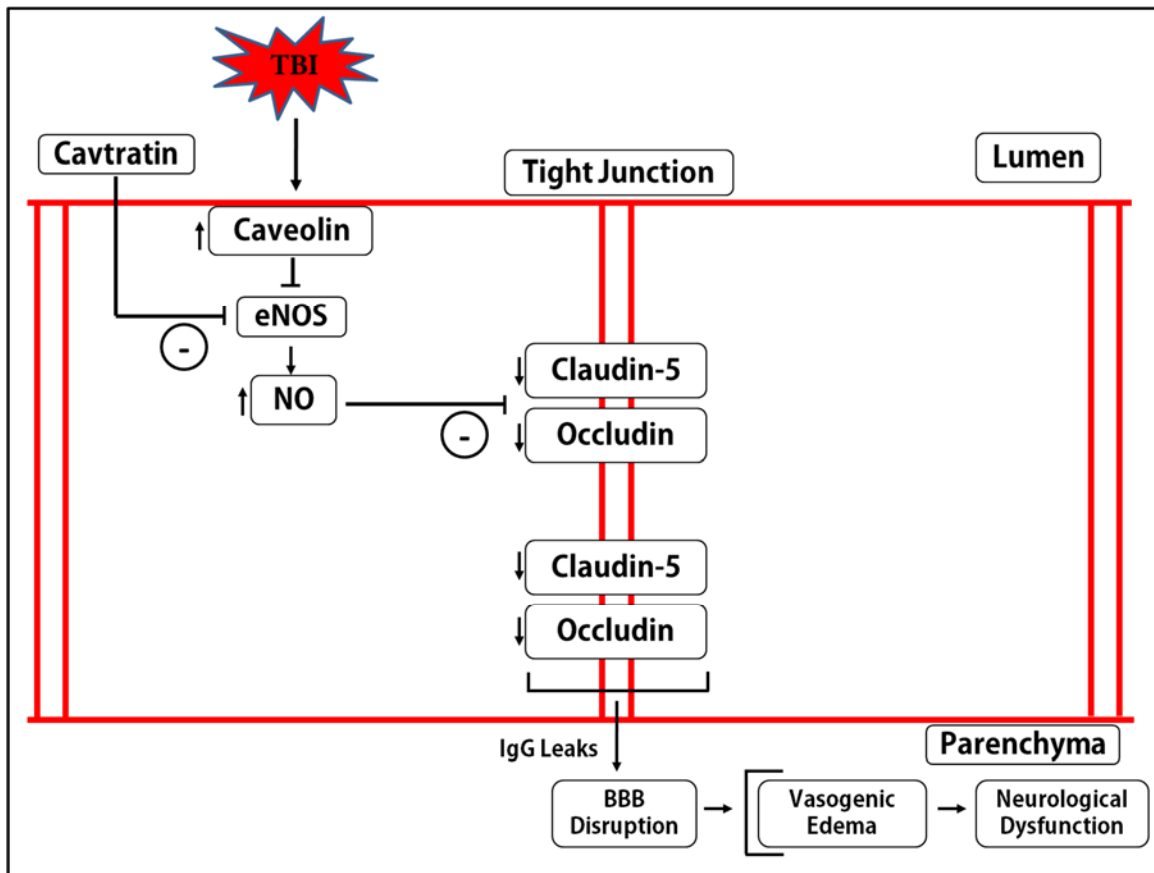


Figure A: Proposed Intervention Strategy in Experimental Juvenile TBI.

TBI in the juvenile brain produces several stress factors which effect increased expression and activation of endothelial caveolins, among others things. Increased expression and activity of caveolins in this model is proposed to inactivate eNOS and inhibit NO production, thereby reversing brain vascular permeability. NO is a highly potent vascular permeability factor. Caveolins has been shown to inhibit JNK hyperactivation in the periphery, but this is yet to be shown in brain endothelial cells. It is also not known whether changes in endothelial caveolins in this model has any effect on observed functional deficits. The proposed intervention strategy involves acute administration of cavtratin – an injectable peptide mimetic of the caveolin scaffolding domain – which can mimic the function of endogenous caveolins with respect to repair of tight junction and reduction of edema. Cavtratin can act on various cell types in the brain (including neurons, astrocytes and endothelial cells), and may promote additive or synergistic therapeutic effects following juvenile TBI.

TBI – Traumatic Brain Injury; eNOS – Endothelial Nitric Oxide Synthase; NO – Nitric Oxide; IgG – Immunoglobulin G; BBB – Blood-Brain Barrier

CHAPTER 4
CAVTRATIN AMELIORATES EDEMA AND REDUCES BRAIN
LESION VOLUME AT ACUTE TIME POINTS AFTER JUVENILE
TRAUMATIC BRAIN INJURY

David O. Ajao¹, Jérôme Badaut^{1, 2*}

Departments of Physiology¹ and Pediatrics², Loma Linda University, Loma Linda, CA.

**Running Title: Cavtratin Ameliorates Brain Damage in Juvenile
TBI**

Key words

Blood-brain barrier, endothelium, juvenile traumatic brain injury, caveolin, cavtratin

Abstract

Blood-brain barrier (BBB) breakdown and the resultant edema formation are emergent therapeutic targets for addressing traumatic brain injury (TBI) in the juvenile brain, which is known to be vulnerable to these two secondary pathophysiological processes of brain trauma. Caveolin-1 has also emerged as an important protein that modulates brain endothelial permeability. We investigate the therapeutic potential of cavtratin – a caveolin mimetic peptide injected systemically – on the brain, following juvenile TBI (jTBI) in P17 rats. We show that intraperitoneal administration of cavtratin at 3 hours post-jTBI results in reduction of brain lesion volume in treated rats at 1d (by 47.9%) and 3d (by 65.8%) post-injury. In addition, edema formation in the lesion ROI – measured with T2-weighted MRI – undergoes significant reduction with cavtratin treatment at both acute time points (1d and 3d). There is however no rapid recovery of neurological functions (tested with foot-faults, beam balance, and rotarod) observable in cavtratin-treated rats compared to saline-controls at 1d and 3d. We therefore conclude that systemic, acute treatment with cavtratin following jTBI protects against enlargement of brain lesion and edema formation, and this suggests future potential development of cavtratin as a therapeutic tool.

Introduction

Two of the secondary pathophysiological processes most commonly associated with traumatic brain injury (TBI) are blood-brain barrier (BBB) disruption and concomitant edema formation (Werner and Engelhard, 2007, Shlosberg et al., 2010). These processes are especially common in juvenile cases of TBI (jTBI) and are a deadly duo responsible for deaths, disability and enormous economic burden (Yeates et al., 2002, Schneier et al., 2006, Coronado et al., 2011). The juvenile brain is susceptible to disruption of its BBB and to diffuse edema formation owing to some unique developmental features which include weak ligamentous protection, less myelination of white matter fibers, and higher brain water content (Battin, 2001, Campbell et al., 2007, Giza et al., 2007, Freeman et al., 2008). Subtle forms of BBB disruption have been observed for months to years following initial TBI assault on young brains (Tomkins et al., 2001, Tomkins et al., 2011). In addition, the juvenile brain has a greater risk for hemodynamic dysfunction (Armstead, 1999, Udomphorn et al., 2008), and together, these unresolved pathological processes translate into long-term functional deficits (Thomsen, 1992, Sbordone et al., 1995, Giza, 2006). These and many more studies highlight post-TBI BBB disruption and edema as bona fide therapeutic targets that require further investigation (Aldrich et al., 1992, Adelson et al., 1997, Shlosberg et al., 2010).

Caveolin-1 – the first member of the caveolin family to be discovered (Rothberg et al., 1992) – is abundant within lipid rafts of brain endothelial cells (Cameron et al., 1997, Virgintino et al., 2002). Together with caveolin-2, caveolin-1 forms the fundamental structural framework of the caveolae (Sargiacomo et al., 1995, Predescu et al., 2007), and is very crucial in mediating transcellular transport through the endothelium into brain parenchyma via transcytosis (Schubert et al., 2002, Predescu et al., 2007, Frank et al., 2009). The rate of transcytosis is, however, very low, and the

process is tightly regulated across the BBB (Wolburg and Lippoldt, 2002). In addition to its role in transcytosis, caveolin-1 has the capacity to scaffold several signaling proteins, some of which are crucial to regulating BBB permeability (Razani et al., 2002, Bernatchez et al., 2005). It performs this role through its caveolin scaffolding domain (CSD) which recognizes specific caveolin binding motifs (CBM) on signaling proteins, ligands and receptors (Razani et al., 2002). A classic example of this CSD-CBM binding and functional interaction is found in the negative regulation of endothelial nitric oxide synthase (eNOS) by caveolin-1, with the resultant reduction in production of nitric oxide (NO) – a highly potent endogenous vasodilator and inducer of BBB permeability (Garcia-Cardena et al., 1997, Bucci et al., 2000). In order to investigate the mechanism and therapeutic potential of endogenous CSD, a synthetic cell-permeable peptide which mimics the scaffolding domain of caveolin – termed CSD peptide or cavtratin (CSD peptide sequence fused with the cell-permeable antennapedia internalization sequence) – has been developed and used extensively (Bucci et al., 2000, Bernatchez et al., 2005, Argaw et al., 2012).

In the search for therapeutic agents to combat post-traumatic BBB disruption in the juvenile setting, CSD mimetic peptide cavtratin is a potentially strong candidate based on multiple literature evidence. Caveolin-1 knockout mice are known to display microvascular hyperpermeability among other phenotypic defects (Razani et al., 2001, Schubert et al., 2002). Using caveolin-1 knockout mice and silencing RNA against caveolin-1 (siCav-1), it was shown that caveolin-1 protects against BBB hyperpermeability after focal cerebral ischemia and reperfusion injury through a negative regulation of nitric oxide (NO)-mediated matrix metalloproteinases (MMPs) activity in the brain (Gu et al., 2011). Using cavtratin as a selective inhibitor of eNOS, improvement in BBB dysfunction and associated reduction in neurologic deficits were observed in a model of multiple sclerosis (MS) (Argaw et al., 2012). Moreover, cavtratin protects

against chemokine-induced breakdown of brain endothelial junctional proteins including occludin and ZO-1 in an *in vitro* model of brain microvascular endothelial cells (BMECs) (Song et al., 2007).

We therefore propose the use of intraperitoneal injection of cavtratin following juvenile TBI in P17 rats to investigate the drug's potential therapeutic benefits. Our objective was to determine whether cavtratin, which mimics some activities of endogenous caveolin-1, is effective in improving BBB integrity and behavioral outcomes post-jTBI. We showed that cavtratin protects against TBI-induced edema formation and remarkably reduced the size of ensuing brain lesion. Our findings showed, however, that there are no appreciable sensorimotor improvements associated with cavtratin administration at least at the acute time points.

Materials and Methods

Subjects

This experiment generally follows previously described animal and experimental protocols in chapters 2, 3 and 4 of this dissertation. Briefly, 12 ten-day old (P10) male Sprague-Dawley rats were ordered from Harlan Laboratories (Harlan, Indianapolis, IN). Upon delivery, they were housed with their dam on a 12-hour light-dark cycle at constant temperature and humidity, in accordance with standard guidelines. The rats were allowed to acclimatize for 7 days prior to induction of controlled cortical injury (CCI) – the key experimental surgical procedure – carried out on the pups at P17. The pups were fed with standard lab chow and water *ad libitum*. All groups of animals used in the study (total n = 12, comprising of 2 different cohorts) had identical CCI surgical parameters, and were randomly divided into saline-injected control and cavtratin-treated groups. The first cohort is comprised of 8 randomly selected rat pups (4 cavtratin-treated and 4 saline-controls) which were all subjected to both MRI and neurological tests at 1dpi and

3dpi before being euthanized. The second cohort comprising of 4 rat pups (2 cavtratin-treated and 2 saline-controls) underwent only neurological testing but no MRI. Euthanization and brain collection were carried out at 3dpi. All protocols and procedures used in this study were approved by the Institutional Animal Care and Use Committee of Loma Linda University and are in compliance with the U.S. Department of Health and Human Services Guide.

Juvenile Traumatic Brain Injury Procedure

The procedure was carried out as we have previously described in literature (Ajao et al., 2012) and as earlier described in this dissertation (see chapters 2, 3 and 4). The same CCI surgery method and parameters were used. Briefly, each rat was subjected to light anesthesia with isoflurane (Webster Veterinary Supply, Inc., Sterling, MA) and placed in a mouse stereotaxic frame (David Kopf Instruments, USA). Following a midline incision on the scalp, a 5-mm craniotomy was bored over the right fronto-parietal cortex at the following coordinate: 3 mm anterior-posterior and 4 mm medial-lateral relative to Bregma. The brain was then impacted by an electromagnetic impactor (impactor tip diameter = 2.7mm) (Leica Microsystems Company, Richmond, IL) to a depth of 1.5 mm from cortical surface, at a 20° angle to dura surface, at a velocity of 6m/s and with impact duration of 200ms. Morphological aberrations to the cortex such as hemorrhage and herniation were recorded. The surgical site was then sutured close followed by subcutaneous administration of an analgesic drug – Buprenorphine (0.01 mg/kg; dilution: 0.01 mg/ml).

Systemic Administration of Cavtratin

The cavtratin dose used in this study is 2.5mg/kg. This dose was effective for selective eNOS inhibition in previously reported *in vivo* studies (Gratton et al., 2003,

Hagendoorn et al., 2004, Bernatchez et al., 2005). The peptide was dissolved in 1% DMSO and diluted 1000-fold in saline to a desired volume before intraperitoneal injection (Gratton et al., 2003). The peptide was injected first at 3 hours post-TBI, and then at 1dpi, 2dpi and 3dpi (between 7am and 9am). Control animals received equivalent volume of 0.9% saline. The rats were returned to their dam after treatment.

Magnetic Resonance Imaging (MRI): Acquisition and Analyses

Image Acquisition

In vivo MRI was performed at 1 and 3 dpi for a subset of the animals (n = 8). Rats were prepared for in vivo MRI as previously described (Ajao et al., 2012). Briefly, following induction of anesthesia (with 1-2% isofluorane), each rat was placed in a temperature controlled cradle containing a volume radiofrequency (RF) coil and imaged mostly on a 11.7T MRI (8.9 cm bore) at 1d and 3d. Some animals were scanned on a larger bore (40 cm) 4.7T MRI (Bruker Biospin, Billerica, MA) at 3d. T2 weighted imaging (T2WI) was acquired in vivo with the following parameters: repetition time/echo time (TR/TE) = 2357.9/10.2 ms; 128 X 128 matrix; 1 mm slice thickness; 1 mm interleaved; average of 4 acquisitions; number of slices = 20; and field of view (FOV) = 2.0 cm for a total imaging time of 20 min on 11.7T MRI; and repetition time/echo time (TR/TE) = 3563.4/20 ms; 128 X 128 matrix; 1 mm slice thickness; 1 mm interleaved; average of 2 acquisitions; number of slices = 20; field of view (FOV) = 2.0 cm for a total imaging time of 15 min on the 4.7T MRI. As previously reported, the use of two different field strengths for *in vivo* MRI did not alter our relative measurements (Obenaus and Hayes, 2011, Ajao et al., 2012).

Lesion Volume Analysis

As previously described (Ajao et al., 2012), volumetric analyses of brain and

lesion volumes were performed using the T2WI in Cheshire software (Hayden Image Processing Group, Waltham, MA). Lesion volumes were defined as the cortical brain regions containing abnormal hypo- and/or hyperintense signals compared to normal-appearing cortical brain matter on the contralateral hemisphere (Fig. 1A). Total brain volume encompasses both normal-appearing and abnormal brain tissues, while herniated tissue, if present, was excluded. In some animals, subcortical and extracortical abnormalities were present but were not included in the lesion. In order to correct for individual brain size differences in the animals and age-related brain growth, the injury volumes were normalized to the brain volumes. Hemispheric volumes were also analyzed using the same inclusion and exclusion criteria.

T2 Analysis

For each T2WI scan, a region of Interest (ROI) was drawn on the slice with the largest lesion area for each of the following areas: lesion, perilesion, striatum and hippocampus on both ipsilateral and contralateral hemispheres. The lesion and perilesion ROIs encompass both hypointense (which may indicate hemorrhage) and hyperintense pixels [which may indicate edema (Gomori et al., 1985, Kato et al., 1986)] within the brain parenchyma (Fig. 2A). ROIs for the hippocampus encompass all visible hippocampal regions along the anterior-posterior axis. All the aforementioned ROIs were later posted on co-registered T2 maps corresponding to each chosen brain slice for acquisition of T2 values. T2 value was extracted for each of the ROIs using Cheshire software.

Neurological Tests

Each behavioral test used in this report has been previously detailed (Ajao et al., 2012). All tests on both saline-controls and cavtratin-treated animals were carried out

within a 3-hour time-block between 8am and 11am, and the animals from both groups were interleaved. The tests were carried out in the sequence in which they are listed below.

Foot-fault

This was performed using an elevated wire mesh (2.5 cm X 30 cm rectangular holes/grid spacing) raised 76 cm above the floor. Movements of each rat placed in the middle of the mesh were video-recorded for 60 sec in two separate trials at 1 and 3dpi. A foot-fault was counted when a rodent's paw slipped completely through the wire mesh. The number of foot-fault for both groups were compared.

Beam Balance

Juvenile animals were tested on a 0.65 cm wide plexiglass beam which is commensurate to their size at 1 and 3dpi. Each animal walked unrestricted for 60 sec for each of two trials 20 min apart, and the distance covered was recorded and compared between saline-controls and cavtratin group.

Rotarod

A constant velocity rotarod paradigm consisting of 2 trials at a slow speed (10rpm) and 2 trials at a faster speed (20rpm) is used at 1 and 3dpi. The rotarod (Rotamex-5, Columbus Instruments, Columbus, OH) operates until each animals falls off. Latency to fall was recorded as a measure of motor coordination and balance and compared between the two groups.

Statistical Analyses

All data are presented as mean \pm SEM. Statistical analyses were done using SPSS, and graphs were obtained using Sigmaplot (SPSS Inc.). All the data were analyzed using student t-tests for normally distributed data with comparison between the cavtratin and control groups for each of the time points. Repeated measures ANOVAs (rm ANOVAs) were used for serial data collected on the same groups.

Results

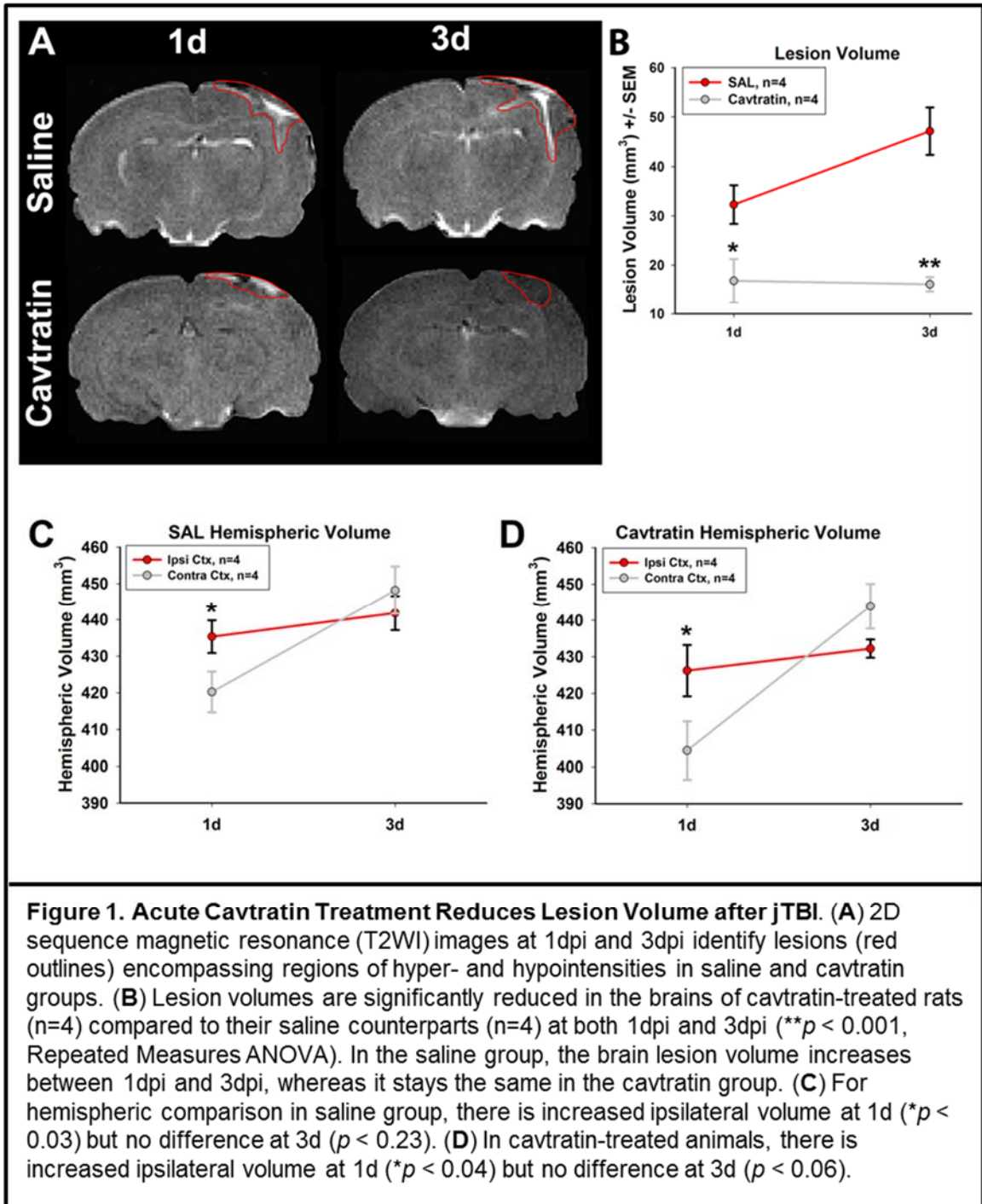
Cavtratin Reduces Cortical Lesion Volume and Ameliorates Some Morphological Alterations

To investigate the potential therapeutic effect of caveolin in brain injuries, cavtratin was injected intraperitoneally at 3 hours following jTBI in P17 rats. Following previously established protocol (Ajao et al., 2012), T2-weighted MRI (T2WI) was utilized to outline and quantify cortical lesion volumes in the brains of both saline-controls and cavtratin-treated animals (Fig. 1A, red outlines). The lesion encompassed both visible hyperintense and hypointense pixels (Fig. 1A). We found that systemic administration of cavtratin results in significant reductions of brain lesion volume in treated rats at 1d (47.9 \pm 13.7% reduction) and 3d (65.8 \pm 3.1% reduction; ** $p < 0.001$, rm ANOVA) post-injury compared to controls (Fig. 1B). Another key difference between the two groups is increase in lesion volume in TBI-saline group between 1d and 3d, not seen in the cavtratin-treated group (Fig. 1B).

There are intragroup differences in hemispheric volumes (Fig. 1C, D). In the SAL group, the ipsilateral hemisphere volumes are significantly increased compared to the contralateral hemisphere at 1d ($*p < 0.03$, t-test), but these differences have been neutralized by 3d ($p < 0.23$, t-test) (Fig. 1C). Similarly, in the treated group, the ipsilateral

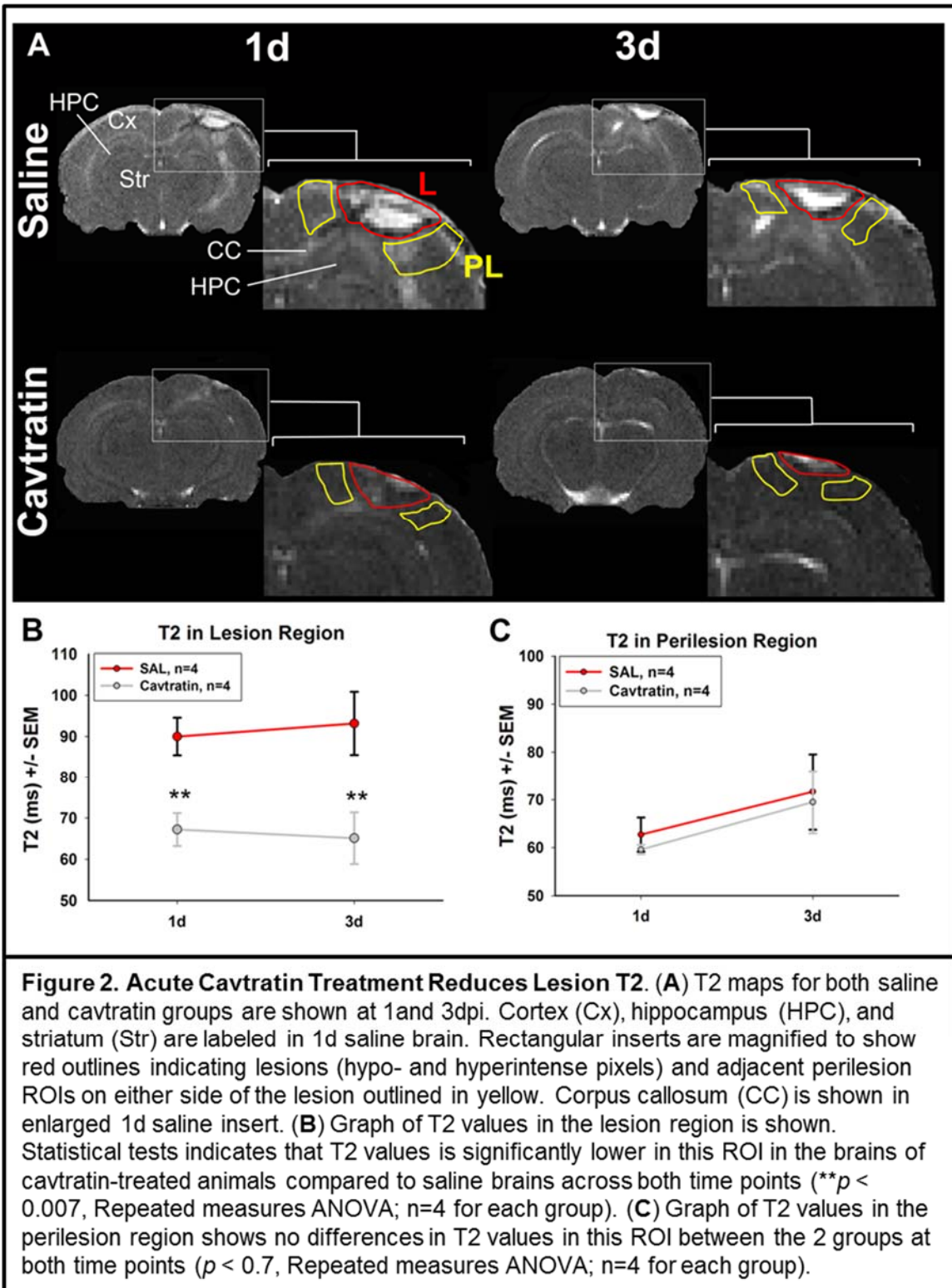
hemisphere volumes are significantly increased at 1d ($*p < 0.04$, t-test) but not at 3d ($*p < 0.06$, t-test) (Fig. 1D).

Moreover, there were no prominent midline shifts observed in brains of both saline and cavtratin-treated subjects. There were also no significant weight differences between the two groups over the experimental period.



Cavtratin Reduces Edema in the Lesion Region Following Brain Injury

We used serially acquired T2WI on the animal subjects to profile T2 changes over the acute time points (Fig. 2A). Shown in Fig. 2A are representative T2WI from saline and cavtratin groups at 1d and 3d, with boxed regions enlarged in the lower panes, and with some major brain structures and ROIs labeled (HPC = Hippocampus; Cx = Cortex; Str = Striatum; CC = Corpus Callosum; L = Lesion; PL = Perilesion). Interestingly, there was a statistically significant decrease in T2 values acquired from lesion ROI (Fig. 2A, red outlines with red letter "L") in the cavtratin-treated animals compared to saline controls at both 1dpi and 3dpi (** $p < 0.007$, rm ANOVA) following jTBI (Fig. 2A, B), suggesting that cavtratin treatment attenuates edema formation acutely. Not surprisingly, there are no significant intragroup changes in T2 values at the lesion ROI between 1d and 3d (Fig. 2B; $p < 0.635$, rm ANOVA). In the brains of saline control rats, T2 values in the perilesion ROIs (Fig. 2A, yellow outlines with yellow letter "PL") at 1d and 3d were significantly lower compared to corresponding T2 values in lesion ROIs (Fig. 2A, red outlines with red letter "L") (** $p < 0.001$, Student's t-test). This distinction is, however, not seen in brains from cavtratin-treated rats which had similar T2 values from both lesion and perilesion ROIs over the acute time points (Fig. 2B, C) ($p < 0.748$, Student's t-test). Unlike T2 values in lesion ROI, there are no intergroup differences in T2 values in the perilesion ROI at both 1d and 3d (Fig. 2C; $p < 0.703$, rm ANOVA). Other regions of the brain besides lesion and perilesion (e.g. contralateral Cx, HPC, and Str, and ipsilateral HPC and Str) show no significant changes in T2 values between the two groups at both time points (data not shown).



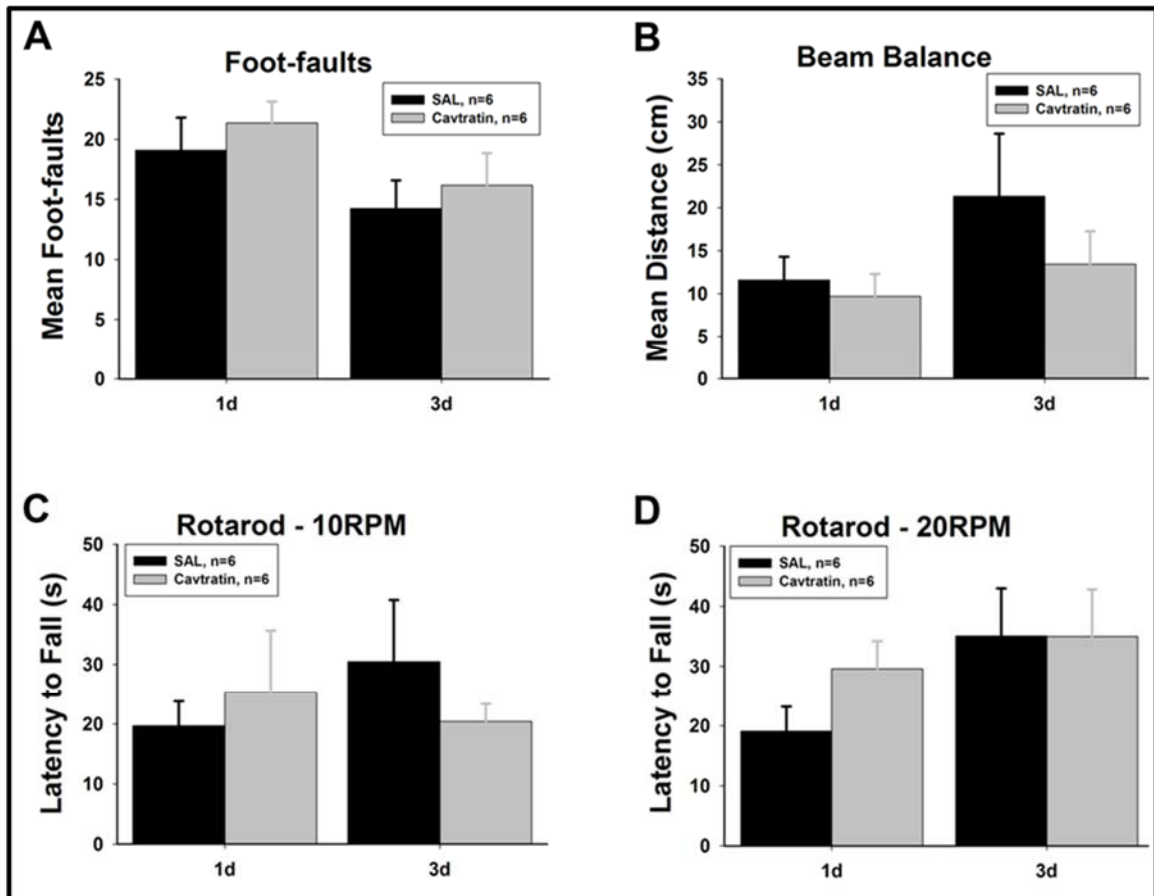


Figure 3. Neurological Test (Foot-faults, Beam Balance and Rotarod) Outcome following Cavtratin Treatment. (A) Graph of foot-fault test (which tests sensorimotor functions) shows no differences in the number of faults between saline-controls (SAL) and their cavtratin-treated counterparts at both 1 and 3dpi ($p < 0.352$, Repeated Measures ANOVA). (B) Likewise, the distance covered on the beam in beam balance test (which examines balance and coordination skills) is not significantly different between the two groups at both time points ($p < 0.332$, Repeated Measures ANOVA). (C) Slow rotarod test set to a constant velocity of 10RPM was used to examine motor balance and coordination. The graph shows no differences in latency to fall between cavtratin-treated rats and controls ($p < 0.788$, Repeated Measures ANOVA). (D) Rotarod set to a constant velocity of 20 RPM was used to further test motor balance and coordination. There is no difference between the 2 groups at over the 2 time points. ($p < 0.48$, Repeated Measures ANOVA; $n=6$ for each group).

Cavtratin Does Not Improve Sensorimotor Functions at Acute Time Point

Because the injury is centered on the somatosensory cortex, it was important to test for the functional impact of the treatment during the peak of edema. To this end, a previously validated set of neurological and behavioral tests were carried out to investigate the impairment and/or recovery of sensorimotor functions which include foot-fault, beam balance and rotarod tests at 1d and 3d post-treatment (Fig. 3) (Ajao et al., 2012). There were no significant differences in the number of foot-faults between the two groups at 1dpi and 3dpi (Fig. 3A; $p < 0.35$, rm ANOVA). Likewise, beam balance test showed no differences between the two groups at both time points (Fig. 3B; $p < 0.33$, rm ANOVA). Consistent with the two previous tests above, rotarod tests showed no intergroup differences either in the 10RPM ($p < 0.79$, rm ANOVA) or 20RPM ($p < 0.48$, rm ANOVA) constant speed paradigm at 1d and 3d (Fig. 3D). Overall, these neurological test results suffer from low statistical power. With increased group sizes, sensitivity may be enhanced for detecting fine motor improvements in between the groups for some of the tests.

Discussion

Multiple reports in scientific literature have highlighted some beneficial effects of the synthetic caveolin-1 scaffolding domain (CSD) peptide, cavtratin, in various experimental models, but not yet in juvenile TBI models. These include studies that utilized *in vitro* (Song et al., 2007, Schmitz et al., 2011) and *in vivo* (Bucci et al., 2000, Gratton et al., 2003, Jasmin et al., 2006, Desjardins et al., 2008) models of disease and system. Caveolin-1 plays a role in regulating endothelial hyperpermeability as demonstrated by the microvascular hyperpermeability of caveolin-1 knockout (-/-) mice (Razani et al., 2001, Schubert et al., 2002). In addition, Song and colleagues (2007)

showed *in vitro* that cavtratin is effective in inhibiting microvascular hyperpermeability in chemokine-stimulated brain microvascular endothelial cells (BMECs) which models BBB *in vitro*. They also found that treatment of BMECs with silencing RNA against caveolin-1 not only reduced caveolin-1 expression, but also reduced expression of key tight junction proteins (Song et al., 2007). More studies are providing further evidence of strong link between endothelial caveolins and TJ proteins. Claudins and occludins are found in isolated caveolae, putatively interacting with caveolins (Nusrat et al., 2000, McCaffrey et al., 2007, Song et al., 2007, Stamatovic et al., 2009). The level of oligomeric claudin-5 and occludin seen in normal brain endothelial caveolae is reduced during pathological conditions such as hypoxia-reoxygenation (McCaffrey et al., 2009). Such reduction engenders TJ and BBB disruption (McCaffrey et al., 2008). Gu and colleagues (2011) recently showed that caveolin-1 protects the BBB against hyperpermeability following focal cerebral ischemia and reperfusion injury through its negative regulation of nitric oxide (NO)-mediated matrix metalloproteinases (MMPs) activity in the brain. These studies above and many more (Miyawaki-Shimizu et al., 2006, Siddiqui et al., 2011) suggest that caveolin-1 is functionally associated with brain endothelial junctional integrity.

Interestingly, recent studies have suggested that caveolin-1 plays crucial roles in regulating efflux transporters in the BBB (Barakat et al., 2007, McCaffrey et al., 2012). McCaffrey and colleagues (2012), for instance, showed that in λ -carrageenan-induced paw edema model (a peripheral inflammatory model in rats), P-glycoprotein (P-gp) – a key efflux transporter at the BBB – was rapidly trafficked to the membrane lipid raft domain, where it colocalized with phosphorylated caveolin-1. This colocalization promoted the redistribution of P-gp at the microvascular endothelial luminal membrane with increased ATPase activity, which suggests functionally active P-gp. Using a rat brain endothelial cell line, Barakat et al (2007) previously suggested that phosphorylated

caveolin-1 may impact the transport property of P-gp. Hence, caveolin-1 is implicated in the maintenance of both molecular TJ proteins as well as transport barriers at the BBB.

A crucial secondary pathophysiological phenomenon commonly observed in juvenile brain trauma that needs to be addressed therapeutically is BBB disruption – which has been shown to last for months and in some cases years after primary injury (Seiffert et al., 2004, Tomkins et al., 2011) – with resultant edema formation (Bolton and Perry, 1998, Schutzman and Greenes, 2001, Stock, 2011). Given literature evidence stated above linking caveolin-1 to regulation of endothelial permeability, we set out to study the effect of systemic administration of caveolin-1 mimetic peptide, cavtratin, on brain lesion, edema formation and, by extension, on neurological function at acute time points following juvenile TBI in P17 rats.

Reduction of Lesion Volume and Amelioration of Morphological Alterations by Cavtratin

We found that cavtratin treatment results in significantly lower lesion volumes in the brains of treated rats compared to saline controls at both 1dpi and 3dpi (Figs. 1A, B). Analyzed along hemispheric lines (Fig. 1C - F), the ipsilateral hemispheres of both control (Fig. 1E) and cavtratin brains (Fig. 1F) had higher volumes compared to their contralateral hemispheres, suggesting a uniformity in injury profile for both groups. The lowered lesion volume in cavtratin group (Figs. 1A, B) however suggests that cavtratin is functionally limiting the extent of the injury. This set of results is important for potential therapeutic application of cavtratin as a caveolin-mimicking pharmacological agent (Desjardins et al., 2008) in jTBI.

There are a few studies in other models of brain injuries that support these findings. In an ischemic stroke (MCAO) study in mice, Jasmin and colleagues (2007) reported that caveolin-1 knockouts (KOs) have a generally worse outcome than the wild-

type (WT), with increased cerebral volume of infarction coupled with impaired angiogenesis and increased apoptotic cell death. Acute and sometimes sustained increase in caveolin-1 expression has been reported following various forms of CNS injuries (Shin et al., 2005, Nag et al., 2007, Shin, 2007, Nag et al., 2009), but opinions are divided on whether this is beneficial or detrimental to the structural and functional recovery of the BBB and brain tissues (Nag et al., 2007, Song et al., 2007). Based on findings in this study, endogenous increase in caveolin-1 could be a form of innate protective mechanism that the brain deploys during active evolution of injury to minimize damage. In further support of this hypothesis, down-regulation of caveolin-1 expression in ischemic-reperfusion stroke model in rodents is concomitant with increased infarction volume, neurological deficit and BBB disruption (Ding-Zhou et al., 2002, Shen et al., 2006, Gu et al., 2011).

Reduction of Acute Edema Formation at Lesioned Brain Region by Cavtratin

Our findings on reduced edema formation (indexed by reduced T2 values) in the lesion ROIs of brains of cavtratin-treated animals (Fig. 2A, B) constitute a strong support for the theory that this CSD mimetic peptide helps in maintaining and protecting the BBB. This effect however was not found in the outlying perilesion ROI (Fig. 2C), suggesting that the drug's therapeutic effect is focused more on clearly lesioned brain regions. In a study that utilized an *in vivo* model of multiple sclerosis (MS) in mice, researchers confirmed that systemic administration of cavtratin reduced eNOS-associated BBB disruption and its resultant edema (Argaw et al., 2012). Argaw and colleagues (2012) further showed that cavtratin increases the expression of TJ proteins claudin-5 and occludin both *in vitro* in human brain microvascular endothelial cells and *in vivo* in VEGF-A null mice model of MS. These findings support a tight junction protein-

maintaining role for caveolin-1 and provide solid support for its role in preventing BBB permeability and edema formation.

Absence of Improvement in Neurological Function

There was a general lack of functional improvements at acute time points (1d and 3d) following cavtratin treatment (Fig. 3), which could be explained in two possible ways. A possible drawback is the shortness of testing period (within 3 days following jTBI) which coincides with period of maximum edema formation (Fukuda et al., 2012). We have previously shown that in this brain injury model, there were no clear increases in the number of foot-faults in jTBI animals compared to shams until 7d post-injury (Ajao et al., 2012). Hence, testing both sensorimotor and cognitive functions at later time points (7d, 30d and 60d) could provide an extended opportunity for picking up subtle functional differences that might have been masked by the evolution of the injury at earlier time points. Later time point testing also affords cavtratin the opportunity to act for a longer time. Given the effects of cavtratin on lesion volume and edema, it is plausible that there would be beneficial functional effects that could be picked out by the right tests at the right time points. Secondly, drugs may confer other functional benefits that may not be reflected in neurological and cognitive tests. For instance, electrophysiological recordings of neuronal firing (such as the measurement of compound action potential – CAP) may be helpful in picking out more subtle functional changes like we demonstrated in a previous report using this jTBI model (Ajao et al., 2012). Given the effects of cavtratin stated above, there is a need for investigating the mechanism(s) of action of this drug.

A Potential Mechanism of Action for Cavtratin – Blood-Brain Barrier Protection

One of the mechanistic possibilities for cavtratin action is through BBB protection. Caveolins are highly enriched in brain microvasculature, although they are found, albeit in smaller amounts, in other cells in the brain such as neurons and vascular astrocytes (Cameron et al., 1997, Virgintino et al., 2002, Head et al., 2010). Caveolins act as scaffolding proteins which bind and modulate the activities of a wide variety of signaling molecules that are segregated within the caveolae compartments not only in brain endothelial cells but also in the periphery (Palade, 1953, Sargiacomo et al., 1995, Cameron et al., 1997, Razani et al., 2002, Lajoie et al., 2009, Lajoie and Nabi, 2010). Tight junction proteins have been shown to actively bind to and be regulated by caveolins (McCaffrey et al., 2007, Stamatovic et al., 2009). Hence, a logical mechanism for the neuroprotective effect of cavtratin seen through reduced lesion volume is the protection against uncontrolled and prolonged BBB breakdown through decreased tight junction protein expression (Song et al., 2007, Gu et al., 2011). This BBB-focused mechanism is evidenced by reduction in edema formation (Fig. 2A, B) – which often results from disrupted BBB – seen in cavtratin-treated subjects and discussed in the next section below. Furthermore, caveolin-1 is known to negatively regulate eNOS which produces NO which in turn activates tight junction proteins-degrading MMPs in the brain (Gu et al., 2011).

There is also a strong positive correlation reported in TBI literature between extent or size of post-TBI brain lesion and BBB disruption (Tomkins et al., 2011). Tomkins and colleagues (2011) noted in their study that the set of patients with larger volume of BBB disruption (measured with T1-weighted MRI and the contrast agent gadolinium/Gd-DTPA) also had significantly larger volume of lesioned and dysfunctional cortex (measured with standardized low-resolution brain electromagnetic tomography

[sLORETA]). Subtle BBB disruption with concomitant functional cortical dysfunction was found in up to four TBI patients in the study (Tomkins et al., 2011). These reports support the theory that cavtratin may be acting mechanistically through protection of TJ proteins and BBB. Increased endogenous caveolin post-TBI may also constitute a compensatory mechanism aimed at limiting BBB damage. These proposed mechanisms need to be investigated by further studies.

Meanwhile, increased immunoreactivity of claudin-5 and decreased immunoreactivity of the efflux transporter p-gp at the BBB have been reported at 2 months following the juvenile TBI model used in this study (Pop et al., 2012). Since caveolin-1 have been implicated in the regulation of both claudin-5 (Liu et al., 2012) and p-gp (Barakat et al., 2007, McCaffrey et al., 2012), it is possible that cavtratin may modulate beneficial changes in these BBB components at long-term following juvenile TBI. This hypothesis needs to be investigated in the future.

Conclusion

We have shown in this study that systemic administration of cavtratin at 3 hours after juvenile TBI is effective in reducing lesion volume and edema formation. We further proposed that these protective effects might be modulated by cavtratin's beneficial activities on the tight junction proteins that make up the BBB. More elaborate studies are highly encouraged to investigate mechanistic details of cavtratin with respect to BBB maintenance, as well as test for functional improvements in cavtratin-treated animals. Such studies may shed further light on the caveolins as potential therapeutic targets in combating BBB disruption following juvenile TBI.

PROLOGUE TO CHAPTER 5
ACUTE ADMINISTRATION OF DJNKI-1 FOLLOWING JUVENILE
TBI IN RATS IMPROVES NEUROIMAGING, HISTOLOGICAL AND
FUNCTIONAL OUTCOMES

Having dealt with the caveolins and cavtratin in chapters 3 and 4 respectively, the second set of molecules that are of interest for early intervention in juvenile TBI (jTBI) are c-Jun N-terminal kinases (JNKs). DJNKI-1 is used as a competitive inhibitor of JNK pathway. See **Fig. 1** below for a diagrammatic representation of the proposed intervention strategy for juvenile TBI using DJNKI-1.

The aim of this chapter is to examine the effect of acute DJNKI-1 treatment on BBB disruption, edema formation, and neurological and behavioral outcomes following juvenile TBI. The underlying hypothesis is that acute inhibition of the JNK pathway through the administration of DJNKI-1 will limit the extent of BBB disruption and vasogenic edema, with concomitant improvements in histological and functional outcomes both short-term and long-term.

Results in this section show that intraperitoneal administration of DJNKI-1 at 3 hours post-jTBI produces a reduction of brain lesion volume in DJNKI-1 treated rats at both acute and chronic time points. Furthermore, there is concomitant reduction in edema formation at acute time point in lesioned cortical region with DJNKI-1 treatment. Immunohistochemical staining showed lower Immunoglobulin G (IgG) extravasation in the brains of treated subjects. There is also a significant recovery of neurological functions in the DJNKI-1 treated rats compared with controls as examined by a battery of

tests which include: foot-fault, rotarod, zero maze, and Morris Water Maze (MWM) tests.

These results suggest beneficial effects of early DJNKI-1 intervention in jTBI.

The chapter follows the blueprint of a scientific manuscript with abstract, introduction, methods, results and discussion sections. It is also replete with detailed figures and legends, and a table.

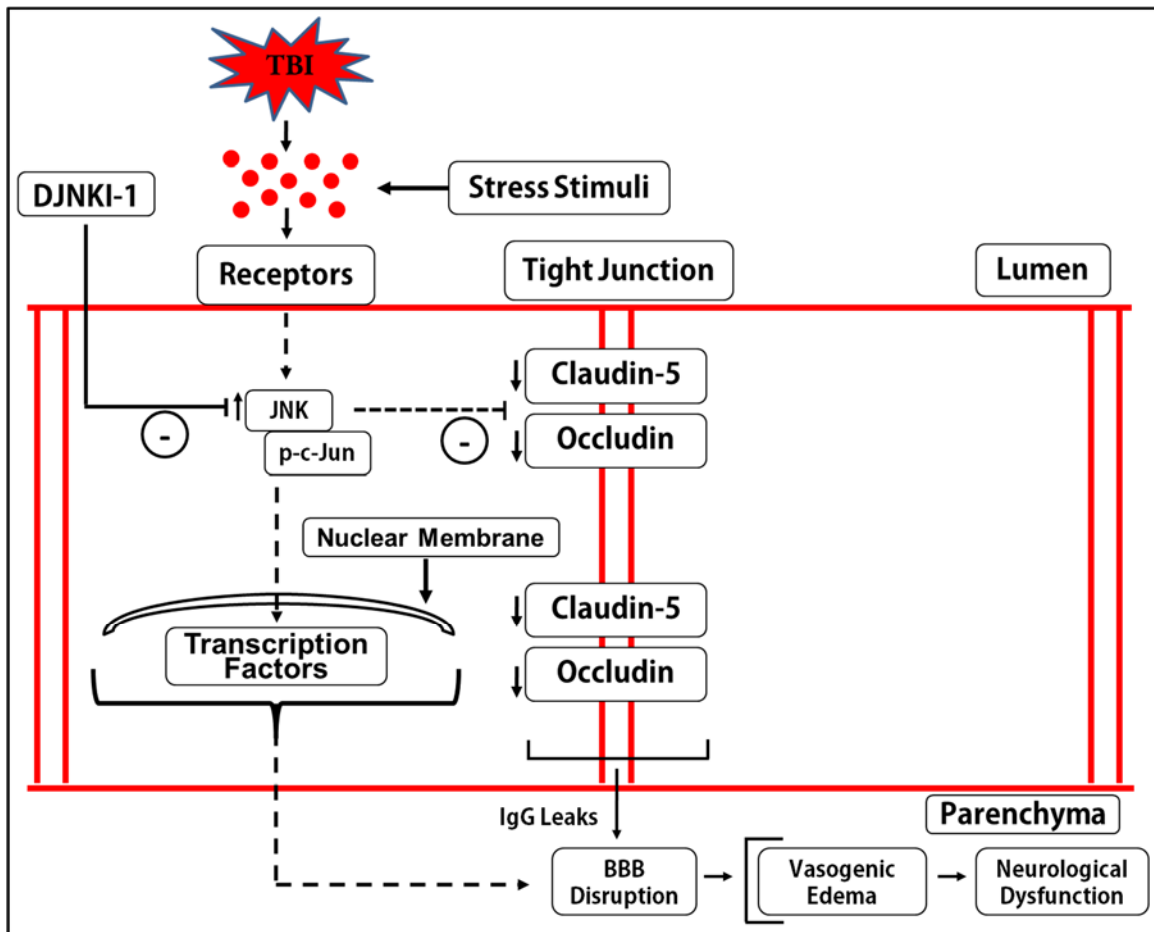


Figure 1: Proposed Intervention Strategy in Experimental Juvenile TBI.

TBI in the juvenile brain produces several stress factors which effect increased activation of the JNK signalling pathway, among others. Activated JNKs can phosphorylate various downstream substrates, including transcription factors (such as c-Jun) that regulate gene expression. Consequences of JNK hyperactivation is cell-type dependent, and may include: regulation of vascular permeability factors (e.g. NO) that may cause BBB damage and edema (in endothelial cells), excitotoxicity (e.g. in neurons), and apoptosis (in both neurons and endothelial cells), followed by functional deficits. The proposed intervention strategy involves acute administration of DJNKI-1 which competitively blocks the interactions between JNK and its various substrates, thereby abrogating their downstream effects. This may be promising for repair of brain endothelial tight junctions and reduction of edema. DJNKI-1 can act on various cell types in the brain (including neurons, astrocytes and endothelial cells), and have the potential to promote additive or synergistic therapeutic effects following juvenile TBI.

TBI – Traumatic Brain Injury; JNK – c-Jun N-Terminal Kinase; p-c-Jun – Phosphorylated c-Jun; IgG – Immunoglobulin G; BBB – Blood-Brain Barrier

CHAPTER 5

ACUTE ADMINISTRATION OF DJNKI-1 FOLLOWING JUVENILE
TBI IN RATS IMPROVES NEUROIMAGING, HISTOLOGICAL AND
FUNCTIONAL OUTCOMES

David O. Ajao¹, Jérôme Badaut^{1, 2*}

Departments of Physiology¹ and Pediatrics², Loma Linda University, Loma Linda, CA.

**Running Title: DJNKI-1 Ameliorates Brain Damage in Juvenile
TBI**

Key words

Blood-brain barrier, c-Jun N-terminal Kinase, JNK, DJNKI-1, juvenile traumatic brain
injury, edema, neurological, cognitive functions, T2-weighted MRI

Abstract

The juvenile brain is known to be susceptible to Blood-Brain Barrier (BBB) damaging secondary processes which occur for days to weeks following brain trauma. In this study, we investigate the therapeutic potential of competitively inhibiting the activation of c-Jun N-terminal kinases (JNKs) acutely in the brain following an experimental model of juvenile TBI (jTBI) in P17 rats. We show that intraperitoneal administration of DJNKI-1 – a competitive inhibitor of JNK pathway – at 3 hours post-jTBI results in reduction of brain lesion volume in DJNKI-1 treated rats at 1d (by 47.3%), 3d (by 37.2%), 7d (by 51.7%), 30d (by 38.1%), and 60d (by 45.8%) post-injury. Furthermore, edema in the cortical lesion – measured with T2-weighted magnetic resonance imaging (MRI) – is reduced significantly at acute time points (e.g. 3d by 26.4% and 7d by 26.9%) with DJNKI-1 treatment. Immunohistochemical staining for IgG showed lower IgG extravasation in DJNKI-1 treated subjects. In addition, there is significant recovery of neurological functions in the DJNKI-1 treated rats compared with controls as examined by foot-fault (** $p < 0.0001$, rm ANOVA at 1d – 60d), rotarod (at 3d, * $p < 0.02$ and at 7d, ** $p < 0.002$, t-test), zero maze (at 60d, * $p < 0.04$, t-test), and Morris Water Maze tests (e.g. 30d West spatial, ** $p < 0.008$, rm ANOVA). We conclude that acute inhibition of JNK pathway following jTBI protects against prolonged BBB disruption and edema formation, and aids in the recovery of some sensorimotor and neurocognitive functions at both acute and later time points.

Introduction

The mechanical impact that initiates traumatic brain injury (TBI) is known to induce secondary pathophysiological and biochemical processes, which progressively determine the consequent outcomes of the injury (Adelson and Kochanek, 1998, Park et al., 2008). Among these secondary processes are: blood-brain barrier disruption, edema formation, impaired metabolism, alteration in cerebral blood flow (CBF) and hemodynamic regulation, hypotension, hypoxia, free radical formation, neuroinflammation, and excitotoxicity (Werner and Engelhard, 2007, Shlosberg et al., 2010). TBI in the juvenile population (jTBI) is particularly associated with greater risks of cerebral hemodynamic dysfunction (Armstead, 1999, 2005, Freeman et al., 2008, Udomphorn et al., 2008, Chaiwat et al., 2009, Armstead et al., 2011), hypoxic-ischemic injury (Armstead, 2005), and diffuse cerebral edema (Suh et al., 2001, Giza et al., 2007), with resultant long-term functional deficits (Giza, 2006). The susceptibility of juvenile brain to tight junction (TJ) protein breakdown, edema, and dysfunction of cerebral hemodynamics are bona fide therapeutic targets that require further investigation (Aldrich et al., 1992, Adelson and Kochanek, 1998, Huh and Raghupathi, 2009, Fukuda et al., 2012).

The c-Jun N-terminal kinases (JNKs) constitute a subfamily of mitogen-activated protein kinases (MAPKs) which respond to various forms of internal and external stress stimuli such as: UV light, inflammatory cytokines, reactive oxygen species (ROS), growth factors, as well as physical and biomechanical perturbations (Hibi et al., 1993, Derijard et al., 1994). All 3 isoforms of JNKs are highly conserved across various species ranging from yeast to mammals (Goberdhan and Wilson, 1998, Kirkham et al., 2008), and are found in various cell types in the brain, including neurons (Lannuzel et al., 1997, Herdegen et al., 1998), endothelial cells (Etienne et al., 1998, Waetzig et al., 2006), and astrocytes (Migheli et al., 1997, Xie et al., 2004). Basal JNK activity level in the brain is

15 to 30-fold higher than in other tissues under physiological conditions (Xu et al., 1997, Coffey et al., 2000). JNKs in the brain are activated even further following external stimuli and pathological events (Borsello and Bonny, 2004). Most studies on JNK pathway in the brain have focused predominantly on neuronal activation triggered by excitotoxic events in adult rodents (Borsello et al., 2003, Cui et al., 2007, Haeusgen et al., 2009) or human (Ortolano et al., 2009). There is however increasing evidence that JNK is also activated in glial cells (Xie et al., 2004, Cui et al., 2007) and brain endothelial cells (Lenmyr et al., 2002, Lo et al., 2005, Kacimi et al., 2011, Tu et al., 2011), and that such activation in non-neuronal cells negatively impacts neuronal function and cell death (Xie et al., 2004, Kaminska et al., 2009).

Hyperactivation of JNKs is a phenomenon that could mediate the secondary events of TJ protein breakdown and the formation of edema, which can lead to functional and behavioral consequences. JNK hyperactivation has been documented both clinically (Ortolano et al., 2009) and experimentally (Otani et al., 2002a, Otani et al., 2002b, Raghupathi et al., 2003, Tran et al., 2012) post-TBI, in parallel with secondary injuries. It has also been shown in models of stroke (Borsello et al., 2003, Michel-Monigadon et al., 2010, Nijboer et al., 2010), Parkinson's disease (Peng and Andersen, 2003, Kuan and Burke, 2005), and Alzheimer's disease (Okazawa and Estus, 2002, Wei et al., 2002).

Hyperactivation of JNKs has been shown to result in downregulation of TJ proteins in both *in vitro* brain endothelial cell cultures (Tai et al., 2010) and *in vivo* in the periphery (Kojima et al., 2010, Samak et al., 2010), consequently affecting the BBB integrity (Tai et al., 2010, Tu et al., 2011). Interestingly, JNK inhibition with SP600125 was shown to reverse decrease in TJ proteins such as claudin-5 in the periphery (Carrozzino et al., 2009). In an experimental model of pancreatitis, JNK inhibition with CEP-1347 was found to reduce edema formation in rat pancreas (Wagner et al., 2000).

Inhibition of JNK with SP600125 was also found to reduce brain swelling in experimental subarachnoid hemorrhage (SAH) model (Yatsushige et al., 2007). SAH induces JNK activation in rat cerebral arteries by 24 hours which is concomitant with increased BBB permeability and brain edema (Kusaka et al., 2004). Furthermore, JNK hyperactivation was found to play a role in experimental jTBI-induced cerebrovascular dysregulation in piglets (Armstead et al., 2011). Successful reversal of pial arterial vasoconstriction that occurs following TBI induction was achieved with the use of JNK inhibitors, SP600125 and DJNKI-1 (Armstead et al., 2011). JNK antagonist SP600125 has also been used in combination with glucagon to achieve full reversal of cerebral vasoconstriction in jTBI model in piglets (Armstead et al., 2012). These studies provide evidence that the hyperactivation of JNK pathway may be involved in jTBI-induced disruption of tight junction and cerebrovascular regulation.

Investigators have up to date experimented with three main types of JNK inhibitors with varying efficacies (Cui et al., 2007). The first group comprises of ATP-competitive inhibitors of JNK, such as SP600125 and CEP-1347, which are small organic compounds that occupy the ATP-binding site of the protein kinase (Herdegen et al., 1998, Haeusgen et al., 2009). However, the disadvantage of this set of inhibitors is that their efficacy is reduced by the high endogenous levels of ATP (Cui et al., 2007). SP600125 has been used in some experimental TBI (Hong et al., 2012), stroke (Gao et al., 2005, Guan et al., 2006) and Parkinson's disease (Kuan and Burke, 2005) studies. The second and third groups of inhibitors target the substrate-binding sites and the allosteric regulatory sites of JNK respectively with non-phosphorylatable analogues (Cui et al., 2007, Comess et al., 2011). Peptide inhibitors are examples of these second and third groups, and these provide a more specific inhibition mechanism than ATP-competitive inhibitors (Haeusgen et al., 2009). Peptide inhibitors which competitively bind to JNK-interacting peptide-1 (JIP-1) – a scaffolding protein that act upstream of the

3 isoforms of JNK – have been used extensively in experimental brain research (Bogoyevitch and Arthur, 2008). JIP-1 scaffolding protein structurally organizes the MAP kinase signaling module by linking MLK-3 and MKK-4/7 (upstream kinases that phosphorylate JNK) with JNK and thereby providing a spatial and temporal platform for regulating the JNK pathway (Borsello and Bonny, 2004, Bogoyevitch and Arthur, 2008) (See **Fig. 2**). L-DJNK-1 and D-JNK-1 are examples of these peptides (Bogoyevitch and Arthur, 2008).

D-JNKI-1 is a synthetic, protease-resistant and cell-penetrating peptide made by linking HIV-TAT transporter peptide sequence to the 20-amino acid JNK-binding motif of JIP-1 (Borsello et al., 2003). The D-retro-inverso synthesis (i.e. made with D-amino acids) of D-JNKI-1 gives it strong resistance against proteolytic degradation and increases its stability in the body (Borsello et al., 2003, Borsello and Bonny, 2004). D-JNKI-1 functions through competitive inhibition of all JNK isoforms (**Fig. 2**). D-JNKI-1 selectively blocks access of JNK to c-Jun and other downstream substrates such as JunB, JunD, and c-myc by competing for the JNK-binding site of JIP-1 (Borsello et al., 2003, Borsello and Forloni, 2007) (See **Fig. 2** below). The therapeutic effectiveness of D-JNKI-1 is pegged on its potential to modulate upstream and downstream arms of the secondary injury cascade following jTBI, including excitotoxicity, hypoxia-ischemia, edema, neuroinflammation and apoptosis (Yang et al., 1997, Kuan et al., 2003, Tu et al., 2011).

Meanwhile, long-term functional deficits of sensorimotor, cognitive, and neuropsychiatric nature which could last for years have been reported in patients with incidence of jTBI (Chadwick et al., 1981, Yeates et al., 2002, Jonsson et al., 2013). Most experimental studies of jTBI in animals have, however, focused on acute time-points following trauma (Saatman et al., 2008), making them inapplicable and nongeneralizable to clinically observed long-term sequelae of TBI (Doppenberg et al., 2004, Saatman et

al., 2008). This justifies the establishment of models for long-term profiling of functional and behavioral parameters following experimental jTBI as have been reported (Giza et al., 2005, Ajao et al., 2012). Such models that assess both sensorimotor (e.g. through the use of foot-fault, beam balance, and rotarod tests) and cognitive (e.g. through the use of Morris Water Maze [MWM] test) parameters can be used to determine the long-term efficacy of potential therapeutic agents such as D-JNKI-1. D-JNKI-1 has been shown to ameliorate behavioral deficits in experimental models of stroke (Esneault et al., 2008), neuroinflammation (Palin et al., 2008), and spinal cord injury (Repici et al., 2012) in adult rodents. D-JNKI-1 was also successfully used to arrest the progression of hearing loss in a model of cochlear implantation trauma (Eshraghi et al., 2006).

To date, there have been no reports on the potential link between juvenile TBI-induced JNK activation and post-injury BBB disruption and edema. Neither have there been studies on the therapeutic potential of DJNKI-1 in this model. The working hypothesis for this study is that acute competitive inhibition of JNK in the brain will mediate rapid recovery at BBB level, and lead to reduced edema formation and lesion volume, reflected in improved motor and behavioral outcomes at both acute and delayed time points following jTBI. We report that acute treatment with DJNKI-1 following jTBI in P17 rats results in remarkable reduction in edema, lesion volume and neurological deficit, alongside with reduced BBB disruption.

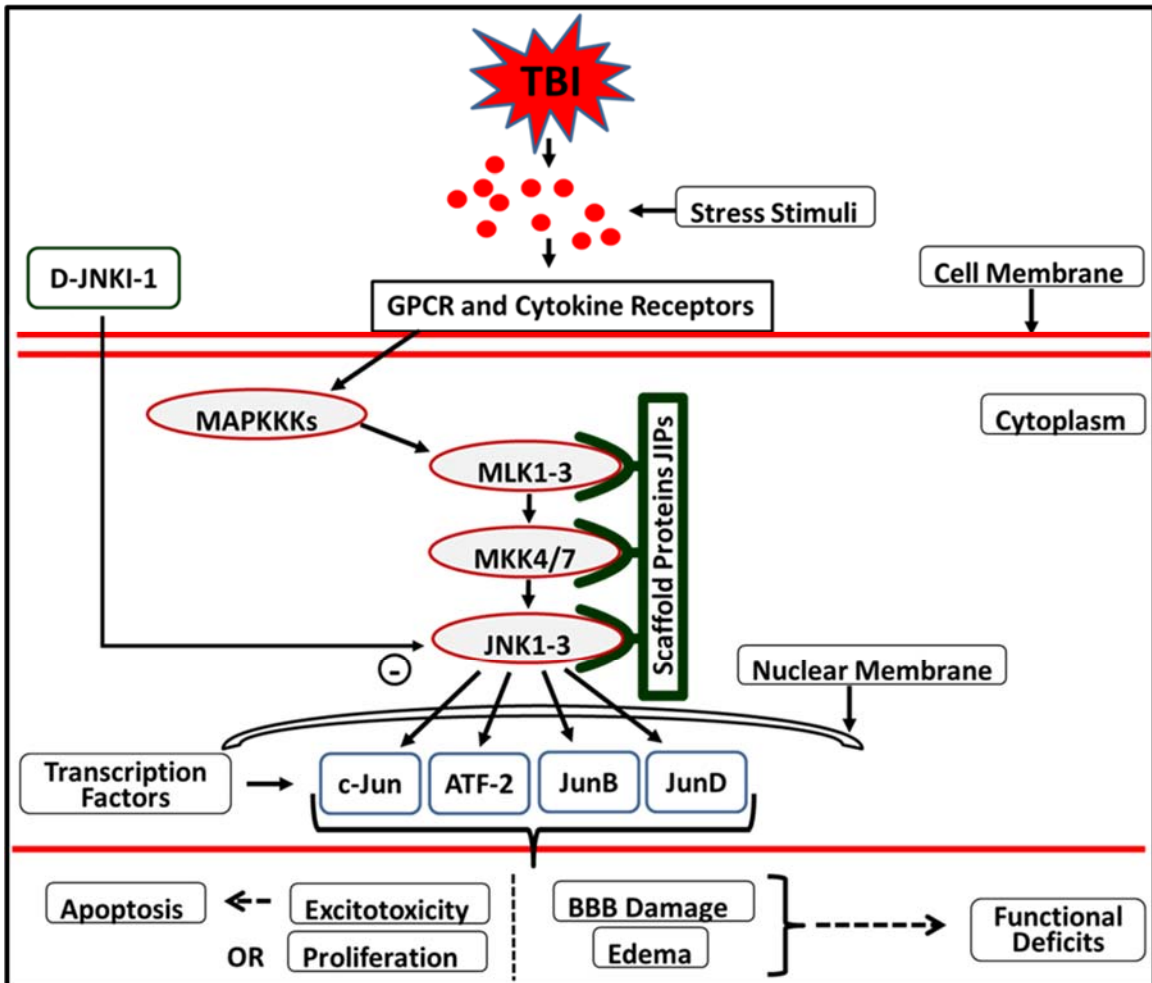


Figure 2: Pathway of JNK Activation in a Generalized Brain Cell and Theorized Mechanism of Action of D-JNKI-1. Following jTBI, stress stimuli including cytokines activate the stress receptors on the cell membrane in various brain cells (e.g. neurons, astrocytes & endothelial cells). The cascade follows a sequential activation of various MAP kinases: MLKs phosphorylate MKK4 or 7 which in turn phosphorylate JNK1-3. Activated JNK translocates to the nucleus where it activates c-Jun and other transcription factors (TFs). Gene transcription by these TFs could lead to excitotoxicity and apoptosis (e.g. in neurons), cell growth and proliferation, or increased BBB permeability and edema (e.g. in cerebral endothelial cells) which could engender functional deficits. JIPs provide scaffolding platforms to structurally organize various MAPKs and facilitate the signaling cascade. D-JNKI-1 acts by competitively inhibiting JNKs' interaction with the JIPs with its specificity to the JNK-binding domain of the scaffolding protein.

Abbreviations: GPCR = G-Protein Coupled Receptor; MAPKKKs = Mitogen-Activated Protein Kinase (MAPK) Kinase-Kinase; MLK = Mixed Linkage Kinase; MKK = MAPK Kinase; JNK = c-Jun N-Terminal Kinase; ATF-2 = Activating Transcription Factor 2; JIPs = JNK-Interacting Proteins; jTBI = Juvenile Traumatic Brain Injury.

Materials and Methods

Subjects

Juvenile (P10) male Sprague-Dawley rats were ordered from Harlan Laboratories (Harlan, Indianapolis, IN). They were housed with their dams upon delivery on a 12-hour light-dark cycle at constant temperature and humidity, in accordance with standard guidelines, and allowed to acclimatize for 7 days. Key surgical procedures were carried out on the pups at P17. Subsequently, the pups were weaned at P24, housed 2 rats per cage, and fed with standard lab chow and water ad libitum. All groups of animals used in the study (total n = 28, comprising of 3 different cohorts) had identical CCI surgical parameters, and were randomly divided into saline-injected control and DJNKI-1 treated groups. The first cohort of subjects (n = 5 SAL, n = 5 DJNKI-1) was studied acutely with MRI and behavioral tests (i.e. at 1 and 3dpi), and then euthanized, followed by brain collection at 3dpi. The second cohort (n = 5 SAL, n = 5 DJNKI-1) was studied longitudinally for MRI (at 1, 3, 7, 30 and 60 dpi) and all behavioral tests (at 1, 3, 7, 30 and 60 dpi) over a 2-month period. The third cohort (n = 4 SAL, n = 4 DJNKI-1) was identical to the second cohort with the exception of MRI scans. Euthanization and brain collection for the second and third cohorts occurred at 60dpi, and the brains were prepared for immunohistochemistry. All protocols and procedures used in this study were approved by the Institutional Animal Care and Use Committee of Loma Linda University and are in compliance with the U.S. Department of Health and Human Services Guide.

Juvenile Traumatic Brain Injury Procedure

TBI was induced in juvenile rats at P17 through a controlled cortical impact (CCI) as previously described (Ajao et al., 2012). Briefly, the rats were anesthetized with isoflurane (Webster Veterinary Supply, Inc., Sterling, MA) and afterwards placed into a mouse stereotaxic frame (David Kopf Instruments, USA). A midline scalp incision

followed by a 5 mm craniotomy was performed unilaterally over the right fronto-parietal cortex (Bregma: 3 mm anterior-posterior and 4 mm medial-lateral). A controlled impact on the brain was delivered using a 3 mm rounded-tip metal impactor fixed to an electromechanical actuator and centered over the exposed dura at a 20° angle to be parallel to the cortical surface (Leica Microsystems Company, Richmond, IL). The impact was delivered at a 1.5 mm depth from the cortical surface, with impact duration of 200 ms, and at a velocity of 6 m/s. Aberrations to the cortical tissue, such as bleeding and protrusion of cortical tissue through the craniotomy, were duly recorded. Thereafter, the surgical site was sutured closed. Subject's body temperature was maintained throughout the surgery at 37°C. For pain relief, Buprenorphine (0.01 mg/kg; dilution: 0.01 mg/ml) was injected subcutaneously into the subjects before they were returned to their dams. The time between the end of surgery and when subjects wake up were also recorded. There was close daily monitoring of the subjects for at least 7 days post injury, followed by more spaced out examinations afterwards.

DJNKI-1 Treatment

D-JNKI-1 (11mg/kg) or normal saline was intraperitoneally administered to each subject at 3 hours post-injury. This dosage was based on previously reported efficacy of DJNKI-1 in middle cerebral artery occlusion (MCAO) model in male P14 Wistar rats (Repici et al., 2007) where the drug was injected intraperitoneally. The same dosage has also been used effectively in spinal cord injury model in adult mice (Repici et al., 2012). The rats were returned to their dams right after injection.

Magnetic Resonance Imaging (MRI): Acquisition and Analyses

Image Acquisition

In vivo MRI was performed at 1 and 3 dpi for all animals, while a subset of the animals was also scanned at 7 and 30 dpi, followed by high resolution *ex vivo* imaging at 60 dpi. Rats were prepared for *in vivo* MRI as previously described (Ajao et al., 2012). Briefly, following induction of anesthesia (with 1-2% isoflurane), each rat was placed in a temperature controlled cradle containing a volume radio frequency (RF) coil and imaged on a 11.7T MRI (8.9 cm bore) at 1d and 3d, and on a larger bore (40 cm) 4.7T MRI (Bruker Biospin, Billerica, MA) at 7d and 30d. *Ex vivo* imaging at 60d was carried out in the 11.7T magnet.

T2 weighted imaging (T2WI) was acquired *in vivo* with the following parameters: repetition time/echo time (TR/TE) = 2357.9/10.2 ms; 128 X 128 matrix; 1 mm slice thickness; 1 mm interleaved; average of 4 acquisitions; number of slices = 20; and field of view (FOV) = 2.0 cm for a total imaging time of 20 min on 11.7T MRI; and repetition time/echo time (TR/TE) = 3563.4/20 ms; 256 X 256 matrix; 1 mm slice thickness; 1 mm interleaved; average of 2 acquisitions; number of slices = 25; field of view (FOV) = 3.0 cm for a total imaging time of 30 min on the 4.7T MRI. Diffusion-weighted imaging (DWI) was acquired using a repetition time/echo time (TR/TE) = 1096.5/50 ms; 128 X 128 matrix; 1 mm slice thickness; 1 mm interleaved; average of 2 acquisitions; number of slices = 20; field of view (FOV) = 2.0 cm; and b values = 116.96 s/mm², 1044.422 s/mm² for a total imaging time of 17 min on 11.7T MRI; and a repetition time/echo time (TR/TE) = 3000/50 ms; 256 X 256 matrix; 1 mm slice thickness; 1 mm interleaved; average of 2 acquisitions; number of slices = 25; field of view (FOV) = 3.0 cm; and b values = 43.05 s/mm², 441.991 s/mm² for a total imaging time of 51 min on 4.7T MRI.

At 60 dpi, perfusion-fixed brains were prepared as previously described (Ajao et al., 2012) before undergoing *ex vivo* scanning using the 11.7T magnet. T2WI were

acquired using: a repetition time/echo time (TR/TE) = 1769.9/10.2 ms; 256 X 256 matrix; 1 mm slice thickness; 1 mm interleaved; average of 4 acquisitions; number of slices = 15; and a field of view (FOV) = 2.0 cm for a total imaging time of 30 min on 11.7T MRI. DWI was carried on the same scanner and with the same parameters as the T2WI, with the exception of TR/TE (552.5/15.1 ms), acquisition time (70 min), and b values (116.96 s/mm²; 1044.422 s/mm²). Apparent Diffusion Coefficient (ADC) was calculated from six gradient vectors. As previously reported, the use of two different field strengths and the use of both *in vivo* and *ex vivo* MRI did not alter our relative measurements (Obenaus et al., 2011, Obenaus and Hayes, 2011, Ajao et al., 2012). Acquisition of both T2WI and DWI was done in sequence without any apparent change in the positioning of the animals.

Lesion Volume Analysis

As previously described (Ajao et al., 2012), volumetric analyses of brain and lesion volumes were performed using the T2WI in either Cheshire (Hayden Image Processing Group, Waltham, MA) or Amira (Mercury Computer Systems, Visage Imaging, Inc., San Diego, CA, USA) software. Lesion volumes were defined as the cortical brain regions containing abnormal hypo- and/or hyperintense signals compared to normal-appearing cortical brain matter on the contralateral hemisphere (Fig. 1C). Total brain volume encompassed both normal-appearing and abnormal brain tissues, while herniated tissue, if present, was excluded. In some animals, subcortical and extracortical abnormalities were present but were not included in the lesion. These abnormalities were recorded as injury-related morphological alterations (Table 1), and included: ventricular hypertrophy, hemorrhage, shrunken hippocampus, disrupted corpus callosum (and other affected white matter structures), and cortical herniation. In order to correct for individual brain size differences among the animals and age-related brain

growth, the injury volumes were normalized to the brain volumes. Hemispheric volumes were also analyzed using the same inclusion and exclusion criteria.

T2 Analysis

For each T2WI scan, a region of Interest (ROI) was drawn on the slice with the largest lesion area for each of the following areas: lesion, perilesion, striatum and hippocampus on both ipsilateral and contralateral hemispheres. The lesion and perilesion ROIs encompass both hypointense (which may indicate hemorrhage) and hyperintense pixels (which may indicate edema) within the brain parenchyma (Fig. 3A, D). A rectangular box measuring 6-by-8 pixels constitutes the ROI for both ipsilateral and contralateral striatum. ROIs for the hippocampus encompass all visible hippocampal regions along the anterior-posterior axis. All these aforementioned ROIs were subsequently posted on co-registered T2 maps corresponding to each chosen brain slice for acquisition of T2 values. T2 values were compared between DJNKI-1 group and saline-control group.

Apparent Diffusion Coefficient (ADC) Analysis

The ROIs drawn for T2WI scans were copied to co-registered diffusion-weighted MRI-derived ADC maps on the slice with the largest lesion for each subject. Extraction of ADC values from these ROIs on the maps followed. There were no overt differences in ADC values resulting from the use of *in vivo* versus *ex vivo* MRIs in all ROIs.

Area Measurements of the Corpus Callosum Thickness

A ROI was drawn around the portion of visible corpus callosum in each hemisphere from a selected T2-weighted MR image at bregma level +1mm, anterior to

the lesion in each animal. The chosen coronal slice often corresponds to the slice that is directly anterior to the visible lesion. Equivalent anatomical landmarks were used for selection of the slice chosen for analysis for all animals. The corpus callosal areas for each image were extracted with Cheshire software.

Neurological and Behavioral Tests

Detailed procedure for each behavioral test used in this study has been previously described (Ajao et al., 2012). All tests on both saline and DJNKI-treated animals were carried out within a 3-hour time-block between 8am and 11am, and the animals from both groups were interleaved. The tests were carried out in the sequence in which they are listed below.

Foot-fault

This was performed using an elevated wire mesh (2.5 cm X 30 cm rectangular holes/grid spacing) raised 76 cm above the floor. Movements of each rat placed in the middle of the mesh were video-recorded for 60 sec in two separate trials. A foot-fault was counted when a rodent's paw slipped completely through the wire mesh. The number of foot-fault for both groups were compared.

Beam Balance

Juvenile animals were tested on a 0.65 cm wide plexiglass beam at 1, 3, and 7 dpi. Adult animals were tested on a 2.5 cm wide beam at 30 and 60 dpi commensurate to their size increase. Each animal walked unrestricted for 60 sec for each of two trials 20 min apart, and the distance covered was recorded and compared between saline-controls and DJNKI-1 group.

Rotarod

Two different rotarod paradigms were used: constant velocity (at 1, 3, 7, 30 and 60dpi), and constant acceleration (2rpm/5s and 5rpm/5s at 30 and 60 dpi). The rotarod (Rotamex-5, Columbus Instruments, Columbus, OH) operates until each animals falls off. Latency to fall was recorded as a measure of motor coordination and balance.

Open-field

General activity level and exploratory behavior of the animals were assessed with open-field test at 30 and 60 dpi. Each subject was video-recorded for 30 min (Noldus Ethovision, Noldus Information Technology, Inc., Leesburg, VA) inside an empty plastic bin. Total distance traveled was recorded as a measure of overall activity levels and compared between groups.

Zero Maze

This test was carried out on an elevated circular apparatus fitted with a brightly lit, open half, and also with an enclosed half. A 5-min trial was conducted at 30 and 60 dpi, and the percentage of time spent in the enclosed half was recorded. Increased percentage of time spent in the dark quadrants of the track is associated with increased anxiety-like behaviors as previously shown (Ajao et al., 2012).

Morris Water Maze (MWM)

A 3-day assessment of subject performance in cued and spatial water maze paradigms was used as a measure of learning and spatial memory functions at 30 and 60 dpi. The water maze metal tank was filled with opaque water. An escape platform (11 cm diameter) was adjusted so that its surface was 2 cm above the water surface for cued testing, and submerged 1 cm below the water surface for the spatial learning and memory tasks. Rodent's swim paths were recorded with a computerized tracking device

(Noldus Information Technology, Inc., Leesburg, VA) (Hartman et al., 2005, Ajao et al., 2012). In the cued task, platform location was changed for each of 5 trial blocks – each block consisting of 2 consecutive trials (60 sec maximum for each) with a 5 sec inter-trial interval. For the spatial testing, platform location was kept constant for all 10 trials, and there were four release points. 1.5 hrs following the spatial trials, a 60 sec probe trial was performed, in which the platform was removed from the tank and the rats were allowed to swim in search of it. Outcomes for the MWM include: distance traveled to reach the platform, number of entries into the target quadrant, percentage of time spent in the target quadrant, and swim speed.

Tissue Processing and Immunohistochemistry

A cohort of rats were transcardially perfused with 4% PFA prepared in PBS at 3d and 60d post-jTBI. The brains, upon removal, were immersed in 30% sucrose solution at 4°C for 48 hours, until they sink to the bottom. They were then frozen on dry ice and stored at -20°C pending cryosectioning. Coronal cryostat sections were pre-mounted on glass slides (thickness = 20µm) (Leica CM1850, Leica Microsystems GmbH, Wetzlar, Germany). The sections were stored at -20°C until used.

Extravasated Serum Immunoglobulin G (IgG) Staining and Analysis

To evaluate disruption at the BBB, staining for extravasated IgG was performed as previously described (Badaut et al., 2011). Briefly, pre-mounted sections were twice washed (10min each) in PBS and then blocked with 1% BSA in PBS for 1.5 hrs. The sections were then incubated for 2 hrs at RT with biotinylated, affinity-purified goat anti-rat IgG, coupled with an 800nm wavelength infrared dye (1:500 dilution; Rockland, Gilbertsville, PA), in a PBS-based antibody incubation buffer containing 0.1% Triton X-100 and 1% BSA. The sections were washed in PBS and dried. The sections were then

scanned on an infra-red scanner (Odyssey-system, LiCor, Germany) to quantify the area of IgG extravasation on 3 to 5 adjacent slices covering the lesion. ROIs were drawn with LI-COR Odyssey system around the regions where extravasated IgG is observed in each section. The areas of these regions were then extracted for each section, summated for each brain, and averaged for each group.

Statistical Analyses

All data are presented as mean \pm SEM. Statistical analyses were done using SPSS, and graphs were obtained using Sigmaplot (SPSS Inc.). All the data were analyzed using student t-tests for normally distributed data with comparison between the DJNKI-1 and control groups for each of the time points. Repeated measures ANOVAs were used in cases where longitudinal data were collected on the same groups.

Results

DJNKI-1 Reduces Lesion Volume and Ameliorates Morphological Alterations

Data gathered from non-invasive MRI was used to quantify lesion volume at 1d, 3d, 7d, and 30d. It was also used for lesion volume measurements following removal of brains from euthanized rat subjects at the 60d time points. 3D reconstructions of representative saline and DJNKI brains along the rostral-caudal axis show that the lesions (red) constitute 1.9% and 2.2% of DJNKI brains compared to 3.5% and 3.9% of saline brains respectively at 3d and 60d (Fig. 3B). The lesion is located on frontoparietal cortex that encompasses the motor and somatosensory cortices. Intraperitoneal administration of DJNKI-1 at 3 hours post-jTBI (Fig. 3A) results in significant reductions of brain lesion volume in DJNKI-1 treated rats at 1d (by 47.3 \pm 11.1 %), 3d (by 37.2 \pm 17.5 %), 7d (by 51.7 \pm 12.7 %), 30d (by 38.1 \pm 19.9 %), and 60d (by 45.8 \pm 11.3 %)

post-injury (Fig. 3D). Repeated measures ANOVA confirms a reduction in lesion volume in DJNKI-treated rat brains across all time points compared to brains of saline control rats (** $p < 0.001$; Fig. 3D). Fig. 3D shows lesion volumes as percentages of total brain volumes for both saline and DJNKI-1 groups. In addition, pairwise comparisons (with rm ANOVA) reveal intragroup variations in lesion volume as a percentage of brain volume in the saline group but not in the DJNKI-1 group (Fig. 3D). Compared to 1d value, lesion volume (in the saline group) is significantly lower at 7d ($*p < 0.02$) and 30d (** $p < 0.005$). Juxtaposed brain sections (consisting of the brain slice that is most central to the lesion and that has the largest lesion volume, for each time point) and lesion ROIs demarcated in red are shown in saline and DJNKI-1 brains for each time point in Fig. 3C. Visual comparison reveals that DJNKI-1 brain sections have smaller lesion volume across all time points compared to saline brains (Fig. 3C).

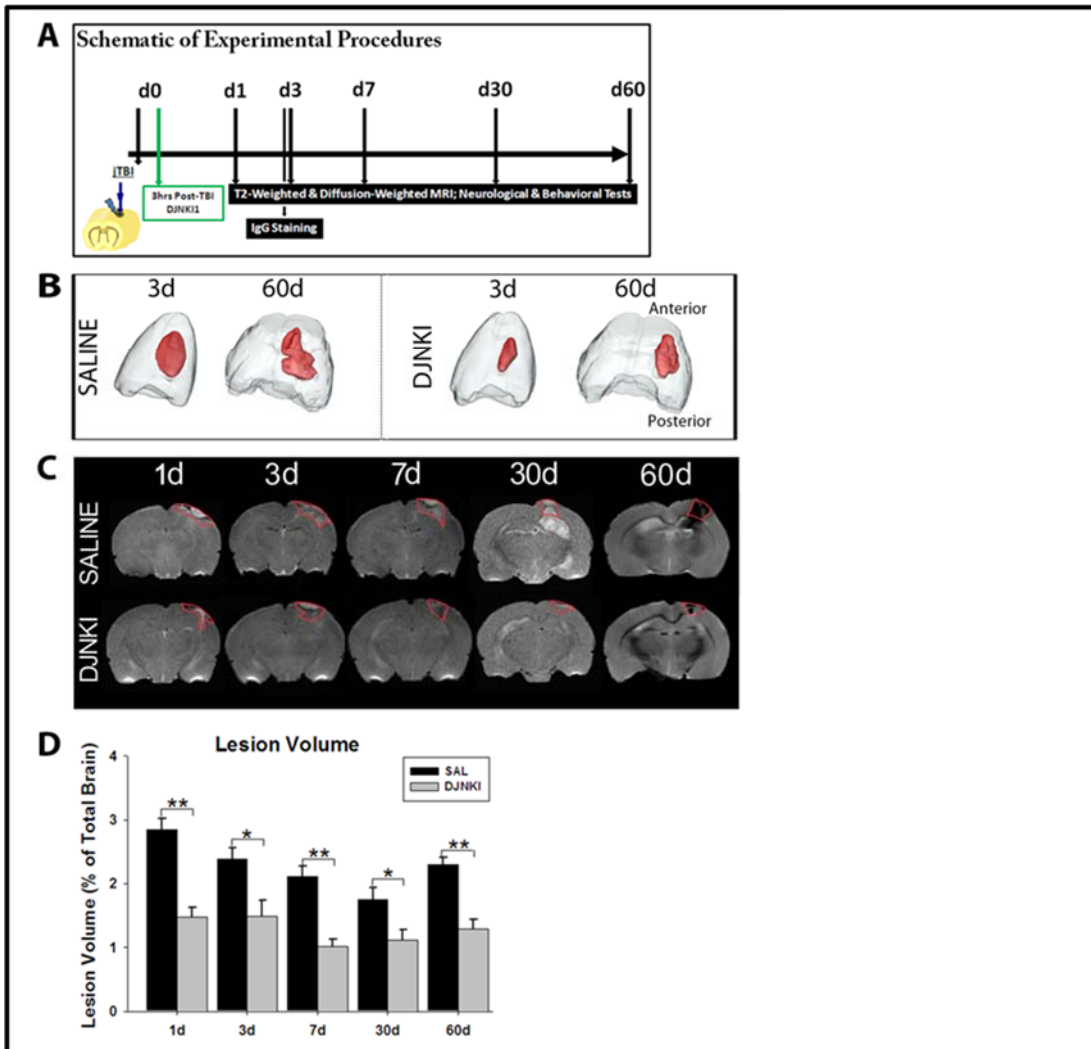


Figure 3. Experimental Timeline, and Images and Quantification of Lesion Volume. **(A)** A schematic of experimental timeline and procedures from induction of jTBI (d0) until euthanasia (d60) is shown. T2- and diffusion-weighted MRI were serially obtained at 1d, 3d, 7d, 30d, and 60d post-jTBI. Neurological and behavioral tests were carried out at the same time points. Immunohistochemical staining was performed for extravasated IgG at 3dpi. **(B)** 3D reconstructions of normal appearing brain (gray) and lesion (red) are shown at 3 and 60 dpi. The lesion encompasses 2.9 +/- 0.2% and 2.5 +/- 0.2% of saline brains at 3 and 60dpi respectively, while accounts for 1.5 +/- 0.2% and 1.5 +/- 0.3% of DJNKI brains at the same time points. **(C)** 2D sequence MR (T2WI) images at 1, 3, 7, 30 and 60 dpi are shown with lesions (red outlines) encompassing regions of hyper- and hypointensities on the cortex and lesion cavity in saline and DJNKI groups. Regions of hyper- and hypointensity below the corpus callosum are excluded. **(D)** Lesion volume was significantly smaller in the brains of DJNKI-treated rats compared to their saline counterparts (** $p < 0.001$; * $p < 0.05$). Repeated measures ANOVA shows reduced lesion volume in DJNKI-treated rat brains across all time points ($p < 0.001$). (1d and 3d: $n=10$ for each group; 7d: $n=5$ for each group; 30d and 60d: $n=4$ for SAL, and $n=5$ for DJNKI).

Table 1: Morphological Observations of Tissue Alterations

Morphological Observation	Experimental Group	1d	3d	7d	30d	60d
Ventricular Hypertrophy (Ipsil. Cortex)	SAL	70%*	90%	100%	100%	100%
	DJNKI	20%	40%	40%	100%	80%
Ventricular Hypertrophy (Contra. Cortex)	SAL	60%	30%	80%	75%	100%
	DJNKI	10%	20%	60%	40%	40%
Cortical Thinning (Ipsil. Cortex)	SAL	50%	90%	80%	100%	100%
	DJNKI	0%	0%	60%	100%	80%
Damaged HPC (Ipsil. Cortex)	SAL	90%	90%	100%	100%	100%
	DJNKI	0%	0%	60%	20%	60%
Damaged HPC (Contra. Cortex)	SAL	0%	0%	10%	0%	0%
	DJNKI	0%	0%	0%	0%	0%
Hemorrhage (Ipsil. Cortex)	SAL	90%	100%	100%	50%	0%
	DJNKI	90%	80%	80%	40%	0%
Herniation (Ipsil. Cortex)	SAL	50%	80%	100%	100%	50%
	DJNKI	40%	50%	80%	100%	40%
Cyst (Ipsil. Cortex)	SAL	0%	10%	60%	100%	100%
	DJNKI	0%	10%	0%	80%	20%
Disrupted Corpus Cal. (Ipsil. Hemisphere)	SAL	70%	80%	60%	100%	100%
	DJNKI	0%	20%	60%	80%	100%
Total n (SAL)		10	10	5	4	4
Total n (DJNKI)		10	10	5	5	5

* Percentage of animals in the group with the observed morphological alteration

Comparison of the two hemispheric volumes in saline group shows increased contralateral hemisphere volume at 3, 7 and 30dpi ($*p = 0.03$, $**p = 0.003$, and $**p = 0.01$ respectively; t-test) (Fig. 4A). In the DJNKI-1 group, there is increased contralateral volume at 7 and 60dpi ($**p = 0.002$, and $*p = 0.02$ respectively; t-test) (Fig. 4B). As expected, the raw volumes of both hemispheres in saline and DJNKI-1 brains are significantly increased at 30d and 60d compared to the volumes at earlier time points ($**p < 0.001$ for each comparison), reflecting brain growth with increasing age (Figs. 4A and B). When compared, ipsilateral hemispheres volumes for the saline group is higher than that of the DJNKI-1 group only at the 60d time point ($**p < 0.01$) (Fig. 4C). There are no differences at other time points. The contralateral hemisphere volumes are however similar for both groups at all time-points (Fig. 4D).

Some alterations in brain morphology were observed at varying frequencies in the T2WI of the two groups (see Table 1). Of particular note are: ventricular hypertrophy (enlargement of the ventricles) which was less frequent in DJNKI animals at 1, 3, and 7dpi on both ipsilateral (70% [saline] vs. 20% [DJNKI], 90% vs. 40%, and 100% vs. 40% respectively at 1, 3 and 7dpi) and contralateral cortices (60% vs. 10%, 30% vs. 20%, and 80% vs. 60% respectively) (Table 1); cortical thinning (reduction in cortical thickness) which was less frequent in DJNKI animals at 1, 3, and 7dpi on ipsilateral cortex (50% vs. 0%, 90% vs. 0%, and 80% vs. 60% respectively at 1, 3 and 7dpi), and damaged hippocampus on ipsilateral cortex (90% vs. 0%, 90% vs. 0%, and 100% vs. 60%, 100% vs. 20%, and 100% vs. 60% respectively at 1, 3, 7, 30 and 60dpi). Other morphological changes include hemorrhage/hematoma which was less frequent on DJNKI brain at 3 (100% vs. 80%) and 7dpi (100% vs. 80%) on ipsilateral cortex, herniation (displacement and protrusion of brain tissue) which was less common in DJNKI brains at 1 (50% vs. 40%), 3 (80% vs. 50%), and 7dpi (100% vs. 80%) on the ipsilateral cortex, formation of cyst (enclosed sphere separated from the brain that is

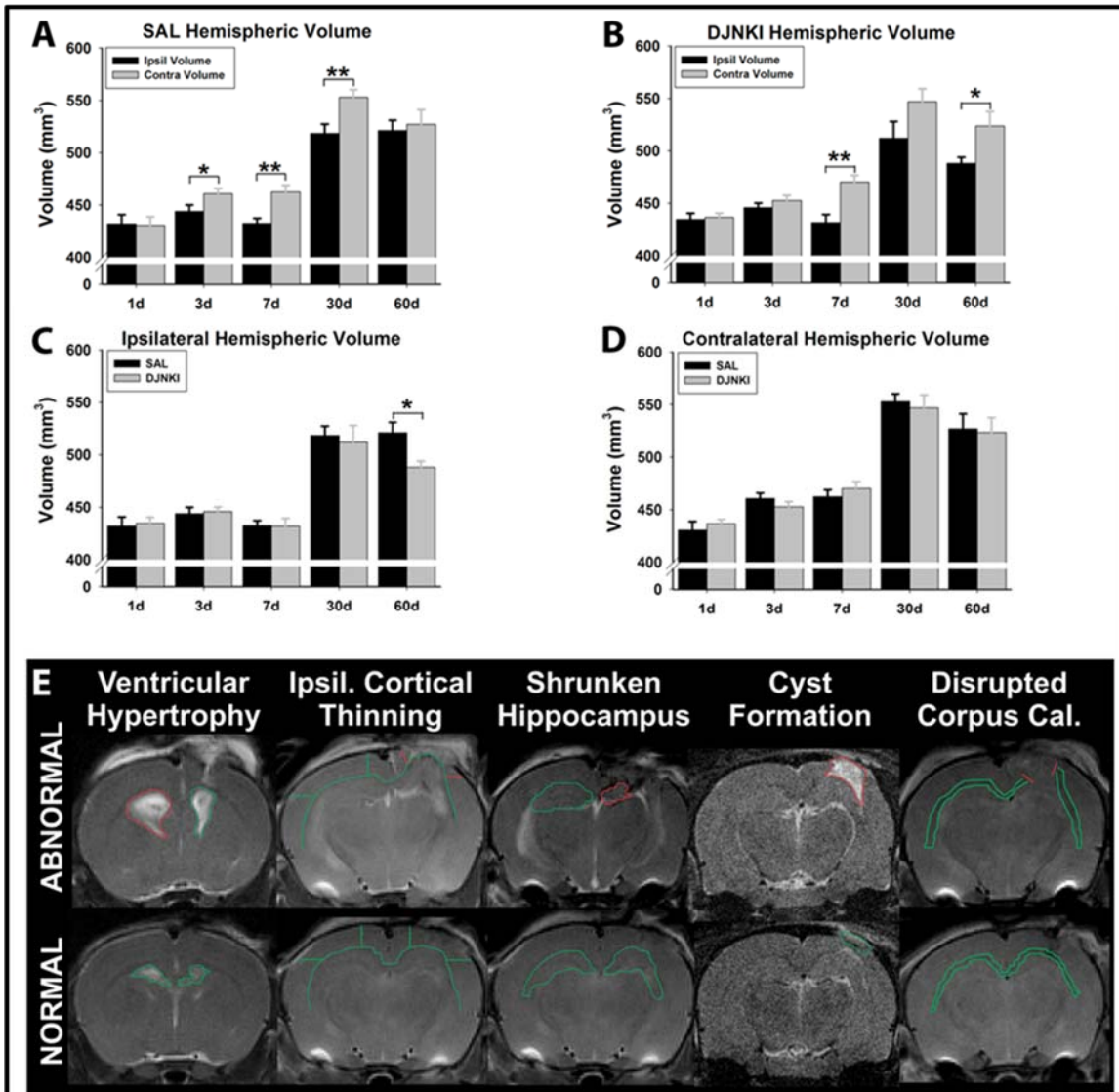


Figure 4. Changes in Hemispheric Volumes and Brain Morphology. (A) Comparison of hemispheric volumes in the saline group shows increased contralateral hemisphere volume at 3, 7 and 30dpi ($*p = 0.03$, $**p = 0.003$, and $**p = 0.01$ respectively). (B) In the DJNKI-1 group, there is increased contralateral volume at 7 and 60dpi ($**p = 0.002$, and $*p = 0.02$ respectively). (C) Graph comparing ipsilateral hemispheres volumes between the groups shows that at 60dpi, saline group has higher volumes than DJNKI-1 group ($**p < 0.01$). There are no differences at other time points. (D) Graph comparing contralateral hemispheres volumes between the groups shows no difference at all time points. (1d and 3d: $n=10$ for each group; 7d: $n=5$ for each group; 30d and 60d: $n=4$ for SAL, and $n=5$ for DJNKI). (E) Morphological abnormalities appear in higher frequency in the saline group versus DJNKI-treated group.

made up of a mixture of fluid and abnormal brain mater) which was less frequent on DJNKI brain at 7 (60% vs. 0%) and 60dpi (100% vs. 20%) on ipsilateral cortex, and disrupted corpus callosum which was less frequent on DJNKI brain at 1 (70% vs. 0%) and 3dpi (80% vs. 20%) on the ipsilateral cortex (Table 1). Representative samples of these morphological changes are presented in Fig. 4E with abnormalities demarcated in red. The reduced frequencies of these alterations in brain morphology in DJNKI-treated animals' brains suggest that the DJNKI-1 treatment is protective at various levels in the brain. No prominent midline shifts were observed in both saline and DJNKI-treated brains. There were also no significant weight differences between the two groups over the experimental period.

To investigate possible effect of acute DJNKI-1 treatment on white matter structure, we quantified the surface area of regional corpus callosum (CC) from T2-weighted images (T2WI) at the level of +1mm from bregma (just anterior to the lesion) at each of the time points in each group. Overall increase in total CC surface areas was observed for DJNKI-1 animals across all time points compared to saline-controls (** $p < 0.001$, repeated measures ANOVA; Fig. 5A, B). Individual t-test for total CC showed that the increased CC size was more evident at later time points, especially at 7d ($p = 0.021$), 30d ($p = 0.005$), and 60d ($p = 0.005$) time points in the DJNKI-1 animals, although CC size at 1d is also higher for DJNKI-1 animals ($p = 0.012$) (Fig. 5B, C). Comparison of CC size along hemispheric lines further shows overall increase for the DJNKI-1 group across all time points (for ipsilateral CC, ** $p < 0.009$; for contralateral CC, ** $p < 0.003$) (Fig. 5D, E). These results are suggestive of beneficial role for DJNKI-1 in maintaining white matter structural integrity, especially at later time points.

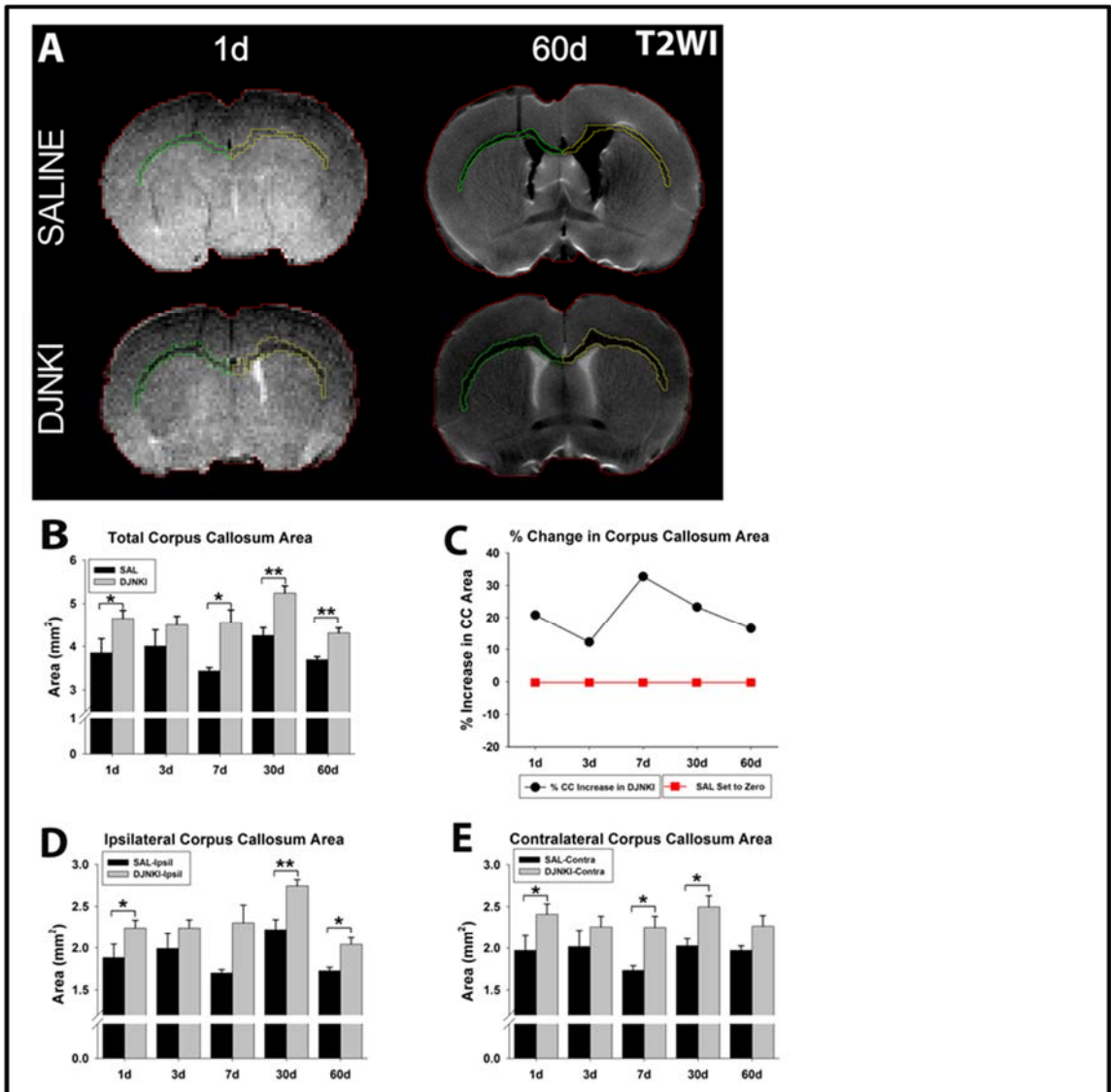


Figure 5. Corpus Callosum (CC) Area Increases with DJNKI-1 Treatment. **(A)** T2-weighted MR images for both saline (SAL) and DJNKI groups are shown at 1dpi and 60dpi at a coronal slice that is 1mm from last slice showing sign of injury. Yellow and green outlines encompass the ipsilateral and contralateral regions of interest (ROIs) for the CC respectively. The red outlines encompass the entire coronal brain slice. The DJNKI-1 slices appear to have larger CC surface area at each time of the time points shown. **(B)** Quantification of combined CC surface area in equivalent coronal slices for all animal at each time point shows that DJNKI animals have increased overall surface area (** $p < 0.001$, repeated measures ANOVA) compared to saline animals. The increased CC area in DJNKI-1 group is more pronounced at 7, 30 and 60 days post-injury. **(C)** Percent change in CC area in DJNKI-1 group is shown compared to saline group. **(D, E)** Inter-group comparison of CC surface area is shown for ipsilateral **(D)** and contralateral **(E)** CC. Both graphs show that the most evident increase in CC area in DJNKI-1 animals occurred at 7, 30, and 60d, although repeated measures ANOVAs show overall increase in CC (for ipsilateral CC, $p < 0.009$; for contralateral CC, $p < 0.003$).

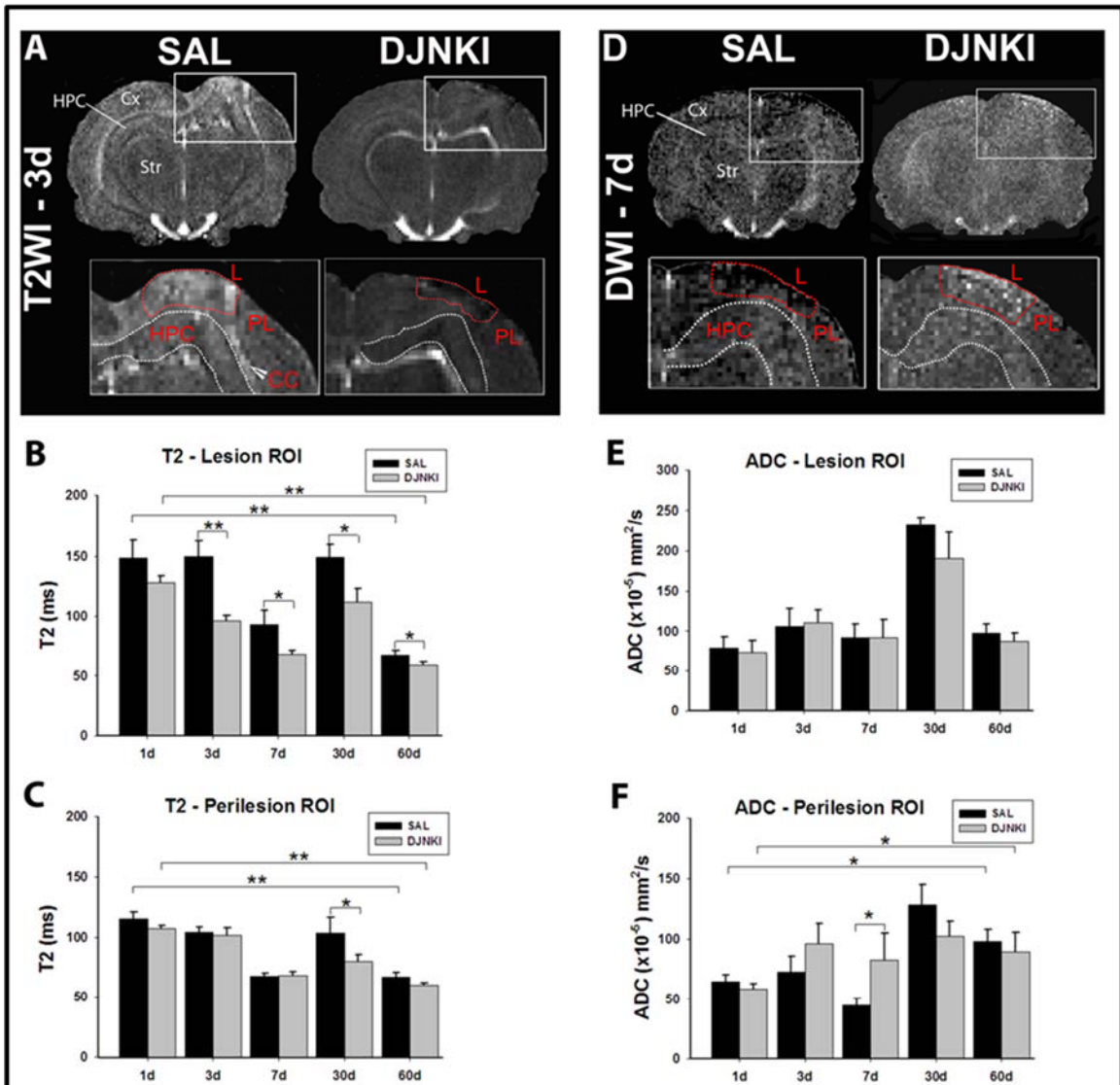


Figure 6. Changes in T2 and Apparent Diffusion Coefficient (ADC) with DJNKI treatment. **(A)** T2 maps for both saline (SAL) and DJNKI groups are shown at 3 dpi. White rectangular boxes encompass the lesion and perilesion regions of interest (ROIs) which are more hyperintense in the saline vs. DJNKI group. The boxed regions are enlarged in the lower pane. **(B)** Graph of T2 values at the lesion ROI indicates higher T2 values in the saline group at 3, 7, 30, and 60dpi ($*p < 0.05$; $**p < 0.01$) compared to DJNKI brains. **(C)** Graph of T2 values at the perilesion ROI indicates higher T2 values in the saline group at 30 dpi ($*p < 0.05$) compared to DJNKI brains. **(D)** ADC maps for both saline (SAL) and DJNKI groups are shown at 7dpi. White boxes (enlarged in lower pane) encompass the lesion and perilesion ROIs coregistered with T2 maps. **(E)** Graph of ADC values in the lesion ROI indicates similar water diffusion profiles of the brains of saline and DJNKI animals across all time points examined. **(F)** ADC graph for perilesion ROI indicates reduced water diffusion in the brains of saline animals at 7dpi ($*p < 0.05$) compared to their DJNKI-treated counterparts. There are no differences at all other time points. (1d, 3d, and 7d: $n=5$ for each group; 30d and 60d: $n=4$ for SAL, and $n=5$ for DJNKI).

DJNKI-1 Reduces Edema and Improves Water Diffusion after Juvenile TBI

Hyperintensity on T2-weighted MRI (T2WI) has long been used as an index of water accumulation possibly related to edema formation (Gomori et al., 1985, Kato et al., 1986) as shown in Fig. 6A (SAL, white box). In this study, we serially acquired T2WI on the subjects to profile T2 changes over the experimental timeline (Figs. 3A, 6B & C). Shown in Fig. 6A are representative T2WI of saline and DJNKI brains at 3d, with the boxed region enlarged in the lower pane and the important regions labeled (L = Lesion; PL = Perilesion; CC = Corpus Callosum; HPC = Hippocampus; Cx = Cortex; and Str = Striatum).

The overall T2 profile in lesion ROI shows increase in T2 values at the acute injury phase (1d and 3d), followed by a decrease back to normal values by 7d, and another rise in T2 values by 30d, followed by decrease by 60d (Fig. 6B). This intragroup variation in T2 value over time is statistically significant ($**p < 0.001$, rm ANOVA, Fig. 6B). Pairwise comparisons show that the T2 values from the lesion ROI at 7d and 60d are significantly lower than the T2 values at the same ROI at 1d ($**p < 0.001$) and 3d ($**p < 0.001$) (Fig. 6B). Overall, T2 values are higher in the lesion (Fig. 6B) than in the perilesion (Fig. 6C). Inter-group differences are also observed. T2 values acquired from lesion ROI in the DJNKI-treated animals are significantly decreased compared to controls at both acute (3dpi [$**p < 0.003$] and 7dpi [$*p < 0.04$], t-tests) and later (30dpi [$*p < 0.03$] and 60dpi [$*p < 0.04$], t-tests) time points following jTBI (Fig. 6B), suggesting that DJNKI treatment ameliorates edema formation acutely. The treatment may also reduce continued cell death and water accumulation in the lesion cavity at later time points (Fig. 6B). Repeated measures ANOVA confirms the reduced T2 in DJNKI-treated group over all time points ($**p < 0.002$). The use of *ex vivo* MRI modality at 60d does not

significantly affect value comparison with *in vivo* MRI scans at earlier time points as earlier reported (Obenaus et al., 2011, Ajao et al., 2012).

Significant intergroup difference in perilesion T2 is found only at 30dpi with reduced T2 in DJNKI-1 brains ($*p < 0.05$, Fig. 6C). Intragroup variation in perilesion T2 value over time is statistically significant ($**p < 0.001$, rm ANOVA, Fig. 6C). Pairwise comparisons show that the T2 values from the perilesion ROI at 7d and 60d are significantly lower than the T2 values at the same ROI at 1d ($**p < 0.001$) and 3d ($**p < 0.001$) (Fig. 6C). Other brain regions besides lesion and perilesion show the same pattern of stepwise T2 decrease from 1d to 60d without the transitory, upsurge in T2 values at 30d (data not shown).

Apparent diffusion coefficient (ADC), which is a quantitative parameter of diffusion-weighted MRI (DWI), is often used as a measure of water mobility in the brain (Le Bihan, 2007, Badaut et al., 2011). Shown in Fig. 6D are representative DWI of saline and DJNKI brains at 7d, with the boxed region enlarged in the lower pane and the important regions labeled as in Fig. 6A. There were no detectable intergroup differences in the ADC values in the lesion ROI across the experimental timeline (Fig. 6E). Whereas ADC values in the lesion ROI were fairly at the same levels at 1, 3, 7, and 60dpi, there was a significant spike at 30dpi in both groups (Fig. 6E; $**p < 0.008$).

There is significant variation in ADC values in the perilesion ROI over the course of the experiment ($**p < 0.01$). ADC profile of the perilesion ROI is strikingly similar to that of the lesion ROI over the experimental timeline (Fig. 6F) with the exception of a significant increase in ADC in DJNKI-1 group compared to saline group at 7dpi ($p < 0.05$) (Fig. 6F). The similarity in the profiles of ADC changes in both lesion and perilesion ROIs suggests intragroup uniformity with respect to jTBI model and effect of DJNKI-1 treatment.

DJNKI-1 Improves Neurological Functions at Acute Time Points and Cognitive Functions at Chronic Time Points.

To test the efficacy of DJNKI-1 to reverse functional deficits such as motor coordination impairment, the rats were subjected to foot-fault, beam balance and rotarod tests over the experimental timeline (Fig. 7A). Significant reduction in the number of foot-faults was found in DJNKI-treated rats at 3, 7, 30 and 60 dpi (** $p < 0.01$) compared to control rats (Fig. 7A), suggesting that DJNKI improves motor function not just acutely but also chronically. A repeated-measures ANOVA confirms significant intergroup differences in number of foot-faults over time (** $p < 0.001$; Fig. 7A). There was a progressive, stepwise decrease in the number of foot-faults registered by all subjects over time regardless of group (Fig. 7A; ** $p < 0.001$, rm ANOVA). The beam balance test, however, does not show any significant intergroup differences in mean distance travelled across all time points (Fig. 7B; $p < 0.67$, rm ANOVA). Nonetheless, profile of distance travelled over the experimental timeline shows a stepwise decrease in value that is similar (although less steep) to the foot-fault graph (Fig. 7B; ** $p < 0.001$, rm ANOVA).

Two different rotarod paradigms (with 2 velocity/acceleration settings on each) were used to further test motor balance, coordination and endurance (Figs. 7C, D, and E). Constant speed paradigms (consisting of 10RPM and 20RPM trials) were used at all experimental time points, while constant acceleration paradigms (consisting of 2RPM/5s and 5RPM/5s) were employed only at 30dpi and 60dpi. DJNKI-treated animals performed better in the 10RPM rotarod with higher latencies at 3dpi (* $p < 0.02$, t-test) and 7dpi (** $p < 0.002$, t-test) (Fig. 7C), and at 7dpi (** $p < 0.001$, t-test) in the 20RPM rotarod (Fig. 7D). Constant acceleration rotarod paradigms (2RPM/5s and 5RPM/5s) showed no differences in latency to fall between the 2 groups at 30d and 60d (Fig. 7E). Taken together, results from foot-fault and rotarod (constant speed paradigm) tests suggest that acute DJNKI-1 administration ameliorates motor deficits following jTBI.

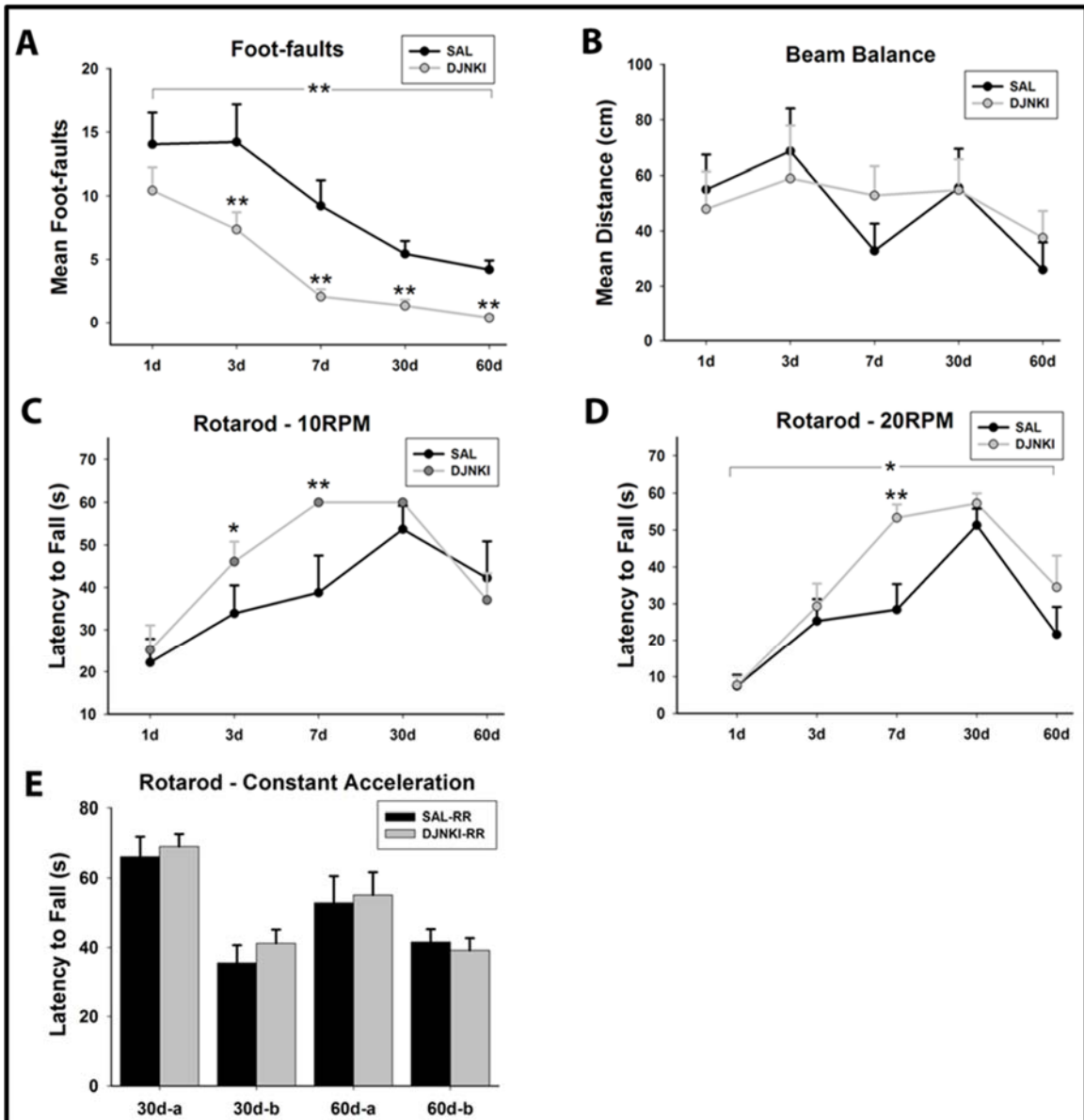


Figure 7. DJNKI Treatment Changes Neurological Outcomes. **(A)** Graph of foot-fault test shows significant increase in the number of faults in saline-control (SAL) rats compared to their DJNKI-treated (DJNKI) counterparts across examined time points (** $p < 0.001$; repeated measures ANOVA). **(B)** Balance and coordination skills were measured with the beam balance test. The distances covered on the beam were not different between the two groups. **(C)** Motor balance and coordination functions were examined with a rotarod test set to a constant velocity of 10 RPM. The graph reveals that fall latency was significantly higher in DJNKI-treated group at 3 and 7dpi (* $p < 0.05$; ** $p < 0.01$) compared to controls. **(D)** Graph of rotarod test set to a constant velocity of 20 RPM shows that fall latency was significantly higher in DJNKI-treated group at 7dpi (** $p < 0.01$) compared to controls. **(E)** Constant acceleration rotarod paradigm at **(a)** 2RPM per 5s and **(b)** 5RPM per 5s shows no difference in fall latency between the two groups at 30d and 60d. (1d and 3d: $n=14$ for each group; 7d: $n=9$ for each group; 30d and 60d: $n=8$ for SAL, and $n=9$ for DJNKI).

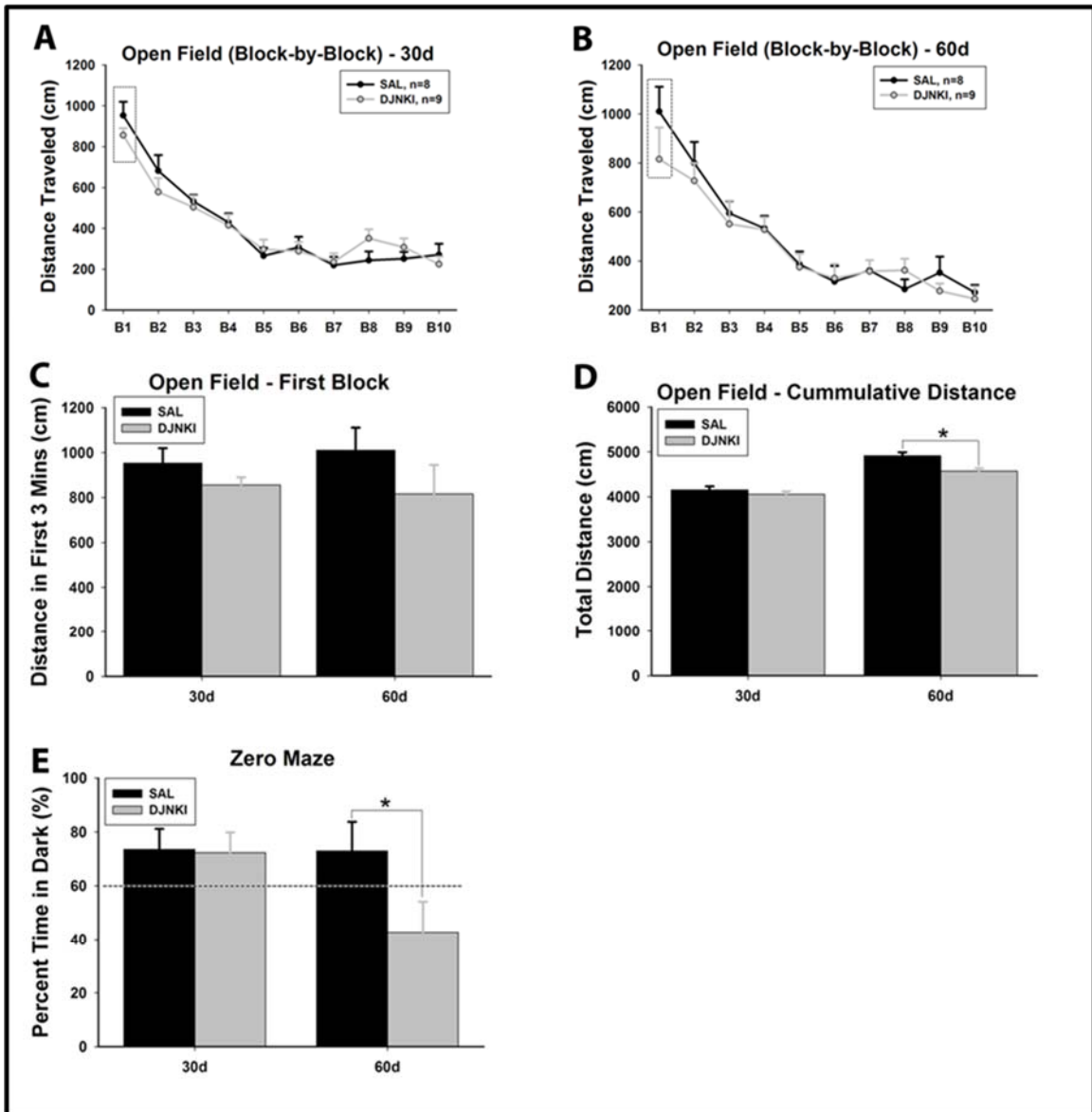


Figure 8. DJNKI Treatment Effects Behavioral Changes in Open Field and Zero Maze Tests. **(A)** Graph of open field recordings across 10 time blocks is shown at 30dpi, showing no between group differences. The first block is enclosed in a box. **(B)** Similarly, an open field graph is shown for recordings at 60dpi with no between group differences. The first block is enclosed in a box. **(C)** Evaluation of the first 3-min block of activity as an index of exploratory behavior shows no significant differences between the two groups. **(D)** Graph of cumulative distance traveled over 30 min (10 blocks of 3 min each) in the open field test shows no significant differences at 30dpi, but indicates decreased distance travelled in DJNKI animals at 60 dpi ($*p < 0.05$). **(E)** Graph of zero maze test – used to assess anxiety-like behaviors – shows significant decrease in time spent in the dark by DJNKI-treated animals at 60 dpi ($*p < 0.05$) compared to saline group. (At both 30d and 60d: $n=8$ for SAL, and $n=9$ for DJNKI).

The open field (OF) test consists of 10 3-mins continuous recording period, with each 3 mins constituting a trial block. There are no significant intergroup changes in distance travelled across the 10 blocks either at 30d (Fig. 8A) or 60d (Fig. 8B). The OF profiles follow a pattern of progressive decrease in distance moved from one block to the next resulting in overall variation in distance traveled across the 10 blocks for both groups (** $p < 0.001$, rm ANOVA; Figs. 8A & B). The cumulative distance graph shows a significant increase in total distance traveled by saline animals compared to their DJNKI-treated counterparts at 60 dpi ($*p < 0.05$) (Fig. 8D), suggesting an overall decrease of activity in DJNKI-1 treated rats. Distance traveled during the first 3 mins of the 10-block test – used as a measure of exploratory behavior – showed no inter-group differences at 30dpi and 60dpi (Fig. 8C). In addition, to evaluate anxiety behavior, the rats were subjected to Zero Maze test, which showed significantly reduced percentage of time spent in the dark arm by DJNKI animals compared to saline (42.7% vs. 73%; $*p < 0.04$) at 60dpi (Fig. 8E).

Cognitive outcomes were assessed by a combination of MWM trials, which includes cued, spatial and probe trials (Figs. 9A-E). Cued MWM test was carried out at 30 and 60dpi to test for equivalence in visual, swimming and motor abilities between the 2 groups. There were no intergroup differences at 30dpi (Fig. 9A; $*p = 0.72$, rm ANOVA). At 60dpi however, rm ANOVA ran on cued MWM indicates significantly lower distance covered by DJNKI animals to reach submerged platforms across the 5 trial blocks (Fig. 9B; $*p < 0.03$, rm ANOVA). This suggests that the DJNKI-1 animals had either higher motor and swimming or visual ability compared to the controls at 60d. The distance traveled to reach submerged platforms in MWM spatial trials are indicators of spatial learning and working memory. Spatial MWM was carried out with a western (W) start location. In spatial MWM, cumulative distance covered by DJNKI-treated rats at 30dpi was significantly lower compared to controls across the blocks (Fig. 9C; $**p < 0.008$, rm

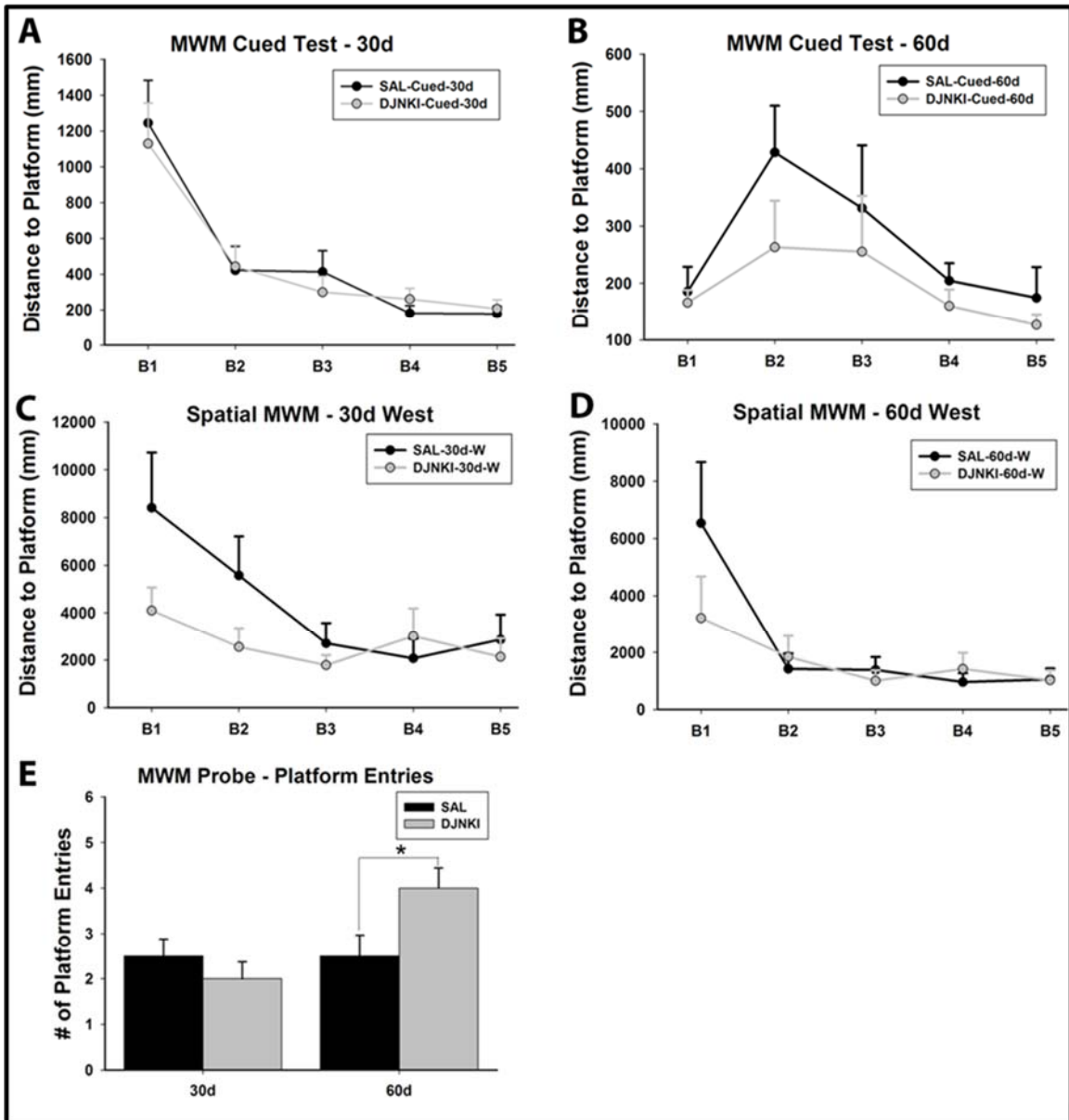


Figure 9. DJNKI Treatment Improves Behavioral Outcomes in Morris Water Maze (MWM) Tests. **(A)** Cued MWM test was carried out at 30dpi to test for equivalence in visual, swimming and motor abilities between the 2 groups. The graph indicates that there were no between group differences at 30dpi. **(B)** Repeated measures ANOVA ran on cued MWM at 60dpi indicates significantly lower distance covered by DJNKI animals across the 5 trial blocks ($*p < 0.03$). **(C)** In spatial MWM at 30dpi (start location = West), cumulative distance covered by DJNKI-treated rats was significantly lower compared to controls across the blocks ($**p < 0.01$, repeated measures ANOVA). **(D)** There were no differences in MWM spatial test at 60d (West) across the trial blocks, although there is a group-distance interaction ($*p < 0.04$). **(E)** Entries to platform location (an indicator of spatial memory) was higher in DJNKI-treated rats compared to controls at 60dpi ($*p = 0.02$). (For both 30d and 60d: $n=8$ for SAL, and $n=9$ for DJNKI).

ANOVA). There was, however, no significant between-group difference in MWM spatial test at 60d (W) across the trial blocks, although there was a group-distance interaction ($*p < 0.04$). Meanwhile, in the probe trials, the number of entries to platform location, which is an index of spatial memory, was significantly higher in DJNKI-treated rats compared to controls at 60dpi (Fig. 9E; $*p < 0.02$, t-test), but not at 30dpi. Taken together, these MWM results indicate that the effect of acute DJNKI-1 treatment on cognitive deficits at long-term following jTBI may be sensitive to both test repetition which can reduce the sensitivity of the MWM tests, and to the evolution of the injury across time (see section 4.1 for an elaborate discussion on this).

DJNKI-1 Protects Blood-Brain Barrier Integrity Acutely after Brain Injury

Immunohistochemical staining for extravasated IgG was carried out to assess BBB disruption at 3dpi as previously described (Pop et al., 2012). Representative coronal slices with extravasated IgG (shown as intense green) at varying depths from Bregma at 3dpi are shown for each group on Fig. 10A. Student's t-test on IgG-stained areas on these sections indicates that DJNKI-treated animals had significantly lower IgG-stained surface area compared to controls ($*p < 0.02$) (Fig. 10B). This suggests that DJNKI-1 administration helps ameliorate acute BBB disruption following jTBI.

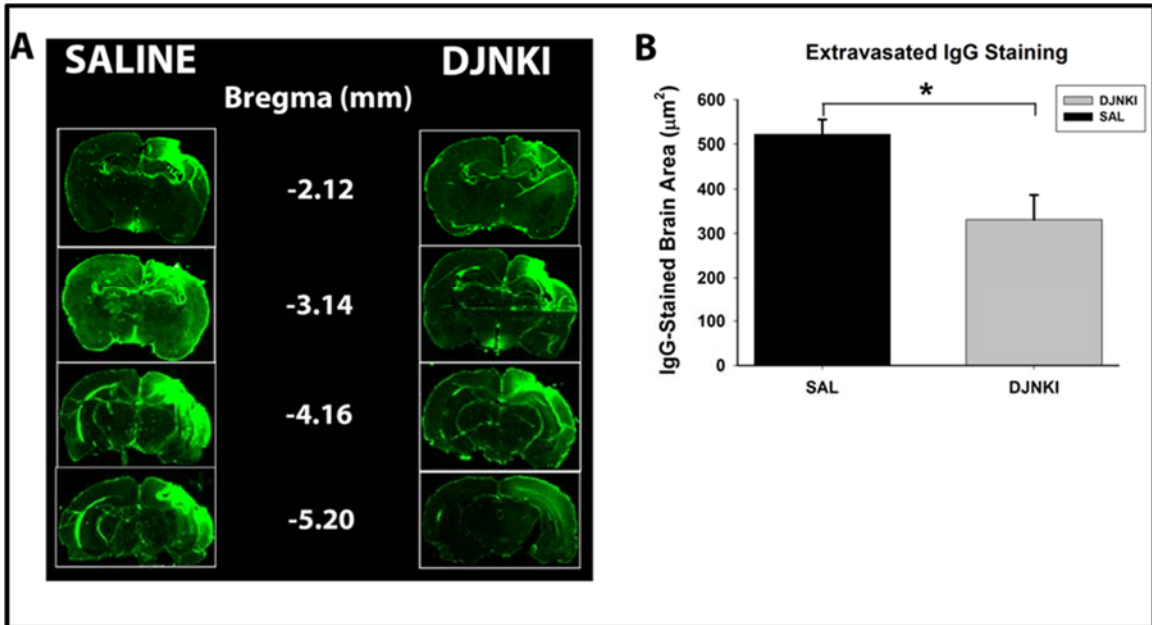


Figure 10. IgG Extravasation Decreases with DJNKI-1 Treatment.

(A) Immunohistochemical staining for immunoglobulin G (IgG) extravasation (seen as intense green) is shown on coronal slices at varying depths from Bregma at 3dpi.

(B) A graph of quantified extravasated IgG shows a significantly lower IgG staining in brains of DJNKI-treated animals compared to saline-controls ($*p = 0.02$).

Discussion

This study was aimed at investigating the potential therapeutic impact of competitive inhibition of JNK pathway in a juvenile TBI (jTBI) model. Hyperactivation of the JNK pathway is a phenomenon that has been reported in various forms of brain injuries (Borsello et al., 2003, Michel-Monigadon et al., 2010, Nijboer et al., 2010). Experimental data from animal studies show that activation of JNK pathway peaks early – in usually less than 12 hours – following brain injuries (Michel-Monigadon et al., 2010, Nijboer et al., 2010). In broad agreement with these animal studies, Ortolano et al. reported an increase in phospho-JNK (an index of JNK activation) from 1 to 48 hours post-injury in brain tissue samples from 6 TBI patients, and confirmed this phospho-JNK temporal profile experimentally in a CCI model in adult mice (Ortolano et al., 2009). Other experimental data from murine ischemia-reperfusion model suggest that JNK phosphorylation may initially drop, and then begin to rise from 1 hour until it peaks at 9 hours following stroke (Gao et al., 2005). Phosphorylation of c-Jun – a JNK substrate – follows a similar pattern, peaking at 8 hours post-stroke, although it remains significantly elevated at 24 hours (Gao et al., 2005). The choice of 3 hour post-injury DJNKI-1 administration time for this study therefore is appropriate, as it falls within a period of active JNK hyperactivation, and is linked with positive outcomes in both permanent ischemic brain injury model in 14d rat pups (Borsello et al., 2003) and in neonatal hypoxic-ischemic brain injury model in 7d rat pups (Nijboer et al., 2010).

The drug of choice – DJNKI-1 – is a synthetic cell-penetrating peptide that is protease-resistant and has been shown to be very promising in inhibiting JNK action competitively at various levels of the pathway (Borsello et al., 2003, Borsello and Bonny, 2004). The drug was synthesized by linking HIV-TAT carrier peptide sequence to the 20-amino acid JNK-binding motif of the scaffold protein JIP-1 (Borsello et al., 2003). D-JNK-1 acts by competitively inhibiting the interaction of all JNK isoforms with JIP-1 and

with their downstream substrates (Borsello et al., 2003, Borsello and Forloni, 2007). The dosage used – 11mg/kg – was based on its previously reported efficacy in permanent middle cerebral artery occlusion (MCAO) model in juvenile (P14) rats (Borsello et al., 2003) and in other CNS injury models (Repici and Borsello, 2006, Repici et al., 2007) where the drug was injected intraperitoneally (i.p.). Previous reports have indicated that the drug is able to cross the BBB and penetrate the cerebral cortex within 1.5 hours after i.p. injection in rodents, and could remain stable in brain parenchyma for at least 3 weeks (Repici et al., 2007, Ploia et al., 2011, Scip et al., 2011).

The key finding of this study is that early administration of DJNKI-1 not only improves histological, sensorimotor and cognitive outcomes at early time points but also confers neuroimaging and functional improvements at later time points as observed at 4 to 8 weeks post-injury (Figs. 3D, 6B, 7A, 8E, etc.). This property is important for potential clinical use and bodes well for long-term clinical efficacy of DJNKI-1 in juvenile TBI. In the following sections, the main effects of early DJNK-1 intervention following jTBI in this study are discussed, together with insights into potential mechanisms mediating these effects.

DJNKI-1 and Improvement of Neurological and Cognitive Functions

In this study, we found remarkable improvements in sensorimotor and cognitive functions at both acute and later time points following DJNKI-1 treatment in our jTBI model (Figs 7, 8, and 9). These findings are important with respect to scientific reports that highlighted the persistence of neurological, cognitive, and behavioral sequelae following moderate to severe TBI during childhood (Schwartz et al., 2003, Catroppa and Anderson, 2009, Anderson et al., 2012), which have been confirmed in some animal models of jTBI (Russell et al., 2011, Ajao et al., 2012).

We found robust improvement in sensorimotor functions with the use of foot-fault test (Fig. 7A, both short-term and long-term post-injury) and constant speed paradigm of rotarod test (Figs. 7C and D, only at short-term), but not with either beam balance test (Fig. 7B) or the constant acceleration paradigms of rotarod (Fig. 7E). Other labs that used comparable acceleration paradigm have established that motor deficits on rotarod are greatest and most evident at acute phases (1 – 7 days) following experimental TBI in rodents, with recovery up to 88% of preinjury values by 14 days (Onyszchuk et al., 2007). This is consistent with our results in constant speed paradigm (Figs. 7C, D), and makes it improbable to see treatment effects on accelerating rotarod at later time points (Fig. 7E). Lack of both pre-training and customized rotarod apparatus to accommodate the smaller sizes of juvenile rats have been suggested to affect performance on accelerating rotarod more adversely compared to constant speed rotarod following jTBI (Russell et al., 2011). Rats have also been observed to use change in gait strategy and motor skill learning to improve their performance on accelerating rotarod (Buitrago et al., 2004, Barreto et al., 2010). These results suggest that DJNKI-1 improves neurological function, although not all tests are sensitive enough to reveal the improvements in fine motor skills (Russell et al., 2011). The motor deficits observed are warranted because the injury encompasses parts of the motor cortex on the rat brains (Soblosky et al., 1996, Ajao et al., 2012). On-going morphological and functional changes in white matter tracts in this model (Ajao et al., 2012, Kamper et al., 2013) may also account for the persistent motor dysfunction observed (Caeyenberghs et al., 2011b), and as such the impact of DJNKI-1 treatment on the white matter should be further investigated. We have reported long-term sensorimotor deficits up to 6 months in this jTBI model (Kamper et al., 2013). Potential correction of these long-term deficits with DJNKI-1 should be studied.

With respect to emotional disorders, the decreased cumulative distance by DJNKI animals in open field test (Fig. 8D) coupled with decrease in time spent in the dark arm of zero maze at 60d by DJNKI animals (Fig. 8E) could indicate reduced anxiety-like behavior compared to their saline counterparts (Kodama et al., 2008) as we have previously reported (Ajao et al., 2012). Amelioration of anxiety-like behavior on zero maze test (Fig. 8E) further substantiates DJNKI-1's positive effects on functional changes involving multiple brain networks. Anxiety-like symptoms and anxiety disorders have been reported within 6 months in over 25% of clinical cases of juvenile TBI across all severity levels according to one report (Max et al., 2011). Late onset of anxiety disorders in adult patients has been previously reported (Whelan-Goodinson et al., 2009). Younger children were found to be at an increased risk for developing anxiety disorders following TBI (Vasa et al., 2002, Max et al., 2011). Damaged frontal lobe and frontal white-matter systems are also associated with these anxiety-related disorders in young TBI victims (Max et al., 2011). We have previously shown that the jTBI model used in this study causes alterations in some white matter tracts both proximal to and distal from the site of impact (Ajao et al., 2012). DJNKI-1 could hold some potential for counteracting these post-injury symptoms.

Moreover, DJNKI-1 also confers some cognitive improvements at select time points as seen in various MWM test formats (cued, spatial, and probe) (Fig. 9) which assessed spatial learning and spatial memory functions. In a previous study (Ajao et al., 2012) where the injury location was more anterior and less lateral to Bregma (1mm by 2mm) than in this current study (3mm by 4mm), we found no spatial learning or memory differences at 30d and 60d between shams and injured rats in this jTBI model. However, in a follow-up study, despite not showing overt spatial learning deficits, TBI animals in this model use cruder MWM swim strategies which are more dependent on chance at 60d post-injury compared to sham animals which rely more on direct spatial learning

strategy (Pop et al., 2012). DJNKI-1 treatment may be correcting for this subtle shortfall in spatial learning strategy in treated animals (Fig. 9). Decrease in distance moved to reach the platform by DJNKI-1 animals in the 60d cued MWM test (Fig. 9B), rather than confounding the results of the spatial MWM, may be a further indication that DJNKI-1 improves motor coordination capabilities of the treated animals. While DJNKI-1 animals displayed better spatial learning at 30d and 60d (Fig. 9C, D), all animals might have become used to the repetitive nature of the test, thereby potentially limiting the test's sensitivity at later time points. Cognitive deficits, however, evolved over time following injury (Kamper et al., 2013). While not explicit at 1 and 2 months post-injury (Ajao et al., 2012), there are spatial memory differences at 3 and 5 months post-injury, and these resolved at 6 months (Kamper et al., 2013). Therefore, differences in MWM test could show up at much later time points with DJNKI-1 treatment, and this underscores the potential of testing DJNKI-1 to arrest some long-term sequelae of juvenile TBI that have been well-documented (Sbordone et al., 1995, Yeates et al., 2002, Schwartz et al., 2003, Ajao et al., 2012).

The developmental time period is very important for formation of crucial sensorimotor and cognitive abilities, and injury to the brain during this phase could elicit unresolved imbalances in functional behavior (Giza, 2006, Giza et al., 2007, Ajao et al., 2012). Scientific reports on genetic deletion (Wang et al., 2007, Yamasaki et al., 2011, Yamasaki et al., 2012) and pharmacological inhibition (Borsello et al., 2003, Armstead et al., 2011) of JNK or its upstream MAPK activators in developmental animal models have highlighted the importance of JNK to normal brain development as well as its deleterious role in developmental brain disorders. For example, deletion of JNK3 gene protects neonatal mice against cerebral hypoxic-ischemic (HI) injury (Kuan et al., 2003, Pirianov et al., 2007). BBB damage is strongly mediated by JNK hyperactivation in experimental hypoxic-ischemic brain injury in P7 rat pups (Tu et al., 2011). These reports underscore

the importance of JNK pathway in various forms of brain insults during development and highlight the therapeutic importance of DJNKI-1.

Improvement in neurological and cognitive functions has been reported following DJNKI treatment in CNS injury models such as: MCAO (Borsello et al., 2003, Esneault et al., 2008), neonatal hypoxic-ischemia (Nijboer et al., 2010), intracerebral hemorrhage (Michel-Monigadon et al., 2010), spinal cord injury (Repici et al., 2012), and controlled cortical injury in adult mice (Ortolano et al., 2009). Tests utilized in these referenced reports (rotarod, adhesive removal, beam walking, object recognition, cylinder rearing, modified hole board, footprint, and forelimb placement tests) were customized and standardized for assessing several neuromotor, proprioceptive, and cognitive abilities. Chronic treatment with D-JNKI-1 has recently been shown to rescue memory impairments and long term potentiation deficits in an Alzheimer disease mouse (TgCRND8) model without any major side effects (Sclip et al., 2011). Our study provides additional evidence that DJNKI-1 could ameliorate functional deficits following jTBI.

TBI in the pediatric brain exhibits both acute and chronic phases linked to the disruption of learning and memory consolidation (Schwartz et al., 2003, Chapman, 2006, Babikian and Asarnow, 2009). The pediatric population may be especially vulnerable to this post-TBI cognitive deficits due to disruption of normal brain development and emerging skills which often lead to neurocognitive stall (Chapman, 2006, Catroppa and Anderson, 2009). JNK hyperactivation has been shown experimentally to specifically mediate such stressful event in the hippocampus (Sherrin et al., 2010). The report further shows that injection of DJNKI-1 reduced the activity of hippocampal JNK and ameliorated the stress-induced functional deficit. It is plausible that in our study, DJNKI-1 treatment is mediating similar reduction of JNK activity in the hippocampus with resultant improvements seen in learning and memory test (Fig. 9). We cannot however rule out potential beneficial effects of JNK inhibition by DJNKI-1 in peripheral systems as inferred

in models where DJNKI-1 was injected at a low dose that was not detected in the brain (Benakis et al., 2010, Benakis et al., 2012). Peripheral actions of DJNKI-1 such as reduction of peripheral inflammation may indirectly effect cognitive improvement (Wilson et al., 2002, Benakis et al., 2010).

While it is not entirely clear how DJNKI-1 elicits these long-term improvements, reduced neuronal apoptosis and resultant preservation of the brain's sensorimotor networks is a potential mechanism (Borsello et al., 2003). So also is preservation of BBB integrity and prevention of edema formation. Neuromotor abilities have been shown to correlate with brain edema and BBB integrity in experimental TBI (Li et al., 2012).

Very few pharmacological agents including several ones that failed clinical trials (Doppenberg et al., 2004, Beauchamp et al., 2008, Janowitz and Menon, 2010) have demonstrated such strong neurological and cognitive effects and for the length of time comparable to those shown by DJNKI-1 in these results (Figs. 7 - 9). Some of the problems that led to failure of several TBI-targeted clinical trials, such as insufficient brain penetration and lack of long-term neurobehavioral testing (Doppenberg et al., 2004) have been addressed with the use of D-JNKI-1 in this study. Its ability to penetrate the brain (Repici et al., 2007) and its beneficial effect on both short-term and long-term neurological and cognitive functions (Repici et al., 2012) (Figs. 7 - 9) increases its profile as an ideal therapeutic candidate. It should also be noted that most of the clinical trials in TBI have been carried out in severe TBI cases in adult patients (Doppenberg et al., 2004). The potential suitability of D-JNKI-1 as a candidate drug for moderate TBI in pediatric patients is another highlight of this study.

DJNKI-1, Reduction of Lesion Volume and Amelioration of Morphological Alterations

In our search for additional evidence of DJNKI-1's effects following jTBI, we found a consistent reduction in lesion volume over the experimental timeline in DJNKI-1 treated rats (Fig. 3B, C, D). Similar reduction in lesion volume through inhibition of JNK pathway – either with the use of DJNKI-1 or SP600125 (another small molecule JNK-specific inhibitor) – has been reported in various models of brain injuries, which include transient and permanent middle cerebral artery occlusion (MCAO) (Borsello et al., 2003, Hirt et al., 2004), focal ischemic brain injury (SP600125 was used here) (Gao et al., 2005), intracerebral hemorrhage (ICH) (Michel-Monigadon et al., 2010), and neonatal hypoxic-ischemic brain injury (Nijboer et al., 2010). Abnormal morphological alterations that are coincident with massive brain contusion such as ventricular hypertrophy, cortical thinning, hemorrhage/hematoma, herniation, cyst formation and disrupted corpus callosum are also reduced in DJNKI-1 group (Table 1). This could be attributed to reduced lesion volume in the brains of DJNKI-1 treated animals. In another study, we reported long-term cortical thinning in jTBI animals at 3 and 6 months post-injury (Kamper et al., 2013). DJNKI-1 may have the potential to correct this in the long-term. The therapeutic effect of DJNKI-1 with respect to reduced lesion volume has previously been attributed to: (1) inhibition of excitotoxicity and prevention of neuronal loss [as shown in models of MCAO (Borsello et al., 2003, Hirt et al., 2004), and in TBI (Ortolano et al., 2009)]; and (2) reduction in the loss of glial cells through reduction of glutamate toxicity [for example in oligodendrocytes in the brain (Rosin et al., 2004)].

Another potential mechanism of action for DJNKI-1 is through salvaging of oligodendrocytes, which could ameliorate the negative effects of jTBI on white matter structure and function. We have previously reported a significant decrease in area measurement of corpus callosum (through NF-200 and MBP staining, and through MRI

measurement) together with a concomitant increase in MBP immunoreactivity at early (3d) and later (60d) time points following jTBI (Ajao et al., 2012). In another study, we reported that the area of corpus callosum remains decreased in jTBI animals at 3 and 6 months post-injury (Kamper et al., 2013). Some studies have reported possible links between JNK pathway inhibition, viability of oligodendrocytes, and resultant sparing of white matter (Chew et al., 2010, Repici et al., 2012, Wang et al., 2012). Repici and colleagues (Repici et al., 2012) in particular reported long-term (4 months) locomotor recovery following administration of DJNKI-1 in a mouse model of spinal cord injury, and positively correlated this functional recovery with white matter sparing. It is therefore plausible that the short- and long-term functional recovery seen in this study is related to DJNKI's positive effects on the brain's white matter structures and functions (Ajao et al., 2012, Kamper et al., 2013).

To investigate possible effect of DJNKI-1 treatment on the white matter, we measured the surface area of corpus callosum (CC) from T2-weighted images (T2WI) at each of the time points. Increase in CC surface areas especially at 7d, 30d, and 60d time points in the DJNKI-1 animals (Fig. 5) suggests that the drug is effecting structural changes along the white matter that may be beneficial to recovery of function. We have previously shown that this jTBI model decreases CC surface area in the injured animals at 60d with respect to shams, and also decreases neurofilament-200 (NF200) immunostaining along the CC at 7d, 30d, and 60d post-TBI (Ajao et al., 2012). This data on CC area is consistent with the previous report. The CC contains commissural pathways that enable interhemispheric communication which is essential for bimanual motor function and other coordinated movements. The CC is highly vulnerable to TBI, and damage to the CC in humans TBI patients has been linked with deficits in bimanual motor functioning and coordinated movements (Caeyenberghs et al., 2011a). Decrease in size and microstructural integrity of CC also underpin the poorer sensorimotor

coordination on tasks requiring high degree of interhemispheric interactions seen in older adults compared with their younger counterparts (Fling et al., 2011). Furthermore, loss in the volume of deep white matter structures such as CC in children with TBI has been strongly linked with poorer long-term social reintegration and neuropsychological performance (Gale and Prigatano, 2010). DJNKI-1's effect on the CC and possibly other white matter structures may therefore have a potential for ameliorating not only sensorimotor deficits but also behavioral deficits as well. Additional studies are being carried out in Dr. Badaut's lab to determine the cellular and downstream molecular targets for DJNKI-1 supporting the neuroimaging and behavioral benefits.

DJNKI-1, Blood-Brain Barrier, and Edema Formation

We showed in this study that DJNKI-1 administration at 3 hours post-jTBI significantly reduced IgG extravasation at 3d post-jTBI around the lesion and perilesion ROIs (Fig. 10A, B). Water accumulation measured with T2 in these same 2 ROIs was significantly reduced in DJNKI-treated compared to non-treated rats not just acutely but also at later time points (Fig. 6A - C), suggesting that DJNKI prevents the edema formation early one after jTBI by improving the BBB integrity. Meanwhile, ADC measurements [which is used as an indicator of water mobility in the brain (Le Bihan, 2007, Obenaus and Ashwal, 2008)] showed no differences in the lesion and perilesion ROIs (Figs. 6D - F) except for the increased ADC value found in DJNKI-1 group at 7d in perilesion ROI (Fig. 6F). This may indicate a transient availability of larger intercellular space in the perilesion of DJNKI-1-treated animals at this 7d time point only. While the increased ADC value in the DJNKI-1 group could indicate some cell death, the reduced ADC value in the saline group may also indicate an on-going neuronal and astrocytic swelling (Badaut et al., 2011) which DJNKI-1 treatment counteracted.

Edema formation is one of the secondary processes evident in TBI (Werner and Engelhard, 2007, Shlosberg et al., 2010), and it is especially pronounced in juvenile TBI (Giza et al., 2007, Fukuda et al., 2012, Fukuda et al., 2013). A mechanistic explanation for the observation on edema above is a possible protective action of DJNKI-1 on BBB and brain endothelial TJ, which prevents prolonged BBB opening and preserves endothelial TJ integrity. In line with the proposed mechanism of action, attenuation of BBB disruption, edema, and apoptosis by DJNKI-1 could result in salvaging more neurons and glia that could have succumbed to premature cell death, and eventually lead to the preservation of neuronal networks that are vital to various neurological and cognitive functions. For example, in another study in this jTBI model in our lab that looked at a different treatment strategy, edema formation was decreased acutely alongside improved outcomes in BBB integrity and neurological functions, and reduction in neuronal cell death and astrogliosis (Fukuda et al., 2013).

The action of JNK hyperactivation in disrupting inter-epithelial and inter-endothelial tight junctional proteins have been reported in the periphery, like in tricellular tight junctions in human pancreatic duct epithelial cells, intestinal epithelial tight junctions (Betanzos et al., 2004, Kojima et al., 2010, Samak et al., 2010) and in *in vitro* brain endothelial cell cultures (Etienne et al., 1998, Adamson et al., 1999, Wolburg and Lippoldt, 2002, Tai et al., 2010). Moreover, JNK hyperactivation appears to contribute tremendously to TJ and BBB disruption in some brain disease models (Tai et al., 2010, Kacimi et al., 2011, Tu et al., 2011). Conversely, inhibition of JNK reversed decrease in TJ proteins including claudin-5 in the periphery (Carrozzino et al., 2009). JNK is actively involved in ICAM-1-mediated lymphocyte transmigration across brain microvascular endothelial cells in an *in vitro* model of neuroinflammation (Hudson, 2012). In human brain endothelial cells exposed to inflammatory cytokines, JNK inhibition reduced the cytokine-induced paracellular permeability (Lopez-Ramirez et al., 2012). Since capillary

endothelial cells are one of the first points of contact in the brain for intraperitoneally-injected, blood-borne DJNKI-1, the agent may conceivably be acting to reverse the reduction in BBB TJ proteins (Berezowski et al., 2012). The reduction in IgG extravasation at acute time-point provides an indirect, but fairly strong support for this (Fig. 10A, B). Corroborating evidence for this comes from a recently reported study of spinal cord injury (SCI) model performed in male Swiss mice where i.p. injection of the same dose of DJNKI-1 that we used (11 mg/kg) at 6 hour post-injury resulted in significantly lower IgG extravasation volume and erythrocyte extravasation in DJNKI-1 group compared to saline controls (Repici et al., 2012). Further studies (such as staining TJ proteins, etc. following DJNKI-1 treatment in JTBI) will however be needed to solidify this hypothesis.

The main sites of action for DJNKI-1 in the brain endothelium that could result in JNK inhibition are the JNK-binding motifs of the scaffolding protein, JIP-1 (Borsello et al., 2003, Borsello and Forloni, 2007). All 3 isoforms of JNK are present in the brain endothelium (Berezowski et al., 2012). DJNKI-1 competitively inhibits the interactions between JNK isoforms and their upstream mediators and downstream substrates. More than 50 substrates of JNK have been identified (Bogoyevitch and Kobe, 2006), and the functions of some are yet to be determined.

Repair of disrupted BBB and preservation of brain endothelial junctional integrity is a unique therapeutic avenue that has been proposed for traumatic brain injury (Hawkins and Davis, 2005, Shlosberg et al., 2010). Disruption of BBB and brain regulatory vascular mechanisms is of particular concern to the juvenile population due to its susceptibility to brain injury-induced cerebral hemodynamic dysfunction (Armstead, 1999, 2005, Freeman et al., 2008, Udomphorn et al., 2008, Chaiwat et al., 2009, Armstead et al., 2011), diffuse cerebral edema, and tight junction breakdown (Anthony et al., 1997, Suh et al., 2001, Campbell et al., 2007, Giza et al., 2007, Freeman et al.,

2008). Occurrence of impaired cerebral hemodynamic autoregulation has been established in several clinical cases and experimental models of TBI (Armstead, 1999, 2000) and it appears to be more pronounced in pediatric/juvenile model of TBI versus adult model (Armstead and Kurth, 1994, Armstead, 2000, 2004, 2005). Armstead and colleagues have identified hyperactivation of JNK as a major mechanism for this secondary consequence of jTBI (Armstead, 2003, Armstead et al., 2011). Using porcine (piglet) model of lateral fluid percussion injury (FPI) which mimics many of the pathophysiological features of jTBI including cerebral autoregulation impairment seen clinically (Armstead and Kurth, 1994), they reported that JNK MAPK concentration was increased in CSF by FPI, but blocked by JNK antagonists SP600125 and DJNKI-1 (Armstead et al., 2011). DJNKI administration following FPI blocked NMDA-induced vasoconstriction and fully restored pial artery vasodilation (Armstead et al., 2011). Although measurements of JNK was obtained from CSF in these studies, the increased concentration of JNK in CSF reflects events in brain parenchyma (Armstead et al., 2011). A major caveat is that the major cellular origin of this increased JNK is unknown, with the possibility of neuronal, glial, smooth muscle, and endothelial origins, or a combination of these sources. These reports nonetheless strengthen the theory that DJNKI-1 may confer a protective effect on brain vascular system and BBB. More investigation is needed, however, in this jTBI model to address the effect of DJNKI-1 on neuroinflammation and on some other relevant pathways such as the JAK-STAT pathway.

Conclusion

In this study, we provide evidence showing that administration of the competitive JNK inhibitor – DJNKI-1 – at 3 hours post-jTBI is not only effective in reducing edema formation and blood-brain barrier disruption at acute time points following juvenile TBI,

but also confers reduction in lesion volume and recovery of neurological and cognitive abilities that last into adulthood. Certain morphological alterations commonly seen in brain-injured rodents are also less frequent following acute treatment with DJNKI-1. These include reduction in the surface area of corpus callosum, ventricular hypertrophy, cortical thinning, damaged hippocampus, herniation, and hematoma.

DJNKI-1 has the potential to mediate cellular processes in various types of brain cells, including neurons, glial, smooth muscle, and endothelial, all of which could experience JNK hyperactivation. Processes that DJNKI-1 could ameliorate in the brain following jTBI may include: excitotoxicity (in neurons), apoptosis (in neurons and endothelial cells), and vascular permeability and edema (in capillary endothelial cells). Administration of DJNKI-1 through the intraperitoneal route, its facilitated passage through the cell membrane (by virtue of its carrier peptide sequence, HIV-TAT), and its lengthy half-life in brain tissue (up to 3 weeks) could ensure access of the drug to most of these cell types, and potentially elicit additive or synergistic effects in the brain. These beneficial effects appear to result in improved neurological and behavioral outcomes. Major effects of DJNKI-1 in the periphery can however not be ruled out.

The prolonged efficacy of this agent makes it promising for potential clinical applications. But further studies are needed to expound the mechanisms of action of DJNKI at the BBB interface, in the gray and white matter, and in the periphery. The molecular targets of DJNKI-1 that mediate reduced structural and histological damage secondary to the primary insult, and engender beneficial functional outcomes need to be further investigated. Such elucidation may help move DJNKI-1 into a clinical trial phase.

CHAPTER 6

GENERAL CONCLUSIONS AND FUTURE DIRECTIONS

Model Development for Juvenile TBI

Clinical observations and research evidence have shown that TBI is complex and heterogeneous in terms of its location, severity and pathophysiology (Saatman et al., 2008). This heterogeneity is considered a major barrier in finding effective therapeutic intervention (Saatman et al., 2008) and necessitated the development of various experimental models of TBI (Dixon et al., 1987, Dixon et al., 1991, Cernak, 2005, Morales et al., 2005, Morrison et al., 2011), each of which can model only parts of the pathophysiological processes associated with brain injuries. Controlled cortical injury (CCI) and fluid percussion injury (FPI) are the two most commonly used models of TBI (Morales et al., 2005, Chodobski et al., 2011). Efforts have also been made to develop suitable models of juvenile TBI (jTBI) mostly in piglets and rodents (Armstead and Kurth, 1994, Adelson et al., 1998, Prins and Hovda, 2003).

In this project, electromagnetically-actuated CCI on P17 rats was used to model TBI in the developing brain (Brody et al., 2007). This model of choice has a number of advantages. First is the ability to control the deformation parameters (velocity, impact depth, time delay) of the model, which allows improved reproducibility of injury severity in our lab and in other labs (Morales et al., 2005, Ajao et al., 2012). Secondly, this CCI model is associated with key pathophysiological processes including acute hemorrhage and hematoma, axonal injury, BBB dysfunction, and edema, all of which have been observed clinically in young TBI patients (Duhaime et al., 1992, Giza et al., 2007, Chodobski et al., 2011, Maxwell, 2012). Our findings confirmed that following jTBI, there

were: acute increase in BBB permeability and edema, neuronal loss, white matter changes, and brain deformities such as ventricular hypertrophy, herniation, and hemorrhage (Ajao et al., 2012). These observations demonstrate the usefulness and suitability of this model in investigating some important aspects of juvenile TBI.

Histological and Functional Effects of Juvenile TBI in Rodents

The traditional theory that prevailed for many decades is that brain injuries in young humans would be far less damaging structurally and functionally due to putative high plasticity and repair potential of the young brain (Kennard, 1936, Teuber and Rudel, 1962, Anderson et al., 2005, Dennis, 2010). Several findings in this project, however, suggest otherwise. Some functional deficits associated with the initial injury, which are sensorimotor, cognitive and behavioral in nature, remained unresolved up to 2 months post-injury (Ajao et al., 2012, Pop et al., 2012). Electrophysiological measurement also showed dysfunction in axonal conductance along a major white matter fiber at two months post-injury (Ajao et al., 2012). This supports our hypothesis that TBI on P17 rats will engender neurological dysfunction and deficits that will last for weeks after the initial insult. Furthermore, data from similar animal cohorts have confirmed the persistence of sensorimotor and cognitive deficits up to 6 months following jTBI (Kamper et al., 2013). These observations are consistent with epidemiological data that showed prolonged cognitive and behavioral deficits for years following TBI (Jonsson et al., 2013), and suggest that injury at an early age could be detrimental to future brain development. Such observations have triggered a rethink of how the developing brain responds to TBI (Yeates et al., 2002, Anderson et al., 2005) with increasing number of investigators now viewing the young brain as being more vulnerable than the adult brain for pathophysiological signatures of TBI, such as subdural hematomas and diffuse cerebral edema (Aldrich et al., 1992, Giza et al., 2007, Huh and Raghupathi, 2009).

While there are literature evidence that the developing brain retains some 'plasticity' (defined as the ability to be remolded or reshaped after damage) (Anderson et al., 2012), this plasticity does not fully compensate for deficits resulting from brain injuries (McQuillen and Ferriero, 2004, Anderson et al., 2012, Levin, 2012). Several developmental processes (e.g. white matter myelination and size) (see Chapter 5) and overall maturation of the brain are disrupted by juvenile TBI (Ajao et al., 2012). Furthermore, clinical reports of long-term deficits arise not just from moderate and severe TBI (Yeates et al., 2002), but also in some forms of mild TBI (Rees, 2003, Carroll et al., 2004, Stern et al., 2011). Recognition of the potentially life-long functional deficits facing children who have experienced TBI, coupled with the significant socioeconomic burden that is associated, should spur more research aimed at both prevention (Keenan and Bratton, 2006) and mitigation of TBI effects (Kochanek et al., 2010).

Meanwhile, results from chapters 2 (Fig. 6: global increase of myelin basic protein [MBP] in the corpus callosum observed at regions proximal and distal to lesion cavity) and 5 (Fig. 4: ventricular hypertrophy of the contralateral hippocampus) reinforced the idea that brain responses to focal brain injury is not just localized to the immediate surroundings of the impact locus, but reaches distal brain regions (both grey and white matter) as well (Ajao et al., 2012). Diffuse brain injuries have long been associated with global (i.e. widely distributed) changes in the brain (Andriessen et al., 2010), but focal TBI may also trigger non-localized responses (Dunn-Meynell et al., 1994, Ding et al., 2011). The distal effects associated with focal TBI could be partly attributed to the spreading out of the initial impact forces to vulnerable brain regions (such as hippocampus, amygdala, and basal ganglia) (Wilde et al., 2007, McAllister, 2011) and to changes in the connection network of various brain parts (as seen with herniation and injury to white matter tracts) (Huh and Raghupathi, 2009). For example, in a follow-up study, we have reported reduced immunoreactivity for NF200 (a

neurofilament that forms part of the neuronal cytoskeleton which supports and maintains axonal/neuronal structure, and has also been implicated in intracellular transport to axons and dendrites) in gray and white matter regions that are proximal and distal to the point of initial brain impact following juvenile TBI in rats (Kemper et al., 2013).

Interestingly, these changes were measured at 6 months post-injury in adult rat brains.

The vulnerability of the central structures of the brain which support conveyance of sensory and motor information to the cerebral cortex is partly responsible for sensorimotor deficits seen after TBI (Wilde et al., 2007, Ajao et al., 2012) (chapter 5, figure 5). Moreover, TBI in all its forms affect all major cell types in the neurovascular unit – e.g. neurons, astrocytes, endothelial cells – as attested to in our findings (Ajao et al., 2013; Submitted). Any form of therapeutic intervention would therefore be more beneficial if it has the potential to target multiple protein molecule(s) and pathway(s) in more than one cell type in the brain (Vink and Van Den Heuvel, 2004, Stoica et al., 2009). Such multidimensional effects are afforded by the two pharmacological agents used in this project – DJNKI-1 (for suppression of JNK hyperactivation following jTBI) and cavtratin (for pharmacological mimicry of endogenous caveolin scaffolding domain). See Figure 1 for a diagrammatical representation of the pathways affected by these two pharmacological agents.

JNK Activation as a Therapeutic Target for Juvenile TBI

This project provides evidence in support of the theory that DJNKI-1 confers protection against secondary processes of jTBI. This is through: prevention of excessive brain tissue damage (e.g. reduction in lesion volume over a 60-day period with acute DJNKI-1 treatment), reduction of injury-associated morphological alterations (e.g. reduced frequency of ventricular hypertrophy and prevention of white matter size reduction over time), reversal of BBB disruption and hyperpermeability, and consequent

reduction in vasogenic edema (see chapter 5). In addition, acute administration of DJNKI-1 promotes recovery of motor and cognitive functions both acutely and in the long-term (see chapter 5, figs. 7 - 9). This ability to influence longitudinal recovery makes DJNKI-1 particularly promising for ameliorating long-term dysfunction associated with juvenile TBI. However, the mechanism of action of DJNKI-1 has not been fully elucidated in juvenile TBI.

One possible mechanism highlighted in this work (chapter 5) is the reduction in vascular permeability and edema. We conclude from the observed reduction in IgG extravasation in DJNKI1-treated rats (chapter 5, fig. 10), and in T2 values at the lesion and perilesion brain ROIs in the same rats (chapter 5, fig. 6A - C), that DJNKI-1 protects against vasogenic edema, while not ruling out protection against other forms of cerebral edema (e.g. cytotoxic edema). We earlier hypothesized that DJNKI-1 treatment will ameliorate BBB disruption and hyperpermeability in this model, and these findings mostly support the hypothesis. Meanwhile, the action of DJNKI-1 may be conferring a global neuroprotection following jTBI. The premise for this is that JNK isoforms (JNK-1, -2, and -3) are present not only in neurons but in other brain cell types such as endothelial cells, astrocytes, etc. (Waetzig et al., 2006, Haeusgen et al., 2009, Tu et al., 2011) whose actions are vital to neuronal survival and function. Hyperactivation of these JNK isoforms has been shown extensively in neurons following various forms of brain injuries or damage (Borsello et al., 2003, Ortolano et al., 2009). Activation in glia and brain microvascular endothelial cells has also been highlighted (Xie et al., 2004, Wang et al., 2012). In fact, Wang et al (2012) showed in a juvenile model of brain inflammation that JNK hyperactivation is the common thread linking BBB disruption, oligodendroglial

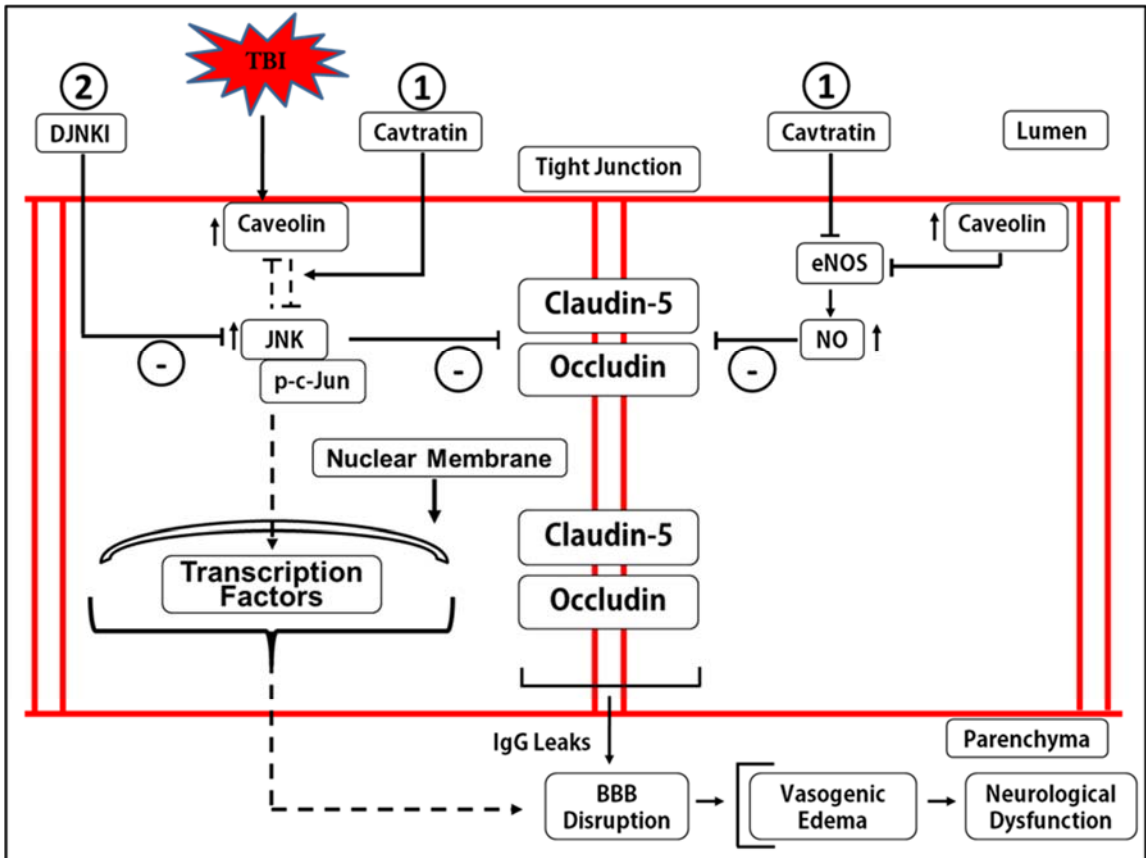


Figure 1: Proposed Intervention Strategies in Experimental Juvenile TBI.

TBI in the juvenile brain produces several stress factors which effect: (1) increased expression and activation of endothelial caveolins, and (2) activation of JNK pathway, among others. Increased expression and activity of caveolins in this model is proposed to inactivate eNOS and inhibit NO production, thereby reversing brain vascular permeability. NO is a highly potent vascular permeability factor. Caveolins has been shown to inhibit JNK hyperactivation in the periphery, but this is yet to be shown in brain endothelial cells. Activated JNKs can phosphorylate various downstream substrates, including transcription factors (such as c-Jun) that regulate gene expression. Consequences of JNK hyperactivation is cell-type dependent, and may include: production of vascular permeability factors (e.g. NO) that cause BBB damage and edema (in endothelial cells), excitotoxicity (e.g. in neurons), and apoptosis (neurons and endothelial cells), followed by functional deficits. The first intervention strategy involves the acute administration of cavtratin – an injectable peptide mimetic of the caveolin scaffolding domain – which can mimic the function of endogenous caveolins with respect to repair of tight junction and reduction of edema. The second intervention strategy involves the acute administration of DJNKI-1 which competitively blocks the interactions between JNK and its various substrates, thereby abrogating their downstream effects. Both cavtratin and DJNKI-1 can act on various cell types in the brain (including neurons, astrocytes and endothelial cells), and may promote additive or synergistic therapeutic effects following juvenile TBI.

TBI – Traumatic Brain Injury; JNK – c-Jun N-Terminal Kinase; p-c-Jun – Phosphorylated c-Jun; eNOS – Endothelial Nitric Oxide Synthase; NO – Nitric Oxide; IgG – Immunoglobulin G; BBB – Blood-Brain Barrier

apoptosis in the white matter, and microglial activation with its consequent cytokine production. The long-term difference in corpus callosal (CC) thickness observed between DJNKI1-treated rats and control (with DJNKI-1 group showing increased CC thickness especially at later time points, see chapter 5, fig. 5) is suggestive of a protective role of JNK inhibition in the white matter structures of a developing brain. Since DJNKI-1 is capable of inhibiting the hyperactivation of all 3 JNK isoforms in the varied cell types in the brain, its actions may therefore constitute a form of global neuroprotection following jTBI.

It is however important to further investigate the mechanisms of brain protection that DJNKI-1 confers following post-TBI administration in the juvenile brain. It has been suggested that DJNKI-1 may be playing a role in the periphery (e.g. in the liver, spleen, etc.) that positively influences brain recovery following cerebral ischemia (Lehnert et al., 2008, Touchard et al., 2010, Benakis et al., 2012). This route of action should be further investigated in jTBI models.

Caveolins in Brain Homeostasis and in Recovery and Repair after Juvenile TBI

Caveolins are believed to play important roles in brain homeostasis under normal conditions and in response to brain pathology. In this project, we found increase in caveolin-1 following jTBI at both acute and later time points (chapter 3, fig. 3). This long-term increase following jTBI suggests that caveolin-1 may be exerting some modulatory effects long after the initial injury. We also found increase in caveolin-3 at acute time points (chapter 3, fig. 5). These agree with literature evidence showing increase in caveolins-1 and -3 in some forms of CNS injuries and disorders, including cold cortical injury (Nag et al., 2007, Nag et al., 2009), spinal cord injury (Shin, 2007), and experimental autoimmune encephalopathy (Shin et al., 2005). The increase in caveolins-

1 and 3 coincided with the acute decrease in claudin-5 immunoreactivity and increased in extravasated IgG, showing that caveolins may be associated with BBB disruption and hyperpermeability. This is in broad agreement with our hypothesis that decreased tight junction protein levels and BBB hyperpermeability will be associated with an increase in expression of the caveolins, although we did not find a significant increase in the expression of caveolin-2. Meanwhile, some reports have shown a lowering of caveolin-1 expression in some forms of brain injury such as ischemic-reperfusion injury (IR) (Shen et al., 2006, Gu et al., 2011). This endogenous reduction in caveolin-1 in IR is associated with increased nitric oxide production, increased activation of matrix metalloproteinases (MMPs), BBB disruption, and overall poor histological and functional outcomes (Gu et al., 2011, Gottschall and Barone, 2012).

We found a ubiquitous distribution of caveolin-1 in the brain following jTBI (in neurons, astrocytes, etc., in addition to cerebral endothelium) (chapter 3, fig. 2), which agrees with current literature reports (Cameron et al., 1997, Shin et al., 2005). Cav-1, (as well as cav-2, and -3) have been reported to be present in non-caveolae regions in neurons, and are associated with pro-growth and pro-survival signaling functions (Head and Insel, 2007).

The role of prolonged increase in caveolin-1 expression should be a subject of future research. It may be a compensatory mechanism to counteract long-term damage in brain cells and improve function, or it could be detrimental to long-term functional recovery (Patel et al., 2008, Gu et al., 2011, Stary et al., 2012) (Also see chapter 3).

We studied the effect of pharmacological mimicry of the caveolin scaffolding domain (CSD) with the use of cavtratin. The CSD is not restricted to brain endothelial cells (Song et al., 2007), but is also present in neurons (Head et al., 2008) and astrocytes (Cameron et al., 1997). The ability of both of cavtratin to permeabilize the

brain through its cell permeable adjunct (Antennapedia internalization sequence) and influence multiple brain targets makes it a promising pharmacological tool.

Acute administration of cavtratin resulted in reduced lesion volume at 1d and 3d post-injury (Chapter 4, Fig. 1). Cavtratin also reduced edema formation (as determined by T2-weighted MRI) acutely in the lesion region of interest (ROI), but not in the perilesion ROI (Chapter 4, Fig. 2). There was however no behavioral benefits (only sensorimotor functions were tested) associated with cavtratin treatment at acute time points (Chapter 4, Fig. 3). We therefore conclude that cavtratin could reduce edema formation and ameliorate brain damage acutely. Future work should concentrate on long-term study of the effect of cavtratin both on the pathophysiology of the brain and on brain function as several secondary processes occurring acutely after jTBI could mask some positive effects of the drug. Injection of cavtratin at multiple time points following jTBI may also show if its effect could be optimized acutely and beneficial at long-term. The effect of cavtratin on brain endothelial tight junction proteins (e.g. claudin-5, occludin, etc.) as well as on IgG extravasation should be studied to further establish examine the effect of the drug on the BBB integrity. The effect of cavtratin on eNOS, NO production and MMP9 activation [which has been implicated in BBB disruption in ischemic models (Gu et al., 2011)] should also be investigated to gain more insight into the mechanism of action of the drug. In addition, the question of how caveolin-1 interacts with JNKs in the brain should be studied through *in vitro* models. Combinatorial use of both DJNKI-1 and cavtratin in jTBI should also be investigated for potential additive or synergistic effects.

Overall, we have shown that acute administration of DJNKI-1 and cavtratin could be beneficial in ameliorating some secondary processes associated with jTBI. In-depth studies looking at the mechanisms of action of these drugs in juvenile TBI models should be undertaken to further ascertain their clinical potential.

REFERENCES

- Abbott NJ, Patabendige AA, Dolman DE, Yusof SR, Begley DJ (2010) Structure and function of the blood-brain barrier. *Neurobiol Dis* 37:13-25.
- Abbott NJ, Ronnback L, Hansson E (2006) Astrocyte-endothelial interactions at the blood-brain barrier. *Nat Rev Neurosci* 7:41-53.
- Adams JH, Graham DI, Murray LS, Scott G (1982) Diffuse axonal injury due to nonmissile head injury in humans: an analysis of 45 cases. *Ann Neurol* 12:557-563.
- Adams RA, Bauer J, Flick MJ, Sikorski SL, Nuriel T, Lassmann H, Degen JL, Akassoglou K (2007) The fibrin-derived gamma377-395 peptide inhibits microglia activation and suppresses relapsing paralysis in central nervous system autoimmune disease. *J Exp Med* 204:571-582.
- Adamson P, Etienne S, Couraud PO, Calder V, Greenwood J (1999) Lymphocyte migration through brain endothelial cell monolayers involves signaling through endothelial ICAM-1 via a rho-dependent pathway. *J Immunol* 162:2964-2973.
- Adelson PD (2000) Pediatric trauma made simple. *Clin Neurosurg* 47:319-335.
- Adelson PD (2009) Hypothermia following pediatric traumatic brain injury. *J Neurotrauma* 26:429-436.
- Adelson PD, Bratton SL, Carney NA, Chesnut RM, du Coudray HE, Goldstein B, Kochanek PM, Miller HC, Partington MD, Selden NR, Warden CR, Wright DW, American Association for Surgery of T, Child Neurology S, International Society for Pediatric N, International Trauma A, Critical Care S, Society of Critical Care M, World Federation of Pediatric I, Critical Care S (2003) Guidelines for the acute medical management of severe traumatic brain injury in infants, children, and adolescents. Chapter 1: Introduction. *Pediatr Crit Care Med* 4:S2-4.
- Adelson PD, Clyde B, Kochanek PM, Wisniewski SR, Marion DW, Yonas H (1997) Cerebrovascular response in infants and young children following severe traumatic brain injury: a preliminary report. *Pediatr Neurosurg* 26:200-207.
- Adelson PD, Dixon CE, Kochanek PM (2000) Long-term dysfunction following diffuse traumatic brain injury in the immature rat. *J Neurotrauma* 17:273-282.
- Adelson PD, Kochanek PM (1998) Head injury in children. *J Child Neurol* 13:2-15.
- Adelson PD, Robichaud P, Hamilton RL, Kochanek PM (1996) A model of diffuse traumatic brain injury in the immature rat. *J Neurosurg* 85:877-884.

- Adelson PD, Srinivas R, Chang Y, Bell M, Kochanek PM (2011) Cerebrovascular response in children following severe traumatic brain injury. *Child's nervous system : ChNS : official journal of the International Society for Pediatric Neurosurgery* 27:1465-1476.
- Adelson PD, Whalen MJ, Kochanek PM, Robichaud P, Carlos TM (1998) Blood brain barrier permeability and acute inflammation in two models of traumatic brain injury in the immature rat: a preliminary report. *Acta Neurochir Suppl* 71:104-106.
- Agarwal SS, Sheikh I, Kumar L (2005) Cranio-Cerebral Trauma Deaths: A Postmortem Study on 0-15 Years Age Group. *Journal of Indian Academy of Forensic Medicine* 27.
- Ajao D, Pop V, Kamper J, Adami A, Rudobeck E, Huang L, Vlkolinsky R, Hartman R, Ashwal S, Obenaus A, Badaut J (2012) Traumatic brain injury in young rats leads to progressive behavioral deficits coincident with altered tissue properties in adulthood. *J Neurotrauma*.
- Akiyama K, Ichinose S, Omori A, Sakurai Y, Asou H (2002) Study of expression of myelin basic proteins (MBPs) in developing rat brain using a novel antibody reacting with four major isoforms of MBP. *Journal of neuroscience research* 68:19-28.
- Al Ahmad A, Gassmann M, Ogunshola OO (2009) Maintaining blood-brain barrier integrity: pericytes perform better than astrocytes during prolonged oxygen deprivation. *J Cell Physiol* 218:612-622.
- Aldrich EF, Eisenberg HM, Saydjari C, Luerssen TG, Foulkes MA, Jane JA, Marshall LF, Marmarou A, Young HF (1992) Diffuse brain swelling in severely head-injured children. A report from the NIH Traumatic Coma Data Bank. *J Neurosurg* 76:450-454.
- Alwis DS, Yan EB, Morganti-Kossmann MC, Rajan R (2012) Sensory cortex underpinnings of traumatic brain injury deficits. *PLoS One* 7:e52169.
- Amasheh S, Schmidt T, Mahn M, Florian P, Mankertz J, Tavalali S, Gitter AH, Schulzke JD, Fromm M (2005) Contribution of claudin-5 to barrier properties in tight junctions of epithelial cells. *Cell Tissue Res* 321:89-96.
- Anderson V, Catroppa C, Morse S, Haritou F, Rosenfeld J (2005) Functional plasticity or vulnerability after early brain injury? *Pediatrics* 116:1374-1382.
- Anderson V, Godfrey C, Rosenfeld JV, Catroppa C (2012) Predictors of cognitive function and recovery 10 years after traumatic brain injury in young children. *Pediatrics* 129:e254-261.
- Anderson V, Yeates KO (2010) Introduction: Pediatric traumatic brain injury: New frontiers in clinical and translational research. Cambridge, UK: Cambridge University Press.

- Andras IE, Eum SY, Huang W, Zhong Y, Hennig B, Toborek M (2010) HIV-1-induced amyloid beta accumulation in brain endothelial cells is attenuated by simvastatin. *Molecular and cellular neurosciences* 43:232-243.
- Andriessen TM, Jacobs B, Vos PE (2010) Clinical characteristics and pathophysiological mechanisms of focal and diffuse traumatic brain injury. *J Cell Mol Med* 14:2381-2392.
- Anthony DC, Bolton SJ, Fearn S, Perry VH (1997) Age-related effects of interleukin-1 beta on polymorphonuclear neutrophil-dependent increases in blood-brain barrier permeability in rats. *Brain* 120 (Pt 3):435-444.
- Argaw AT, Asp L, Zhang J, Navrazhina K, Pham T, Mariani JN, Mahase S, Dutta DJ, Seto J, Kramer EG, Ferrara N, Sofroniew MV, John GR (2012) Astrocyte-derived VEGF-A drives blood-brain barrier disruption in CNS inflammatory disease. *J Clin Invest* 122:2454-2468.
- Argaw AT, Zhang Y, Snyder BJ, Zhao ML, Kopp N, Lee SC, Raine CS, Brosnan CF, John GR (2006) IL-1beta regulates blood-brain barrier permeability via reactivation of the hypoxia-angiogenesis program. *J Immunol* 177:5574-5584.
- Armstead WM (1997) Brain injury impairs ATP-sensitive K⁺ channel function in piglet cerebral arteries. *Stroke* 28:2273-2279; discussion 2280.
- Armstead WM (1999) Cerebral hemodynamics after traumatic brain injury of immature brain. *Exp Toxicol Pathol* 51:137-142.
- Armstead WM (2000) Age-dependent cerebral hemodynamic effects of traumatic brain injury in newborn and juvenile pigs. *Microcirculation* 7:225-235.
- Armstead WM (2003) PTK, ERK and p38 MAPK contribute to impaired NMDA-induced vasodilation after brain injury. *Eur J Pharmacol* 474:249-254.
- Armstead WM (2004) NMDA and age dependent cerebral hemodynamics after traumatic brain injury. *Exp Toxicol Pathol* 56:75-81.
- Armstead WM (2005) Age and cerebral circulation. *Pathophysiology* 12:5-15.
- Armstead WM, Kiessling JW, Riley J, Cines DB, Higazi AA (2011a) tPA contributes to impaired NMDA cerebrovasodilation after traumatic brain injury through activation of JNK MAPK. *Neurol Res* 33:726-733.
- Armstead WM, Kiessling JW, Riley J, Kofke WA, Vavilala MS (2011b) Phenylephrine infusion prevents impairment of ATP- and calcium-sensitive potassium channel-mediated cerebrovasodilation after brain injury in female, but aggravates impairment in male, piglets through modulation of ERK MAPK upregulation. *J Neurotrauma* 28:105-111.

- Armstead WM, Kurth CD (1994a) Different cerebral hemodynamic responses following fluid percussion brain injury in the newborn and juvenile pig. *J Neurotrauma* 11:487-497.
- Armstead WM, Kurth CD (1994b) The role of opioids in newborn pig fluid percussion brain injury. *Brain Res* 660:19-26.
- Armstead WM, Riley J, Cines DB, Higazi AA (2012) Combination therapy with glucagon and a novel plasminogen activator inhibitor-1-derived peptide enhances protection against impaired cerebrovasodilation during hypotension after traumatic brain injury through inhibition of ERK and JNK MAPK. *Neurological research* 34:530-537.
- Asahi M, Wang X, Mori T, Sumii T, Jung JC, Moskowitz MA, Fini ME, Lo EH (2001) Effects of matrix metalloproteinase-9 gene knock-out on the proteolysis of blood-brain barrier and white matter components after cerebral ischemia. *J Neurosci* 21:7724-7732.
- Babikian T, Asarnow R (2009) Neurocognitive outcomes and recovery after pediatric TBI: meta-analytic review of the literature. *Neuropsychology* 23:283-296.
- Babikian T, Prins ML, Cai Y, Barkhoudarian G, Hartonian I, Hovda DA, Giza CC (2010) Molecular and physiological responses to juvenile traumatic brain injury: focus on growth and metabolism. *Dev Neurosci* 32:431-441.
- Badaut J, Ashwal S, Adami A, Tone B, Recker R, Spagnoli D, Ternon B, Obenaus A (2011a) Brain water mobility decreases after astrocytic aquaporin-4 inhibition using RNA interference. *J Cereb Blood Flow Metab* 31:819-831.
- Badaut J, Ashwal S, Obenaus A (2011b) Aquaporins in cerebrovascular disease: a target for treatment of brain edema? *Cerebrovasc Dis* 31:521-531.
- Badaut J, Ashwal S, Tone B, Regli L, Tian HR, Obenaus A (2007) Temporal and regional evolution of aquaporin-4 expression and magnetic resonance imaging in a rat pup model of neonatal stroke. *Pediatr Res* 62:248-254.
- Baethmann A, Maier-Hauff K, Kempfski O, Unterberg A, Wahl M, Schurer L (1988) Mediators of brain edema and secondary brain damage. *Critical care medicine* 16:972-978.
- Baldwin SA, Fugaccia I, Brown DR, Brown LV, Scheff SW (1996) Blood-brain barrier breach following cortical contusion in the rat. *J Neurosurg* 85:476-481.
- Ballabh P, Braun A, Nedergaard M (2004) The blood-brain barrier: an overview: structure, regulation, and clinical implications. *Neurobiol Dis* 16:1-13.
- Ballesteros MC, Hansen PE, Soila K (1993) MR imaging of the developing human brain. Part 2. Postnatal development. *Radiographics* 13:611-622.

- Balligand JL, Feron O, Dessy C (2009) eNOS activation by physical forces: from short-term regulation of contraction to chronic remodeling of cardiovascular tissues. *Physiol Rev* 89:481-534.
- Barakat S, Demeule M, Pilorget A, Regina A, Gingras D, Baggetto LG, Beliveau R (2007) Modulation of p-glycoprotein function by caveolin-1 phosphorylation. *J Neurochem* 101:1-8.
- Barcroft J (1938) *The Brain and its Environment. 1. The Activity of the Brain in Mid-Foetal Life.* New Haven: Yale University Press.
- Barie PS, Ghajar JB, Firlik AD, Chang VA, Hariri RJ (1993) Contribution of increased cerebral blood volume to posttraumatic intracranial hypertension. *J Trauma* 35:88-95; discussion 95-86.
- Barresi V, Grosso M, Bulfamante G, Vitarelli E, Ghioni MC, Barresi G (2006) Caveolin-1 immuno-expression in human fetal tissues during mid and late gestation. *Eur J Histochem* 50:183-190.
- Barreto G, Huang TT, Giffard RG (2010) Age-related defects in sensorimotor activity, spatial learning, and memory in C57BL/6 mice. *J Neurosurg Anesthesiol* 22:214-219.
- Bart J, Nagengast WB, Coppes RP, Wegman TD, van der Graaf WT, Groen HJ, Vaalburg W, de Vries EG, Hendrikse NH (2007) Irradiation of rat brain reduces P-glycoprotein expression and function. *British journal of cancer* 97:322-326.
- Barzo P, Marmarou A, Fatouros P, Hayasaki K, Corwin F (1997) Contribution of vasogenic and cellular edema to traumatic brain swelling measured by diffusion-weighted imaging. *J Neurosurg* 87:900-907.
- Baskaya MK, Rao AM, Dogan A, Donaldson D, Dempsey RJ (1997) The biphasic opening of the blood-brain barrier in the cortex and hippocampus after traumatic brain injury in rats. *Neurosci Lett* 226:33-36.
- Battin M (ed.) (2001) *Magnetic resonance imaging of the brain in preterm infants: 24 weeks' gestation to term.* Saunders Ltd.
- Bauer PM, Yu J, Chen Y, Hickey R, Bernatchez PN, Looft-Wilson R, Huang Y, Giordano F, Stan RV, Sessa WC (2005) Endothelial-specific expression of caveolin-1 impairs microvascular permeability and angiogenesis. *Proc Natl Acad Sci U S A* 102:204-209.
- Bauer R, Walter B, Fritz H, Zwiener U (1999) Ontogenetic aspects of traumatic brain edema--facts and suggestions. *Exp Toxicol Pathol* 51:143-150.
- Bayir H, Kagan VE, Tyurina YY, Tyurin V, Ruppel RA, Adelson PD, Graham SH, Janesko K, Clark RS, Kochanek PM (2002) Assessment of antioxidant reserves and oxidative stress in cerebrospinal fluid after severe traumatic brain injury in infants and children. *Pediatr Res* 51:571-578.

- Bazzoni G (2003) The JAM family of junctional adhesion molecules. *Curr Opin Cell Biol* 15:525-530.
- Bazzoni G, Martinez-Estrada OM, Orsenigo F, Cordenonsi M, Citi S, Dejana E (2000) Interaction of junctional adhesion molecule with the tight junction components ZO-1, cingulin, and occludin. *J Biol Chem* 275:20520-20526.
- Beauchamp K, Mutlak H, Smith WR, Shohami E, Stahel PF (2008) Pharmacology of traumatic brain injury: where is the "golden bullet"? *Mol Med* 14:731-740.
- Becker DP, Miller JD, Ward JD, Greenberg RP, Young HF, Sakalas R (1977) The outcome from severe head injury with early diagnosis and intensive management. *J Neurosurg* 47:491-502.
- Benakis C, Bonny C, Hirt L (2010) JNK inhibition and inflammation after cerebral ischemia. *Brain Behav Immun* 24:800-811.
- Benakis C, Vaslin A, Pasquali C, Hirt L (2012) Neuroprotection by inhibiting the c-Jun N-terminal kinase pathway after cerebral ischemia occurs independently of interleukin-6 and keratinocyte-derived chemokine (KC/CXCL1) secretion. *J Neuroinflammation* 9:76.
- Berezowski V, Fukuda AM, Cecchelli R, Badaut J (2012) Endothelial cells and astrocytes: a concerto en duo in ischemic pathophysiology. *Int J Cell Biol* 2012:176287.
- Berger RP, Adelson PD, Pierce MC, Dulani T, Cassidy LD, Kochanek PM (2005) Serum neuron-specific enolase, S100B, and myelin basic protein concentrations after inflicted and noninflicted traumatic brain injury in children. *Journal of neurosurgery* 103:61-68.
- Bernatchez PN, Bauer PM, Yu J, Prendergast JS, He P, Sessa WC (2005) Dissecting the molecular control of endothelial NO synthase by caveolin-1 using cell-permeable peptides. *Proc Natl Acad Sci U S A* 102:761-766.
- Bertolizio G, Bissonnette B, Mason L, Ashwal S, Hartman R, Marcantonio S, Obenaus A (2011) Effects of hemodilution after traumatic brain injury in juvenile rats. *Paediatric anaesthesia* 21:1198-1208.
- Betanzos A, Huerta M, Lopez-Bayghen E, Azuara E, Amerena J, Gonzalez-Mariscal L (2004) The tight junction protein ZO-2 associates with Jun, Fos and C/EBP transcription factors in epithelial cells. *Exp Cell Res* 292:51-66.
- Biagas KV, Grundl PD, Kochanek PM, Schiding JK, Nemoto EM (1996) Posttraumatic hyperemia in immature, mature, and aged rats: autoradiographic determination of cerebral blood flow. *J Neurotrauma* 13:189-200.
- Bjelke B, Seiger A (1989) Morphological distribution of MBP-like immunoreactivity in the brain during development. *International journal of developmental neuroscience* :

the official journal of the International Society for Developmental Neuroscience
7:145-164.

- Blaiss CA, Yu TS, Zhang G, Chen J, Dimchev G, Parada LF, Powell CM, Kernie SG (2011) Temporally specified genetic ablation of neurogenesis impairs cognitive recovery after traumatic brain injury. *The Journal of neuroscience : the official journal of the Society for Neuroscience* 31:4906-4916.
- Blakemore SJ, Choudhury S (2006) Development of the adolescent brain: implications for executive function and social cognition. *J Child Psychol Psychiatry* 47:296-312.
- Bogoyevitch MA (2006) The isoform-specific functions of the c-Jun N-terminal Kinases (JNKs): differences revealed by gene targeting. *Bioessays* 28:923-934.
- Bogoyevitch MA, Arthur PG (2008) Inhibitors of c-Jun N-terminal kinases: JuNK no more? *Biochimica et biophysica acta* 1784:76-93.
- Bogoyevitch MA, Kobe B (2006) Uses for JNK: the many and varied substrates of the c-Jun N-terminal kinases. *Microbiology and molecular biology reviews : MMBR* 70:1061-1095.
- Bolton CF, Carter KM (1980) Human sensory nerve compound action potential amplitude: variation with sex and finger circumference. *Journal of neurology, neurosurgery, and psychiatry* 43:925-928.
- Bolton SJ, Perry VH (1998) Differential blood-brain barrier breakdown and leucocyte recruitment following excitotoxic lesions in juvenile and adult rats. *Exp Neurol* 154:231-240.
- Bor-Seng-Shu E, Kita WS, Figueiredo EG, Paiva WS, Fonoff ET, Teixeira MJ, Panerai RB (2012) Cerebral hemodynamics: concepts of clinical importance. *Arquivos de neuro-psiquiatria* 70:352-356.
- Borregaard N, Sorensen OE, Theilgaard-Monch K (2007) Neutrophil granules: a library of innate immunity proteins. *Trends in immunology* 28:340-345.
- Borsello T, Bonny C (2004) Use of cell-permeable peptides to prevent neuronal degeneration. *Trends Mol Med* 10:239-244.
- Borsello T, Clarke PG, Hirt L, Vercelli A, Repici M, Schorderet DF, Bogousslavsky J, Bonny C (2003) A peptide inhibitor of c-Jun N-terminal kinase protects against excitotoxicity and cerebral ischemia. *Nat Med* 9:1180-1186.
- Borsello T, Forloni G (2007) JNK signalling: a possible target to prevent neurodegeneration. *Curr Pharm Des* 13:1875-1886.
- Brecht S, Kirchhof R, Chromik A, Willesen M, Nicolaus T, Raivich G, Wessig J, Waetzig V, Goetz M, Claussen M, Pearse D, Kuan CY, Vaudano E, Behrens A, Wagner

- E, Flavell RA, Davis RJ, Herdegen T (2005) Specific pathophysiological functions of JNK isoforms in the brain. *Eur J Neurosci* 21:363-377.
- Bremner JD, Randall P, Scott TM, Bronen RA, Seibyl JP, Southwick SM, Delaney RC, McCarthy G, Charney DS, Innis RB (1995) MRI-based measurement of hippocampal volume in patients with combat-related posttraumatic stress disorder. *The American journal of psychiatry* 152:973-981.
- Brenn A, Grube M, Peters M, Fischer A, Jedlitschky G, Kroemer HK, Warzok RW, Vogelgesang S (2011) Beta-Amyloid Downregulates MDR1-P-Glycoprotein (Abcb1) Expression at the Blood-Brain Barrier in Mice. *International journal of Alzheimer's disease* 2011:690121.
- Brenner LA, Dise-Lewis JE, Bartles SK, O'Brien SE, Godleski M, Selinger M (2007) The long-term impact and rehabilitation of pediatric traumatic brain injury: a 50-year follow-up case study. *The Journal of head trauma rehabilitation* 22:56-64.
- Brightman MW, Klatzo I, Olsson Y, Reese TS (1970) The blood-brain barrier to proteins under normal and pathological conditions. *J Neurol Sci* 10:215-239.
- Brightman MW, Palay SL (1963) The Fine Structure of Ependyma in the Brain of the Rat. *J Cell Biol* 19:415-439.
- Brody DL, Holtzman DM (2006) Morris water maze search strategy analysis in PDAPP mice before and after experimental traumatic brain injury. *Experimental Neurology* 197:330-340.
- Brody DL, Mac Donald C, Kessens CC, Yuede C, Parsadarian M, Spinner M, Kim E, Schwetye KE, Holtzman DM, Bayly PV (2007) Electromagnetic controlled cortical impact device for precise, graded experimental traumatic brain injury. *J Neurotrauma* 24:657-673.
- Brown G, Chadwick O, Shaffer D, Rutter M, Traub M (1981) A prospective study of children with head injuries: III. Psychiatric sequelae. *Psychol Med* 11:63-78.
- Bucci M, Gratton JP, Rudic RD, Acevedo L, Roviezzo F, Cirino G, Sessa WC (2000) In vivo delivery of the caveolin-1 scaffolding domain inhibits nitric oxide synthesis and reduces inflammation. *Nat Med* 6:1362-1367.
- Buitrago MM, Schulz JB, Dichgans J, Luft AR (2004) Short and long-term motor skill learning in an accelerated rotarod training paradigm. *Neurobiol Learn Mem* 81:211-216.
- Butt AM (1995) Effect of inflammatory agents on electrical resistance across the blood-brain barrier in pial microvessels of anaesthetized rats. *Brain Res* 696:145-150.
- Butt AM, Jones HC, Abbott NJ (1990) Electrical resistance across the blood-brain barrier in anaesthetized rats: a developmental study. *J Physiol* 429:47-62.

- Buttram SD, Wisniewski SR, Jackson EK, Adelson PD, Feldman K, Bayir H, Berger RP, Clark RS, Kochanek PM (2007) Multiplex assessment of cytokine and chemokine levels in cerebrospinal fluid following severe pediatric traumatic brain injury: effects of moderate hypothermia. *J Neurotrauma* 24:1707-1717.
- Caeyenberghs K, Leemans A, Coxon J, Leunissen I, Drijkoningen D, Geurts M, Gooijers J, Michiels K, Sunaert S, Swinnen SP (2011a) Bimanual coordination and corpus callosum microstructure in young adults with traumatic brain injury: a diffusion tensor imaging study. *Journal of neurotrauma* 28:897-913.
- Caeyenberghs K, Leemans A, Geurts M, Linden CV, Smits-Engelsman BC, Sunaert S, Swinnen SP (2011b) Correlations between white matter integrity and motor function in traumatic brain injury patients. *Neurorehabilitation and neural repair* 25:492-502.
- Cameron PL, Ruffin JW, Bollag R, Rasmussen H, Cameron RS (1997) Identification of caveolin and caveolin-related proteins in the brain. *J Neurosci* 17:9520-9535.
- Campbell SJ, Carare-Nnadi RO, Losey PH, Anthony DC (2007) Loss of the atypical inflammatory response in juvenile and aged rats. *Neuropathol Appl Neurobiol* 33:108-120.
- Carroll LJ, Cassidy JD, Peloso PM, Borg J, von Holst H, Holm L, Paniak C, Pepin M, Injury WHOCCCTFoMTB (2004) Prognosis for mild traumatic brain injury: results of the WHO Collaborating Centre Task Force on Mild Traumatic Brain Injury. *Journal of rehabilitation medicine : official journal of the UEMS European Board of Physical and Rehabilitation Medicine* 84-105.
- Carrozzino F, Pugnale P, Feraille E, Montesano R (2009) Inhibition of basal p38 or JNK activity enhances epithelial barrier function through differential modulation of claudin expression. *Am J Physiol Cell Physiol* 297:C775-787.
- Castejon OJ (2012) Ultrastructural pathology of endothelial tight junctions in human brain oedema. *Folia neuropathologica / Association of Polish Neuropathologists and Medical Research Centre, Polish Academy of Sciences* 50:118-129.
- Catroppa C, Anderson V (2009) Neurodevelopmental outcomes of pediatric traumatic brain injury. *Future Neurology* 4:811-821.
- Cattelani R, Lombardi F, Brianti R, Mazzucchi A (1998) Traumatic brain injury in childhood: intellectual, behavioural and social outcome into adulthood. *Brain injury : [BI]* 12:283-296.
- Cederberg D, Siesjo P (2010) What has inflammation to do with traumatic brain injury? *Child's nervous system : ChNS : official journal of the International Society for Pediatric Neurosurgery* 26:221-226.
- Centeno C, Repici M, Chatton JY, Riederer BM, Bonny C, Nicod P, Price M, Clarke PG, Papa S, Franzoso G, Borsello T (2007) Role of the JNK pathway in NMDA-mediated excitotoxicity of cortical neurons. *Cell Death Differ* 14:240-253.

- Centers for Disease C, Prevention (1997) Sports-related recurrent brain injuries--United States. *MMWR Morb Mortal Wkly Rep* 46:224-227.
- Cernak I (2005) Animal models of head trauma. *NeuroRx* 2:410-422.
- Chadwick DL, Chin S, Salerno C, Landsverk J, Kitchen L (1991) Deaths from falls in children: how far is fatal? *J Trauma* 31:1353-1355.
- Chadwick O, Rutter M, Brown G, Shaffer D, Traub MU (1981) A prospective study of children with head injuries: II. Cognitive sequelae. *Psychol Med* 11:49-61.
- Chaiwat O, Sharma D, Udomphorn Y, Armstead WM, Vavilala MS (2009) Cerebral hemodynamic predictors of poor 6-month Glasgow Outcome Score in severe pediatric traumatic brain injury. *J Neurotrauma* 26:657-663.
- Chan JR, Phillips LJ, 2nd, Glaser M (1998) Glucocorticoids and progestins signal the initiation and enhance the rate of myelin formation. *Proceedings of the National Academy of Sciences of the United States of America* 95:10459-10464.
- Chapman SB (2006) Neurocognitive stall: A paradox in long term recovery from pediatric brain injury. *Brain Injury Professional* 3:10-13.
- Chaudhury H, Zakkar M, Boyle J, Cuhlmann S, van der Heiden K, Luong le A, Davis J, Platt A, Mason JC, Krams R, Haskard DO, Clark AR, Evans PC (2010) c-Jun N-terminal kinase primes endothelial cells at atheroprone sites for apoptosis. *Arterioscler Thromb Vasc Biol* 30:546-553.
- Chen C, Sheppard D (2007) Identification and molecular characterization of multiple phenotypes in integrin knockout mice. *Methods Enzymol* 426:291-305.
- Chen LW, Chang WJ, Wang JS, Hsu CM (2006) Thermal injury-induced peroxynitrite production and pulmonary inducible nitric oxide synthase expression depend on JNK/AP-1 signaling. *Critical care medicine* 34:142-150.
- Chew LJ, Coley W, Cheng Y, Gallo V (2010) Mechanisms of regulation of oligodendrocyte development by p38 mitogen-activated protein kinase. *J Neurosci* 30:11011-11027.
- Chini B, Parenti M (2004) G-protein coupled receptors in lipid rafts and caveolae: how, when and why do they go there? *J Mol Endocrinol* 32:325-338.
- Chodobski A, Zink BJ, Szmydynger-Chodobska J (2011) Blood-brain barrier pathophysiology in traumatic brain injury. *Transl Stroke Res* 2:492-516.
- Choudhury A, Marks DL, Proctor KM, Gould GW, Pagano RE (2006) Regulation of caveolar endocytosis by syntaxin 6-dependent delivery of membrane components to the cell surface. *Nat Cell Biol* 8:317-328.

- Christensen J, Pedersen MG, Pedersen CB, Sidenius P, Olsen J, Vestergaard M (2009) Long-term risk of epilepsy after traumatic brain injury in children and young adults: a population-based cohort study. *Lancet* 373:1105-1110.
- Cirrito JR, Deane R, Fagan AM, Spinner ML, Parsadanian M, Finn MB, Jiang H, Prior JL, Sagare A, Bales KR, Paul SM, Zlokovic BV, Pivnicka-Worms D, Holtzman DM (2005) P-glycoprotein deficiency at the blood-brain barrier increases amyloid-beta deposition in an Alzheimer disease mouse model. *The Journal of clinical investigation* 115:3285-3290.
- Coffey ET, Hongisto V, Dickens M, Davis RJ, Courtney MJ (2000) Dual roles for c-Jun N-terminal kinase in developmental and stress responses in cerebellar granule neurons. *J Neurosci* 20:7602-7613.
- Cohen AW, Hnasko R, Schubert W, Lisanti MP (2004) Role of caveolae and caveolins in health and disease. *Physiol Rev* 84:1341-1379.
- Colasanti M, Persichini T, Fabrizi C, Cavalieri E, Venturini G, Ascenzi P, Lauro GM, Suzuki H (1998) Expression of a NOS-III-like protein in human astroglial cell culture. *Biochemical and biophysical research communications* 252:552-555.
- Comess KM, Sun C, Abad-Zapatero C, Goedken ER, Gum RJ, Borhani DW, Argiriadi M, Groebe DR, Jia Y, Clampit JE, Haasch DL, Smith HT, Wang S, Song D, Coen ML, Cloutier TE, Tang H, Cheng X, Quinn C, Liu B, Xin Z, Liu G, Fry EH, Stoll V, Ng TI, Banach D, Marcotte D, Burns DJ, Calderwood DJ, Hajduk PJ (2011) Discovery and characterization of non-ATP site inhibitors of the mitogen activated protein (MAP) kinases. *ACS Chem Biol* 6:234-244.
- Cooke JP, Dzau VJ (1997) Nitric oxide synthase: role in the genesis of vascular disease. *Annual review of medicine* 48:489-509.
- Coronado VG, Xu L, Basavaraju SV, McGuire LC, Wald MM, Faul MD, Guzman BR, Hemphill JD (2011) Surveillance for traumatic brain injury-related deaths--United States, 1997-2007. *MMWR Surveill Summ* 60:1-32.
- Couet J, Li S, Okamoto T, Ikezu T, Lisanti MP (1997a) Identification of peptide and protein ligands for the caveolin-scaffolding domain. Implications for the interaction of caveolin with caveolae-associated proteins. *J Biol Chem* 272:6525-6533.
- Couet J, Sargiacomo M, Lisanti MP (1997b) Interaction of a receptor tyrosine kinase, EGF-R, with caveolins. Caveolin binding negatively regulates tyrosine and serine/threonine kinase activities. *J Biol Chem* 272:30429-30438.
- Couet J, Shengwen L, Okamoto T, Scherer PE, Lisanti MP (1997c) Molecular and cellular biology of caveolae paradoxes and plasticities. *Trends Cardiovasc Med* 7:103-110.
- Counsell SJ, Rutherford MA (2002) Magnetic resonance imaging of the newborn brain. *Current Paediatrics* 12:401-413.

- CRASH-2 C (2011) Effect of tranexamic acid in traumatic brain injury: a nested randomised, placebo controlled trial (CRASH-2 Intracranial Bleeding Study). *BMJ* 343:d3795.
- Crowe LM, Catroppa C, Babl FE, Anderson V (2012) Intellectual, behavioral, and social outcomes of accidental traumatic brain injury in early childhood. *Pediatrics* 129:e262-268.
- Cui J, Zhang M, Zhang YQ, Xu ZH (2007) JNK pathway: diseases and therapeutic potential. *Acta Pharmacol Sin* 28:601-608.
- Cunningham KE, Turner JR (2012) Myosin light chain kinase: pulling the strings of epithelial tight junction function. *Ann N Y Acad Sci* 1258:34-42.
- Das M, Cui J, Das DK (2007a) Generation of survival signal by differential interaction of p38MAPK α and p38MAPK β with caveolin-1 and caveolin-3 in the adapted heart. *J Mol Cell Cardiol* 42:206-213.
- Das M, Das S, Das DK (2007b) Caveolin and MAP kinase interaction in angiotensin II preconditioning of the myocardium. *J Cell Mol Med* 11:788-797.
- David Y, Cacheaux LP, Ivens S, Lapilover E, Heinemann U, Kaufer D, Friedman A (2009) Astrocytic dysfunction in epileptogenesis: consequence of altered potassium and glutamate homeostasis? *J Neurosci* 29:10588-10599.
- Davis AS, Dean RS (2010) Assessing sensory-motor deficits in pediatric traumatic brain injury. *Appl Neuropsychol* 17:104-109.
- Davis RJ (1999) Signal transduction by the c-Jun N-terminal kinase. *Biochem Soc Symp* 64:1-12.
- Dawodu ST (2011) Traumatic Brain Injury (TBI) - Definition, Epidemiology, Pathophysiology. In: *e-Medicine*, pp 1-10: e-Medicine.
- del Valle J, Duran-Vilaregut J, Manich G, Pallas M, Camins A, Vilaplana J, Pelegri C (2011) Cerebral amyloid angiopathy, blood-brain barrier disruption and amyloid accumulation in SAMP8 mice. *Neurodegener Dis* 8:421-429.
- Dennis M (2010) Margaret Kennard (1899-1975): not a 'principle' of brain plasticity but a founding mother of developmental neuropsychology. *Cortex* 46:1043-1059.
- Derijard B, Hibi M, Wu IH, Barrett T, Su B, Deng T, Karin M, Davis RJ (1994) JNK1: a protein kinase stimulated by UV light and Ha-Ras that binds and phosphorylates the c-Jun activation domain. *Cell* 76:1025-1037.
- Desjardins F, Lobysheva I, Pelat M, Gallez B, Feron O, Dessy C, Balligand JL (2008) Control of blood pressure variability in caveolin-1-deficient mice: role of nitric oxide identified in vivo through spectral analysis. *Cardiovasc Res* 79:527-536.

- Dietrich WD, Alonso O, Halley M (1994) Early microvascular and neuronal consequences of traumatic brain injury: a light and electron microscopic study in rats. *J Neurotrauma* 11:289-301.
- Ding-Zhou L, Marchand-Verrecchia C, Croci N, Plotkine M, Margaille I (2002) L-NAME reduces infarction, neurological deficit and blood-brain barrier disruption following cerebral ischemia in mice. *Eur J Pharmacol* 457:137-146.
- Ding MC, Wang Q, Lo EH, Stanley GB (2011) Cortical excitation and inhibition following focal traumatic brain injury. *J Neurosci* 31:14085-14094.
- Dixon CE, Clifton GL, Lighthall JW, Yaghmai AA, Hayes RL (1991) A controlled cortical impact model of traumatic brain injury in the rat. *J Neurosci Methods* 39:253-262.
- Dixon CE, Lyeth BG, Povlishock JT, Findling RL, Hamm RJ, Marmarou A, Young HF, Hayes RL (1987) A fluid percussion model of experimental brain injury in the rat. *J Neurosurg* 67:110-119.
- Donkin JJ, Vink R (2010) Mechanisms of cerebral edema in traumatic brain injury: therapeutic developments. *Curr Opin Neurol* 23:293-299.
- Doppenberg EM, Choi SC, Bullock R (2004) Clinical trials in traumatic brain injury: lessons for the future. *J Neurosurg Anesthesiol* 16:87-94.
- Dore-Duffy P, Owen C, Balabanov R, Murphy S, Beaumont T, Rafols JA (2000) Pericyte migration from the vascular wall in response to traumatic brain injury. *Microvasc Res* 60:55-69.
- Drab M, Verkade P, Elger M, Kasper M, Lohn M, Lauterbach B, Menne J, Lindschau C, Mende F, Luft FC, Schedl A, Haller H, Kurzchalia TV (2001) Loss of caveolae, vascular dysfunction, and pulmonary defects in caveolin-1 gene-disrupted mice. *Science* 293:2449-2452.
- Duhaime AC, Alario AJ, Lewander WJ, Schut L, Sutton LN, Seidl TS, Nudelman S, Budenz D, Hertle R, Tsiaras W, et al. (1992) Head injury in very young children: mechanisms, injury types, and ophthalmologic findings in 100 hospitalized patients younger than 2 years of age. *Pediatrics* 90:179-185.
- Dunn-Meynell A, Pan S, Levin BE (1994) Focal traumatic brain injury causes widespread reductions in rat brain norepinephrine turnover from 6 to 24 h. *Brain Res* 660:88-95.
- Dunn KM, Hill-Eubanks DC, Liedtke WB, Nelson MT (2013) TRPV4 channels stimulate Ca²⁺-induced Ca²⁺ release in astrocytic endfeet and amplify neurovascular coupling responses. *Proceedings of the National Academy of Sciences of the United States of America* 110:6157-6162.
- Echarri A, Del Pozo MA (2006) Caveolae internalization regulates integrin-dependent signaling pathways. *Cell Cycle* 5:2179-2182.

- Edwards P, Arango M, Balica L, Cottingham R, El-Sayed H, Farrell B, Fernandes J, Gogichaisvili T, Golden N, Hartzenberg B, Husain M, Ulloa MI, Jerbi Z, Khamis H, Komolafe E, Laloe V, Lomas G, Ludwig S, Mazairac G, Munoz Sanchez Mde L, Nasi L, Oildashi F, Plunkett P, Roberts I, Sandercock P, Shakur H, Soler C, Stocker R, Svoboda P, Trenkler S, Venkataramana NK, Wasserberg J, Yates D, Yutthakasemsunt S (2005) Final results of MRC CRASH, a randomised placebo-controlled trial of intravenous corticosteroid in adults with head injury-outcomes at 6 months. *Lancet* 365:1957-1959.
- Ek CJ, Dziegielewska KM, Habgood MD, Saunders NR (2012) Barriers in the developing brain and Neurotoxicology. *Neurotoxicology* 33:586-604.
- Ek CJ, Wong A, Liddelow SA, Johansson PA, Dziegielewska KM, Saunders NR (2010) Efflux mechanisms at the developing brain barriers: ABC-transporters in the fetal and postnatal rat. *Toxicology letters* 197:51-59.
- el-Bacha RS, Minn A (1999) Drug metabolizing enzymes in cerebrovascular endothelial cells afford a metabolic protection to the brain. *Cellular and molecular biology* 45:15-23.
- El-Yazbi AF, Cho WJ, Schulz R, Daniel EE (2008) Calcium extrusion by plasma membrane calcium pump is impaired in caveolin-1 knockout mouse small intestine. *Eur J Pharmacol* 591:80-87.
- Engelman JA, Zhang X, Galbiati F, Volonte D, Sotgia F, Pestell RG, Minetti C, Scherer PE, Okamoto T, Lisanti MP (1998) Molecular genetics of the caveolin gene family: implications for human cancers, diabetes, Alzheimer disease, and muscular dystrophy. *Am J Hum Genet* 63:1578-1587.
- Eshraghi AA, He J, Mou CH, Polak M, Zine A, Bonny C, Balkany TJ, Van De Water TR (2006) D-JNKI-1 treatment prevents the progression of hearing loss in a model of cochlear implantation trauma. *Otology & neurotology : official publication of the American Otological Society, American Neurotology Society [and] European Academy of Otology and Neurotology* 27:504-511.
- Esneault E, Castagne V, Moser P, Bonny C, Bernaudin M (2008) D-JNKi, a peptide inhibitor of c-Jun N-terminal kinase, promotes functional recovery after transient focal cerebral ischemia in rats. *Neuroscience* 152:308-320.
- Etienne S, Adamson P, Greenwood J, Strosberg AD, Cazaubon S, Couraud PO (1998) ICAM-1 signaling pathways associated with Rho activation in microvascular brain endothelial cells. *J Immunol* 161:5755-5761.
- Fan P, Yamauchi T, Noble LJ, Ferriero DM (2003) Age-dependent differences in glutathione peroxidase activity after traumatic brain injury. *J Neurotrauma* 20:437-445.
- Farquhar MG, Palade GE (1963) Junctional complexes in various epithelia. *J Cell Biol* 17:375-412.

- Faul MX, L.; Wald, M. M.; Coronado, V. G.; (2010) Traumatic Brain Injury in the United States: Emergency Department Visits, Hospitalizations and Deaths 2002–2006., pp 1 - 74 Atlanta (GA): Centers for Disease Control and Prevention, National Center for Injury Prevention and Control
- Feigin I, Budzilovich G, Weinberg S, Ogata J (1973) Degeneration of white matter in hypoxia, acidosis and edema. *J Neuropathol Exp Neurol* 32:125-143.
- Feldman GJ, Mullin JM, Ryan MP (2005) Occludin: structure, function and regulation. *Advanced drug delivery reviews* 57:883-917.
- Feng Y, Venema VJ, Venema RC, Tsai N, Behzadian MA, Caldwell RB (1999a) VEGF-induced permeability increase is mediated by caveolae. *Invest Ophthalmol Vis Sci* 40:157-167.
- Feng Y, Venema VJ, Venema RC, Tsai N, Caldwell RB (1999b) VEGF induces nuclear translocation of Flk-1/KDR, endothelial nitric oxide synthase, and caveolin-1 in vascular endothelial cells. *Biochem Biophys Res Commun* 256:192-197.
- Fernandez-Lopez D, Faustino J, Daneman R, Zhou L, Lee SY, Derugin N, Wendland MF, Vexler ZS (2012) Blood-brain barrier permeability is increased after acute adult stroke but not neonatal stroke in the rat. *The Journal of neuroscience : the official journal of the Society for Neuroscience* 32:9588-9600.
- Fling BW, Walsh CM, Bangert AS, Reuter-Lorenz PA, Welsh RC, Seidler RD (2011) Differential callosal contributions to bimanual control in young and older adults. *Journal of cognitive neuroscience* 23:2171-2185.
- Frank PG, Lisanti MP (2006) Role of caveolin-1 in the regulation of the vascular shear stress response. *J Clin Invest* 116:1222-1225.
- Frank PG, Pavlides S, Lisanti MP (2009) Caveolae and transcytosis in endothelial cells: role in atherosclerosis. *Cell Tissue Res* 335:41-47.
- Freeman SS, Udomphorn Y, Armstead WM, Fisk DM, Vavilala MS (2008) Young age as a risk factor for impaired cerebral autoregulation after moderate to severe pediatric traumatic brain injury. *Anesthesiology* 108:588-595.
- Friess SH, Kilbaugh TJ, Huh JW (2012) Advanced neuromonitoring and imaging in pediatric traumatic brain injury. *Critical care research and practice* 2012:361310.
- Fujii D, Ahmed I (2002) Psychotic disorder following traumatic brain injury: a conceptual framework. *Cogn Neuropsychiatry* 7:41-62.
- Fukuda AM, Adami A, Pop V, Bellone JA, Coats JS, Hartman RE, Ashwal S, Obenaus A, Badaut J (2013) Posttraumatic reduction of edema with aquaporin-4 RNA interference improves acute and chronic functional recovery. *Journal of cerebral blood flow and metabolism : official journal of the International Society of Cerebral Blood Flow and Metabolism* 33:1621-1632.

- Fukuda AM, Pop V, Spagnoli D, Ashwal S, Obenaus A, Badaut J (2012) Delayed increase of astrocytic aquaporin 4 after juvenile traumatic brain injury: Possible role in edema resolution? *Neuroscience* 222:366-378.
- Furuse M, Fujita K, Hiiragi T, Fujimoto K, Tsukita S (1998a) Claudin-1 and -2: novel integral membrane proteins localizing at tight junctions with no sequence similarity to occludin. *J Cell Biol* 141:1539-1550.
- Furuse M, Hata M, Furuse K, Yoshida Y, Haratake A, Sugitani Y, Noda T, Kubo A, Tsukita S (2002) Claudin-based tight junctions are crucial for the mammalian epidermal barrier: a lesson from claudin-1-deficient mice. *J Cell Biol* 156:1099-1111.
- Furuse M, Hirase T, Itoh M, Nagafuchi A, Yonemura S, Tsukita S (1993) Occludin: a novel integral membrane protein localizing at tight junctions. *J Cell Biol* 123:1777-1788.
- Furuse M, Sasaki H, Fujimoto K, Tsukita S (1998b) A single gene product, claudin-1 or -2, reconstitutes tight junction strands and recruits occludin in fibroblasts. *J Cell Biol* 143:391-401.
- Furuse M, Sasaki H, Tsukita S (1999) Manner of interaction of heterogeneous claudin species within and between tight junction strands. *J Cell Biol* 147:891-903.
- Gaetz M (2004) The neurophysiology of brain injury. *Clinical neurophysiology : official journal of the International Federation of Clinical Neurophysiology* 115:4-18.
- Galbiati F, Volonte D, Engelman JA, Watanabe G, Burk R, Pestell RG, Lisanti MP (1998a) Targeted downregulation of caveolin-1 is sufficient to drive cell transformation and hyperactivate the p42/44 MAP kinase cascade. *EMBO J* 17:6633-6648.
- Galbiati F, Volonte D, Gil O, Zanazzi G, Salzer JL, Sargiacomo M, Scherer PE, Engelman JA, Schlegel A, Parenti M, Okamoto T, Lisanti MP (1998b) Expression of caveolin-1 and -2 in differentiating PC12 cells and dorsal root ganglion neurons: caveolin-2 is up-regulated in response to cell injury. *Proc Natl Acad Sci U S A* 95:10257-10262.
- Gale SD, Prigatano GP (2010) Deep white matter volume loss and social reintegration after traumatic brain injury in children. *The Journal of head trauma rehabilitation* 25:15-22.
- Gao X, Deng P, Xu ZC, Chen J (2011) Moderate traumatic brain injury causes acute dendritic and synaptic degeneration in the hippocampal dentate gyrus. *PLoS One* 6:e24566.
- Gao Y, Signore AP, Yin W, Cao G, Yin XM, Sun F, Luo Y, Graham SH, Chen J (2005) Neuroprotection against focal ischemic brain injury by inhibition of c-Jun N-terminal kinase and attenuation of the mitochondrial apoptosis-signaling pathway. *J Cereb Blood Flow Metab* 25:694-712.

- Garcia-Cardena G, Martasek P, Masters BS, Skidd PM, Couet J, Li S, Lisanti MP, Sessa WC (1997) Dissecting the interaction between nitric oxide synthase (NOS) and caveolin. Functional significance of the nos caveolin binding domain in vivo. *J Biol Chem* 272:25437-25440.
- Garcia-Cardena G, Oh P, Liu J, Schnitzer JE, Sessa WC (1996) Targeting of nitric oxide synthase to endothelial cell caveolae via palmitoylation: implications for nitric oxide signaling. *Proc Natl Acad Sci U S A* 93:6448-6453.
- Gennarelli TA (1993) Mechanisms of brain injury. *J Emerg Med* 11 Suppl 1:5-11.
- Giza CC (2006) Lasting effects of pediatric traumatic brain injury. *Indian Journal of Neurotrauma* 3:19-26.
- Giza CC, Griesbach GS, Hovda DA (2005) Experience-dependent behavioral plasticity is disturbed following traumatic injury to the immature brain. *Behavioural brain research* 157:11-22.
- Giza CC, Mink RB, Madikians A (2007) Pediatric traumatic brain injury: not just little adults. *Curr Opin Crit Care* 13:143-152.
- Giza CC, Prins ML (2006) Is being plastic fantastic? Mechanisms of altered plasticity after developmental traumatic brain injury. *Dev Neurosci* 28:364-379.
- Gleckman AM, Bell MD, Evans RJ, Smith TW (1999) Diffuse axonal injury in infants with nonaccidental craniocerebral trauma: enhanced detection by beta-amyloid precursor protein immunohistochemical staining. *Archives of pathology & laboratory medicine* 123:146-151.
- Glezer I, Rivest S (2004) Glucocorticoids: protectors of the brain during innate immune responses. *The Neuroscientist : a review journal bringing neurobiology, neurology and psychiatry* 10:538-552.
- Goberdhan DC, Wilson C (1998) JNK, cytoskeletal regulator and stress response kinase? A *Drosophila* perspective. *Bioessays* 20:1009-1019.
- Golding EM (2002) Sequelae following traumatic brain injury. The cerebrovascular perspective. *Brain Res Brain Res Rev* 38:377-388.
- Gomori JM, Grossman RI, Goldberg HI, Zimmerman RA, Bilaniuk LT (1985) Intracranial hematomas: imaging by high-field MR. *Radiology* 157:87-93.
- Gonzalez MI, Krizman-Genda E, Robinson MB (2007) Caveolin-1 regulates the delivery and endocytosis of the glutamate transporter, excitatory amino acid carrier 1. *The Journal of biological chemistry* 282:29855-29865.
- Goold D, Vane DW (2009) Evaluation of functionality after head injury in adolescents. *The Journal of trauma* 67:71-74; discussion 74.

- Gottschall PE, Barone FC (2012) Important role for endothelial calveolin-1 in focal cerebral ischemia-induced blood-brain barrier injury. *J Neurochem* 120:4-6.
- Graham DI (2001) Paediatric head injury. *Brain* 124:1261-1262.
- Grammas P (2011) Neurovascular dysfunction, inflammation and endothelial activation: implications for the pathogenesis of Alzheimer's disease. *J Neuroinflammation* 8:26.
- Gratton JP, Lin MI, Yu J, Weiss ED, Jiang ZL, Fairchild TA, Iwakiri Y, Groszmann R, Claffey KP, Cheng YC, Sessa WC (2003) Selective inhibition of tumor microvascular permeability by cavtratin blocks tumor progression in mice. *Cancer Cell* 4:31-39.
- Groeschel S, Vollmer B, King MD, Connelly A (2010) Developmental changes in cerebral grey and white matter volume from infancy to adulthood. *International journal of developmental neuroscience : the official journal of the International Society for Developmental Neuroscience* 28:481-489.
- Grontoft O (1954) Intracranial haemorrhage and blood-brain barrier problems in the newborn; a pathologico-anatomical and experimental investigation. *Acta pathologica et microbiologica Scandinavica Supplementum* 100:8-109.
- Grossetete M, Phelps J, Arko L, Yonas H, Rosenberg GA (2009) Elevation of matrix metalloproteinases 3 and 9 in cerebrospinal fluid and blood in patients with severe traumatic brain injury. *Neurosurgery* 65:702-708.
- Gu Y, Zheng G, Xu M, Li Y, Chen X, Zhu W, Tong Y, Chung SK, Liu KJ, Shen J (2011) Caveolin-1 regulates nitric oxide-mediated matrix metalloproteinases activity and blood-brain barrier permeability in focal cerebral ischemia and reperfusion injury. *J Neurochem*.
- Guan QH, Pei DS, Xu TL, Zhang GY (2006) Brain ischemia/reperfusion-induced expression of DP5 and its interaction with Bcl-2, thus freeing Bax from Bcl-2/Bax dimmers are mediated by c-Jun N-terminal kinase (JNK) pathway. *Neuroscience letters* 393:226-230.
- Guerra A (2011) Occludin and Claudin-5 are Comparably Abundant and Co-localized in the Rat's Blood Brain Barrier from Late Gestation to Adulthood. *The e-Journal of Neonatology Research* 1:31-43.
- Gupta S, Barrett T, Whitmarsh AJ, Cavanagh J, Sluss HK, Derijard B, Davis RJ (1996) Selective interaction of JNK protein kinase isoforms with transcription factors. *EMBO J* 15:2760-2770.
- Gupta YK, Gupta M (2006) Post traumatic epilepsy: a review of scientific evidence. *Indian journal of physiology and pharmacology* 50:7-16.

- Gursoy-Ozdemir Y, Bolay H, Saribas O, Dalkara T (2000) Role of endothelial nitric oxide generation and peroxynitrite formation in reperfusion injury after focal cerebral ischemia. *Stroke* 31:1974-1980; discussion 1981.
- Gursoy-Ozdemir Y, Can A, Dalkara T (2004) Reperfusion-induced oxidative/nitrative injury to neurovascular unit after focal cerebral ischemia. *Stroke* 35:1449-1453.
- Haasemann M, Cartaud J, Muller-Esterl W, Dunia I (1998) Agonist-induced redistribution of bradykinin B2 receptor in caveolae. *J Cell Sci* 111 (Pt 7):917-928.
- Haeusgen W, Boehm R, Zhao Y, Herdegen T, Waetzig V (2009) Specific activities of individual c-Jun N-terminal kinases in the brain. *Neuroscience* 161:951-959.
- Hagendoorn J, Padera TP, Kashiwagi S, Isaka N, Noda F, Lin MI, Huang PL, Sessa WC, Fukumura D, Jain RK (2004) Endothelial nitric oxide synthase regulates microlymphatic flow via collecting lymphatics. *Circ Res* 95:204-209.
- Hartman RE, Izumi Y, Bales KR, Paul SM, Wozniak DF, Holtzman DM (2005a) Treatment with an amyloid-beta antibody ameliorates plaque load, learning deficits, and hippocampal long-term potentiation in a mouse model of Alzheimer's disease. *The Journal of neuroscience : the official journal of the Society for Neuroscience* 25:6213-6220.
- Hartman RE, Lee JM, Zipfel GJ, Wozniak DF (2005b) Characterizing learning deficits and hippocampal neuron loss following transient global cerebral ischemia in rats. *Brain research* 1043:48-56.
- Haskins J, Gu L, Wittchen ES, Hibbard J, Stevenson BR (1998) ZO-3, a novel member of the MAGUK protein family found at the tight junction, interacts with ZO-1 and occludin. *J Cell Biol* 141:199-208.
- Hawkins BT, Davis TP (2005) The blood-brain barrier/neurovascular unit in health and disease. *Pharmacol Rev* 57:173-185.
- Head BP, Insel PA (2007) Do caveolins regulate cells by actions outside of caveolae? *Trends Cell Biol* 17:51-57.
- Head BP, Patel HH, Tsutsumi YM, Hu Y, Mejia T, Mora RC, Insel PA, Roth DM, Drummond JC, Patel PM (2008) Caveolin-1 expression is essential for N-methyl-D-aspartate receptor-mediated Src and extracellular signal-regulated kinase 1/2 activation and protection of primary neurons from ischemic cell death. *FASEB J* 22:828-840.
- Head BP, Peart JN, Panneerselvam M, Yokoyama T, Pearn ML, Niesman IR, Bonds JA, Schilling JM, Miyanohara A, Headrick J, Ali SS, Roth DM, Patel PM, Patel HH (2010) Loss of caveolin-1 accelerates neurodegeneration and aging. *PLoS One* 5:e15697.
- Heiskala M, Peterson PA, Yang Y (2001) The roles of claudin superfamily proteins in paracellular transport. *Traffic* 2:93-98.

- Herdegen T, Claret FX, Kallunki T, Martin-Villalba A, Winter C, Hunter T, Karin M (1998) Lasting N-terminal phosphorylation of c-Jun and activation of c-Jun N-terminal kinases after neuronal injury. *The Journal of neuroscience : the official journal of the Society for Neuroscience* 18:5124-5135.
- Herman ST (2002) Epilepsy after brain insult: targeting epileptogenesis. *Neurology* 59:S21-26.
- Hibi M, Lin A, Smeal T, Minden A, Karin M (1993) Identification of an oncoprotein- and UV-responsive protein kinase that binds and potentiates the c-Jun activation domain. *Genes Dev* 7:2135-2148.
- Hirase T, Kawashima S, Wong EY, Ueyama T, Rikitake Y, Tsukita S, Yokoyama M, Staddon JM (2001) Regulation of tight junction permeability and occludin phosphorylation by RhoA-p160ROCK-dependent and -independent mechanisms. *J Biol Chem* 276:10423-10431.
- Hirt L, Badaut J, Thevenet J, Granziera C, Regli L, Maurer F, Bonny C, Bogousslavsky J (2004) D-JNK11, a cell-penetrating c-Jun-N-terminal kinase inhibitor, protects against cell death in severe cerebral ischemia. *Stroke* 35:1738-1743.
- Hirt L, Ternon B, Price M, Mastour N, Brunet JF, Badaut J (2009) Protective role of early aquaporin 4 induction against postischemic edema formation. *J Cereb Blood Flow Metab* 29:423-433.
- Holshouser BA, Tong KA, Ashwal S (2005) Proton MR spectroscopic imaging depicts diffuse axonal injury in children with traumatic brain injury. *AJNR American journal of neuroradiology* 26:1276-1285.
- Honer WG, Barr AM, Sawada K, Thornton AE, Morris MC, Leurgans SE, Schneider JA, Bennett DA (2012) Cognitive reserve, presynaptic proteins and dementia in the elderly. *Transl Psychiatry* 2:e114.
- Hong MY, Gao JL, Cui JZ, Wang KJ, Tian YX, Li R, Wang HT, Wang H (2012) Effect of c-Jun NH(2)-terminal kinase-mediated p53 expression on neuron autophagy following traumatic brain injury in rats. *Chinese medical journal* 125:2019-2024.
- Hoofien D, Gilboa A, Vakil E, Donovick PJ (2001) Traumatic brain injury (TBI) 10-20 years later: a comprehensive outcome study of psychiatric symptomatology, cognitive abilities and psychosocial functioning. *Brain Inj* 15:189-209.
- Hooper C, Pinteaux-Jones F, Fry VA, Sevastou IG, Baker D, Heales SJ, Pocock JM (2009) Differential effects of albumin on microglia and macrophages; implications for neurodegeneration following blood-brain barrier damage. *J Neurochem* 109:694-705.
- Hooper C, Taylor DL, Pocock JM (2005) Pure albumin is a potent trigger of calcium signalling and proliferation in microglia but not macrophages or astrocytes. *J Neurochem* 92:1363-1376.

- Hu CH, Xiao K, Luan ZS, Song J (2013) Early weaning increases intestinal permeability, alters expression of cytokine and tight junction proteins, and activates mitogen-activated protein kinases in pigs. *Journal of animal science* 91:1094-1101.
- Huang T, Solano J, He D, Loutfi M, Dietrich WD, Kuluz JW (2009) Traumatic injury activates MAP kinases in astrocytes: mechanisms of hypothermia and hyperthermia. *J Neurotrauma* 26:1535-1545.
- Huber D, Balda MS, Matter K (2000) Occludin modulates transepithelial migration of neutrophils. *J Biol Chem* 275:5773-5778.
- Hudson N (2012) The Role of Brain Endothelial MAP Kinases in ICAM-1-Mediated Lymphocyte Transmigration. In: *Institute of Ophthalmology*, vol. Doctor of Philosophy, p 277 London: University College London.
- Huh JW, Raghupathi R (2007) Chronic cognitive deficits and long-term histopathological alterations following contusive brain injury in the immature rat. *Journal of neurotrauma* 24:1460-1474.
- Huh JW, Raghupathi R (2009) New concepts in treatment of pediatric traumatic brain injury. *Anesthesiol Clin* 27:213-240.
- Huh JW, Widing AG, Raghupathi R (2008) Midline brain injury in the immature rat induces sustained cognitive deficits, bihemispheric axonal injury and neurodegeneration. *Exp Neurol* 213:84-92.
- Hynes RO (1987) Integrins: a family of cell surface receptors. *Cell* 48:549-554.
- Iadecola C, Nedergaard M (2007) Glial regulation of the cerebral microvasculature. *Nat Neurosci* 10:1369-1376.
- Ibrahim NG, Wood J, Margulies SS, Christian CW (2012) Influence of age and fall type on head injuries in infants and toddlers. *Int J Dev Neurosci* 30:201-206.
- Ihara M, Polvikoski TM, Hall R, Slade JY, Perry RH, Oakley AE, Englund E, O'Brien JT, Ince PG, Kalaria RN (2010) Quantification of myelin loss in frontal lobe white matter in vascular dementia, Alzheimer's disease, and dementia with Lewy bodies. *Acta neuropathologica* 119:579-589.
- Ikezu T, Ueda H, Trapp BD, Nishiyama K, Sha JF, Volonte D, Galbiati F, Byrd AL, Bassell G, Serizawa H, Lane WS, Lisanti MP, Okamoto T (1998) Affinity-purification and characterization of caveolins from the brain: differential expression of caveolin-1, -2, and -3 in brain endothelial and astroglial cell types. *Brain Res* 804:177-192.
- Ikonomovic MD, Uryu K, Abrahamson EE, Ciallella JR, Trojanowski JQ, Lee VM, Clark RS, Marion DW, Wisniewski SR, DeKosky ST (2004) Alzheimer's pathology in human temporal cortex surgically excised after severe brain injury. *Experimental Neurology* 190:192-203.

- Ip YT, Davis RJ (1998) Signal transduction by the c-Jun N-terminal kinase (JNK)--from inflammation to development. *Curr Opin Cell Biol* 10:205-219.
- Istrate AN, Tsvetkov PO, Mantsyzov AB, Kulikova AA, Kozin SA, Makarov AA, Polshakov VI (2012) NMR solution structure of rat abeta(1-16): toward understanding the mechanism of rats' resistance to Alzheimer's disease. *Biophysical journal* 102:136-143.
- Itallie CM, Anderson JM (2012) Caveolin binds independently to claudin-2 and occludin. *Ann N Y Acad Sci* 1257:103-107.
- Itoh M, Furuse M, Morita K, Kubota K, Saitou M, Tsukita S (1999) Direct binding of three tight junction-associated MAGUKs, ZO-1, ZO-2, and ZO-3, with the COOH termini of claudins. *J Cell Biol* 147:1351-1363.
- Iudice A, Murri L (2000) Pharmacological prophylaxis of post-traumatic epilepsy. *Drugs* 59:1091-1099.
- Jane JA, Francel PC (1996) Age and outcome of head injury. In: *Neurotrauma*(Narayan, R. K. et al., eds), pp 723-741 New York: McGraw-Hill.
- Janowitz T, Menon DK (2010) Exploring new routes for neuroprotective drug development in traumatic brain injury. *Science translational medicine* 2:27rv21.
- Jasmin JF, Malhotra S, Singh Dhallu M, Mercier I, Rosenbaum DM, Lisanti MP (2007) Caveolin-1 deficiency increases cerebral ischemic injury. *Circ Res* 100:721-729.
- Jasmin JF, Mercier I, Dupuis J, Tanowitz HB, Lisanti MP (2006) Short-term administration of a cell-permeable caveolin-1 peptide prevents the development of monocrotaline-induced pulmonary hypertension and right ventricular hypertrophy. *Circulation* 114:912-920.
- Jicha GA, Parisi JE, Dickson DW, Johnson K, Cha R, Ivnik RJ, Tangalos EG, Boeve BF, Knopman DS, Braak H, Petersen RC (2006) Neuropathologic outcome of mild cognitive impairment following progression to clinical dementia. *Arch Neurol* 63:674-681.
- Jodoin J, Demeule M, Fenart L, Cecchelli R, Farmer S, Linton KJ, Higgins CF, Beliveau R (2003) P-glycoprotein in blood-brain barrier endothelial cells: interaction and oligomerization with caveolins. *J Neurochem* 87:1010-1023.
- Johnson VE, Stewart W, Smith DH (2010) Traumatic brain injury and amyloid-beta pathology: a link to Alzheimer's disease? *Nature reviews Neuroscience* 11:361-370.
- Johnson VE, Stewart W, Smith DH (2012) Widespread tau and amyloid-beta pathology many years after a single traumatic brain injury in humans. *Brain pathology* 22:142-149.

- Jonsson CA, Catroppa C, Godfrey C, Smedler AC, Anderson V (2013) Cognitive recovery and development after traumatic brain injury in childhood: a person-oriented, longitudinal study. *Journal of neurotrauma* 30:76-83.
- Ju H, Venema VJ, Liang H, Harris MB, Zou R, Venema RC (2000) Bradykinin activates the Janus-activated kinase/signal transducers and activators of transcription (JAK/STAT) pathway in vascular endothelial cells: localization of JAK/STAT signalling proteins in plasmalemmal caveolae. *Biochem J* 351:257-264.
- Juliano RL (2002) Signal transduction by cell adhesion receptors and the cytoskeleton: functions of integrins, cadherins, selectins, and immunoglobulin-superfamily members. *Annual review of pharmacology and toxicology* 42:283-323.
- Kachar B, Reese TS (1982) Evidence for the lipidic nature of tight junction strands. *Nature* 296:464-466.
- Kacimi R, Giffard RG, Yenari MA (2011) Endotoxin-activated microglia injure brain derived endothelial cells via NF-kappaB, JAK-STAT and JNK stress kinase pathways. *J Inflamm (Lond)* 8:7.
- Kallunki T, Su B, Tsigelny I, Sluss HK, Derijard B, Moore G, Davis R, Karin M (1994) JNK2 contains a specificity-determining region responsible for efficient c-Jun binding and phosphorylation. *Genes Dev* 8:2996-3007.
- Kaminska B, Gozdz A, Zawadzka M, Ellert-Miklaszewska A, Lipko M (2009) MAPK signal transduction underlying brain inflammation and gliosis as therapeutic target. *Anat Rec (Hoboken)* 292:1902-1913.
- Kamper JE, Pop V, Fukuda A, Ajao D, Hartman R, Badaut J (2013) Juvenile traumatic brain injury evolves into a chronic brain disorder: Behavioral histological changes over 6months. *Experimental Neurology*.
- Kang WH, Simon MJ, Gao S, Banta S, Morrison B, 3rd (2011) Attenuation of astrocyte activation by TAT-mediated delivery of a peptide JNK inhibitor. *J Neurotrauma* 28:1219-1228.
- Kato H, Kogure K, Ohtomo H, Izumiyama M, Tobita M, Matsui S, Yamamoto E, Kohno H, Ikebe Y, Watanabe T (1986) Characterization of experimental ischemic brain edema utilizing proton nuclear magnetic resonance imaging. *J Cereb Blood Flow Metab* 6:212-221.
- Keenan HT, Bratton SL (2006) Epidemiology and outcomes of pediatric traumatic brain injury. *Dev Neurosci* 28:256-263.
- Kennard MA (1936) Age and other factors in motor recovery from precentral lesions in monkeys. *American Journal of Physiology* 115:138-146.
- Kenne E, Erlandsson A, Lindbom L, Hillered L, Clausen F (2012) Neutrophil depletion reduces edema formation and tissue loss following traumatic brain injury in mice. *J Neuroinflammation* 9:17.

- Khan AA, Banerjee A (2010) The role of prophylactic anticonvulsants in moderate to severe head injury. *Int J Emerg Med* 3:187-191.
- Khan M, Im YB, Shunmugavel A, Gilg AG, Dhindsa RK, Singh AK, Singh I (2009) Administration of S-nitrosoglutathione after traumatic brain injury protects the neurovascular unit and reduces secondary injury in a rat model of controlled cortical impact. *J Neuroinflammation* 6:32.
- Khilnani P (2004) Management of pediatric head injury. *Indian Journal of Critical Care Medicine* 8.
- Kiening K, Unterberg A (2007) Trauma care in Germany: a European perspective. *Clin Neurosurg* 54:206-208.
- Kim KA, Wang MY, Griffith PM, Summers S, Levy ML (2000) Analysis of pediatric head injury from falls. *Neurosurgical focus* 8:e3.
- Kimelberg HK (1995) Current concepts of brain edema. Review of laboratory investigations. *J Neurosurg* 83:1051-1059.
- Kimelberg HK, Rutledge E, Goderie S, Charniga C (1995) Astrocytic swelling due to hypotonic or high K⁺ medium causes inhibition of glutamate and aspartate uptake and increases their release. *J Cereb Blood Flow Metab* 15:409-416.
- Kirino T (1982) Delayed neuronal death in the gerbil hippocampus following ischemia. *Brain Res* 239:57-69.
- Kirkham M, Nixon SJ, Howes MT, Abi-Rached L, Wakeham DE, Hanzal-Bayer M, Ferguson C, Hill MM, Fernandez-Rojo M, Brown DA, Hancock JF, Brodsky FM, Parton RG (2008) Evolutionary analysis and molecular dissection of caveola biogenesis. *J Cell Sci* 121:2075-2086.
- Klatzo I (1967) Presidential address. Neuropathological aspects of brain edema. *J Neuropathol Exp Neurol* 26:1-14.
- Kochanek PM, Bell MJ, Bayir H (2010) Quo vadis 2010? - carpe diem: challenges and opportunities in pediatric traumatic brain injury. *Dev Neurosci* 32:335-342.
- Kodama Y, Kikusui T, Takeuchi Y, Mori Y (2008) Effects of early weaning on anxiety and prefrontal cortical and hippocampal myelination in male and female Wistar rats. *Developmental psychobiology* 50:332-342.
- Kojima T, Fuchimoto J, Yamaguchi H, Ito T, Takasawa A, Ninomiya T, Kikuchi S, Ogasawara N, Ohkuni T, Masaki T, Hirata K, Himi T, Sawada N (2010) c-Jun N-terminal kinase is largely involved in the regulation of tricellular tight junctions via tricellulin in human pancreatic duct epithelial cells. *J Cell Physiol* 225:720-733.
- Komarova Y, Malik AB (2010) Regulation of endothelial permeability via paracellular and transcellular transport pathways. *Annu Rev Physiol* 72:463-493.

- Kooij G, van Horssen J, de Lange EC, Reijerkerk A, van der Pol SM, van Het Hof B, Drexhage J, Vennegoor A, Killestein J, Scheffer G, Oerlemans R, Scheper R, van der Valk P, Dijkstra CD, de Vries HE (2010) T lymphocytes impair P-glycoprotein function during neuroinflammation. *J Autoimmun* 34:416-425.
- Kotapka MJ, Gennarelli TA, Graham DI, Adams JH, Thibault LE, Ross DT, Ford I (1991) Selective vulnerability of hippocampal neurons in acceleration-induced experimental head injury. *J Neurotrauma* 8:247-258.
- Kraus MF, Susmaras T, Caughlin BP, Walker CJ, Sweeney JA, Little DM (2007) White matter integrity and cognition in chronic traumatic brain injury: a diffusion tensor imaging study. *Brain : a journal of neurology* 130:2508-2519.
- Kriel RL, Krach LE, Panser LA (1989) Closed head injury: comparison of children younger and older than 6 years of age. *Pediatr Neurol* 5:296-300.
- Kuan CY, Burke RE (2005) Targeting the JNK signaling pathway for stroke and Parkinson's diseases therapy. *Curr Drug Targets CNS Neurol Disord* 4:63-67.
- Kuan CY, Whitmarsh AJ, Yang DD, Liao G, Schloemer AJ, Dong C, Bao J, Banasiak KJ, Haddad GG, Flavell RA, Davis RJ, Rakic P (2003) A critical role of neural-specific JNK3 for ischemic apoptosis. *Proc Natl Acad Sci U S A* 100:15184-15189.
- Kumar P, Shen Q, Pivetti CD, Lee ES, Wu MH, Yuan SY (2009) Molecular mechanisms of endothelial hyperpermeability: implications in inflammation. *Expert Rev Mol Med* 11:e19.
- Kuppermann N, Holmes JF, Dayan PS, Hoyle JD, Jr., Atabaki SM, Holubkov R, Nadel FM, Monroe D, Stanley RM, Borgialli DA, Badawy MK, Schunk JE, Quayle KS, Mahajan P, Lichenstein R, Lillis KA, Tunik MG, Jacobs ES, Callahan JM, Gorelick MH, Glass TF, Lee LK, Bachman MC, Cooper A, Powell EC, Gerardi MJ, Melville KA, Muizelaar JP, Wisner DH, Zuspan SJ, Dean JM, Wootton-Gorges SL (2009) Identification of children at very low risk of clinically-important brain injuries after head trauma: a prospective cohort study. *Lancet* 374:1160-1170.
- Kurozumi T, Imamura T, Tanaka K, Yae Y, Koga S (1983) Effects of hypertension and hypercholesteremia on the permeability of fibrinogen and low density lipoprotein in the coronary artery of rabbits. Immunoelectron-microscopic study. *Atherosclerosis* 49:267-276.
- Kusaka G, Ishikawa M, Nanda A, Granger DN, Zhang JH (2004) Signaling pathways for early brain injury after subarachnoid hemorrhage. *J Cereb Blood Flow Metab* 24:916-925.
- Kyriakis JM, Avruch J (2001) Mammalian mitogen-activated protein kinase signal transduction pathways activated by stress and inflammation. *Physiol Rev* 81:807-869.

- Labrecque L, Royal I, Surprenant DS, Patterson C, Gingras D, Beliveau R (2003) Regulation of vascular endothelial growth factor receptor-2 activity by caveolin-1 and plasma membrane cholesterol. *Mol Biol Cell* 14:334-347.
- Lacaz-Vieira F, Jaeger MM, Farshori P, Kachar B (1999) Small synthetic peptides homologous to segments of the first external loop of occludin impair tight junction resealing. *J Membr Biol* 168:289-297.
- Laird MD, Vender JR, Dhandapani KM (2008) Opposing roles for reactive astrocytes following traumatic brain injury. *Neurosignals* 16:154-164.
- Lajoie P, Goetz JG, Dennis JW, Nabi IR (2009) Lattices, rafts, and scaffolds: domain regulation of receptor signaling at the plasma membrane. *J Cell Biol* 185:381-385.
- Lajoie P, Nabi IR (2010) Lipid rafts, caveolae, and their endocytosis. *Int Rev Cell Mol Biol* 282:135-163.
- Lal BK, Varma S, Pappas PJ, Hobson RW, 2nd, Duran WN (2001) VEGF increases permeability of the endothelial cell monolayer by activation of PKB/akt, endothelial nitric-oxide synthase, and MAP kinase pathways. *Microvasc Res* 62:252-262.
- Langlois JA, Rutland-Brown W, Wald MM (2006) The epidemiology and impact of traumatic brain injury: a brief overview. *J Head Trauma Rehabil* 21:375-378.
- Lannuzel A, Barnier JV, Hery C, Huynh VT, Guibert B, Gray F, Vincent JD, Tardieu M (1997) Human immunodeficiency virus type 1 and its coat protein gp120 induce apoptosis and activate JNK and ERK mitogen-activated protein kinases in human neurons. *Annals of neurology* 42:847-856.
- Le Bihan D (2007) The 'wet mind': water and functional neuroimaging. *Phys Med Biol* 52:R57-90.
- Lee H, Park DS, Wang XB, Scherer PE, Schwartz PE, Lisanti MP (2002) Src-induced phosphorylation of caveolin-2 on tyrosine 19. Phospho-caveolin-2 (Tyr(P)19) is localized near focal adhesions, remains associated with lipid rafts/caveolae, but no longer forms a high molecular mass hetero-oligomer with caveolin-1. *J Biol Chem* 277:34556-34567.
- Lehnert M, Relja B, Sun-Young Lee V, Schwestka B, Henrich D, Czerny C, Froh M, Borsello T, Marzi I (2008) A peptide inhibitor of C-jun N-terminal kinase modulates hepatic damage and the inflammatory response after hemorrhagic shock and resuscitation. *Shock* 30:159-165.
- Lehning M, Leplow B, Herzog A, Benz B, Ritz A, Stolze H, Mehdorn M, Ferstl R (2001) Children's spatial behavior is differentially affected after traumatic brain injury. *Child neuropsychology : a journal on normal and abnormal development in childhood and adolescence* 7:59-71.

- Lenmyr F, Karlsson S, Gerwins P, Ata KA, Terent A (2002) Activation of mitogen-activated protein kinases in experimental cerebral ischemia. *Acta Neurol Scand* 106:333-340.
- Lenroot RK, Giedd JN (2006) Brain development in children and adolescents: insights from anatomical magnetic resonance imaging. *Neuroscience and biobehavioral reviews* 30:718-729.
- Levin H, Hanten G, Max J, Li X, Swank P, Ewing-Cobbs L, Dennis M, Menefee DS, Schachar R (2007) Symptoms of attention-deficit/hyperactivity disorder following traumatic brain injury in children. *Journal of developmental and behavioral pediatrics* : JDBP 28:108-118.
- Levin HS (2012) Long-term intellectual outcome of traumatic brain injury in children: limits to neuroplasticity of the young brain? *Pediatrics* 129:e494-495.
- Levin HS, Amparo E, Eisenberg HM, Williams DH, High WM, Jr., McArdle CB, Weiner RL (1987) Magnetic resonance imaging and computerized tomography in relation to the neurobehavioral sequelae of mild and moderate head injuries. *Journal of neurosurgery* 66:706-713.
- Li WP, Liu P, Pilcher BK, Anderson RG (2001) Cell-specific targeting of caveolin-1 to caveolae, secretory vesicles, cytoplasm or mitochondria. *J Cell Sci* 114:1397-1408.
- Li X, McClellan ME, Tanito M, Garteiser P, Towner R, Bissig D, Berkowitz BA, Fliesler SJ, Woodruff ML, Fain GL, Birch DG, Khan MS, Ash JD, Elliott MH (2012a) Loss of caveolin-1 impairs retinal function due to disturbance of subretinal microenvironment. *J Biol Chem* 287:16424-16434.
- Li YH, Wang JB, Li MH, Li WB, Wang D (2012b) Quantification of brain edema and hemorrhage by MRI after experimental traumatic brain injury in rabbits predicts subsequent functional outcome. *Neurol Sci* 33:731-740.
- Liao CW, Cho WL, Kao TC, Su KE, Lin YH, Fan CK (2008) Blood-brain barrier impairment with enhanced SP, NK-1R, GFAP and claudin-5 expressions in experimental cerebral toxocarasis. *Parasite Immunol* 30:525-534.
- Liebner S, Czupalla CJ, Wolburg H (2011) Current concepts of blood-brain barrier development. *Int J Dev Biol* 55:467-476.
- Lin JL, Huang YH, Shen YC, Huang HC, Liu PH (2010) Ascorbic acid prevents blood-brain barrier disruption and sensory deficit caused by sustained compression of primary somatosensory cortex. *Journal of cerebral blood flow and metabolism* : official journal of the International Society of Cerebral Blood Flow and Metabolism 30:1121-1136.
- Lindbom L (2003) Regulation of vascular permeability by neutrophils in acute inflammation. *Chem Immunol Allergy* 83:146-166.

- Linder AE, McCluskey LP, Cole KR, 3rd, Lanning KM, Webb RC (2005) Dynamic association of nitric oxide downstream signaling molecules with endothelial caveolin-1 in rat aorta. *J Pharmacol Exp Ther* 314:9-15.
- Lippert-Gruner M, Kuchta J, Hellmich M, Klug N (2006) Neurobehavioural deficits after severe traumatic brain injury (TBI). *Brain injury : [BI]* 20:569-574.
- Lisanti MP, Scherer PE, Tang Z, Sargiacomo M (1994a) Caveolae, caveolin and caveolin-rich membrane domains: a signalling hypothesis. *Trends Cell Biol* 4:231-235.
- Lisanti MP, Scherer PE, Vidugiriene J, Tang Z, Hermanowski-Vosatka A, Tu YH, Cook RF, Sargiacomo M (1994b) Characterization of caveolin-rich membrane domains isolated from an endothelial-rich source: implications for human disease. *J Cell Biol* 126:111-126.
- Liu F, Schafer DP, McCullough LD (2009) TTC, fluoro-Jade B and NeuN staining confirm evolving phases of infarction induced by middle cerebral artery occlusion. *Journal of neuroscience methods* 179:1-8.
- Liu J, Jin X, Liu KJ, Liu W (2012) Matrix metalloproteinase-2-mediated occludin degradation and caveolin-1-mediated claudin-5 redistribution contribute to blood-brain barrier damage in early ischemic stroke stage. *J Neurosci* 32:3044-3057.
- Liu LB, Xue YX, Liu YH (2010) Bradykinin increases the permeability of the blood-tumor barrier by the caveolae-mediated transcellular pathway. *J Neurooncol* 99:187-194.
- Liu MC, Akle V, Zheng W, Kitlen J, O'Steen B, Lerner SF, Dave JR, Tortella FC, Hayes RL, Wang KK (2006) Extensive degradation of myelin basic protein isoforms by calpain following traumatic brain injury. *Journal of neurochemistry* 98:700-712.
- Lo EH, Moskowitz MA, Jacobs TP (2005) Exciting, radical, suicidal: how brain cells die after stroke. *Stroke* 36:189-192.
- Lok J, Gupta P, Guo S, Kim WJ, Whalen MJ, van Leyen K, Lo EH (2007) Cell-cell signaling in the neurovascular unit. *Neurochem Res* 32:2032-2045.
- Lopez-Ramirez MA, Fischer R, Torres-Badillo CC, Davies HA, Logan K, Pfizenmaier K, Male DK, Sharrack B, Romero IA (2012) Role of caspases in cytokine-induced barrier breakdown in human brain endothelial cells. *Journal of immunology* 189:3130-3139.
- Lowry JL, Brovkovich V, Zhang Y, Skidgel RA (2013) Endothelial nitric-oxide synthase activation generates an inducible nitric-oxide synthase-like output of nitric oxide in inflamed endothelium. *J Biol Chem* 288:4174-4193.
- Luna B, Garver KE, Urban TA, Lazar NA, Sweeney JA (2004) Maturation of cognitive processes from late childhood to adulthood. *Child Dev* 75:1357-1372.

- Maas AI, Stocchetti N, Bullock R (2008) Moderate and severe traumatic brain injury in adults. *Lancet neurology* 7:728-741.
- Marmarou A (2003) Pathophysiology of traumatic brain edema: current concepts. *Acta Neurochir Suppl* 86:7-10.
- Marshall LF, Smith RW, Shapiro HM (1979) The outcome with aggressive treatment in severe head injuries. Part I: the significance of intracranial pressure monitoring. *J Neurosurg* 50:20-25.
- Martin-Padura I, Lostaglio S, Schneemann M, Williams L, Romano M, Fruscella P, Panzeri C, Stoppacciaro A, Ruco L, Villa A, Simmons D, Dejana E (1998) Junctional adhesion molecule, a novel member of the immunoglobulin superfamily that distributes at intercellular junctions and modulates monocyte transmigration. *J Cell Biol* 142:117-127.
- Masuda K, Katagiri C, Nomura M, Sato M, Kakumoto K, Akagi T, Kikuchi K, Tanuma N, Shima H (2010) MKP-7, a JNK phosphatase, blocks ERK-dependent gene activation by anchoring phosphorylated ERK in the cytoplasm. *Biochem Biophys Res Commun* 393:201-206.
- Mawuenyega KG, Sigurdson W, Ovod V, Munsell L, Kasten T, Morris JC, Yarasheski KE, Bateman RJ (2010) Decreased clearance of CNS beta-amyloid in Alzheimer's disease. *Science* 330:1774.
- Max JE, Keatley E, Wilde EA, Bigler ED, Levin HS, Schachar RJ, Saunders A, Ewing-Cobbs L, Chapman SB, Dennis M, Yang TT (2011) Anxiety disorders in children and adolescents in the first six months after traumatic brain injury. *J Neuropsychiatry Clin Neurosci* 23:29-39.
- Max JE, Koele SL, Castillo CC, Lindgren SD, Arndt S, Bokura H, Robin DA, Smith WL, Jr., Sato Y (2000) Personality change disorder in children and adolescents following traumatic brain injury. *J Int Neuropsychol Soc* 6:279-289.
- Max JE, Lansing AE, Koele SL, Castillo CS, Bokura H, Schachar R, Collings N, Williams KE (2004) Attention deficit hyperactivity disorder in children and adolescents following traumatic brain injury. *Developmental neuropsychology* 25:159-177.
- Maxwell WL (2012) Traumatic brain injury in the neonate, child and adolescent human: an overview of pathology. *Int J Dev Neurosci* 30:167-183.
- McAllister TW (2011) Neurobiological consequences of traumatic brain injury. *Dialogues in clinical neuroscience* 13:287-300.
- McCaffrey G, Seelbach MJ, Staatz WD, Nametz N, Quigley C, Campos CR, Brooks TA, Davis TP (2008) Occludin oligomeric assembly at tight junctions of the blood-brain barrier is disrupted by peripheral inflammatory hyperalgesia. *J Neurochem* 106:2395-2409.

- McCaffrey G, Staats WD, Quigley CA, Nametz N, Seelbach MJ, Campos CR, Brooks TA, Egleton RD, Davis TP (2007) Tight junctions contain oligomeric protein assembly critical for maintaining blood-brain barrier integrity in vivo. *J Neurochem* 103:2540-2555.
- McCaffrey G, Staats WD, Sanchez-Covarrubias L, Finch JD, Demarco K, Laracuate ML, Ronaldson PT, Davis TP (2012) P-glycoprotein trafficking at the blood-brain barrier altered by peripheral inflammatory hyperalgesia. *Journal of neurochemistry* 122:962-975.
- McCaffrey G, Willis CL, Staats WD, Nametz N, Quigley CA, Hom S, Lochhead JJ, Davis TP (2009) Occludin oligomeric assemblies at tight junctions of the blood-brain barrier are altered by hypoxia and reoxygenation stress. *J Neurochem* 110:58-71.
- McGowan E, Pickford F, Kim J, Onstead L, Eriksen J, Yu C, Skipper L, Murphy MP, Beard J, Das P, Jansen K, Delucia M, Lin WL, Dolios G, Wang R, Eckman CB, Dickson DW, Hutton M, Hardy J, Golde T (2005) Abeta42 is essential for parenchymal and vascular amyloid deposition in mice. *Neuron* 47:191-199.
- McQuillen PS, Ferriero DM (2004) Selective vulnerability in the developing central nervous system. *Pediatr Neurol* 30:227-235.
- Meng J, Zou Y, Hu C, Zhu Y, Peng Z, Hu G, Wang Z, Tao L (2012) Fluorofenidone Attenuates Bleomycin-Induced Pulmonary Inflammation and Fibrosis in Mice via Restoring Caveolin-1 Expression and Inhibiting MAPK Signaling Pathway. *Shock*.
- Michel-Monigadon D, Bonny C, Hirt L (2010) c-Jun N-terminal kinase pathway inhibition in intracerebral hemorrhage. *Cerebrovasc Dis* 29:564-570.
- Migheli A, Piva R, Atzori C, Troost D, Schiffer D (1997) c-Jun, JNK/SAPK kinases and transcription factor NF-kappa B are selectively activated in astrocytes, but not motor neurons, in amyotrophic lateral sclerosis. *Journal of neuropathology and experimental neurology* 56:1314-1322.
- Miller DS (2010) Regulation of P-glycoprotein and other ABC drug transporters at the blood-brain barrier. *Trends in pharmacological sciences* 31:246-254.
- Minshall RD, Sessa WC, Stan RV, Anderson RG, Malik AB (2003) Caveolin regulation of endothelial function. *Am J Physiol Lung Cell Mol Physiol* 285:L1179-1183.
- Mitic LL, Van Itallie CM, Anderson JM (2000) Molecular physiology and pathophysiology of tight junctions I. Tight junction structure and function: lessons from mutant animals and proteins. *Am J Physiol Gastrointest Liver Physiol* 279:G250-254.
- Miyawaki-Shimizu K, Predescu D, Shimizu J, Broman M, Predescu S, Malik AB (2006) siRNA-induced caveolin-1 knockdown in mice increases lung vascular permeability via the junctional pathway. *Am J Physiol Lung Cell Mol Physiol* 290:L405-413.

- Mo S, Wang L, Li Q, Li J, Li Y, Thannickal VJ, Cui Z (2010) Caveolin-1 regulates dorsoventral patterning through direct interaction with beta-catenin in zebrafish. *Dev Biol* 344:210-223.
- Montine TJ, Phelps CH, Beach TG, Bigio EH, Cairns NJ, Dickson DW, Duyckaerts C, Frosch MP, Masliah E, Mirra SS, Nelson PT, Schneider JA, Thal DR, Trojanowski JQ, Vinters HV, Hyman BT (2012) National Institute on Aging-Alzheimer's Association guidelines for the neuropathologic assessment of Alzheimer's disease: a practical approach. *Acta neuropathologica* 123:1-11.
- Moppett IK (2007) Traumatic brain injury: assessment, resuscitation and early management. *Br J Anaesth* 99:18-31.
- Morales DM, Marklund N, Lebold D, Thompson HJ, Pitkanen A, Maxwell WL, Longhi L, Laurer H, Maegele M, Neugebauer E, Graham DI, Stocchetti N, McIntosh TK (2005) Experimental models of traumatic brain injury: do we really need to build a better mousetrap? *Neuroscience* 136:971-989.
- Morganti-Kossmann MC, Lenzlinger PM, Hans V, Stahel P, Csuka E, Ammann E, Stocker R, Trentz O, Kossmann T (1997) Production of cytokines following brain injury: beneficial and deleterious for the damaged tissue. *Molecular psychiatry* 2:133-136.
- Morita-Fujimura Y, Fujimura M, Gasche Y, Copin JC, Chan PH (2000) Overexpression of copper and zinc superoxide dismutase in transgenic mice prevents the induction and activation of matrix metalloproteinases after cold injury-induced brain trauma. *J Cereb Blood Flow Metab* 20:130-138.
- Morita K, Sasaki H, Furuse K, Furuse M, Tsukita S, Miyachi Y (2003) Expression of claudin-5 in dermal vascular endothelia. *Exp Dermatol* 12:289-295.
- Morita K, Sasaki H, Furuse M, Tsukita S (1999) Endothelial claudin: claudin-5/TMVCF constitutes tight junction strands in endothelial cells. *J Cell Biol* 147:185-194.
- Morrison B, 3rd, Elkin BS, Dolle JP, Yarmush ML (2011) In vitro models of traumatic brain injury. *Annu Rev Biomed Eng* 13:91-126.
- Morton MV, Wehman P (1995) Psychosocial and emotional sequelae of individuals with traumatic brain injury: a literature review and recommendations. *Brain Inj* 9:81-92.
- Myer DJ, Gurkoff GG, Lee SM, Hovda DA, Sofroniew MV (2006) Essential protective roles of reactive astrocytes in traumatic brain injury. *Brain* 129:2761-2772.
- Nag S, Manias JL, Stewart DJ (2009) Expression of endothelial phosphorylated caveolin-1 is increased in brain injury. *Neuropathol Appl Neurobiol* 35:417-426.
- Nag S, Papneja T, Venugopalan R, Stewart DJ (2005) Increased angiopoietin2 expression is associated with endothelial apoptosis and blood-brain barrier breakdown. *Lab Invest* 85:1189-1198.

- Nag S, Venugopalan R, Stewart DJ (2007) Increased caveolin-1 expression precedes decreased expression of occludin and claudin-5 during blood-brain barrier breakdown. *Acta Neuropathol* 114:459-469.
- Nagy Z, Kolev K, Csonka E, Pek M, Machovich R (1995) Contraction of human brain endothelial cells induced by thrombogenic and fibrinolytic factors. An in vitro cell culture model. *Stroke* 26:265-270.
- Natale JE, Joseph JG, Pretzlaff RK, Silber TJ, Guerguerian AM (2006) Clinical trials in pediatric traumatic brain injury: unique challenges and potential responses. *Dev Neurosci* 28:276-290.
- Nicholl J, LaFrance WC, Jr. (2009) Neuropsychiatric sequelae of traumatic brain injury. *Semin Neurol* 29:247-255.
- Nicolakakis N, Hamel E (2011) Neurovascular function in Alzheimer's disease patients and experimental models. *Journal of cerebral blood flow and metabolism : official journal of the International Society of Cerebral Blood Flow and Metabolism* 31:1354-1370.
- Nijboer CH, van der Kooij MA, van Bel F, Ohl F, Heijnen CJ, Kavelaars A (2010) Inhibition of the JNK/AP-1 pathway reduces neuronal death and improves behavioral outcome after neonatal hypoxic-ischemic brain injury. *Brain Behav Immun* 24:812-821.
- Nimmerjahn A, Kirchhoff F, Helmchen F (2005) Resting microglial cells are highly dynamic surveillants of brain parenchyma in vivo. *Science* 308:1314-1318.
- Ning Y, Buranda T, Hudson LG (2007) Activated epidermal growth factor receptor induces integrin alpha2 internalization via caveolae/raft-dependent endocytic pathway. *J Biol Chem* 282:6380-6387.
- Nishibe M, Barbay S, Guggenmos D, Nudo RJ (2010) Reorganization of motor cortex after controlled cortical impact in rats and implications for functional recovery. *Journal of neurotrauma* 27:2221-2232.
- Nishina H, Wada T, Katada T (2004) Physiological roles of SAPK/JNK signaling pathway. *J Biochem* 136:123-126.
- Nusrat A, Parkos CA, Verkade P, Foley CS, Liang TW, Innis-Whitehouse W, Eastburn KK, Madara JL (2000) Tight junctions are membrane microdomains. *J Cell Sci* 113 (Pt 10):1771-1781.
- Obenaus A, Ashwal S (2008) Magnetic resonance imaging in cerebral ischemia: focus on neonates. *Neuropharmacology* 55:271-280.
- Obenaus A, Dilmac N, Tone B, Tian HR, Hartman R, Digicaylioglu M, Snyder EY, Ashwal S (2011) Long-term magnetic resonance imaging of stem cells in neonatal ischemic injury. *Ann Neurol* 69:282-291.

- Obenaus A, Hayes P (2011) Drill hole defects: induction, imaging, and analysis in the rodent. *Methods Mol Biol* 690:301-314.
- Obenaus A, Robbins M, Blanco G, Galloway NR, Snissarenko E, Gillard E, Lee S, Curras-Collazo M (2007) Multi-modal magnetic resonance imaging alterations in two rat models of mild neurotrauma. *J Neurotrauma* 24:1147-1160.
- Ohtsuki S, Sato S, Yamaguchi H, Kamoi M, Asashima T, Terasaki T (2007) Exogenous expression of claudin-5 induces barrier properties in cultured rat brain capillary endothelial cells. *J Cell Physiol* 210:81-86.
- Ohtsuki S, Yamaguchi H, Katsukura Y, Asashima T, Terasaki T (2008) mRNA expression levels of tight junction protein genes in mouse brain capillary endothelial cells highly purified by magnetic cell sorting. *J Neurochem* 104:147-154.
- Oka N, Yamamoto M, Schwencke C, Kawabe J, Ebina T, Ohno S, Couet J, Lisanti MP, Ishikawa Y (1997) Caveolin interaction with protein kinase C. Isoenzyme-dependent regulation of kinase activity by the caveolin scaffolding domain peptide. *J Biol Chem* 272:33416-33421.
- Okamoto T, Schlegel A, Scherer PE, Lisanti MP (1998) Caveolins, a family of scaffolding proteins for organizing "preassembled signaling complexes" at the plasma membrane. *J Biol Chem* 273:5419-5422.
- Okazawa H, Estus S (2002) The JNK/c-Jun cascade and Alzheimer's disease. *American journal of Alzheimer's disease and other dementias* 17:79-88.
- Ono M, Kikusui T, Sasaki N, Ichikawa M, Mori Y, Murakami-Murofushi K (2008) Early weaning induces anxiety and precocious myelination in the anterior part of the basolateral amygdala of male Balb/c mice. *Neuroscience* 156:1103-1110.
- Onyszchuk G, Al-Hafez B, He YY, Bilgen M, Berman NE, Brooks WM (2007) A mouse model of sensorimotor controlled cortical impact: characterization using longitudinal magnetic resonance imaging, behavioral assessments and histology. *J Neurosci Methods* 160:187-196.
- Orlova VV, Economopoulou M, Lupu F, Santoso S, Chavakis T (2006) Junctional adhesion molecule-C regulates vascular endothelial permeability by modulating VE-cadherin-mediated cell-cell contacts. *J Exp Med* 203:2703-2714.
- Ortolano F, Colombo A, Zanier ER, Scip A, Longhi L, Perego C, Stocchetti N, Borsello T, De Simoni MG (2009) c-Jun N-terminal kinase pathway activation in human and experimental cerebral contusion. *J Neuropathol Exp Neurol* 68:964-971.
- Otani N, Nawashiro H, Fukui S, Nomura N, Shima K (2002a) Temporal and spatial profile of phosphorylated mitogen-activated protein kinase pathways after lateral fluid percussion injury in the cortex of the rat brain. *Journal of neurotrauma* 19:1587-1596.

- Otani N, Nawashiro H, Fukui S, Nomura N, Yano A, Miyazawa T, Shima K (2002b) Differential activation of mitogen-activated protein kinase pathways after traumatic brain injury in the rat hippocampus. *Journal of cerebral blood flow and metabolism : official journal of the International Society of Cerebral Blood Flow and Metabolism* 22:327-334.
- Palacios C, Collins MK, Perkins GR (2001) The JNK phosphatase M3/6 is inhibited by protein-damaging stress. *Curr Biol* 11:1439-1443.
- Palade GE (1953a) An electron microscope study of the mitochondrial structure. *J Histochem Cytochem* 1:188-211.
- Palade GE (1953b) Fine structure of blood capillaries. *Journal of Applied Physics* 24:1424-1436.
- Palin K, McCusker RH, Strle K, Moos F, Dantzer R, Kelley KW (2008) Tumor necrosis factor-alpha-induced sickness behavior is impaired by central administration of an inhibitor of c-jun N-terminal kinase. *Psychopharmacology* 197:629-635.
- Palmela I, Sasaki H, Cardoso FL, Moutinho M, Kim KS, Brites D, Brito MA (2012) Time-dependent dual effects of high levels of unconjugated bilirubin on the human blood-brain barrier lining. *Front Cell Neurosci* 6:22.
- Pani B, Singh BB (2009) Lipid rafts/caveolae as microdomains of calcium signaling. *Cell Calcium* 45:625-633.
- Papp KV, Snyder PJ, Maruff P, Bartkowiak J, Pietrzak RH (2011) Detecting subtle changes in visuospatial executive function and learning in the amnesic variant of mild cognitive impairment. *PLoS One* 6:e21688.
- Park E, Bell JD, Baker AJ (2008) Traumatic brain injury: can the consequences be stopped? *CMAJ* 178:1163-1170.
- Park M, Hennig B, Toborek M (2011) Methamphetamine Alters Occludin Expression Via NADPH Oxidase-Induced Oxidative Insult and Intact Caveolae. *J Cell Mol Med*.
- Pasley BN, Freeman RD (2008) Neurovascular coupling. In: *Scholarpedia*, vol. 3.
- Patel HH, Murray F, Insel PA (2008) Caveolae as organizers of pharmacologically relevant signal transduction molecules. *Annual review of pharmacology and toxicology* 48:359-391.
- Pelkmans L, Fava E, Grabner H, Hannus M, Habermann B, Krausz E, Zerial M (2005) Genome-wide analysis of human kinases in clathrin- and caveolae/raft-mediated endocytosis. *Nature* 436:78-86.
- Peng J, Andersen JK (2003) The role of c-Jun N-terminal kinase (JNK) in Parkinson's disease. *IUBMB Life* 55:267-271.

- Peterson EC, Wang Z, Britz G (2011) Regulation of cerebral blood flow. *International journal of vascular medicine* 2011:823525.
- Phillips PG, Birnby LM (2004) Nitric oxide modulates caveolin-1 and matrix metalloproteinase-9 expression and distribution at the endothelial cell/tumor cell interface. *Am J Physiol Lung Cell Mol Physiol* 286:L1055-1065.
- Pirianov G, Brywe KG, Mallard C, Edwards AD, Flavell RA, Hagberg H, Mehmet H (2007) Deletion of the c-Jun N-terminal kinase 3 gene protects neonatal mice against cerebral hypoxic-ischaemic injury. *J Cereb Blood Flow Metab* 27:1022-1032.
- Pitkanen A, McIntosh TK (2006) Animal models of post-traumatic epilepsy. *J Neurotrauma* 23:241-261.
- Ploia C, Antoniou X, Sclip A, Grande V, Cardinetti D, Colombo A, Canu N, Benussi L, Ghidoni R, Forloni G, Borsello T (2011) JNK plays a key role in tau hyperphosphorylation in Alzheimer's disease models. *J Alzheimers Dis* 26:315-329.
- Plotnikov A, Zehorai E, Procaccia S, Seger R (2011) The MAPK cascades: signaling components, nuclear roles and mechanisms of nuclear translocation. *Biochim Biophys Acta* 1813:1619-1633.
- Pop V, Badaut J (2011) A Neurovascular Perspective for Long-Term Changes After Brain Trauma. *Transl Stroke Res* 2:533-545.
- Pop V, Head E, Berchtold NC, Glabe CG, Studzinski CM, Weidner AM, Murphy MP, Cotman CW (2012a) Abeta aggregation profiles and shifts in APP processing favor amyloidogenesis in canines. *Neurobiology of aging* 33:108-120.
- Pop V, Sorensen DW, Kamper JE, Ajao DO, Paul Murphy M, Head E, Hartman RE, Badaut J (2012b) Early brain injury alters the blood-brain barrier phenotype in parallel with beta-amyloid and cognitive changes in adulthood. *J Cereb Blood Flow Metab*.
- Potts MB, Koh SE, Whetstone WD, Walker BA, Yoneyama T, Claus CP, Manvelyan HM, Noble-Haeusslein LJ (2006) Traumatic injury to the immature brain: inflammation, oxidative injury, and iron-mediated damage as potential therapeutic targets. *NeuroRx* 3:143-153.
- Predescu D, Palade GE (1993) Plasmalemmal vesicles represent the large pore system of continuous microvascular endothelium. *Am J Physiol* 265:H725-733.
- Predescu SA, Predescu DN, Malik AB (2007) Molecular determinants of endothelial transcytosis and their role in endothelial permeability. *Am J Physiol Lung Cell Mol Physiol* 293:L823-842.

- Preston E, Webster J, Small D (2001) Characteristics of sustained blood-brain barrier opening and tissue injury in a model for focal trauma in the rat. *J Neurotrauma* 18:83-92.
- Prigatano GP (2008) The problem of not developing normally and pediatric neuropsychological rehabilitation: the Mitchell Rosenthal Lecture. *The Journal of head trauma rehabilitation* 23:414-422.
- Prins ML, Fujima LS, Hovda DA (2005) Age-dependent reduction of cortical contusion volume by ketones after traumatic brain injury. *Journal of neuroscience research* 82:413-420.
- Prins ML, Hovda DA (1998) Traumatic brain injury in the developing rat: effects of maturation on Morris water maze acquisition. *Journal of neurotrauma* 15:799-811.
- Prins ML, Hovda DA (2003) Developing experimental models to address traumatic brain injury in children. *J Neurotrauma* 20:123-137.
- Prisby RD, Wilkerson MK, Sokoya EM, Bryan RM, Jr., Wilson E, Delp MD (2006) Endothelium-dependent vasodilation of cerebral arteries is altered with simulated microgravity through nitric oxide synthase and EDHF mechanisms. *J Appl Physiol* 101:348-353.
- Pullela R, Raber J, Pfankuch T, Ferriero DM, Claus CP, Koh SE, Yamauchi T, Rola R, Fike JR, Noble-Haeusslein LJ (2006) Traumatic injury to the immature brain results in progressive neuronal loss, hyperactivity and delayed cognitive impairments. *Dev Neurosci* 28:396-409.
- Pulverer BJ, Kyriakis JM, Avruch J, Nikolakaki E, Woodgett JR (1991) Phosphorylation of c-jun mediated by MAP kinases. *Nature* 353:670-674.
- Putcha GV, Le S, Frank S, Besirli CG, Clark K, Chu B, Alix S, Youle RJ, LaMarche A, Maroney AC, Johnson EM, Jr. (2003) JNK-mediated BIM phosphorylation potentiates BAX-dependent apoptosis. *Neuron* 38:899-914.
- Puyraimond A, Fridman R, Lemesle M, Arbeille B, Menashi S (2001) MMP-2 colocalizes with caveolae on the surface of endothelial cells. *Exp Cell Res* 262:28-36.
- Raghupathi R, Muir JK, Fulp CT, Pittman RN, McIntosh TK (2003) Acute activation of mitogen-activated protein kinases following traumatic brain injury in the rat: implications for posttraumatic cell death. *Exp Neurol* 183:438-448.
- Ralay Ranaivo H, Hodge JN, Choi N, Wainwright MS (2012) Albumin induces upregulation of matrix metalloproteinase-9 in astrocytes via MAPK and reactive oxygen species-dependent pathways. *J Neuroinflammation* 9:68.
- Ralay Ranaivo H, Wainwright MS (2010) Albumin activates astrocytes and microglia through mitogen-activated protein kinase pathways. *Brain Res* 1313:222-231.

- Ramirez MI, Pollack L, Millien G, Cao YX, Hinds A, Williams MC (2002) The alpha-isoform of caveolin-1 is a marker of vasculogenesis in early lung development. *J Histochem Cytochem* 50:33-42.
- Ramlackhansingh AF, Brooks DJ, Greenwood RJ, Bose SK, Turkheimer FE, Kinnunen KM, Gentleman S, Heckemann RA, Gunanayagam K, Gelosa G, Sharp DJ (2011) Inflammation after trauma: microglial activation and traumatic brain injury. *Ann Neurol* 70:374-383.
- Razani B, Engelman JA, Wang XB, Schubert W, Zhang XL, Marks CB, Macaluso F, Russell RG, Li M, Pestell RG, Di Vizio D, Hou H, Jr., Kneitz B, Lagaud G, Christ GJ, Edelmann W, Lisanti MP (2001) Caveolin-1 null mice are viable but show evidence of hyperproliferative and vascular abnormalities. *J Biol Chem* 276:38121-38138.
- Razani B, Lisanti MP (2001) Two distinct caveolin-1 domains mediate the functional interaction of caveolin-1 with protein kinase A. *Am J Physiol Cell Physiol* 281:C1241-1250.
- Razani B, Wang XB, Engelman JA, Battista M, Lagaud G, Zhang XL, Kneitz B, Hou H, Jr., Christ GJ, Edelmann W, Lisanti MP (2002a) Caveolin-2-deficient mice show evidence of severe pulmonary dysfunction without disruption of caveolae. *Mol Cell Biol* 22:2329-2344.
- Razani B, Woodman SE, Lisanti MP (2002b) Caveolae: from cell biology to animal physiology. *Pharmacol Rev* 54:431-467.
- Readnower RD, Chavko M, Adeeb S, Conroy MD, Pauly JR, McCarron RM, Sullivan PG (2010) Increase in blood-brain barrier permeability, oxidative stress, and activated microglia in a rat model of blast-induced traumatic brain injury. *Journal of neuroscience research* 88:3530-3539.
- Recker R, Adami A, Tone B, Tian HR, Lallas S, Hartman RE, Obenaus A, Ashwal S (2009) Rodent neonatal bilateral carotid artery occlusion with hypoxia mimics human hypoxic-ischemic injury. *Journal of cerebral blood flow and metabolism : official journal of the International Society of Cerebral Blood Flow and Metabolism* 29:1305-1316.
- Rees PM (2003) Contemporary issues in mild traumatic brain injury. *Arch Phys Med Rehabil* 84:1885-1894.
- Reese TS, Karnovsky MJ (1967) Fine structural localization of a blood-brain barrier to exogenous peroxidase. *J Cell Biol* 34:207-217.
- Reeves TM, Smith TL, Williamson JC, Phillips LL (2012) Unmyelinated axons show selective rostrocaudal pathology in the corpus callosum after traumatic brain injury. *Journal of neuropathology and experimental neurology* 71:198-210.

- Regina A, Jodoin J, Khoueir P, Rolland Y, Berthelet F, Moumdjian R, Fenart L, Cecchelli R, Demeule M, Beliveau R (2004) Down-regulation of caveolin-1 in glioma vasculature: modulation by radiotherapy. *J Neurosci Res* 75:291-299.
- Reithmeier T, Speder B, Pakos P, Brinker G, Lohr M, Klug N, Ernestus RI (2005) Delayed bilateral craniectomy for treatment of traumatic brain swelling in children: case report and review of the literature. *Child's nervous system : ChNS : official journal of the International Society for Pediatric Neurosurgery* 21:249-253; discussion 254.
- Repici M, Borsello T (2006) JNK pathway as therapeutic target to prevent degeneration in the central nervous system. *Adv Exp Med Biol* 588:145-155.
- Repici M, Centeno C, Tomasi S, Forloni G, Bonny C, Vercelli A, Borsello T (2007) Time-course of c-Jun N-terminal kinase activation after cerebral ischemia and effect of D-JNKI1 on c-Jun and caspase-3 activation. *Neuroscience* 150:40-49.
- Repici M, Chen X, Morel MP, Doulazmi M, Sclip A, Cannaya V, Veglianese P, Kraftsik R, Mariani J, Borsello T, Dusart I (2012) Specific inhibition of the JNK pathway promotes locomotor recovery and neuroprotection after mouse spinal cord injury. *Neurobiol Dis* 46:710-721.
- Rigor RR, Shen Q, Pivetti CD, Wu MH, Yuan SY (2012) Myosin Light Chain Kinase Signaling in Endothelial Barrier Dysfunction. *Med Res Rev*.
- Robinson JL, Geser F, Corrada MM, Berlau DJ, Arnold SE, Lee VM, Kawas CH, Trojanowski JQ (2011) Neocortical and hippocampal amyloid-beta and tau measures associate with dementia in the oldest-old. *Brain : a journal of neurology* 134:3708-3715.
- Rosen H, Goetzl EJ (2005) Sphingosine 1-phosphate and its receptors: an autocrine and paracrine network. *Nat Rev Immunol* 5:560-570.
- Rosin C, Bates TE, Skaper SD (2004) Excitatory amino acid induced oligodendrocyte cell death in vitro: receptor-dependent and -independent mechanisms. *J Neurochem* 90:1173-1185.
- Rothberg KG, Heuser JE, Donzell WC, Ying YS, Glenney JR, Anderson RG (1992) Caveolin, a protein component of caveolae membrane coats. *Cell* 68:673-682.
- Russell KL, Kutchko KM, Fowler SC, Berman NE, Levant B (2011) Sensorimotor behavioral tests for use in a juvenile rat model of traumatic brain injury: Assessment of sex differences. *J Neurosci Methods* 199:214-222.
- Russell PA, Williams DI (1973) Effects of repeated testing on rats' locomotor activity in the open-field. *Anim Behav* 21:109-111.
- Rutland-Brown W, Langlois JA, Thomas KE, Xi YL (2006) Incidence of traumatic brain injury in the United States, 2003. *J Head Trauma Rehabil* 21:544-548.

- Rybin VO, Xu X, Steinberg SF (1999) Activated protein kinase C isoforms target to cardiomyocyte caveolae : stimulation of local protein phosphorylation. *Circ Res* 84:980-988.
- Ryu J, Pyo H, Jou I, Joe E (2000) Thrombin induces NO release from cultured rat microglia via protein kinase C, mitogen-activated protein kinase, and NF-kappa B. *J Biol Chem* 275:29955-29959.
- Saatman KE, Creed J, Raghupathi R (2010) Calpain as a therapeutic target in traumatic brain injury. *Neurotherapeutics* 7:31-42.
- Saatman KE, Duhaime AC, Bullock R, Maas AI, Valadka A, Manley GT (2008) Classification of traumatic brain injury for targeted therapies. *J Neurotrauma* 25:719-738.
- Sahuquillo J, Poca MA, Amoros S (2001) Current aspects of pathophysiology and cell dysfunction after severe head injury. *Current pharmaceutical design* 7:1475-1503.
- Saitou M, Furuse M, Sasaki H, Schulzke JD, Fromm M, Takano H, Noda T, Tsukita S (2000) Complex phenotype of mice lacking occludin, a component of tight junction strands. *Mol Biol Cell* 11:4131-4142.
- Sakakibara A, Furuse M, Saitou M, Ando-Akatsuka Y, Tsukita S (1997) Possible involvement of phosphorylation of occludin in tight junction formation. *J Cell Biol* 137:1393-1401.
- Salaun C, Gould GW, Chamberlain LH (2005) Lipid raft association of SNARE proteins regulates exocytosis in PC12 cells. *J Biol Chem* 280:19449-19453.
- Samak G, Suzuki T, Bhargava A, Rao RK (2010) c-Jun NH2-terminal kinase-2 mediates osmotic stress-induced tight junction disruption in the intestinal epithelium. *Am J Physiol Gastrointest Liver Physiol* 299:G572-584.
- Sandler SJ, Figaji AA, Adelson PD (2010) Clinical applications of biomarkers in pediatric traumatic brain injury. *Child's nervous system : ChNS : official journal of the International Society for Pediatric Neurosurgery* 26:205-213.
- Sargiacomo M, Scherer PE, Tang Z, Kubler E, Song KS, Sanders MC, Lisanti MP (1995) Oligomeric structure of caveolin: implications for caveolae membrane organization. *Proc Natl Acad Sci U S A* 92:9407-9411.
- Saunders NR, Habgood MD, Dziegielewska KM (1999) Barrier mechanisms in the brain, II. Immature brain. *Clin Exp Pharmacol Physiol* 26:85-91.
- Saunders NR, Liddelow SA, Dziegielewska KM (2012) Barrier mechanisms in the developing brain. *Frontiers in pharmacology* 3:46.
- Sbordone RJ, Liter JC, Pettler-Jennings P (1995) Recovery of function following severe traumatic brain injury: a retrospective 10-year follow-up. *Brain Inj* 9:285-299.

- Schachtrup C, Lu P, Jones LL, Lee JK, Lu J, Sachs BD, Zheng B, Akassoglou K (2007) Fibrinogen inhibits neurite outgrowth via beta 3 integrin-mediated phosphorylation of the EGF receptor. *Proc Natl Acad Sci U S A* 104:11814-11819.
- Scherer PE, Lewis RY, Volonte D, Engelman JA, Galbiati F, Couet J, Kohtz DS, van Donselaar E, Peters P, Lisanti MP (1997) Cell-type and tissue-specific expression of caveolin-2. Caveolins 1 and 2 co-localize and form a stable hetero-oligomeric complex in vivo. *J Biol Chem* 272:29337-29346.
- Schlachetzki F, Pardridge WM (2003) P-glycoprotein and caveolin-1alpha in endothelium and astrocytes of primate brain. *Neuroreport* 14:2041-2046.
- Schmanke TD, Avery RA, Barth TM (1996) The effects of amphetamine on recovery of function after cortical damage in the rat depend on the behavioral requirements of the task. *Journal of neurotrauma* 13:293-307.
- Schmidt OI, Leinhase I, Hasenboehler E, Morgan SJ, Stahel PF (2007) [The relevance of the inflammatory response in the injured brain]. *Orthopade* 36:248, 250-248.
- Schmitz M, Zerr I, Althaus HH (2011) Effect of cavtratin, a caveolin-1 scaffolding domain peptide, on oligodendroglial signaling cascades. *Cell Mol Neurobiol* 31:991-997.
- Schneier AJ, Shields BJ, Hostetler SG, Xiang H, Smith GA (2006) Incidence of pediatric traumatic brain injury and associated hospital resource utilization in the United States. *Pediatrics* 118:483-492.
- Schroder ML, Muizelaar JP, Fatouros PP, Kuta AJ, Choi SC (1998) Regional cerebral blood volume after severe head injury in patients with regional cerebral ischemia. *Neurosurgery* 42:1276-1280; discussion 1280-1271.
- Schubert W, Frank PG, Woodman SE, Hyogo H, Cohen DE, Chow CW, Lisanti MP (2002) Microvascular hyperpermeability in caveolin-1 (-/-) knock-out mice. Treatment with a specific nitric-oxide synthase inhibitor, L-NAME, restores normal microvascular permeability in Cav-1 null mice. *J Biol Chem* 277:40091-40098.
- Schulze C, Firth JA (1993) Immunohistochemical localization of adherens junction components in blood-brain barrier microvessels of the rat. *J Cell Sci* 104 (Pt 3):773-782.
- Schutzman SA, Greenes DS (2001) Pediatric minor head trauma. *Ann Emerg Med* 37:65-74.
- Schwartz L, Taylor HG, Drotar D, Yeates KO, Wade SL, Stancin T (2003) Long-term behavior problems following pediatric traumatic brain injury: prevalence, predictors, and correlates. *J Pediatr Psychol* 28:251-263.

- Schwarzmaier SM, Kim SW, Trabold R, Plesnila N (2010) Temporal profile of thrombogenesis in the cerebral microcirculation after traumatic brain injury in mice. *J Neurotrauma* 27:121-130.
- Schwencke C, Braun-Dullaeus RC, Wunderlich C, Strasser RH (2006) Caveolae and caveolin in transmembrane signaling: Implications for human disease. *Cardiovasc Res* 70:42-49.
- Schwencke C, Yamamoto M, Okumura S, Toya Y, Kim SJ, Ishikawa Y (1999) Compartmentation of cyclic adenosine 3',5'-monophosphate signaling in caveolae. *Mol Endocrinol* 13:1061-1070.
- Sclip A, Antoniou X, Colombo A, Camici GG, Pozzi L, Cardinetti D, Feligioni M, Veglianesi P, Bahlmann FH, Cervo L, Balducci C, Costa C, Tozzi A, Calabresi P, Forloni G, Borsello T (2011) c-Jun N-terminal kinase regulates soluble Abeta oligomers and cognitive impairment in AD mouse model. *J Biol Chem* 286:43871-43880.
- Seiffert E, Dreier JP, Ivens S, Bechmann I, Tomkins O, Heinemann U, Friedman A (2004) Lasting blood-brain barrier disruption induces epileptic focus in the rat somatosensory cortex. *J Neurosci* 24:7829-7836.
- Sellers SL, Trane AE, Bernatchez PN (2012) Caveolin as a potential drug target for cardiovascular protection. *Front Physiol* 3:280.
- Severson EA, Parkos CA (2009) Mechanisms of outside-in signaling at the tight junction by junctional adhesion molecule A. *Ann N Y Acad Sci* 1165:10-18.
- Shapira Y, Setton D, Artru AA, Shohami E (1993) Blood-brain barrier permeability, cerebral edema, and neurologic function after closed head injury in rats. *Anesth Analg* 77:141-148.
- Shen J, Ma S, Chan P, Lee W, Fung PC, Cheung RT, Tong Y, Liu KJ (2006) Nitric oxide down-regulates caveolin-1 expression in rat brains during focal cerebral ischemia and reperfusion injury. *J Neurochem* 96:1078-1089.
- Sherrin T, Blank T, Hippel C, Rayner M, Davis RJ, Todorovic C (2010) Hippocampal c-Jun-N-terminal kinases serve as negative regulators of associative learning. *J Neurosci* 30:13348-13361.
- Shi F, Sottile J (2008) Caveolin-1-dependent beta1 integrin endocytosis is a critical regulator of fibronectin turnover. *J Cell Sci* 121:2360-2371.
- Shin DH, Kim JS, Kwon BS, Lee KS, Kim JW, Kim MH, Cho SS, Lee WJ (2003) Caveolin-3 expression during early chicken development. *Brain Res Dev Brain Res* 141:83-89.
- Shin T (2007) Increases in the phosphorylated form of caveolin-1 in the spinal cord of rats with clip compression injury. *Brain Res* 1141:228-234.

- Shin T, Kim H, Jin JK, Moon C, Ahn M, Tanuma N, Matsumoto Y (2005) Expression of caveolin-1, -2, and -3 in the spinal cords of Lewis rats with experimental autoimmune encephalomyelitis. *J Neuroimmunol* 165:11-20.
- Shlosberg D, Benifla M, Kaufer D, Friedman A (2010) Blood-brain barrier breakdown as a therapeutic target in traumatic brain injury. *Nat Rev Neurol* 6:393-403.
- Siddiqui MR, Komarova YA, Vogel SM, Gao X, Bonini MG, Rajasingh J, Zhao YY, Brovkovich V, Malik AB (2011) Caveolin-1-eNOS signaling promotes p190RhoGAP-A nitration and endothelial permeability. *J Cell Biol* 193:841-850.
- Sifringer M, Stefovská V, Zentner I, Hansen B, Stepulak A, Knaute C, Marzahn J, Ikonomidou C (2007) The role of matrix metalloproteinases in infant traumatic brain injury. *Neurobiol Dis* 25:526-535.
- Silverberg GD, Messier AA, Miller MC, Machan JT, Majmudar SS, Stopa EG, Donahue JE, Johanson CE (2010) Amyloid efflux transporter expression at the blood-brain barrier declines in normal aging. *Journal of neuropathology and experimental neurology* 69:1034-1043.
- Simard JM, Kent TA, Chen M, Tarasov KV, Gerzanich V (2007) Brain oedema in focal ischaemia: molecular pathophysiology and theoretical implications. *Lancet Neurol* 6:258-268.
- Simons K, Ikonen E (1997) Functional rafts in cell membranes. *Nature* 387:569-572.
- Simons K, van Meer G (1988) Lipid sorting in epithelial cells. *Biochemistry* 27:6197-6202.
- Singleton PA, Dudek SM, Ma SF, Garcia JG (2006) Transactivation of sphingosine 1-phosphate receptors is essential for vascular barrier regulation. Novel role for hyaluronan and CD44 receptor family. *J Biol Chem* 281:34381-34393.
- Sloan EK, Stanley KL, Anderson RL (2004) Caveolin-1 inhibits breast cancer growth and metastasis. *Oncogene* 23:7893-7897.
- Soblosky JS, Matthews MA, Davidson JF, Tabor SL, Carey ME (1996) Traumatic brain injury of the forelimb and hindlimb sensorimotor areas in the rat: physiological, histological and behavioral correlates. *Behav Brain Res* 79:79-92.
- Somara S, Bashllari D, Gilmont RR, Bitar KN (2011) Real-time dynamic movement of caveolin-1 during smooth muscle contraction of human colon and aged rat colon transfected with caveolin-1 cDNA. *Am J Physiol Gastrointest Liver Physiol* 300:G1022-1032.
- Song KS, Scherer PE, Tang Z, Okamoto T, Li S, Chafel M, Chu C, Kohtz DS, Lisanti MP (1996) Expression of caveolin-3 in skeletal, cardiac, and smooth muscle cells. Caveolin-3 is a component of the sarcolemma and co-fractionates with dystrophin and dystrophin-associated glycoproteins. *J Biol Chem* 271:15160-15165.

- Song L, Ge S, Pachter JS (2007) Caveolin-1 regulates expression of junction-associated proteins in brain microvascular endothelial cells. *Blood* 109:1515-1523.
- Song L, Pachter JS (2004) Monocyte chemoattractant protein-1 alters expression of tight junction-associated proteins in brain microvascular endothelial cells. *Microvasc Res* 67:78-89.
- Sosin DM, Sniezek JE, Thurman DJ (1996) Incidence of mild and moderate brain injury in the United States, 1991. *Brain Inj* 10:47-54.
- Spisni E, Tomasi V, Cestaro A, Tosatto SC (2005) Structural insights into the function of human caveolin 1. *Biochem Biophys Res Commun* 338:1383-1390.
- Stamatovic SM, Keep RF, Andjelkovic AV (2008) Brain endothelial cell-cell junctions: how to "open" the blood brain barrier. *Curr Neuropharmacol* 6:179-192.
- Stamatovic SM, Keep RF, Wang MM, Jankovic I, Andjelkovic AV (2009) Caveolae-mediated internalization of occludin and claudin-5 during CCL2-induced tight junction remodeling in brain endothelial cells. *J Biol Chem* 284:19053-19066.
- Stary CM, Tsutsumi YM, Patel PM, Head BP, Patel HH, Roth DM (2012) Caveolins: targeting pro-survival signaling in the heart and brain. *Front Physiol* 3:393.
- Stein SC, Chen XH, Sinson GP, Smith DH (2002) Intravascular coagulation: a major secondary insult in nonfatal traumatic brain injury. *J Neurosurg* 97:1373-1377.
- Stern RA, Riley DO, Daneshvar DH, Nowinski CJ, Cantu RC, McKee AC (2011) Long-term consequences of repetitive brain trauma: chronic traumatic encephalopathy. *PM R* 3:S460-467.
- Stock A (2011) Pediatric Head Trauma. In: e-Medicine.
- Stoica B, Byrnes K, Faden AI (2009) Multifunctional drug treatment in neurotrauma. *Neurotherapeutics* 6:14-27.
- Stolp HB, Dziegielewska KM (2009) Review: Role of developmental inflammation and blood-brain barrier dysfunction in neurodevelopmental and neurodegenerative diseases. *Neuropathol Appl Neurobiol* 35:132-146.
- Stolp HB, Dziegielewska KM, Ek CJ, Habgood MD, Lane MA, Potter AM, Saunders NR (2005a) Breakdown of the blood-brain barrier to proteins in white matter of the developing brain following systemic inflammation. *Cell Tissue Res* 320:369-378.
- Stolp HB, Dziegielewska KM, Ek CJ, Potter AM, Saunders NR (2005b) Long-term changes in blood-brain barrier permeability and white matter following prolonged systemic inflammation in early development in the rat. *Eur J Neurosci* 22:2805-2816.
- Strbian D, Durukan A, Pitkonen M, Marinkovic I, Tatlisumak E, Pedrono E, Abo-Ramadan U, Tatlisumak T (2008) The blood-brain barrier is continuously open

- for several weeks following transient focal cerebral ischemia. *Neuroscience* 153:175-181.
- Suh DY, Davis PC, Hopkins KL, Fajman NN, Mapstone TB (2001) Nonaccidental pediatric head injury: diffusion-weighted imaging findings. *Neurosurgery* 49:309-318; discussion 318-320.
- Suzuki K (1990) The changes in regional cerebral blood flow with advancing age in normal children. *Nagoya Medical Journal* 34:159-170.
- Swaiman KF, Ashwal S, Ferriero DM, Schor N (2012) *Swaiman's Pediatric Neurology: Principles and Practice*. China: Saunders Elsevier Inc.
- Taddei A, Giampietro C, Conti A, Orsenigo F, Breviario F, Pirazzoli V, Potente M, Daly C, Dimmeler S, Dejana E (2008) Endothelial adherens junctions control tight junctions by VE-cadherin-mediated upregulation of claudin-5. *Nat Cell Biol* 10:923-934.
- Tagliaferri F, Compagnone C, Korsic M, Servadei F, Kraus J (2006) A systematic review of brain injury epidemiology in Europe. *Acta Neurochir (Wien)* 148:255-268; discussion 268.
- Tai LM, Holloway KA, Male DK, Loughlin AJ, Romero IA (2010) Amyloid-beta-induced occludin down-regulation and increased permeability in human brain endothelial cells is mediated by MAPK activation. *J Cell Mol Med* 14:1101-1112.
- Tanaka H, Ma J, Tanaka KF, Takao K, Komada M, Tanda K, Suzuki A, Ishibashi T, Baba H, Isa T, Shigemoto R, Ono K, Miyakawa T, Ikenaka K (2009) Mice with altered myelin proteolipid protein gene expression display cognitive deficits accompanied by abnormal neuron-glia interactions and decreased conduction velocities. *The Journal of neuroscience : the official journal of the Society for Neuroscience* 29:8363-8371.
- Tang Z, Okamoto T, Boontrakulpoontawee P, Katada T, Otsuka AJ, Lisanti MP (1997) Identification, sequence, and expression of an invertebrate caveolin gene family from the nematode *Caenorhabditis elegans*. Implications for the molecular evolution of mammalian caveolin genes. *J Biol Chem* 272:2437-2445.
- Taylor HG (2004) Research on outcomes of pediatric traumatic brain injury: current advances and future directions. *Dev Neuropsychol* 25:199-225.
- Teuber ML, Rudel RG (1962) Behavior after cerebral lesions in children. *Developmental Medicine & Child Neurology* 4:18.
- Thal SC, Luh C, Schaible EV, Timaru-Kast R, Hedrich J, Luhmann HJ, Engelhard K, Zehendner CM (2012) Volatile anesthetics influence blood-brain barrier integrity by modulation of tight junction protein expression in traumatic brain injury. *PLoS One* 7:e50752.

- Thomsen IV (1984) Late outcome of very severe blunt head trauma: a 10-15 year second follow-up. *J Neurol Neurosurg Psychiatry* 47:260-268.
- Thomsen IV (1992) Late psychosocial outcome in severe traumatic brain injury. Preliminary results of a third follow-up study after 20 years. *Scand J Rehabil Med Suppl* 26:142-152.
- Tian L, Guo R, Yue X, Lv Q, Ye X, Wang Z, Chen Z, Wu B, Xu G, Liu X (2012) Intranasal administration of nerve growth factor ameliorate beta-amyloid deposition after traumatic brain injury in rats. *Brain research* 1440:47-55.
- Tomkins O, Feintuch A, Benifla M, Cohen A, Friedman A, Shelef I (2011) Blood-brain barrier breakdown following traumatic brain injury: a possible role in posttraumatic epilepsy. *Cardiovasc Psychiatry Neurol* 2011:765923.
- Tomkins O, Kaufer D, Korn A, Shelef I, Golan H, Reichenthal E, Soreq H, Friedman A (2001) Frequent blood-brain barrier disruption in the human cerebral cortex. *Cell Mol Neurobiol* 21:675-691.
- Tomkins O, Shelef I, Kaizerman I, Eliushin A, Afawi Z, Misk A, Gidon M, Cohen A, Zumsteg D, Friedman A (2008) Blood-brain barrier disruption in post-traumatic epilepsy. *J Neurol Neurosurg Psychiatry* 79:774-777.
- Touchard E, Omri S, Naud MC, Berdugo M, Deloche C, Abadie C, Jonet L, Jeanny JC, Crisanti P, de Kozak Y, Combette JM, Behar-Cohen F (2010) A peptide inhibitor of c-Jun N-terminal kinase for the treatment of endotoxin-induced uveitis. *Invest Ophthalmol Vis Sci* 51:4683-4693.
- Tourkina E, Richard M, Gooz P, Bonner M, Pannu J, Harley R, Bernatchez PN, Sessa WC, Silver RM, Hoffman S (2008) Antifibrotic properties of caveolin-1 scaffolding domain in vitro and in vivo. *Am J Physiol Lung Cell Mol Physiol* 294:L843-861.
- Tourkina E, Richard M, Oates J, Hofbauer A, Bonner M, Gooz P, Visconti R, Zhang J, Znoyko S, Hatfield CM, Silver RM, Hoffman S (2010) Caveolin-1 regulates leucocyte behaviour in fibrotic lung disease. *Ann Rheum Dis* 69:1220-1226.
- Tran HT, Sanchez L, Brody DL (2012) Inhibition of JNK by a peptide inhibitor reduces traumatic brain injury-induced tauopathy in transgenic mice. *J Neuropathol Exp Neurol* 71:116-129.
- Travis J (1993) Cell biologists explore 'tiny caves'. *Science* 262:1208-1209.
- Tu YF, Tsai YS, Wang LW, Wu HC, Huang CC, Ho CJ (2011) Overweight worsens apoptosis, neuroinflammation and blood-brain barrier damage after hypoxic ischemia in neonatal brain through JNK hyperactivation. *J Neuroinflammation* 8:40.
- Tyagi N, Roberts AM, Dean WL, Tyagi SC, Lominadze D (2008) Fibrinogen induces endothelial cell permeability. *Mol Cell Biochem* 307:13-22.

- Udomphorn Y, Armstead WM, Vavilala MS (2008) Cerebral blood flow and autoregulation after pediatric traumatic brain injury. *Pediatric neurology* 38:225-234.
- Ueno M, Nakagawa T, Wu B, Onodera M, Huang CL, Kusaka T, Araki N, Sakamoto H (2010) Transporters in the brain endothelial barrier. *Curr Med Chem* 17:1125-1138.
- Unterberg AW, Stover J, Kress B, Kiening KL (2004) Edema and brain trauma. *Neuroscience* 129:1021-1029.
- van Assema DM, Lubberink M, Bauer M, van der Flier WM, Schuit RC, Windhorst AD, Comans EF, Hoetjes NJ, Tolboom N, Langer O, Muller M, Scheltens P, Lammertsma AA, van Berckel BN (2012) Blood-brain barrier P-glycoprotein function in Alzheimer's disease. *Brain : a journal of neurology* 135:181-189.
- van Groen T, Puurunen K, Maki HM, Sivenius J, Jolkkonen J (2005) Transformation of diffuse beta-amyloid precursor protein and beta-amyloid deposits to plaques in the thalamus after transient occlusion of the middle cerebral artery in rats. *Stroke; a journal of cerebral circulation* 36:1551-1556.
- van Landeghem FK, Weiss T, Oehmichen M, von Deimling A (2006) Decreased expression of glutamate transporters in astrocytes after human traumatic brain injury. *Journal of neurotrauma* 23:1518-1528.
- Vasa RA, Gerring JP, Grados M, Slomine B, Christensen JR, Rising W, Denckla MB, Riddle MA (2002) Anxiety after severe pediatric closed head injury. *J Am Acad Child Adolesc Psychiatry* 41:148-156.
- Vavilala MS, Lee LA, Boddu K, Visco E, Newell DW, Zimmerman JJ, Lam AM (2004) Cerebral autoregulation in pediatric traumatic brain injury. *Pediatric critical care medicine : a journal of the Society of Critical Care Medicine and the World Federation of Pediatric Intensive and Critical Care Societies* 5:257-263.
- Vaz R, Sarmiento A, Borges N, Cruz C, Azevedo I (1997) Ultrastructural study of brain microvessels in patients with traumatic cerebral contusions. *Acta Neurochir (Wien)* 139:215-220.
- Velumian AA, Wan Y, SamoiloVA M, Fehlings MG (2011) Contribution of fast and slow conducting myelinated axons to single-peak compound action potentials in rat spinal cord white matter preparations. *Journal of Neurophysiology* 105:929-941.
- Verive MJ, Stock A, Singh J, Corden TE (2012) *Pediatric Head Trauma In: eMedicine USA.*
- Vink R, Van Den Heuvel C (2004) Recent advances in the development of multifactorial therapies for the treatment of traumatic brain injury. *Expert opinion on investigational drugs* 13:1263-1274.

- Virgintino D, Errede M, Robertson D, Capobianco C, Girolamo F, Vimercati A, Bertossi M, Roncali L (2004) Immunolocalization of tight junction proteins in the adult and developing human brain. *Histochem Cell Biol* 122:51-59.
- Virgintino D, Robertson D, Errede M, Benagiano V, Tauer U, Roncali L, Bertossi M (2002) Expression of caveolin-1 in human brain microvessels. *Neuroscience* 115:145-152.
- Vogelgesang S, Cascorbi I, Schroeder E, Pahnke J, Kroemer HK, Siegmund W, Kunert-Keil C, Walker LC, Warzok RW (2002) Deposition of Alzheimer's beta-amyloid is inversely correlated with P-glycoprotein expression in the brains of elderly non-demented humans. *Pharmacogenetics* 12:535-541.
- von Oettingen G, Bergholt B, Gyldensted C, Astrup J (2002) Blood flow and ischemia within traumatic cerebral contusions. *Neurosurgery* 50:781-788; discussion 788-790.
- Vorbrodt AW, Dobrogowska DH (2004) Molecular anatomy of interendothelial junctions in human blood-brain barrier microvessels. *Folia Histochem Cytobiol* 42:67-75.
- Vukic V, Callaghan D, Walker D, Lue LF, Liu QY, Couraud PO, Romero IA, Weksler B, Stanimirovic DB, Zhang W (2009) Expression of inflammatory genes induced by beta-amyloid peptides in human brain endothelial cells and in Alzheimer's brain is mediated by the JNK-AP1 signaling pathway. *Neurobiol Dis* 34:95-106.
- Waetzig V, Czeloth K, Hidding U, Mielke K, Kanzow M, Brecht S, Goetz M, Lucius R, Herdegen T, Hanisch UK (2005) c-Jun N-terminal kinases (JNKs) mediate pro-inflammatory actions of microglia. *Glia* 50:235-246.
- Waetzig V, Herdegen T (2005) Context-specific inhibition of JNKs: overcoming the dilemma of protection and damage. *Trends Pharmacol Sci* 26:455-461.
- Waetzig V, Zhao Y, Herdegen T (2006) The bright side of JNKs-Multitalented mediators in neuronal sprouting, brain development and nerve fiber regeneration. *Prog Neurobiol* 80:84-97.
- Wagner AC, Mazzucchelli L, Miller M, Camoratto AM, Goke B (2000) CEP-1347 inhibits caerulein-induced rat pancreatic JNK activation and ameliorates caerulein pancreatitis. *American journal of physiology Gastrointestinal and liver physiology* 278:G165-172.
- Wagner AK, Postal BA, Darrah SD, Chen X, Khan AS (2007) Deficits in novelty exploration after controlled cortical impact. *Journal of neurotrauma* 24:1308-1320.
- Wagner AK, Willard LA, Kline AE, Wenger MK, Bolinger BD, Ren D, Zafonte RD, Dixon CE (2004) Evaluation of estrous cycle stage and gender on behavioral outcome after experimental traumatic brain injury. *Brain research* 998:113-121.

- Wang LW, Tu YF, Huang CC, Ho CJ (2012) JNK signaling is the shared pathway linking neuroinflammation, blood-brain barrier disruption, and oligodendroglial apoptosis in the white matter injury of the immature brain. *J Neuroinflammation* 9:175.
- Wang X, Jung J, Asahi M, Chwang W, Russo L, Moskowitz MA, Dixon CE, Fini ME, Lo EH (2000) Effects of matrix metalloproteinase-9 gene knock-out on morphological and motor outcomes after traumatic brain injury. *J Neurosci* 20:7037-7042.
- Wang X, Nadarajah B, Robinson AC, McColl BW, Jin JW, Dajas-Bailador F, Boot-Handford RP, Tournier C (2007) Targeted deletion of the mitogen-activated protein kinase kinase 4 gene in the nervous system causes severe brain developmental defects and premature death. *Molecular and cellular biology* 27:7935-7946.
- Wang XM, Kim HP, Song R, Choi AM (2006) Caveolin-1 confers antiinflammatory effects in murine macrophages via the MKK3/p38 MAPK pathway. *Am J Respir Cell Mol Biol* 34:434-442.
- Wedmore CV, Williams TJ (1981) Control of vascular permeability by polymorphonuclear leukocytes in inflammation. *Nature* 289:646-650.
- Wei W, Norton DD, Wang X, Kusiak JW (2002) Abeta 17-42 in Alzheimer's disease activates JNK and caspase-8 leading to neuronal apoptosis. *Brain : a journal of neurology* 125:2036-2043.
- Werner C, Engelhard K (2007) Pathophysiology of traumatic brain injury. *Br J Anaesth* 99:4-9.
- Whelan-Goodinson R, Ponsford J, Johnston L, Grant F (2009) Psychiatric disorders following traumatic brain injury: their nature and frequency. *J Head Trauma Rehabil* 24:324-332.
- Widmann C, Gibson S, Jarpe MB, Johnson GL (1999) Mitogen-activated protein kinase: conservation of a three-kinase module from yeast to human. *Physiol Rev* 79:143-180.
- Wiencken AE, Casagrande VA (1999) Endothelial nitric oxide synthetase (eNOS) in astrocytes: another source of nitric oxide in neocortex. *Glia* 26:280-290.
- Wilde EA, Bigler ED, Haider JM, Chu Z, Levin HS, Li X, Hunter JV (2006) Vulnerability of the anterior commissure in moderate to severe pediatric traumatic brain injury. *Journal of child neurology* 21:769-776.
- Wilde EA, Bigler ED, Hunter JV, Fearing MA, Scheibel RS, Newsome MR, Johnson JL, Bachevalier J, Li X, Levin HS (2007) Hippocampus, amygdala, and basal ganglia morphometrics in children after moderate-to-severe traumatic brain injury. *Developmental medicine and child neurology* 49:294-299.

- Wilke GA, Bubeck Wardenburg J (2010) Role of a disintegrin and metalloprotease 10 in Staphylococcus aureus alpha-hemolysin-mediated cellular injury. *Proc Natl Acad Sci U S A* 107:13473-13478.
- Williams TM, Hassan GS, Li J, Cohen AW, Medina F, Frank PG, Pestell RG, Di Vizio D, Loda M, Lisanti MP (2005) Caveolin-1 promotes tumor progression in an autochthonous mouse model of prostate cancer: genetic ablation of Cav-1 delays advanced prostate tumor development in tramp mice. *J Biol Chem* 280:25134-25145.
- Williams TM, Lisanti MP (2005) Caveolin-1 in oncogenic transformation, cancer, and metastasis. *Am J Physiol Cell Physiol* 288:C494-506.
- Wilson CJ, Finch CE, Cohen HJ (2002) Cytokines and cognition--the case for a head-to-toe inflammatory paradigm. *J Am Geriatr Soc* 50:2041-2056.
- Winkler EA, Bell RD, Zlokovic BV (2011) Central nervous system pericytes in health and disease. *Nat Neurosci* 14:1398-1405.
- Wolburg H, Lippoldt A (2002) Tight junctions of the blood-brain barrier: development, composition and regulation. *Vascul Pharmacol* 38:323-337.
- Wolburg H, Noell S, Mack A, Wolburg-Buchholz K, Fallier-Becker P (2009) Brain endothelial cells and the glio-vascular complex. *Cell Tissue Res* 335:75-96.
- Woodman SE, Ashton AW, Schubert W, Lee H, Williams TM, Medina FA, Wyckoff JB, Combs TP, Lisanti MP (2003) Caveolin-1 knockout mice show an impaired angiogenic response to exogenous stimuli. *Am J Pathol* 162:2059-2068.
- Wu H, Mahmood A, Lu D, Jiang H, Xiong Y, Zhou D, Chopp M (2010a) Attenuation of astrogliosis and modulation of endothelial growth factor receptor in lipid rafts by simvastatin after traumatic brain injury. *J Neurosurg* 113:591-597.
- Wu TC, Wilde EA, Bigler ED, Li X, Merkley TL, Yallampalli R, McCauley SR, Schnelle KP, Vasquez AC, Chu Z, Hanten G, Hunter JV, Levin HS (2010b) Longitudinal changes in the corpus callosum following pediatric traumatic brain injury. *Developmental neuroscience* 32:361-373.
- Xi G, Reiser G, Keep RF (2003) The role of thrombin and thrombin receptors in ischemic, hemorrhagic and traumatic brain injury: deleterious or protective? *J Neurochem* 84:3-9.
- Xie Z, Smith CJ, Van Eldik LJ (2004) Activated glia induce neuron death via MAP kinase signaling pathways involving JNK and p38. *Glia* 45:170-179.
- Xing C, Hayakawa K, Lok J, Arai K, Lo EH (2012) Injury and repair in the neurovascular unit. *Neurol Res* 34:325-330.

- Xu X, Raber J, Yang D, Su B, Mucke L (1997) Dynamic regulation of c-Jun N-terminal kinase activity in mouse brain by environmental stimuli. *Proc Natl Acad Sci U S A* 94:12655-12660.
- Yamada E (1955) The fine structure of the gall bladder epithelium of the mouse. *J Biophys Biochem Cytol* 1:445-458.
- Yamasaki T, Kawasaki H, Arakawa S, Shimizu K, Shimizu S, Reiner O, Okano H, Nishina S, Azuma N, Penninger JM, Katada T, Nishina H (2011) Stress-activated protein kinase MKK7 regulates axon elongation in the developing cerebral cortex. *The Journal of neuroscience : the official journal of the Society for Neuroscience* 31:16872-16883.
- Yamasaki T, Kawasaki H, Nishina H (2012) Diverse Roles of JNK and MKK Pathways in the Brain. *J Signal Transduct* 2012:459265.
- Yang DD, Kuan CY, Whitmarsh AJ, Rincon M, Zheng TS, Davis RJ, Rakic P, Flavell RA (1997) Absence of excitotoxicity-induced apoptosis in the hippocampus of mice lacking the Jnk3 gene. *Nature* 389:865-870.
- Yang Y, Estrada EY, Thompson JF, Liu W, Rosenberg GA (2007) Matrix metalloproteinase-mediated disruption of tight junction proteins in cerebral vessels is reversed by synthetic matrix metalloproteinase inhibitor in focal ischemia in rat. *J Cereb Blood Flow Metab* 27:697-709.
- Yatsushige H, Ostrowski RP, Tsubokawa T, Colohan A, Zhang JH (2007) Role of c-Jun N-terminal kinase in early brain injury after subarachnoid hemorrhage. *J Neurosci Res* 85:1436-1448.
- Yeates KO, Taylor HG, Wade SL, Drotar D, Stancin T, Minich N (2002) A prospective study of short- and long-term neuropsychological outcomes after traumatic brain injury in children. *Neuropsychology* 16:514-523.
- Yeung D, Manias JL, Stewart DJ, Nag S (2008) Decreased junctional adhesion molecule-A expression during blood-brain barrier breakdown. *Acta Neuropathol* 115:635-642.
- Yi JH, Hazell AS (2006) Excitotoxic mechanisms and the role of astrocytic glutamate transporters in traumatic brain injury. *Neurochemistry international* 48:394-403.
- Yoon MJ, Cho CH, Lee CS, Jang IH, Ryu SH, Koh GY (2003) Localization of Tie2 and phospholipase D in endothelial caveolae is involved in angiotensin-1-induced MEK/ERK phosphorylation and migration in endothelial cells. *Biochem Biophys Res Commun* 308:101-105.
- Yoshizumi M, Abe J, Haendeler J, Huang Q, Berk BC (2000) Src and Cas mediate JNK activation but not ERK1/2 and p38 kinases by reactive oxygen species. *J Biol Chem* 275:11706-11712.

- Yoshizumi M, Abe J, Tsuchiya K, Berk BC, Tamaki T (2003) Stress and vascular responses: atheroprotective effect of laminar fluid shear stress in endothelial cells: possible role of mitogen-activated protein kinases. *J Pharmacol Sci* 91:172-176.
- Yuan SY, Rigor RR (2010) Regulation of Endothelial Barrier Function. In: *Integrated Systems Physiology: from Molecule to Function to Disease*, vol. Lecture 12 (Granger, D. N. and Granger, J. P., eds) San Rafael (CA): Morgan & Claypool Life Sciences.
- Zaloshnja E, Miller T, Langlois JA, Selassie AW (2008) Prevalence of long-term disability from traumatic brain injury in the civilian population of the United States, 2005. *The Journal of head trauma rehabilitation* 23:394-400.
- Zhang H, Adwanikar H, Werb Z, Noble-Haeusslein LJ (2010) Matrix metalloproteinases and neurotrauma: evolving roles in injury and reparative processes. *The Neuroscientist : a review journal bringing neurobiology, neurology and psychiatry* 16:156-170.
- Zhao BQ, Wang S, Kim HY, Storrie H, Rosen BR, Mooney DJ, Wang X, Lo EH (2006) Role of matrix metalloproteinases in delayed cortical responses after stroke. *Nat Med* 12:441-445.
- Zhao J, Moore AN, Redell JB, Dash PK (2007) Enhancing expression of Nrf2-driven genes protects the blood brain barrier after brain injury. *J Neurosci* 27:10240-10248.
- Zhao X, Ahram A, Berman RF, Muizelaar JP, Lyeth BG (2003) Early loss of astrocytes after experimental traumatic brain injury. *Glia* 44:140-152.
- Zhu L, Wang HD, Yu XG, Jin W, Qiao L, Lu TJ, Hu ZL, Zhou J (2009) Erythropoietin prevents zinc accumulation and neuronal death after traumatic brain injury in rat hippocampus: in vitro and in vivo studies. *Brain research* 1289:96-105.
- Zhu Y, Sun Y, Xie L, Jin K, Sheibani N, Greenberg DA (2003) Hypoxic induction of endoglin via mitogen-activated protein kinases in mouse brain microvascular endothelial cells. *Stroke* 34:2483-2488.
- Zimmerman RA, Bilaniuk LT, Bruce D, Dolinskas C, Obrist W, Kuhl D (1978) Computed tomography of pediatric head trauma: acute general cerebral swelling. *Radiology* 126:403-408.
- Zlokovic BV (2008) The blood-brain barrier in health and chronic neurodegenerative disorders. *Neuron* 57:178-201.
- Zschocke J, Bayatti N, Behl C (2005) Caveolin and GLUT-1 gene expression is reciprocally regulated in primary astrocytes: association of GLUT-1 with non-caveolar lipid rafts. *Glia* 49:275-287.
- Zuckerman GB, Conway EE, Jr. (1997) Accidental head injury. *Pediatr Ann* 26:621-632.

Zweckberger K, Eros C, Zimmermann R, Kim SW, Engel D, Plesnila N (2006) Effect of early and delayed decompressive craniectomy on secondary brain damage after controlled cortical impact in mice. *Journal of neurotrauma* 23:1083-1093.

Zwienenberg M, Muizelaar JP (1999) Severe pediatric head injury: the role of hyperemia revisited. *J Neurotrauma* 16:937-943.